

Cirolana phuketensis, a new species of marine isopod (Crustacea, Isopoda, Cirolanidae) from the Andaman Sea coast of Thailand

Ekmarin Rodcharoen¹, Niel L. Bruce², Pornsilp Pholpunthin³

1 Department of Aquatic Science, Faculty of Natural Resources, Prince of Songkla University, Hat Yai, Songkhla, Thailand 90112 **2** Museum of Tropical Queensland, Queensland Museum, Townsville, Australia; and Water Research Group, Unit for Environmental Sciences and Management, North-West University, Private Bag X6001, Potchefstroom 2520, South Africa **3** Department of Biology, Faculty of Science, Prince of Songkla University, Hat Yai, Songkhla, Thailand 90112

Corresponding author: *Ekmarin Rodcharoen* (ekmarin.r@psu.ac.th)

Academic editor: *T. Horton* | Received 19 May 2017 | Accepted 8 August 2017 | Published 4 September 2017

<http://zoobank.org/A6B4C812-DABB-4D27-9C5C-FA0356FD7336>

Citation: Rodcharoen E, Bruce NL, Pholpunthin P (2017) *Cirolana phuketensis*, a new species of marine isopod (Crustacea, Isopoda, Cirolanidae) from the Andaman Sea coast of Thailand. ZooKeys 695: 1–17. <https://doi.org/10.3897/zookeys.695.13771>

Abstract

Cirolana phuketensis **sp. n.** was collected from coral rubble from the Andaman sea coast of Thailand. *C. phuketensis* **sp. n.** is described and fully illustrated; *C. phuketensis* **sp. n.** can be recognized by the presence of transverse sutures on pereonites 2–4, pereonite 7 having three transverse sutures forming a nodulose ridge, antennula peduncle with articles 1 and 2 fully fused; pleotelson dorsal surface with 2 sub-median longitudinal carinae, each of which has one prominent tubercle, lateral margins weakly convex, and posterior margin narrow and rounded; 6 molariform robust setae pereopod 1 on inferior margin of merus and the penial openings are two low tubercles. A dichotomous key to species of *Cirolana* in Thailand is given.

Keywords

Isopoda, Cirolanidae, *Cirolana*, new species, the Andaman Sea, Thailand

Introduction

Thailand lies in the tropical zone between Pacific Ocean and Indian Ocean. This region has high marine biodiversity (Briggs 2000, 2005; Briggs and Bowen 2013; Carpenter et al. 2011) but knowledge of marine crustaceans still remains minimal in the region,

the non-decapod taxa having received relatively little attention (see Bruce et al. 2002). Since 2000 several new species and new records of marine amphipods (Ariyama et al. 2010; Wongkamhaeng et al. 2012a, b, 2013, 2014), and isopods (Bruce and Olesen 2002; Storey 2002; Svavarsson 2002; Svavarsson and Gísladóttir 2002; Rodcharoen et al. 2014, 2016) have been described.

The family Cirolanidae Dana, 1852 (superfamily Cirolanoidea, suborder Cy-mothoidea following Brandt and Poore 2003), consists of 61 accepted genera and 497 species worldwide (Bruce and Schotte 2015). Forty-three species in twelve genera of Cirolanidae are known from South-East Asia (Nierstrasz 1931; Bruce and Olesen 2002; Sidabalok 2013; Rodcharoen et al. 2014, 2016, present study; Sidabalok and Bruce 2015, 2016, 2017a, b, c in press, and in prep; excluding nomina dubia and synonyms) Bruce (2004b, table 1) compared the diversity of Cirolanidae from different regions, and one can readily assess that, given the relative low level of research on Cirolanidae in South-East Asia the diversity is relatively high and will increase significantly with further research. At present the diversity of South-East Asian Cirolanidae is second only to that of the well-documented Queensland coast that has 16 genera and 65 species (Bruce 2004b, updated). Thailand itself has 18 species in eight genera.

Species of *Cirolana* Leach, 1818 primarily occupy marine and estuarine habitats, and the genus is the largest in the family (Bruce 1981, 1986; Brusca et al. 1995) with 136 named species and a worldwide distribution (Bruce and Schotte 2015). *Cirolana* is found in all oceans from tropical regions to temperate regions. Only *Cirolana mclaughlinae* Bruce & Brandt, 2006, from the Ross Sea, occurs in polar waters. The genus is most common and diverse in the tropics (Bruce 1981, 1986; Kensley and Schotte 1989, 2005; Brusca et al. 1995). Nine species of *Cirolana* have been recorded in Thailand. Of these, five species were reported from the Andaman Sea. Kensley (2001) listed the species known from the Indian Ocean, including the western coasts of Thailand. Bruce and Olesen (2002) reported four marine cirolanid species from Andaman Sea including two new species of *Cirolana*. Recently, Rodcharoen et al. (2016) reported four new species of *Cirolana* ‘*parva* group’ from Thailand two of which are from the Andaman Sea.

Cirolana phuketensis sp. n. is described from the Andaman coast of Thailand and a key of *Cirolana* species occurring in Thai coastal waters is provided.

Materials and methods

2.1 Sampling and collection

Specimens were collected from shallow-water coral-rubble habitats (at depths of 0–10 m) in the coastal zone of the Andaman Sea (Figure 1) using baited traps as described by Keable (1995). Specimens were fixed in 10% formalin in the field and transferred to 70% ethanol.

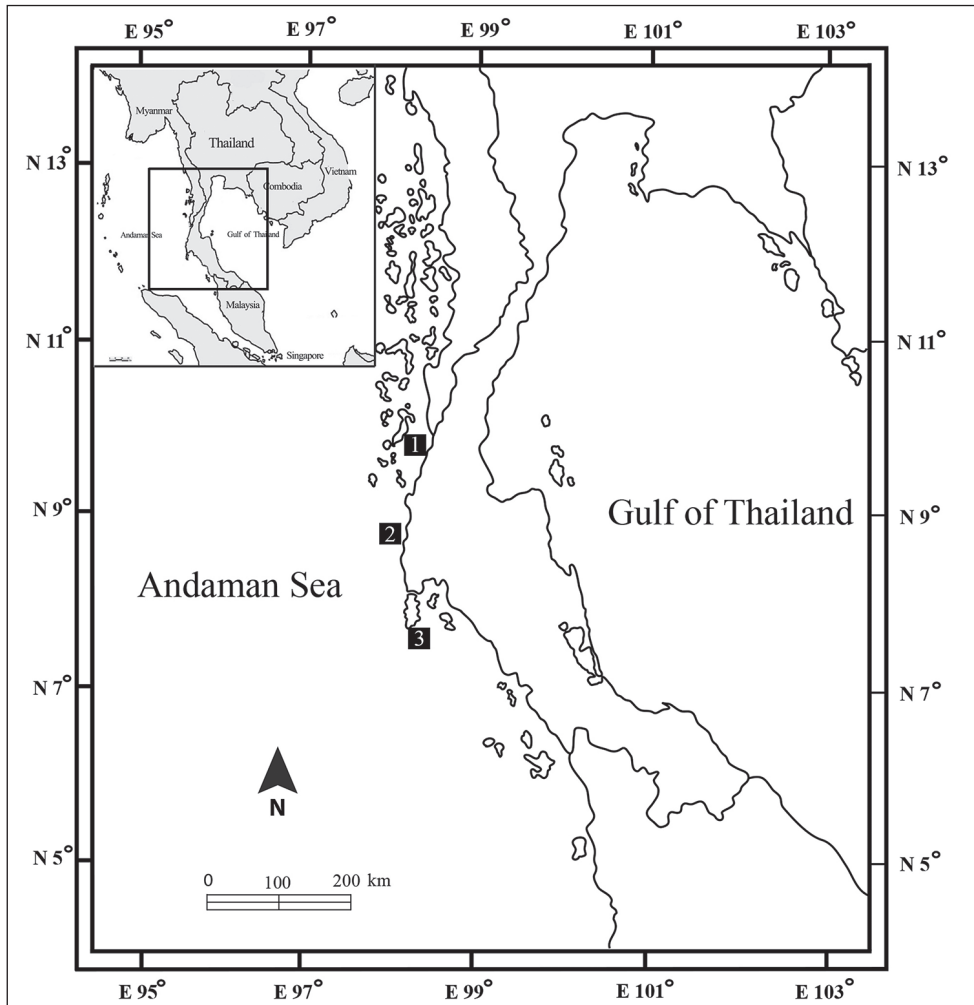


Figure 1. Map of sampling sites **1** Koh Phayam, Ranong Province **2** Laem Pakarang, Phang Nga Province **3** Ao Makham, Phuket Province.

2.2 Morphological study

Appendages of a paratype were dissected for description under Olympus SZ51 stereo microscope and drawn under an Olympus CH30 compound microscope with a *camera lucida*. The holotype dorsal and lateral drawings are based on photos taken by Olympus DP71 microscope digital camera with Olympus SZH10 stereo microscope. Drawings were inked using Adobe Illustrator with Wacom Bamboo drawing tablet. Morphological characters for the descriptions follow Bruce (2004a), and were prepared using DELTA (Descriptive Language for Taxonomy: Coleman et al. 2010; Dallwitz 1980; Dallwitz et al. 1997, 2006).

Abbreviations: **PSUZYC**, Prince of Songkla University Zoological Collection; **MTQ**, Museum of Tropical Queensland. Queensland Museum; **PMS**, plumose marginal setae; **RS**, robust seta/setae; **CPS**, circumplumose setae.

Taxonomy

Family Cirolanidae Dana, 1952

Genus *Cirolana* Leach, 1818

Remarks. For the most recent accounts of this genus in Thai waters see Bruce and Olesen (2002) and Rodcharoen et al (2014, 2016); Bruce and Wong (2015) and Sidalok (2013) while not dealing with the Thai isopod fauna give a useful indication of the genera and species diversity that can be expected in the region. Diagnoses to *Cirolana* have been given most recently Brusca et al. (1995), Kensley and Schotte (1989).

Cirolana phuketensis sp. n.

<http://zoobank.org/CF35E681-77AD-47A1-B3FF-F1493DBDC6C5>

Material examined. Holotype: ♂ (5.0 mm), Ao Makham, Phuket Province, 07°49'51"N, 98°24'14"E, 6 August 2014, trapped in 1 m of depth, coral rubble, coll. E. Rodcharoen (PSUZYC–CR2086-01).

Paratypes: 6 ♂ (4.6, 5.8, 5.2, 5.0, 5.3, 5.1 mm [dissected]), 3 ♀ (5.2, 4.9, 4.9 mm [dissected]), same data as holotype, (PSUZYC–CR2086-02; MTQ W53037). 3 ♂ (5.6, 4.8, 5.3 mm [dissected]), 6 ♀ (5.2, 5.7, 5.3, 5.7, 5.6, 5.4 mm [dissected]), Laem Pakarang, Phang Nga Province, 08°44'11"N, 98°13'13"E, 15 March 2012, trapped in 2 m of depth, coral rubble, coll. E. Rodcharoen (PSUZYC–CR2086-03; MTQ W53038). 3 ♂ (4.7, 4.9, 5.0 mm [dissected]), 7 ♀ (5.0, 4.7, 4.9, 4.9, 5.1, 4.6, 5.1 mm [dissected]), Koh Phayam, Ranong Province, 09°42'36"N, 98°23'41"E, 22 December 2012, trapped in 3 m of depth, coral rubble, coll. E. Rodcharoen (PSUZYC–CR2086-04; MTQ W53039).

Description of male. *Body* 2.8 times as long as greatest width, widest at pereonite 6, lateral margins subparallel (Figure 2A). *Rostral point* absent (Figure 2C). *Eyes* colour dark brown (Figure 2C). *Pereonites* 2–4 with each a single transverse impressed suture; pereonites 5–6 with each 2 transverse impressed sutures; pereonite 7 with 3 transverse sutures each with a nodulose ridge (Figure 2A). *Pereonite 1 and coxae* 2–3 (Figure 2B) each with posteroventral angle rounded; coxae 5–7 with entire oblique carina. *Pleon* (Figure 2E) with pleonite 1 largely concealed by pereonite 7; posterolateral angles of pleonite 2 forming acute point, extending posteriorly to anterior of pleonite 4; pleonite 3 with a row of 13 small tubercles, posterolateral margins not extending to posterior margin of pleonite 5, rounded; pleonite 4 with median tubercles and 5–6 sublateral tubercles on each side, posterolateral margin of pleonite 4 rounded, clearly extending

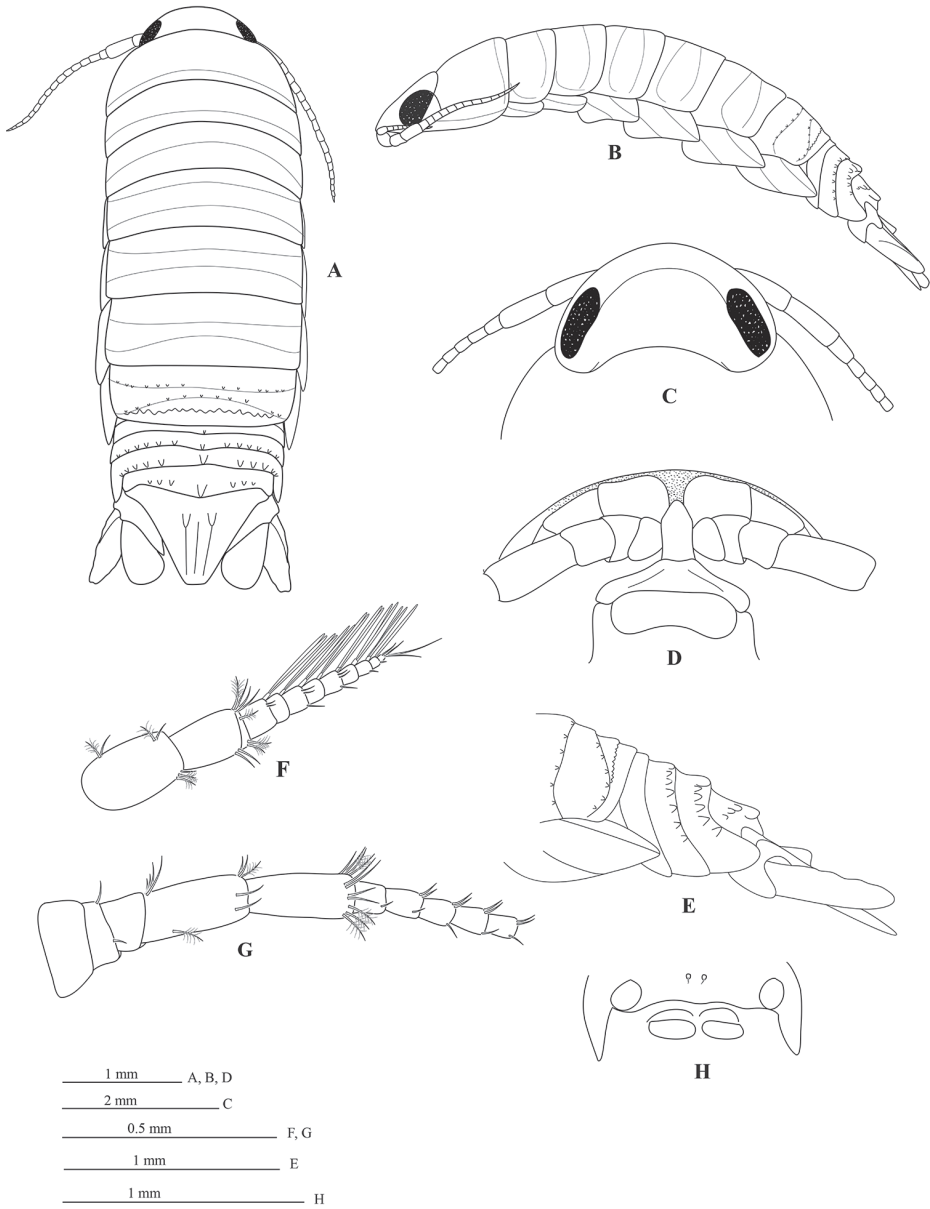


Figure 2. *Cirolana phuketensis* sp. n., male holotype, (PSUZC–CR0286-01) (5.0mm) (**A–E**), male paratype (PSUZC–CR0286-02) (5.1 mm) (**F–G**), male paratype (PSUZC–CR2086-04) (**H**) **A** dorsal view **B** lateral view **C** head **D** frons **E** pleon **F** antennula **G** antenna peduncle **H** penial opening, sternite 7.

beyond posterior margin of pleonite 5; pleonite 5 with prominent median tubercles and 3–4 sublateral tubercles on each side, posterolateral angles overlapped by lateral margins of pleonite 4. *Pleotelson* 0.7 times as long as anterior width, dorsal surface with 2 tubercles and paired submedian longitudinal carina; lateral margins weakly concave,

margins serrate, posterior margin evenly rounded, without median point, with 6 robust setae interspersed among 10 slender plumose setae as figured (Figure 6C, D).

Antennula (Figure 2F) peduncle articles 1 and 2 entirely fused; articles 3 and 4 0.8 times as long as combined lengths of articles 1 and 2; article 3 1.6 times as long as wide, flagellum with 9 articles, antennula extending to anterior margin of pereonite 1.

Antenna (Figure 2G) peduncle article 4 2.2 times as long as wide, 2.4 times as long as article 3, inferior margin with 1 plumose setae, inferodistal margin 1 short simple setae; article 5 1.0 times as long as article 4, 2.4 times as long as wide, inferodistal angle with cluster of 3 pappose setae, anterodistal angle with cluster of 4 short simple setae and 2 plumose setae; flagellum with 16 articles, extending to middle of pereonite 4.

Frontal lamina (Figure 2D) pentagonal, lateral margins concave, anterior margin with narrowly round apex.

Mandible molar process (Figure 3A, C) anterior margin with 12 flat teeth; without proximal cluster of long simple setae; right mandible spine row composed of 8 spines, left with 7 spines; palp articles 2 with 14 distolateral setae; palp article 3 with 17 robust biserrate setae (Figure 3B); *Maxillula* (Figure 3E) mesial lobe with 3 large and circumplumose RS; lateral lobe with 12 RS (plus 1 slender seta). *Maxilla* (Figure 3D) lateral lobe with 5 long simple setae, middle lobe with 12 long simple setae, maxilla mesial lobe with 1 distal simple seta and 12 proximal simple and plumose setae. *Maxilliped palp* (Figure 3F) article 2 mesial margin with 5 slender setae, lateral margin distally with 1 slender setae; article 3 mesial margin with 12 slender setae, lateral margin with 5 slender setae; article 4 mesial margin with 15 slender setae, lateral margin with 3 slender setae; article 5 distal margin 16 setae, lateral margin with 4 setae; maxilliped endite with 5 long CPS and 2 coupling setae (both left and right).

Pereopod 1 (Figure 4A, B) basis 2.0 times as long as greatest width, inferodistal angle with cluster of 2 acute setae; ischium 0.6 times as long as basis, inferior margin with 2 setae, superior distal margin with 2 RS; *merus* inferior margin with 6 molariform RS (set in row of 5 and 2), superior distal angle with 3 setae; *carpus* inferior margin with 1 RS (plus 1 slender seta); *propodus* 1.8 times as long as wide, inferior margin with 2 RS; *dactylus* (Figure 4C) 0.7 times as long as propodus; inferior margin lacking setal fringe. *Pereopod 2* (Figure 4D) *ischium* inferior margin with 2 stout, bluntly rounded RS, superior distal margin with 2 RS; *merus* inferior margin with 4 stout RS (set in row 3 and 1), superior distal margin with 3 acute RS; *carpus* inferodistal angle with 2 RS (plus 1 slender seta); *propodus* 2.3 times as long as wide, with 3 cluster of acute RS; *dactylus* 1.3 times as long as propodus. *Pereopod 3* similar to pereopod 2. *Pereopod 4* (Figure 4E) intermediate in form between pereopod 3 and pereopod 5. *Pereopod 6* similar to pereopod 7. *Pereopod 7* (Figure 4F) *basis* 2.0 times as long as greatest width, superior margin convex, inferior margin with 3 palmate setae; *ischium* 0.6 times as long as basis, inferior margin with 7 RS (set in group 3 and 4), superior distal angle with 5 RS, inferior distal angle with 4 RS; *merus* 0.8 time as long as ischium, 1.5 times as long as wide, inferior margin with 3 RS, superior distal angle with 9 RS, inferior distal angle with 7 RS; *carpus* 0.8 time as long as ischium, 1.5 times as long as wide, inferior margin with 2 RS,

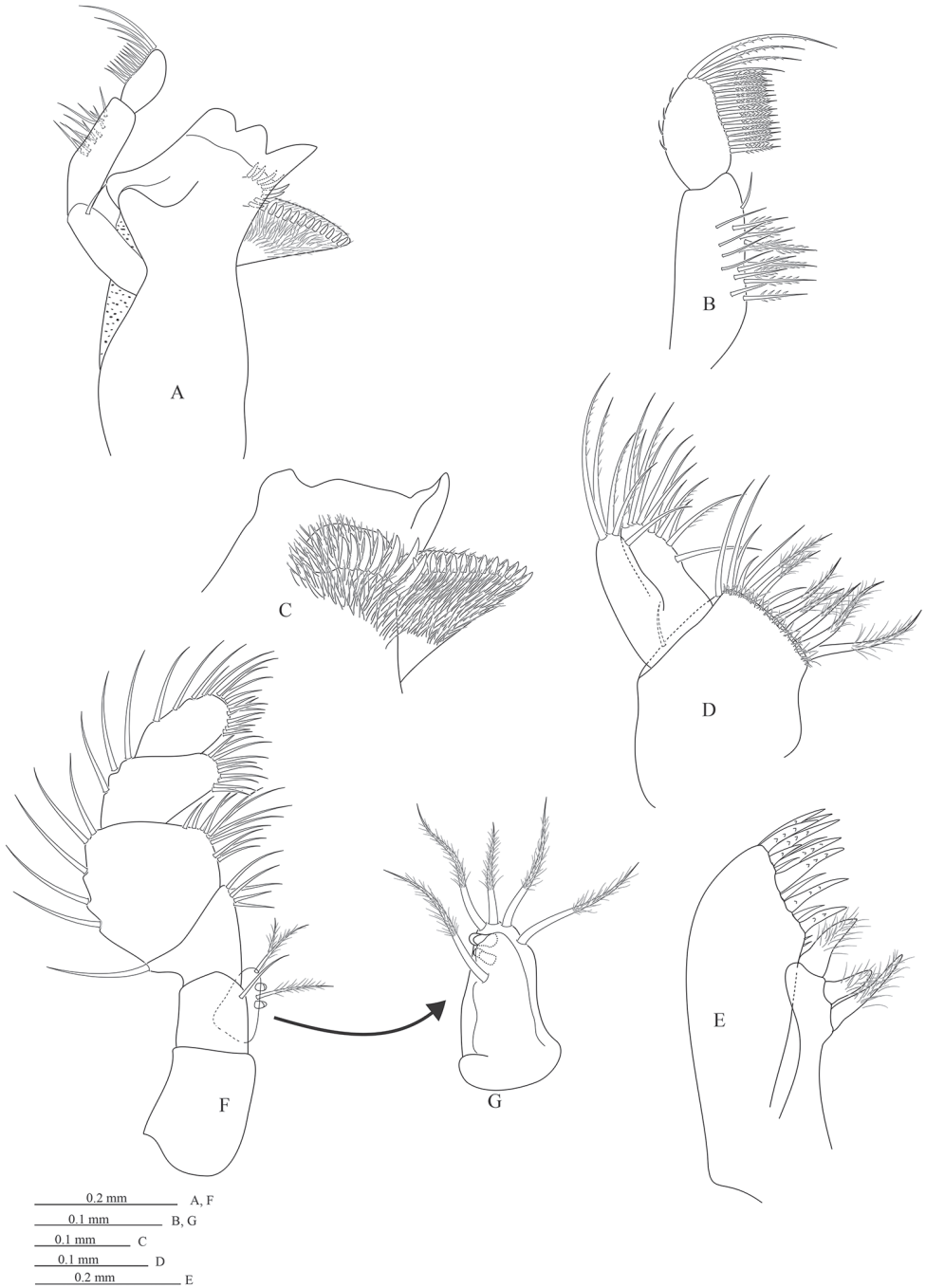


Figure 3. *Cirolana phuketensis* sp. n., male paratype (PSUZC–CR0286-02) (5.1 mm) **A** right mandible **B** dorsal view of article 3 of right mandible palp **C** distal part of left mandible **D** right maxilla **E** right maxillula **F** right maxilliped **G** endite.

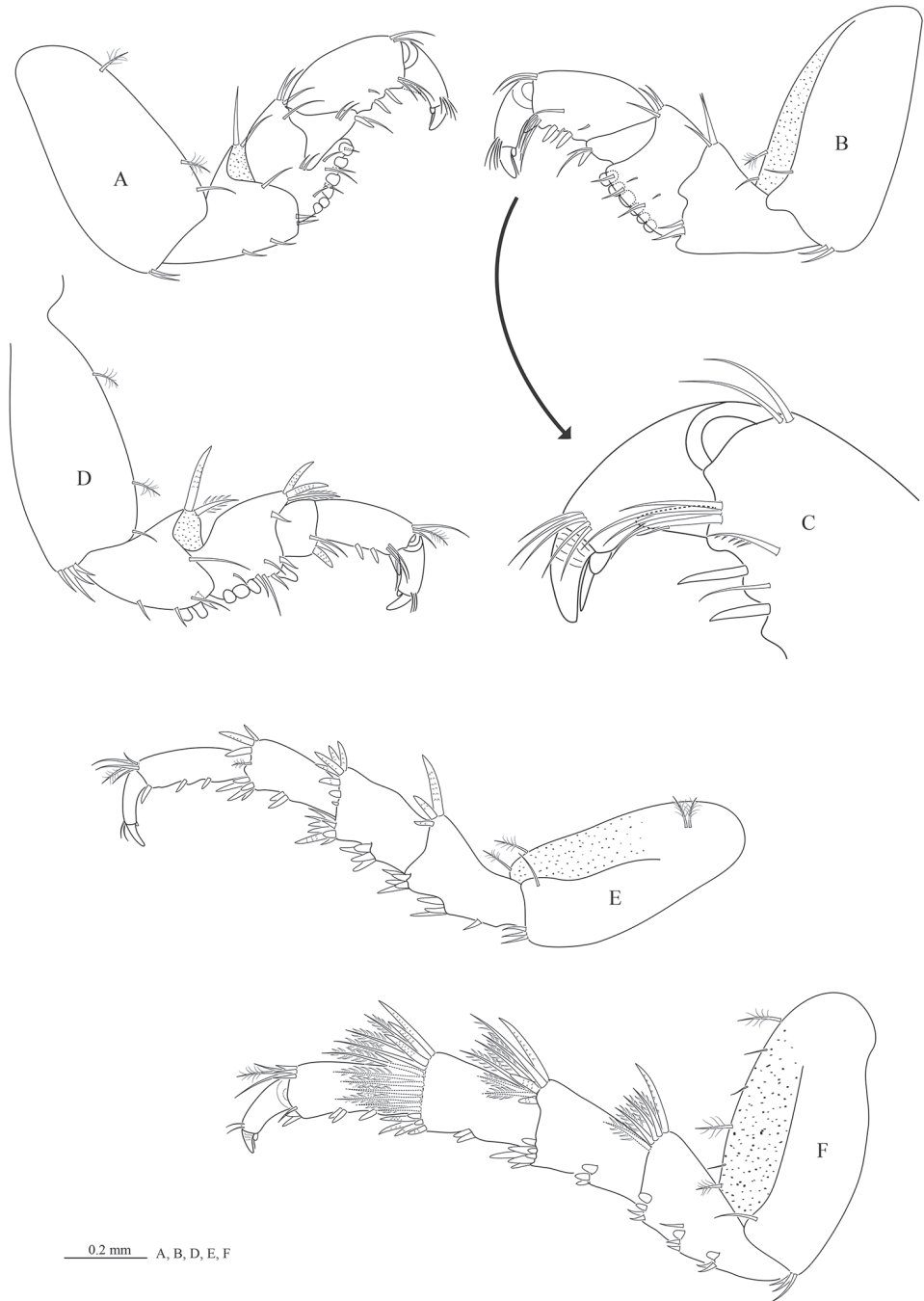


Figure 4. *Cirolana phuketensis* sp. n., male paratype (PSUZC–CR0286-02) (5.1 mm) **A** pereopod 1 **B** mesial view of pereopod 1 **C** mesial view of dactylus of pereopod 1 **D** pereopod 2 **E** pereopod 4 **F** pereopod 7.

superior distal angle with 17 RS, inferior distal angle with 10 RS; *propodus* 0.8 times as long as ischium, 2.3 times as long as wide, inferior margin with 3 clusters of RS (set in group 1 and 2), superior distal angle with 2 slender setae (plus 1 plumose seta and 3RS), inferior distal angle with 2 robust setae; *dactylus* 0.6 times as long as propodus.

Penes (Figure 2H) two low tubercles separated by 3% of sternal width.

Pleopod 1 (Figure 5A) exopod 1.4 times as long as wide, lateral margin straight, distally broadly rounded, mesial margin strongly convex, with 28 PMS from distal one-third; endopod 2.1 times as long as wide, distally broadly rounded, lateral margin strongly concave, with 15 PMS on distal margin only; peduncle 1.6 times as wide as long, mesial margin with 4 coupling hook. *Pleopod 2* (Figure 5B) exopod with 38 PMS, endopod with 14 PMS; appendix masculina with parallel margins, 1.0 times as long as endopod, distally narrowly rounded. *Pleopod 3* (Figure 5C) exopod with 39 PMS, endopod with 11 PMS. *Pleopod 4* (Figure 5D) exopod with 40 PMS, endopod with 10 PMS. *Pleopod 5* (Figure 5E) exopod with 38 PMS. *Pleopods 2–5* peduncle distolateral margin with prominent acute RS.

Uropod peduncle (Figure 6A) ventrolateral margin with 2 RS (Figure 6B), lateral margin with medial short acute RS, posterior lobe about one-half as long as endopod; rami extending beyond pleotelson, marginal setae in single tier. *Endopod* apically not bifid, broadly round, lateral margin straight, without prominent excision, with 2 RS, mesial margin strongly convex, with 7 RS. *Exopod* extending beyond end of endopod, 2.4 times as long as greatest width, apically not bifid, notched, lateral margin straight, with 5 RS, mesial margin weakly convex, with 4 RS.

Female (non-ovigerous). Pereonite 7 without transverse row of tubercles. Pleonites 4–5 and pleotelson with low tubercles.

Size. Adult males (n = 13) 4.6–5.8 mm (mean 5.1 mm); females (n = 16) 4.6–5.7 mm (mean 5.1 mm).

Variation. Pleotelson (n = 28 [12 ♂ and 16 ♀]) with 5–6 RS, with 6 RS (3+3) most frequent (92%). Uropod endopod mesial margin with 6–7 RS, with 6 (82%) and 8 (4%) occurring only once, lateral margin with 1 RS (96%) and 2 (4%) occurring only once; exopod mesial margin with 2–4 RS, with 4 most frequent (92%), 2 and 3 occurring only once (3%), lateral margin with 5–6 RS, with 5 most frequent (92%).

Remarks. *Cirolana phuketensis* sp. n. is characterized by pereonites 2–4 each with a single transverse suture; pereonites 5–6 each with 2 transverse sutures; pereonites 7 with 3 transverse sutures that also form a nodulose ridge; antennula peduncular articles 1 and 2 fused; pleotelson dorsal surface with 2 sub-median longitudinal carinae, each of which has one prominent anterior tubercle, lateral margin weakly convex and posterior margin narrow rounded; pereopod 1 merus inferior margin with 6 molariform RS; penes in the form of two low tubercles.

Cirolana phuketensis sp. n. belongs to a group of species within *Cirolana* that is characterised by dorsal is characterised by dorsal nodular ornamentation on the pereon, pleon and pleotelson (Bruce 1986). This group of species has few widely separated robust setae on the uropodal exopod lateral margin, and the pleotelson posterior mar-

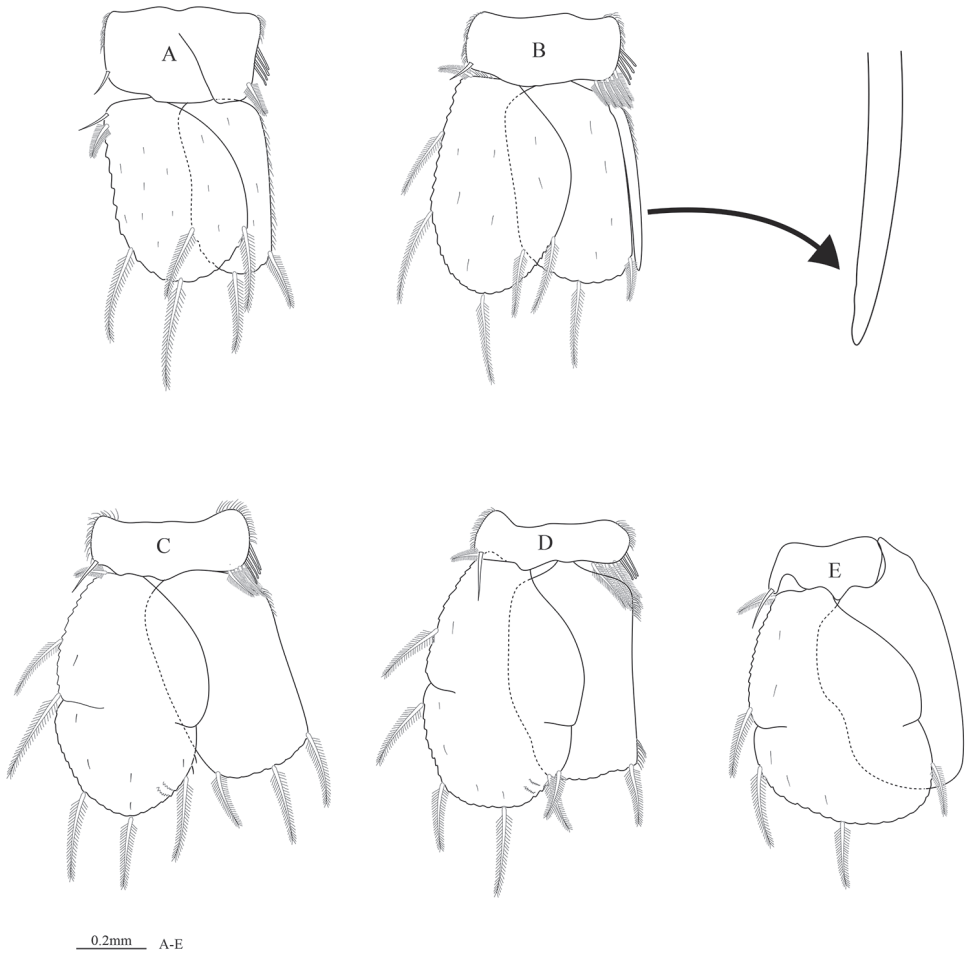


Figure 5. *Cirolana phuketensis* sp. n., male paratype (PSUZC-CR0286-02) (5.1 mm) (A–E) pleopods 1–5 respectively.

gin is truncate to narrowly rounded and has 6 or 8 robust seta; there is often clear sexual dimorphism in this group of species, with females more weakly ornamented than males, and dimorphic uropod shape.

In the South-East Asian region there are few similar species, although undescribed species are known. *Cirolana phuketensis* sp. n. differs from *C. tuberculata* from southern Philippines (see Delaney 1986), the only similar species in the region, by the pereon surface having tubercles on pereonite 7 (vs all pereonites lacking tubercles); coxae 4–7 with two oblique carinae (vs coxae 2–7 with single oblique carina); merus of pereopod 1 has 6 molariform robust setae (vs 4–5 molariform robust setae); pleonites 3–5

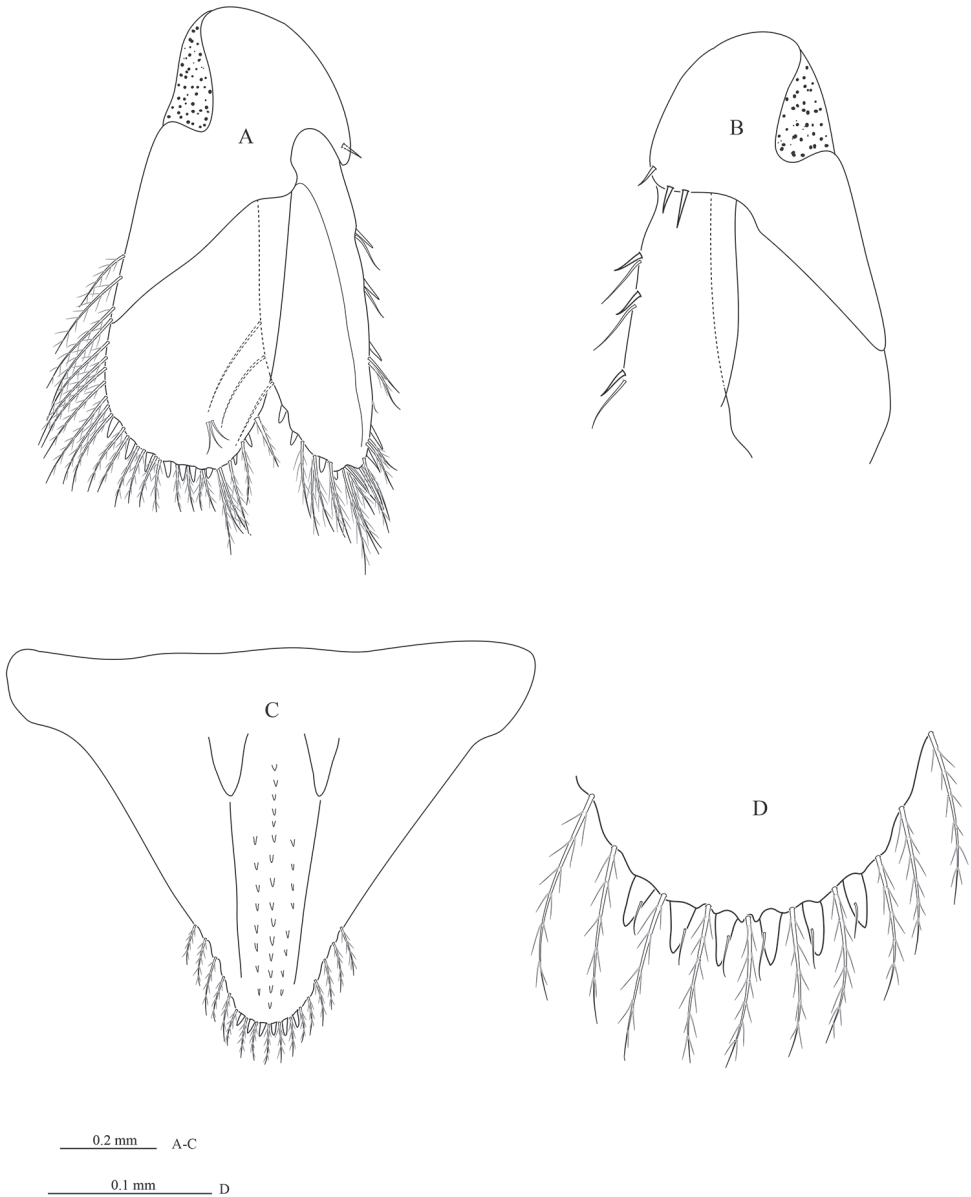


Figure 6. *Cirolana phuketensis* sp. n., male paratype (PSUZC–CR0286-02) (5.1 mm) **A** uropod **B** ventral view of uropod peduncle and exopod **C** pleotelson **D** pleotelson apex.

has tubercles (vs pleon smooth): uropodal exopod apex is notched (vs acute), lateral margin of exopod is straight (vs convex); lateral margin of endopod has two robust setae (vs four robust setae); dorsal surface of pleotelson with two tubercles and paired submedian longitudinal carina (vs parallel rows of four tubercles).

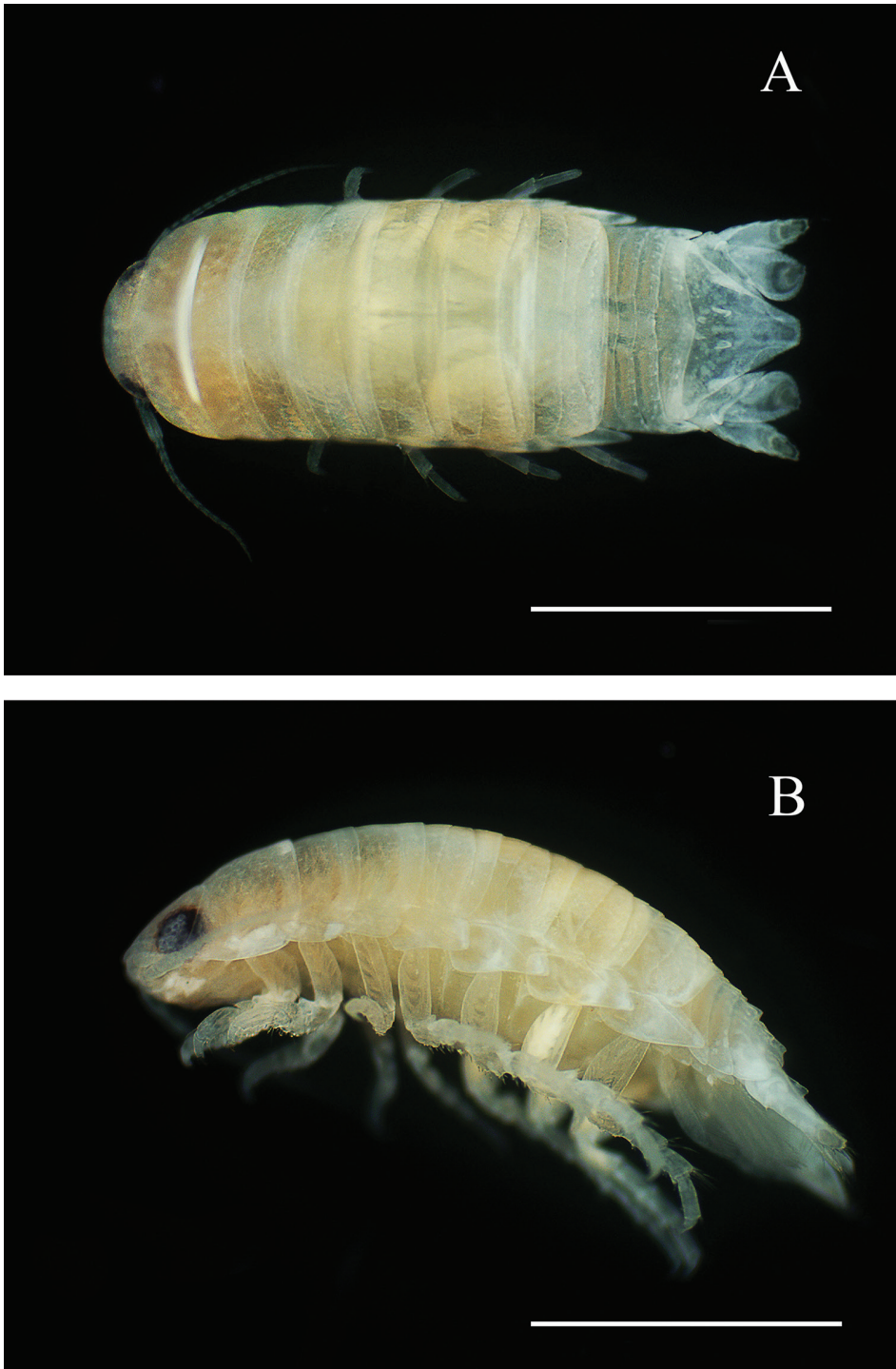


Figure 7. *Cirolana phuketensis* sp. n. male holotype, (PSUZC–CR0286-01) (5.0mm) **A** dorsal view **B** lateral view. Scale bar: 2 mm.

This species is also similar to *Cirolana grumula* Bruce, 1994 (Papua New Guinea) and the Australian species *Cirolana oreonota* Bruce, 1986. However, there are many characters that differentiate *Cirolana phuketensis* sp. n. from these species. *Cirolana phuketensis* sp. n. can be separated from *C. grumula* by having antennula articles 1 and 2 fused (vs unfused in *C. grumula*); pleotelson dorsal surface with 2 sub-median longitudinal carinae, each of which has one prominent tubercle (vs each of which has two prominent tubercles), pleotelson lateral margin weakly convex (vs straight) and posterior margin narrow rounded (vs subtruncate); pereopod 1 merus inferior margin has 6 molariform RS (vs 5 molariform RS); penes has 2 low tubercles (vs opening flush with surface of sternite 7). *Cirolana phuketensis* sp. n. differs from *C. oreonota* by pereonites 2–4 with transverse sutures (vs without transverse sutures on pereonites 2–4); pleotelson dorsal surface with two prominent ridges each with one anterior submedian tubercle (vs ridges not prominent each with 3 of submedian tubercles), pleotelson lateral margin weakly convex (vs straight), posterior margin narrow rounded (vs subtruncate) with 6 RS (vs 8 RS); antennal flagellum extending to middle of pereonite 4 (vs extending to anterior of pereonite 3); pereopod 1 merus inferior margin having 6 molariform RS (vs 5 molariform RS); penes 2 low tubercles (vs opening flush with surface of sternite 7).

Etymology. The epithet is taken from the type locality.

Key to the species of *Cirolana* in Thailand

- 1 Epimera of pleonites 3 and 4 not produced and medially indented..... *C. rachanoi*
- Epimera of pleonites 3 and 4 produced and medially not indented..... 2
- 2 Body dorsal surfaces without tubercles; rostral point present, folded ventrally and posteriorly, in contact with frontal lamina; uropodal rami apically bifid 3
- Body dorsal surfaces with tubercles; anterior margin of head with or without rostral point; uropodal rami apically not bifid..... 7
- 3 Posterior margin of pleotelson with 12–14 RS; endopod of pleopods 3–4 distinctly smaller than exopod, without marginal plumose setae *C. songkhla*
- Posterior margin of pleotelson with 6–10 RS; endopod of pleopods 3–4 about equal to or slightly smaller than exopod, with marginal plumose setae 4
- 4 Antennula peduncle with articles 1 and 2 fused; male pereopod 1 without setal fringe; penial opening separated by 3% of sternal width; uropod peduncle ventrolateral margin with 1 sensory seta..... *C. andamanensis*
- Antennula peduncle with 4 unfused articles; male pereopod 1 with setal fringe; penial opening separated by 12–13% of sternal width; uropod peduncle ventrolateral margin with 3 sensory setae..... 5

- 5 Pleonite 3 with posterolateral margins extending to but not beyond posterior margin of pleonite 5; pleopod 1 endopod with lateral margin concave, appendix masculina 1.4 times as long as pleopod endopod *C. phangnga* 6
- Pleonite 3 with posterolateral margins extending clearly beyond posterior margins of pleonites 4 and 5; pleopod 1 endopod with lateral margin straight, appendix masculina ≤ 1.6 times as long as pleopod endopod..... 6
- 6 Uropodal rami apices equally bifid; appendix masculina lateral curved , 1.6 times as long as pleopod endopod..... *C. siamensis*
- Uropodal rami apices with lateral process prominent; appendix masculina straight, 1.9 times as long as pleopod endopod *C. thailandica*
- 7 Endopod of pleopods 3–4 distinctly smaller than exopod, without marginal plumose setae; found in brackish water habitats 8
- Endopod of pleopods 3–4 with marginal plumose setae; about equal to or slightly smaller than exopod; found in marine habitats 9
- 8 Anterior margin of head without rostral point; frontal lamina anterior margin rounded *C. fluviatilis*
- Anterior margin of head with rostral point, folded ventrally and posteriorly, in contact with frontal lamina; frontal lamina pentagonal..... *C. willeyi*
- 9 Head weakly produced and overriding the antennules/a bases; inferior margins of pereopods 6 and 7 serrate *C. bruscai*
- Head not produced and overriding the antennules/a bases; inferior margins of pereopods 6 and 7 not serrated *C. phuketensis* sp. n.

Acknowledgements

The first author would like to thank Dr. Bongkot Wichachucherd Department of Science, Faculty of Liberal Arts and Science, Kasetsart University, Kamphaeng Saen Campus, for helping to collect the samples. We are grateful to the Department of Aquatic Science and Department of Biology, Prince of Songkla University for access to the laboratory facilities. This work was financed through the Higher Education Research Promotion and National Research University Project of Thailand, Office of the Higher Education Commission, Prince of Songkla University. This is contribution number 195 from the NWU-Water Research Group.

References

- Ariyama H, Angsupanich S, Rodcharoen E (2010) Two New Species of the Genus Kamaka (Crustacea: Amphipoda: Kamakidae) from Songkhla Lagoon, Southern Thailand. *Zootaxa* 2404: 55–68.
- Barnard KH (1936) Isopods collected by the R.I.M.S. “Investigator”. *Records of the Indian Museum* 38(2): 147–191.

- Brandt A, Poore GCB (2003) Higher classification of the flabelliferan and related Isopoda based on a reappraisal of relationships. *Invertebrate Systematics* 17(6): 893–923. <https://doi.org/10.1071/IS02032>
- Briggs JC (2000) Centrifugal speciation and centres of origin. *Journal of Biogeography* 27: 1183–1188. <https://doi.org/10.1046/j.1365-2699.2000.00459.x>
- Briggs JC (2005) The marine East Indies: diversity and speciation. *Journal of Biogeography* 32: 1517–1522. <https://doi.org/10.1111/j.1365-2699.2005.01266.x>
- Briggs JC, Bowen BW (2013) Marine shelf habitat: biogeography and evolution. *Journal of Biogeography* 40: 1023–1035. <https://doi.org/10.1111/jbi.12082>
- Bruce NL (1981) Cirolanidae (Crustacea: Isopoda) of Australia: Diagnoses of *Cirolana* Leach, *Metacirolana* Nierstrasz, *Neocirolana* Hale, *Anopsilana* Paulian & Deboutville, and three new genera—*Natatolana*, *Politolana* and *Cartetolana*. *Australian Journal of Marine and Freshwater Research* 32: 945–966. <https://doi.org/10.1071/MF9810945>
- Bruce NL (1986) Cirolanidae (Crustacea: Isopoda) of Australia. Records of the Australian Museum, Supplement 6: 1–239. <https://doi.org/10.3853/j.0812-7387.6.1986.98>
- Bruce NL (1994) *Cirolana* and related marine isopod crustacean genera (family Cirolanidae) from the coral reefs of Madang, Papua New Guinea. *Cahiers de Biologie Marine* 35: 375–413.
- Bruce NL (2004a) New species of the *Cirolana* “parva-group” (Crustacea: Isopoda: Cirolanidae) from coastal habitats around New Zealand. *Species Diversity* 9: 47–66.
- Bruce NL (2004b) *Cirolana mercuryi* sp. nov., a distinctive cirolanid isopod (Flabellifera) from the corals reefs of Zanzibar, East Africa. *Crustaceana* 76(9): 1071–1081. <https://doi.org/10.1163/156854003322753420>
- Bruce NL, Berggren M, Bussawarit S (Eds) (2002) Proceedings of the International Workshop on the Crustacea in the Andaman Sea, Phuket Marine Biological Center, 29 November–20 December 1998. Phuket Marine Biology Center, Phuket, 532 pp.
- Bruce NL, Brandt A (2006) A new species of *Cirolana* Leach, 1818 (Crustacea, Isopoda, Cirolanidae) from the western Ross Sea, Antarctica, the first record of the genus from polar waters, *Zoosystema* 28(2): 315–324.
- Bruce NL, Olesen J (2002) Cirolanid Isopods from The Andaman Sea off Phuket, Thailand, with description of two new species. In: Bruce NL, Berggren M, Bussawarit S (Eds) Proceedings of the International Workshop on the Crustacea in the Andaman Sea, Phuket Marine Biological Center, 29 November–20 December 1998, Phuket Marine Biological Center Special Publication, 23, Phuket Marine Biological Center, Phuket, 109–131.
- Bruce NL, Schotte M (2015) Cirolanidae. In: Schotte M, Boyko CB, Bruce NL, Poore GCB, Taiti S, Wilson GDF (Eds) World marine, freshwater and terrestrial isopod crustaceans database at <http://www.marinespecies.org/aphia.php?p=taxdetails&id=118399>
- Bruce NL, Wong HPS (2015) An overview of the marine Isopoda (Crustacea) of Singapore. *Raffles Bulletin of Zoology*, Supplement 31: 1–17.
- Brusca RC, Wetzer R, France SC (1995) Cirolanidae (Crustacea: Isopoda: Flabellifera) of the Tropical Eastern Pacific. *Proceedings of the San Diego Natural History Museum* 30: 1–96.
- Carpenter KE, Barber PH, Crandall ED, Ablan-Lagma MA, Ambariyanto G, Ngurah Mahardika G, Manjaji-Matsumoto BM, Juinio-Menes MA, Santos MD, Starger CJ, Toha AHA (2011)

- Comparative Phylogeography of the Coral Triangle and Implications for Marine Management, *Journal of Marine Biology* 2011: 1–14. <https://doi.org/10.1155/2011/396982>
- Coleman CO, Lowry JK, Macfarlane T (2010) DELTA for beginners. An introduction into the taxonomy software package DELTA. *Zookeys* 45: 1–75. <https://doi.org/10.3897/zookeys.45.263>
- Dallwitz MJ (1980) A general system for coding taxonomic descriptions. *Taxon*, 20: 41–46. <https://doi.org/10.2307/1219595>
- Dallwitz MJ, Paine TA, Zurcher EJ (2006) User's guide to the DELTA system: a general system for processing taxonomic descriptions. Available from: <http://delta-intkey.com/> [accessed 15 October 2015]
- Dallwitz MJ, Paine TA, Zurcher EJ (1997) User's guide to the DELTA system. A general system for processing taxonomic descriptions. CSIRO Division of Entomology, Canberra.
- Delaney PM (1986) The Synonymy of *Cirolana tuberculata* (Richardson, 1910) (Isopoda, Flabellifera, Cirolanidae). *Proceedings of the Biological Society of Washington* 99(4): 731–734.
- Keable SJ (1995) Structure of the marine invertebrate scavenging guild of a tropical reef ecosystem: field studies at Lizard Island, Queensland, Australia. *Journal of Natural History* 29: 27–45. <https://doi.org/10.1080/00222939500770021>
- Kensley B, Schotte M (1989) Guide to the marine isopod crustaceans of the Caribbean. Smithsonian Institution Press. Washington, DC and London.
- Kensley B (2001) Biogeography of the marine Isopoda of the Indian Ocean, with a check-list of species and records. In: Kensley B, Brusca RC (Eds) *Isopod systematics and evolution*. *Crustacean Issues* 13: 205–264.
- Leach WE (1818) Cymothoadés. In: Cuvier F (Ed) *Dictionnaire des sciences naturelles*. Paris and Strasbourg 12: 338–354.
- Richardson H (1910) Marine isopods collected in the Philippines by the U.S. Fisheries steamer *Albatross* in 1907–8. Washington D.C. Department of Commerce Bureau of Fisheries. Document No. 736.
- Rodcharoen E, Bruce NL, Pholpunthin P (2014) *Cirolana songkhla*, a new species of brackish-water cirolanid isopod (Crustacea, Isopoda, Cirolanidae) from the lower Gulf of Thailand. *ZooKeys* 375: 1–14. <https://doi.org/10.3897/zookeys.375.6573>
- Rodcharoen E, Bruce NL, Pholpunthin P (2016) Description of four new species of the *Cirolana* 'parva group' (Crustacea: Isopoda: Cirolanidae) from Thailand, with supporting molecular (COI) data. *Journal of Natural History* 50 (NOS31-32): 1935–1981 <https://doi.org/10.1080/00222933.2016.1180718>
- Sidabalok CM (2013) List of marine isopods recorded from Indonesian waters. *Marine Research in Indonesia* 38(1): 49–66. <https://doi.org/10.14203/mri.v38i1.56>
- Sidabalok C, Bruce NL (2015) Revision of the cirolanid isopod genus *Odyssseylana* Malyutina, 1995 (Crustacea) with description of two new species from Singapore. *Zootaxa* 4021(2): 351–367. <https://doi.org/10.11646/zootaxa.4021.2.6>
- Sidabalok CM, Bruce NL (2016) Redescription of three cirolanid isopods (Crustacea: Peracarida) from Indonesia. *Zootaxa* 414(3): 277–290. <https://doi.org/10.11646/zootaxa.414.3.4>
- Sidabalok C, Bruce NL (2017a) Review of the species of the *Cirolana* 'parva-group' (Cirolanidae: Isopoda: Crustacea) in Indonesian and Singaporean waters *Zootaxa* [in press].

- Sidabalok C, Bruce NL (2017b) Review of the *Cirolana* 'pleonastica-group' (Crustacea: Isopoda: Cirolanidae) with description of four new species from the Indo-Malaysian region. Raffles Bulletin of Zoology [submitted].
- Sidabalok C, Bruce NL (2017c) *Cirolana bambang*, a distinctive new species of *Cirolana* Leach, 1818 (Cirolanidae: Isopoda: Crustacea) from Bitung, Indonesia. Zootaxa xxx(submitted).
- Suvatti C (1967) Fauna of Thailand (2nded.). Applied Scientific Research Corporation of Thailand, Bangkok, 143–17.
- Svavarsson J (2002) Gnathiidae (Crustacea, Isopoda) from the Andaman Sea, Thailand: new records and a new species. Phuket Marine Biological Center Special Publication 23(1): 149–156.
- Svavarsson J, Gísladóttir E (2002) *Elaphognathia korachaensis* sp. nov., a new gnathiid species (Crustacea, Isopoda) from Thailand. Phuket Marine Biological Center Special Publication 23(1): 157–164.
- Wongkamhaeng K, Coleman CO, Azman BAR (2013) *Maeropsis paphavasitae* and *Rotomelita longipropoda*, two new species (Crustacea, Amphipoda) from Lower Gulf of Thailand. ZooKeys 307: 15–33 (2013). <https://doi.org/10.3897/zookeys.307.5273>
- Wongkamhaeng K, Azman BAR, Puttapreecha R (2012a). *Cheiriphotis trifurcata*, new species (Crustacea, Amphipoda, Corophiidae, Protomedeiinae) from the Seagrass Bed of the Lower Gulf of Thailand. ZooKeys 187: 71–89. <https://doi.org/10.3897/zookeys.187.3219>
- Wongkamhaeng K, Pattaratumrong MS, Puttapreecha R (2014) Melitid amphipods from the Gulf of Thailand, with a description of *Dulichella pattaniensis*, a new species. ZooKeys 408: 1–18. <https://doi.org/10.3897/zookeys.408.7292>
- Wongkamhaeng K, Pholpunthin P, Azman BAR (2012b). *Grandidierella Halophilus* a new species of the family Aoridae (Crustacea: Amphipoda) from the salt pans of The Inner Gulf of Thailand. The Raffles Bulletin of Zoology 60(2): 433–447.

Taxonomic study of the genus *Neocarpia* Tsaur & Hsu, with descriptions of two new species from China (Hemiptera, Fulgoromorpha, Cixiidae)

Yan Zhi^{1,2,3}, Lin Yang^{1,2}, Pei Zhang⁴, Xiang-Sheng Chen^{1,2}

1 Institute of Entomology, Guizhou University, Guiyang, Guizhou, 550025, P.R. China **2** The Provincial Special Key Laboratory for Development and Utilization of Insect Resources of Guizhou, Guizhou University, Guiyang, Guizhou, 550025, P.R. China **3** Laboratory Animal Center, Guizhou Medical University, Guiyang, Guizhou 550025, P.R. China **4** Xingyi Normal University for Nationalities, Xingyi, Guizhou, 562400, P.R. China

Corresponding author: Xiang-Sheng Chen (chenxs3218@163.com)

Academic editor: Mike Wilson | Received 20 March 2017 | Accepted 24 July 2017 | Published 4 September 2017

<http://zoobank.org/BD15BA2C-951B-469C-90EB-42839551F9DF>

Citation: Zhi Y, Yang L, Zhang P, Chen X-S (2017) Taxonomic study of the genus *Neocarpia* Tsaur & Hsu, with descriptions of two new species from China (Hemiptera, Fulgoromorpha, Cixiidae). ZooKeys 695: 19–35. <https://doi.org/10.3897/zookeys.695.12809>

Abstract

The cixiid planthoppers genus *Neocarpia* Tsaur & Hsu, 2003 is reviewed. Two new species, *N. acutata* Zhi & Chen, **sp. n.** and *N. reversa* Zhi & Chen, **sp. n.**, are described and illustrated from the southwest of China (Yunnan) to give the genus seven species in total. Female genitalia of four Chinese species are described and illustrated for the first time. A key to all known species of *Neocarpia* based on male genitalia, and a key to Chinese species (except for *N. maai*) based on female genitalia, are provided. The morphological characteristics of the posterior vagina, utilized to distinguish female species of *Neocarpia*, are also discussed.

Keywords

Female genitalia, Fulgoroidea, morphology, Oriental region, taxonomy

Introduction

Tsaur and Hsu (2003) established the cixiid planthopper genus *Neocarpia* with the type species *Neocarpia maai* Tsaur & Hsu, 2003 from China (Taiwan), and placed this genus in the tribe Pintaliini of the subfamily Cixiinae (Hemiptera: Fulgoromorpha: Cixiidae). Later, Emeljanov and Hayashi (2007) described *N. okinawana* from Japan and moved *Neocarpia* to the tribe Eucarpiini according to hind margin of the forewing without any convexity situated between the clavus apex and icu. So far, five species of *Neocarpia* are described, including three from China (Tsaur and Hsu 2003; Emeljanov and Hayashi 2007; Löcker et al. 2010; Zhang and Chen 2013).

Herein, two new species of *Neocarpia* are described and illustrated from Yunnan province, China. Female genitalia of four Chinese species are described and illustrated for the first time. The genus *Neocarpia* now contains seven species, including five from China. A key to species based on male genitalia, and to Chinese species (except for *N. maai*) based on female genitalia, are provided. The morphological characters of the posterior vagina are utilized to distinguish female species of *Neocarpia*.

Materials and methods

The morphological terminology and measurements follow Tsaur et al. (1988) and Löcker et al. (2006) and the morphological terminology of female genitalia follows Bourgoïn (1993). Body length was measured from apex of vertex to tip of forewing; vertex length was measured the median length of vertex (from apical transverse carina to tip of basal emargination). External morphology and drawings were done with the aid of a Leica MZ 12.5 stereomicroscope. Photographs of the types were taken with KEYENCE VHX-1000 system. Illustrations were scanned with CanoScan LiDE 200 and imported into Adobe Photoshop CS7 for labelling and plate composition. The dissected male and female genitalia are preserved in glycerine in small plastic tubes pinned together with the specimens.

The type specimens and other specimens examined are deposited in the Institute of Entomology, Guizhou University, Guiyang, Guizhou Province, China (IEGU).

Taxonomy

Neocarpia Tsaur & Hsu, 2003

Neocarpia Tsaur & Hsu, 2003: 440; Löcker et al. 2010: 17; Zhang and Chen 2013: 42.

Type species. *Neocarpia maai* Tsaur & Hsu, 2003, by original designation.

Emended diagnosis. Head slightly narrower than pronotum in dorsal view. Vertex slightly widened to posterior emargination, broader than long and without subapical carina, lateral carinae moderately elevated. Frons with median carina; frontoclypeal suture generally angled or semicircular. Clypeus with well-developed median carina. Rostrum distinctly surpassing hind coxae. Pronotum short with intermediate carinae curved along posterior margins of eyes. Mesonotum tricarinate. Forewing in resting position steeply tectiform, widened towards apex, with rounded apical margin; Sc+R forming a common stem and M emerging separately from basal cell; MA trifid apically; position of fork Sc+R slightly basad or at the same level as fork CuA1+CuA2; first crossvein MP-CuA1 at least as long as MP from M fork to this crossvein, crossvein MP-CuA1 almost at same level as crossvein r-m, subapical cell MP with upper margin (vein MP) fine concave, no crossvein between CuA1 and CuA2. Apical cells 10. Hind tibia lacking lateral spines.

Male genitalia. Pygofer symmetrical and prolonged with symmetrical lateral lobes in lateral view. Medioventral process thumb-like in lateral view. Anal segment tubular, short and stout. Genital styles relative small and symmetrical. Aedeagus slender and flagellum of aedeagus with spinose processes.

Female genitalia. Ovipositor elongate, orthopteroid and slightly curved upwards; anal segment square or rectangular in dorsal view; 9th tergite without wax plate. Gonapophysis VIII slightly sclerotised, blade-like posteriorly. Gonapophysis IX single, blunt and strongly sclerotised, between middle tooth and apex with a row of denticles. Gonoplac slightly sclerotised, with many spinules on ventral edge in inner lateral view. Posterior vagina with sclerites.

Remarks. This genus may be easily distinguished from other genera of Eucarpiini by the following features: frontoclypeal suture generally angled or semicircular; rostrum distinctly surpassing hind coxae; forewing with ten apical cells, Sc+R forking slightly basad or at same level as fork CuA1+CuA2, first crossvein MP-CuA1 as long as or longer than vein MP from M fork to this veinlet, subapical cell MP with upper margin (vein MP) fine concave, no transverse vein between CuA1 and CuA2, position of first crossvein MP-CuA1 almost at same level as first crossvein r-m (Zhang and Chen 2013).

Distribution. China, Japan, Australia.

Checklist and distributions of species of *Neocarpia* Tsaur & Hsu

- N. acutata* Zhi & Chen, **sp. n.**; China (Yunnan).
- N. bidentata* Zhang & Chen, 2013; China (Guizhou).
- N. hamata* Zhang & Chen, 2013; China (Guizhou, Hubei).
- N. maai* Tsaur & Hsu, 2003; China (Taiwan).
- N. okinawana* Emeljanov & Hayashi, 2007; Japan (Ryukyus).
- N. reversa* Zhi & Chen, **sp. n.**; China (Yunnan).
- N. rhizophorae* Löcker, 2010; Australia (Queensland).

Key to species (males) of *Neocarpia* (revised from Zhang and Chen 2013)

- 1 Ventral margin of periandrium without spinose process 2
 – Ventral margin of periandrium with one or two spinose process(es) 3
 2 Dorsal margin of periandrium with one process; flagellum with two processes near apex and without process at base (Emeljanov and Hayashi 2007: Figs 23–24) *N. okinawana*
 – Dorsal margin of periandrium without process; flagellum with one process near apex and a long process near base (Figs 54–55) *N. reversa* sp. n.
 3 Ventral margin of periandrium with one small triangular process at basal 1/3 ... 4
 – Ventral margin of periandrium without triangular process at base, while with one or two process(es) near or at apex 5
 4 Left side of periandrium with a process near apex, dorsal margin with a shovel-shaped process, right side without process in the middle, base of process near apex of flagellum with two denticulations (Zhang and Chen 2013: Figs 10–11); forewing without stripe *N. bidentata*
 – Left side of periandrium without process, dorsal margin without process, right side with a short acute process in the middle, base of process near apex of flagellum without denticulation (Figs 12–13); forewing with yellow stripes along the Y-veins *N. acutata* sp. n.
 5 Flagellum with a prominent long process in the middle (Löcker et al. 2010: Fig. 17A) *N. rhizophorae*
 – Flagellum without process in the middle 6
 6 Dorsal margin of periandrium with a hook-shaped process, ventral margin of periandrium with one process, flagellum with smooth apical margin (Zhang and Chen 2013: Figs 23–24) *N. hamata*
 – Dorsal margin of periandrium without process, ventral margin of periandrium with two processes, flagellum with sinuate apical margin (Tsaur and Hsu 2003: Fig. 6D) *N. maai*

Key to Chinese species (females) of *Neocarpia* (except for *N. maai*)

- 1 Posterior vagina without long longitudinal sclerite (Figs 41–42) .. *N. hamata*
 – Posterior vagina with a long longitudinal sclerite 2
 2 Long longitudinal sclerite on right side ventrally (Figs 65–66)
 *N. reversa* sp. n.
 – Long longitudinal sclerite on left side ventrally 3
 3 Posterior vagina elongate, left side with two longitudinal sclerites; each side with a small sclerite near terminal in ventral view (Figs 23–24)
 *N. acutata* sp. n.
 – Posterior vagina relatively short, left side with one longitudinal sclerite; posterior vagina with a wide sclerite medially and a small longitudinal sclerite on the left side near terminal in ventral view (Figs 32–33) *N. bidentata*

***Neocarpia acutata* Zhi & Chen, sp. n.**

<http://zoobank.org/2AFE0126-5893-40A6-9044-E19D321F762E>

Figs 1–24

Type material. Holotype: ♂, **China:** Yunnan, Jinping County, Fenshuiling (22°86'N, 103°22'E), 8 June 2013, Liang-Jing Yang; paratypes: 1♂, 3♀♀, same data as holotype, Liang-Jing Yang and Ying-Jian Wang; 1♀, **China:** Yunnan, Pingbian County, Daweishan (22°81'N, 103°79'E), 5 June 2013, Liang-Jing Yang.

Description. Body length: male 4.8–5.0 mm ($N = 2$), female 5.1–5.3 mm ($N = 4$); forewing length: male 4.5–4.8 mm ($N = 2$), female 4.8–5.0 mm ($N = 4$).

Coloration. General color brown (Figs 1–6) (blackish brown in female). Eyes brown, ocelli pale yellow. Vertex generally yellow, carinae brown to dark brown (except median carina milky). Face generally yellow, discal area brown to dark brown. Sub-apical segment of rostrum blackish brown, apical segment brown with dark brownish apex. Pronotum with discal areas and mesonotum with area between lateral carinae yellow, lateral areas brownish black. Forewing semihyaline, brown throughout; yellow stripes along the Y-veins, the triangle area between the Y-veins brownish black. Hind tibiae pale yellow. Ventral abdomen blackish brown.

Head and thorax. Vertex (Figs 1, 3, 5) broad, 3.0 times wider than long; anterior margin slightly produced, posterior margin convexly recessed. Frons widest slightly below the level of antennae, 1.4 times as long as wide; frontoclypeal suture nearly concave into an arch; middle carina complete; lateral carinae distinct and elevated. Pronotum (Figs 1, 3, 5) 3.4 times longer than vertex; median carina indistinct, posterior margin nearly at right angle. Mesonotum 1.6 times longer than pronotum and vertex combined. Forewing (Figs 2, 4, 7) amply exceeding the tip of abdomen, 2.6 times longer than wide, with six subapical cells; fork Sc+RP slightly basad of fork CuA1+CuA2, first crossvein r-m slightly basad of fork MA+MP; RP and MP bifid separately; fork MA1+MA2 basad of fork MP1+MP2. Hind tibia with six apical spines; chaetotaxy of hind tarsi: 7/8.

Male genitalia. Pygofer (Figs 8, 9), dorsal margin shallowly concave and U-shaped ventrally, widened towards apex; in lateral view, lateral lobes triangularly extended caudally. Anal segment (Figs 8, 10), dorsal margin almost straight, ventral margin convex in lateral view, apical margin convex and 1.6 times longer than wide in dorsal view; anal style strap-shaped, not beyond anal segment. Apical margin of genital styles (Figs 8, 11) with a small blunt process, dorsal margin bending inwards in the middle. Aedeagus (Figs 12–15) with five spinose processes. Right side of periandrium with a long and broad process, strongly curving near apex directed ventrocephally and a short acute process curved in the middle directed dorsocephally; ventral margin with a small triangular process at basal 1/3, directed ventrocaudally; flagellum moderately sclerotised, generally curved on left side; left side with a short process basally, curved and directed cephalad, and a straight process at apex directed ventrocephally.

Female genitalia. Pygofer (Figs 16–17, 19) moderately sclerotised, with length almost equal to width in caudal view. Anal tube (Figs 16, 18) short, length longer than wide in dorsal view, ventral margin straight in lateral view; anal styles relatively short



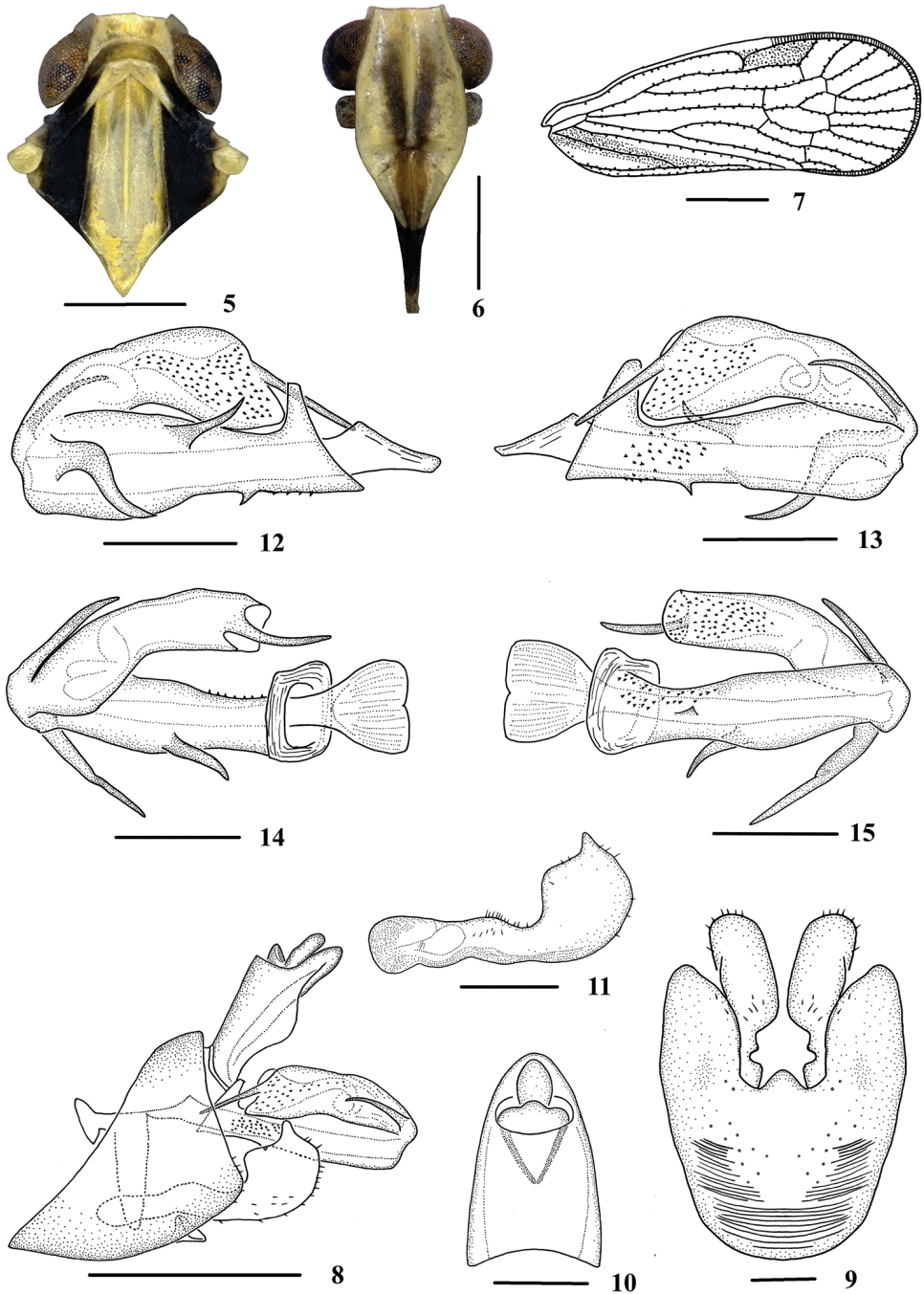
Figures 1–4. *Neocarpia acutata* sp. n. **1** Male, dorsal view **2** Male, lateral view **3** Female, dorsal view **4** Female, lateral view.

and small, apical margin semicircular in dorsal view. Gonapophysis VIII (first valvula) (Fig. 20) elongate, and slightly curved upwards, 2/5 of its inner margin sinuate basally. Gonapophysis IX (second valvula) (Fig. 21), distance ratio between middle tooth to apex and length of denticulate portion is 1.72. Gonoplac (third valvula) (Fig. 22) rod-like, 4.2 times longer than wide, with width of spiculated area less than its 1/10. Posterior vagina (Figs 23–24) elongate, at terminal each lateral side with a sclerite respectively in ventral view; with a large transverse sclerite and several small sclerites in dorsal view; a long longitudinal sclerite in ventral view and a much shorter one in dorsal view on left side basally.

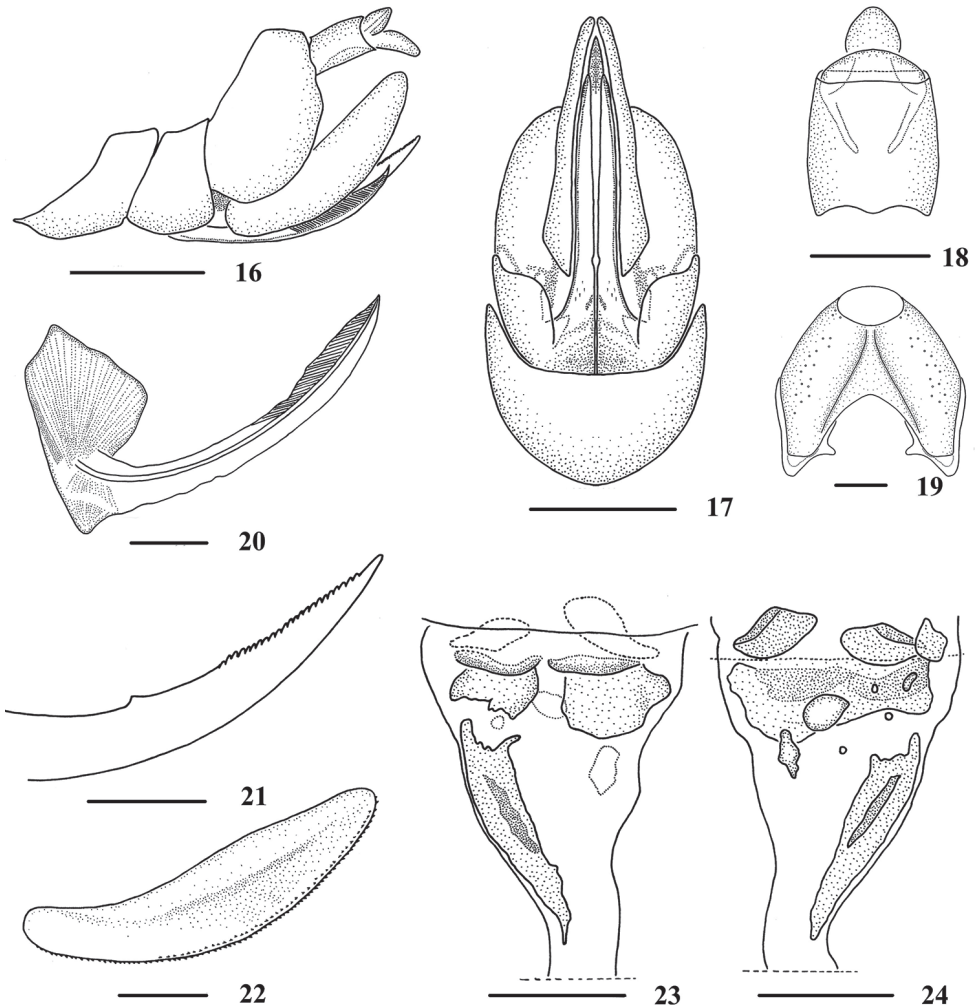
Distribution. China (Yunnan).

Etymology. The specific name is derived from the Latin word “*acutata*”, referring to the right side of periandrium bearing an acute process in the middle near dorsal margin.

Remarks. Male genitalia of *N. acutata* sp. n. is similar to *N. bidentata* Zhang & Chen, 2013, but differs in: (1) right side of periandrium near dorsal margin with a short acute process in the middle curved and directed dorsocephally (in *N. bidentata*, right side without process in the same position); (2) right side of periandrium with a long and broad process strongly curved near apex directed ventrocephally (process on right side of periandrium near apex straight and directed dorsocephally in *N. bidentata*); (3) left side of flagellum with a process basally (in *N. bidentata*, without process in the same position).



Figures 5–15. *Neocarpia acutata* sp. n., male **5** Head and thorax, dorsal view **6** Face, ventral view **7** Forewing **8** Genitalia, lateral view **9** Pygofer and genital styles, ventral view **10** Anal segment, dorsal view **11** Genital styles, inner lateral view **12** Aedeagus, right side **13** Aedeagus, left side **14** Aedeagus, dorsal view **15** Aedeagus, ventral view. Scale bars: 0.5 mm (**5–6, 8**); 1.0 mm (**7**); 0.2 mm (**9–15**).



Figures 16–24. *Neocarpia acutata* sp. n., female **16** Genitalia, lateral view **17** Genitalia, ventral view **18** Anal segment, dorsal view **19** Pygofer, caudal view **20** Gonapophysis VIII and gonocoxa VIII, dorsal view **21** Gonapophysis IX, lateral view **22** Gonoplac, inner lateral view **23** Posterior vagina, ventral view **24** Posterior vagina, dorsal view. Scale bars: 0.5 mm (**16–17**); 0.2 mm (**18–24**).

Female genitalia of *N. acutata* sp. n. is similar to *N. bidentata* Zhang & Chen, 2013, but differs in: (1) posterior vagina elongate, left side with two longitudinal sclerites (in *N. bidentata*, posterior vagina relatively short, left side with one longitudinal sclerite); (2) each side of posterior vagina with a small sclerite near terminal in ventral view (in *N. bidentata*, posterior vagina with a wide sclerite medially and a small longitudinal sclerite on the left side near terminal in ventral view).

***Neocarpia bidentata* Zhang & Chen, 2013**

Figs 25–33

Neocarpia bidentata Zhang & Chen, 2013: 43: figs 1–13; 47: 27–29.

Material examined. 1♂, **China:** Guizhou, Xishui County, Linjiang, 1 June 2006, Xiang-Sheng Chen (Holotype); 3♀♀, same data as holotype (Paratypes); 1♂, **China:** Guizhou, Wangmo County, Dayi, 24 September 1997, Xiang-Sheng Chen (Paratype).

Supplementary description. *Female genitalia.* Pygofer (Figs 25–26, 28) moderately sclerotised, slightly shorter than wide in caudal view. Anal tube (Figs 25, 27) short, slightly longer than wide in dorsal view, ventral margin sinuate in lateral view; anal styles relatively short and small, strap-like. Inner margin of gonapophysis VIII (Fig. 29) concave near base. Gonapophysis IX and gonoplac (Figs 30–31) same as in *N. acutata*, while the width of spiculated area approximately 1/10 of gonoplac, length of gonoplac 4.3 times of its width. Posterior vagina (Figs 32–33) stubby, with a wide sclerite medially and a small longitudinal sclerite on left side near terminal, left side with a long longitudinal sclerite.

Distribution. China (Guizhou).

Remarks. Diagnosis of female see *Neocarpia acutata* Zhi & Chen, sp. n.

Note. The female genitalia of this species is described and illustrated for the first time.

***Neocarpia hamata* Zhang & Chen, 2013**

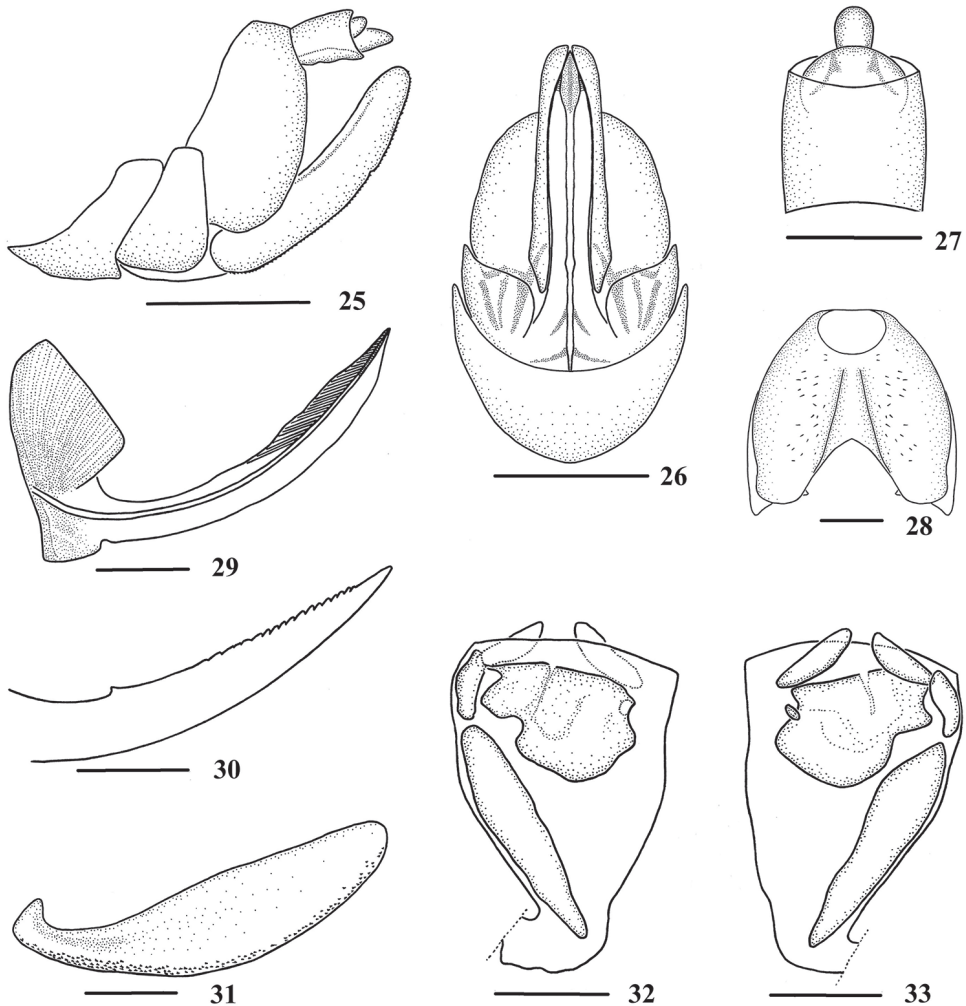
Figs 34–42

Neocarpia hamata Zhang & Chen, 2013: 45: figs 14–26; 47: 30–32.

Material examined. 1♂, **China:** Guizhou, Yanhe County, Daheba, 5–12 June 2007, Pei Zhang (Holotype); 1♀, same data as holotype (Paratype); 3♀♀, **China:** Guizhou, Yanhe County, Lijiaba, 5–12 June 2007, Pei Zhang (Paratypes); 19♂♂, 16♀♀, **China:** Hubei, Luotian County, Qingtaiguan, (31°16'N, 115°69'E), 29 June–3 July 2014, Zhi-Min Chang, Zheng-Xiang Zhou and Mei-Na Guo.

Supplementary description. *Female genitalia.* Pygofer (Figs 34–35, 37) moderately sclerotised, 1.2 times longer than wide in caudal view. Anal tube (Figs 34, 36) short, shorter than wide in dorsal view, ventral margin slightly convex in lateral view; anal styles relatively short and small, strap-like. Gonapophysis VIII and IX and gonoplac (Figs 38–40) same as in *N. acutata*, while width of spiculated area approximately 1/8 of gonoplac, length of gonoplac 4.6 times of its width. Posterior vagina (Figs 41–42) stubby, with a long transverse sclerite near terminal, an irregular sclerite (left edge large and right edge small) and several circular or oval ones in dorsal view, without sclerite near base.

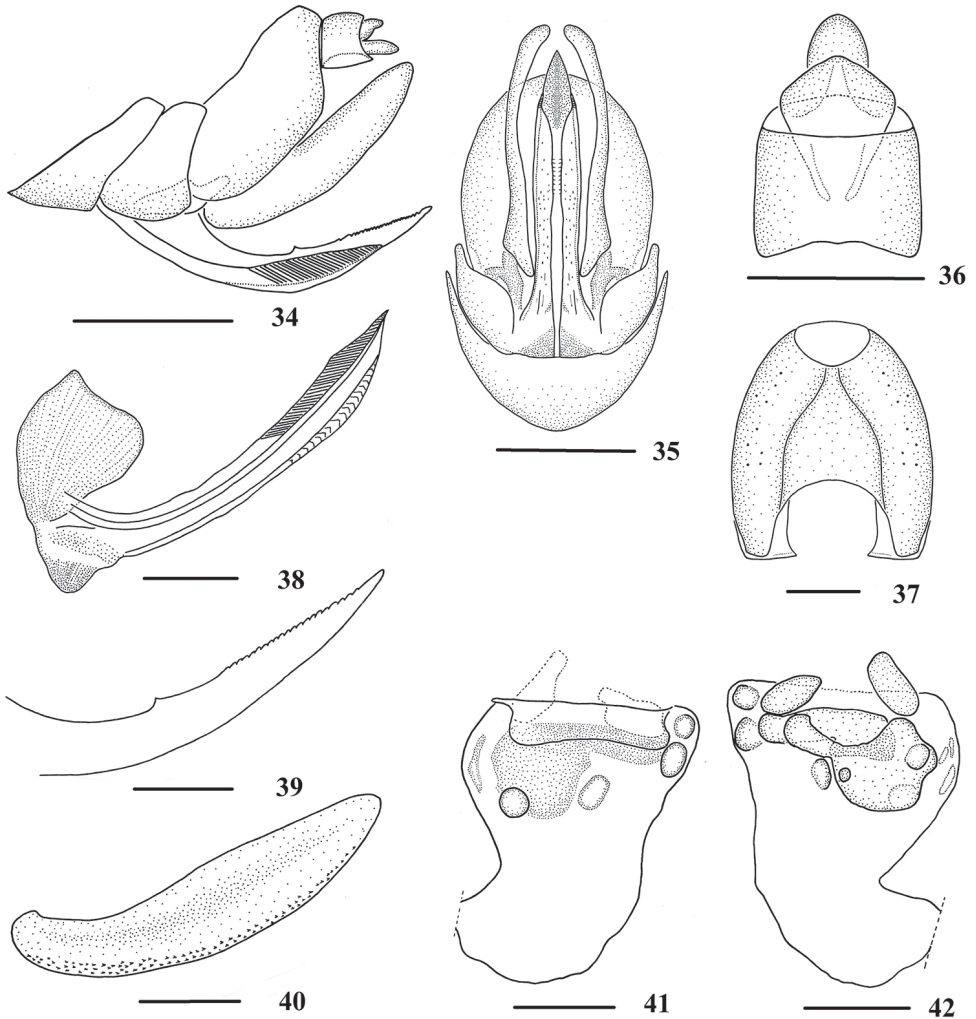
Distribution. China (Guizhou, Hubei).



Figures 25–33. *Neocarpia bidentata* Zhang & Chen, 2013, female **25** Genitalia, lateral view **26** Genitalia, ventral view **27** Anal segment, dorsal view **28** Pygofer, caudal view **29** Gonapophysis VIII and gonocoxa VIII, dorsal view **30** Gonapophysis IX, lateral view **31** Gonoplac, inner lateral view **32** Posterior vagina, ventral view **33** Posterior vagina, dorsal view. Scale bars: 0.5 mm (**25–26**); 0.2 mm (**27–33**).

Remarks. Female of *N. hamata* is similar to *N. acutata* sp. n., but differs in: (1) posterior vagina without sclerite near base (posterior vagina with two longitudinal sclerites near base in *N. acutata*); (2) anal tube shorter than wide in dorsal view (in *N. acutata*, anal tube longer than wide in dorsal view).

Note. The female genitalia of this species is described and illustrated for the first time.



Figures 34–42. *Neocarpia hamata* Zhang & Chen, 2013, female **34** Genitalia, lateral view **35** Genitalia, ventral view **36** Anal segment, dorsal view **37** Pygofer, caudal view **38** Gonapophysis VIII and gonocoxa VIII, dorsal view **39** Gonapophysis IX, lateral view **40** Gonoplac, inner lateral view **41** Posterior vagina, ventral view **42** Posterior vagina, dorsal view. Scale bars: 0.5 mm (**34–35**); 0.2 mm (**36–42**).

Neocarpia maai Tsaour & Hsu, 2003

Neocarpia maai Tsaour & Hsu, 2003: 441: fig. 6A–H.

Distribution. China (Taiwan).

Remarks. Based on the description and the figures by Tsaour and Hsu (2003), this species can be distinguished from other species of the genus by the following charac-

ters: ventral margin of periandrium of aedeagus with 2 processes near apex; one process implanted on right side of periandrium near apex; flagellum with sinuate apical margin, a small awl-shaped production protruding on left side near apex.

Neocarpia okinawana Emeljanov & Hayashi, 2007

Neocarpia okinawana Emeljanov & Hayashi, 2007: 128: figs 4–5; 135: figs 21–24.

Distribution. Japan (Ryukyus).

Remarks. Based on the description and the figures by Emeljanov and Hayashi (2007), this species can be distinguished from other species of the genus by the following characters: periandrium bearing two processes on left side and one on right side near apex; dorsal margin of periandrium with one process, directed caudally; flagellum with two processes near apex.

Neocarpia reversa Zhi & Chen, sp. n.

<http://zoobank.org/B4C95EA6-2EE4-446B-9BF3-72E4339216A3>

Figs 43–66

Type material. Holotype: ♂, **China:** Yunnan, Xichou County, Fadou (23°38'N, 104°78'E), 28 June 2013, Ying-Jian Wang; paratypes: 11♂♂, 29♀♀, same data as holotype, Ying-Jian Wang and Qiang Luo.

Description. Body length: male 5.8–6.3 mm ($N = 7$), female 6.3–6.6 mm ($N = 20$); forewing length: male 5.0–5.3 mm ($N = 7$), female 5.1–5.8 mm ($N = 20$).

Coloration. General color yellowish brown (Figs 43–48) (brown in female). Eyes brown, ocelli yellow. Vertex generally yellowish brown, carinae brown to dark brown (except median carina milky). Face generally yellow, carinae brown to dark brown; rostrum yellowish brown with dark brownish apex. Pronotum and mesonotum with areas between lateral carinae yellow, lateral areas brown. Forewing semihyaline, alternately yellowish brown and pale yellowish brown, with black spots on end of longitudinal veins. Hind tibiae yellowish brown. Ventral abdomen yellowish brown.

Head and thorax. Vertex (Figs 43, 45, 47) broad, 2.0 times wider than long; anterior margin slightly projected, posterior margin convexly recessed. Frons same as *N. acutata*. Pronotum (Figs 43, 45, 47) 2.1 times longer than vertex; median carina indistinct, posterior margin rather right-angled. Mesonotum 1.7 times longer than pronotum and vertex combined. Forewing (Figs 44, 46, 49) amply exceeding tip of abdomen, 2.4 times longer than wide, other veins same as *N. acutata*. Hind tibia with 6 apical spines; chaetotaxy of hind tarsi: 5/7.

Male genitalia. Pygofer (Figs 50, 51), same as *N. acutata*. Anal segment (Figs 50, 52), in lateral view, dorsal margin nearly straight, ventral margin slightly convex, with a horn-like process extending to apex ventrally; in dorsal view 1.8 times longer



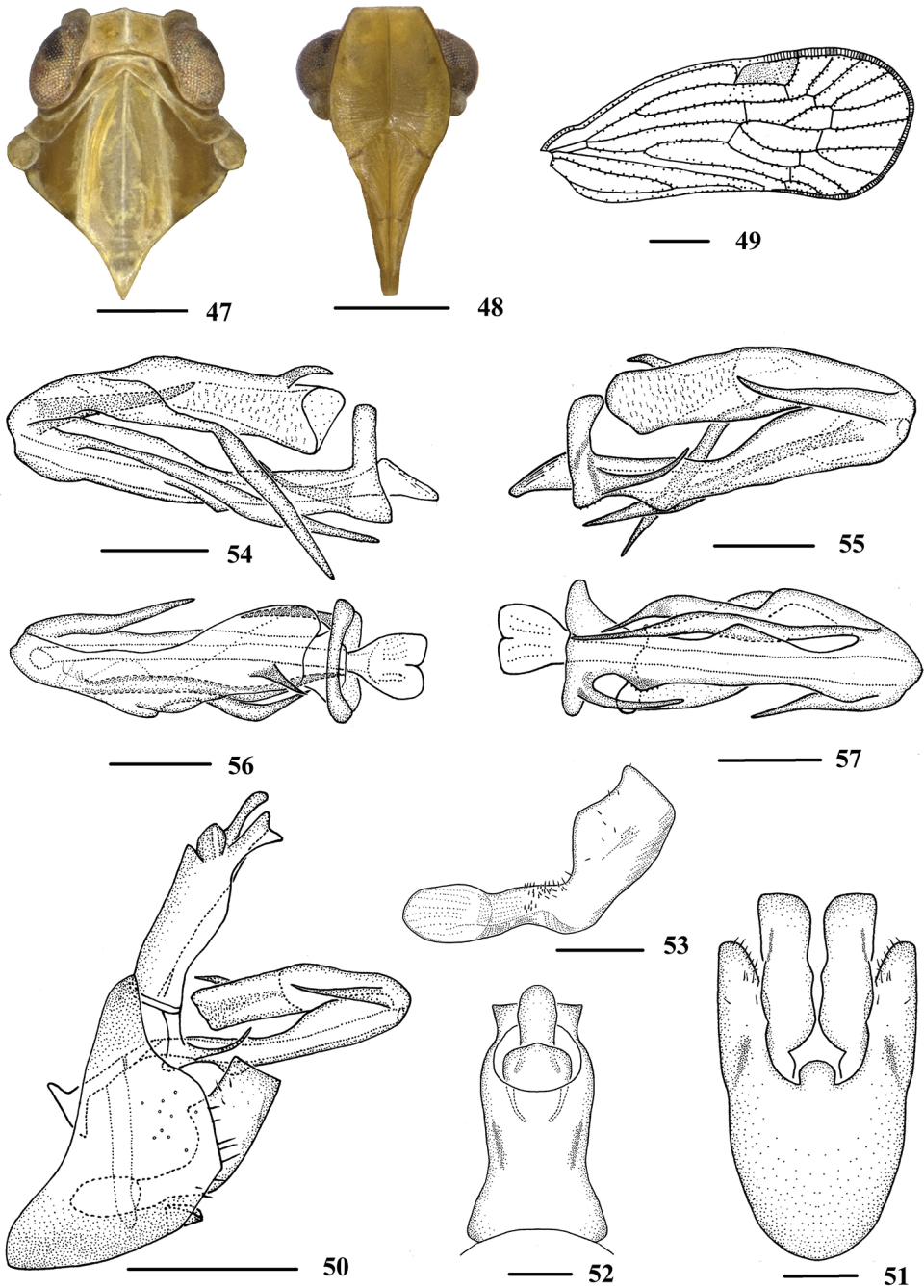
Figures 43–46. *Neocarpia reversa* sp. n. **43** Male, dorsal view **44** Male, lateral view **45** Female, dorsal view **46** Female, lateral view.

than wide; anal style strap-like, beyond anal segment. Apical margin of genital styles (Figs 50, 53) with a small blunt process, dorsal margin bending inwards in the middle. Aedeagus (Figs 54–57) with five spinose processes. Right side of perianthium with a very long process near apex directed ventrocephally. Left side of perianthium with a short reversed process at base directed dorsocaudally, and a medium sized process near apex directed dorsocephally. Flagellum moderately sclerotised. Right side with a long process near base directed ventrocephally. Apex near dorsal margin with a short process, curved towards cephalad.

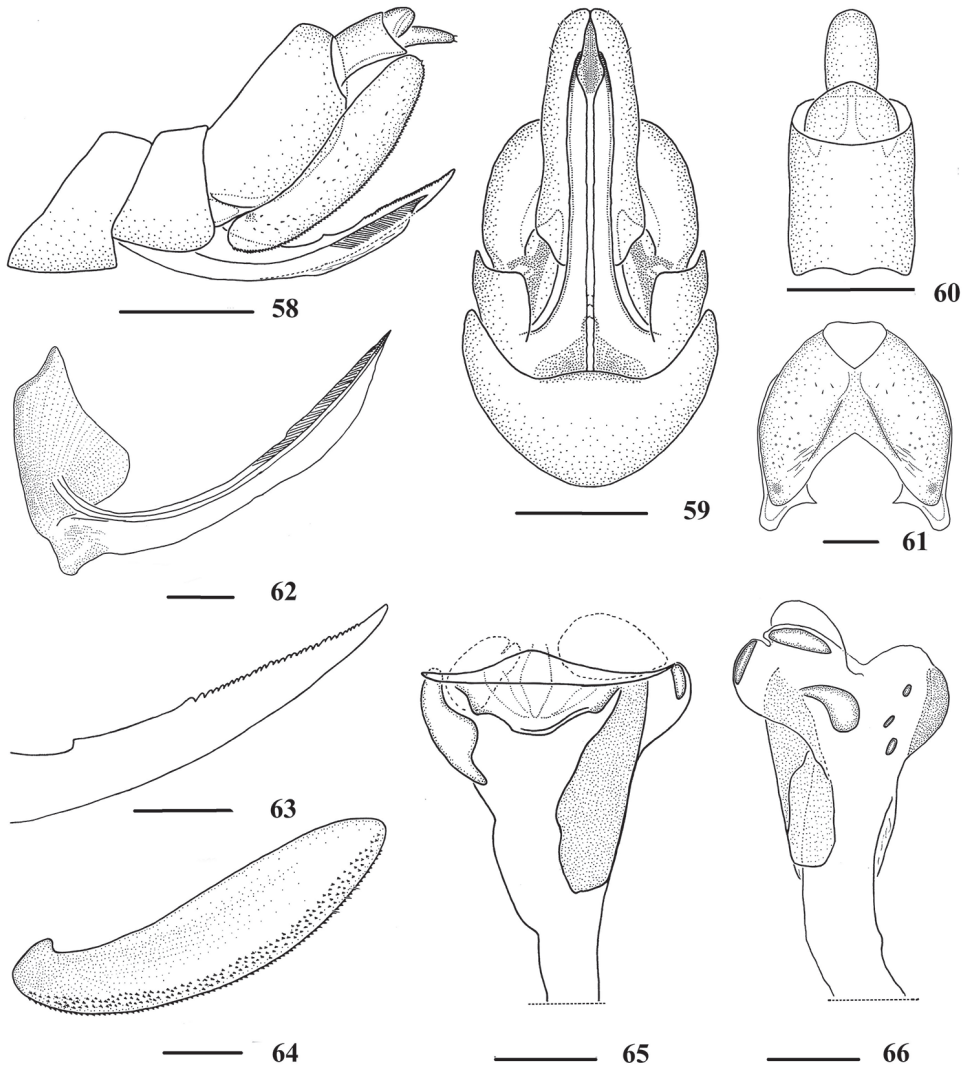
Female genitalia. Pygofer (Figs 58–59, 61) same as in *N. acutata*. Anal tube (Figs 58, 60) short, 1.2 times longer than wide in dorsal view, ventral margin slightly concave in lateral view; anal styles relatively short and small, finger-shaped. Gonapophysis VIII (Fig. 62) slightly concave basally. Gonapophysis IX and gonoplac (Figs 63–64) same as in *N. acutata*, while length of gonoplac 4.3 times of its width, and width of spiculated area approximately 1/5 of gonoplac. Posterior vagina (Figs 65–66) elongate, right side with a long longitudinal sclerite in ventral view and a shorter one in dorsal view, forming a cylindrical structure, left side with a moderately long sclerite in ventral view, hat-shaped. In dorsal view, middle area of posterior vagina with a drop-like sclerite, right side with two small oblong sclerites near terminal.

Distribution. China (Yunnan).

Etymology. The specific name is derived from the Latin word “*reversa*”, referring to the left side of the perianthium with a short reversed process basally.



Figures 47–57. *Neocarpia reversa* sp. n., male **47** Head and thorax, dorsal view **48** Face, ventral view **49** Forewing **50** Genitalia, lateral view **51** Pygofer and genital styles, ventral view **52** Anal segment, dorsal view **53** Genital styles, inner lateral view **54** Aedeagus, right side **55** Aedeagus, left side **56** Aedeagus, dorsal view **57** Aedeagus, ventral view. Scale bars: 0.5 mm (**47–48, 50**); 1.0 mm (**49**); 0.2 mm (**51–57**).



Figures 58–66. *Neocarpia reversa* sp. n., female **58** Genitalia, lateral view **59** Genitalia, ventral view **60** Anal segment, dorsal view **61** Pygofer, caudal view **62** Gonapophysis VIII and gonocoxa VIII, dorsal view **63** Gonapophysis IX, lateral view **64** Gonoplac, inner lateral view **65** Posterior vagina, ventral view **66** Posterior vagina, dorsal view. Scale bars: 0.5 mm (**58–59**); 0.2 mm (**60–66**).

Remarks. Male genitalia of *N. reversa* sp. n. is similar to *N. maai* Tsaur & Hsu, 2003, but differs in: (1) left side of perianthrium with a short reversed process basally (*N. maai* without process in same position); (2) two processes on both lateral sides of perianthrium near apex (three processes on perianthrium near apex, two on ventral margin and one on right side in *N. maai*); (3) flagellum with smooth apical margin (sinuate in *N. maai*).

Female genitalia of *N. reversa* is similar to *N. bidentata* Zhang & Chen, 2013, but differs in: posterior vagina with a long longitudinal sclerite on left side (posterior vagina with a long longitudinal sclerite on right side in *N. bidentata*).

***Neocarpia rhizophorae* Löcker in Löcker, Fletcher & Gurr, 2010**

Neocarpia rhizophorae Löcker, in Löcker, Fletcher & Gurr, 2010: 18: fig. 7A–D; 28: fig. 17A–E.

Distribution. Australia (Queensland).

Remarks. Based on the description and the figures by Löcker et al. (2010), this species can be distinguished from other species of the genus by the following characters: right side of perianthrium with a process near apex and ventral margin of perianthrium with one small triangular process at apical 1/3; flagellum with a prominent long process in the middle.

Discussion

The taxonomic characters of cixiid male genitalia have been sufficiently studied, whereas the descriptions of cixiid female genitalia are quite rare. Although some characters of the female external genitalia like ovipositor, anal segment, anal style and wax plate have been described by several researchers in history, such as: *Cixius* Latreille (Remane and Asche 1979), *Hyalesthes* Signoret (Sforza and Bourgoïn 1998), *Trirhacus* and related taxa (Holzinger 2002) and *Oteana* Hoch (Hoch 2006), these morphological characters are reported only reliable in taxonomic identifications on genus level or higher category, applying them in species identifications is often impracticable (Holzinger et al. 2002; Löcker et al. 2006). Nonetheless, using the characters of female inner genitalia structures, especially those such as the sclerites on the walls of the posterior vagina may provide a practical way for the species level identifications of the female cixiids (Bourgoïn 1993; Holzinger et al. 2002; Orosz 2013).

Tsaur and Hsu described and illustrated the female pygofer and the anal segment of *Neocarpia maai* (Tsaur and Hsu 2003). Löcker et al. (2010) reported the morphological characters of the ovipositor, the 8th abdominal sternite, the anal segment and the anal style of *N. rhizophorae*. However, these characters are not effective when used to distinguish among species of *Neocarpia*. Combined with the type specimens of *Neocarpia*, we found that the characteristics of posterior vaginal walls (Figs 23–24, 32–33, 41–42, 65–66) can be considered as key diagnostic features for female species identification and might provide evidence for the species diagnosis for other *Neocarpia* and Cixiidae. The variety of sclerites in numbers, sizes, and shapes in the walls of the female posterior vagina may be of high potential value in species identification in Cixiidae. In future study, we suggest that the morphological characters of the posterior vagina should be given more attention and their effectiveness in species identifications can be better evaluated and explored through more descriptions and illustrations of this structure.

Acknowledgements

The authors are grateful to collectors for collecting specimens. We also wish to thank Prof. Mike Wilson (National Museum Wales, Cardiff, United Kingdom) for his very kind editorial help with this paper and two anonymous referees for their efforts in improving this paper. This work was supported by the National Natural Science Foundation of China (No. 31472033), the Program of Excellent Innovation Talents, Guizhou Province (No. 20154021) and the Program of Science and Technology Innovation Talents Team, Guizhou Province (No. 20144001).

References

- Bourgoin T (1993) Female genitalia in Hemiptera Fulgoromorpha, morphological and phylogenetic data. *Annales de la Société Entomologique France* 29(3): 225–244.
- Emeljanov AF, Hayashi M (2007) New Cixiidae (Hemiptera, Auchenorrhyncha) from the Ryukyus, Japan. *Japanese Journal of Systematic Entomology* 13(1): 127–140.
- Hoch H (2006) New Cixiidae from eastern Polynesia: *Oteana* gen. nov. and *Manurevana* gen. nov. (Hemiptera: Fulgoromorpha). *Zootaxa* 1209: 1–47.
- Holzinger WE (2002) A review of the European planthopper genus *Trirhacus* and related taxa, with a key to the genera of European Cixiidae (Hemiptera: Fulgoromorpha). *European Journal of Entomology* 99(3): 373–398. <https://doi.org/10.14411/eje.2002.048>
- Holzinger WE, Emeljanov AF, Kammerlander I (2002) The family Cixiidae Spinola, 1839 (Hemiptera: Fulgoromorpha)-a Review. *Denisia* 4: 113–138.
- Löcker B, Fletcher MJ, Gurr GM (2010) Taxonomic revision of the Australian Eucarpiini (Hemiptera: Fulgoromorpha: Cixiidae) with the description of nine new species. *Zootaxa* 2425: 1–31.
- Löcker B, Fletcher MJ, Larivière MC, Gurr GM (2006) The Australian Pentastirini (Hemiptera: Fulgoromorpha: Cixiidae). *Zootaxa* 1290: 1–138.
- Orosz A (2013) A review of the genus *Macrocoxius* with descriptions of five new species (Hemiptera: Fulgoromorpha: Cixiidae). *Acta Musei Moraviae, Scientiae biologicae* 98(2): 97–142.
- Remane R, Asche M (1979) Evolution und Speziation der Gattung *Cixius* Latreille, 1804 (Homoptera, Auchenorrhyncha, Fulgoromorpha, Cixiidae) auf den Azorischen Inseln. *Marburger Entomologische Publikationen* 1: 1–264.
- Sforza R, Bourgoin T (1998) Female genitalia and copulation of the planthopper *Hyalesthes obsoletus* Signoret (Hemiptera: Fulgoromorpha: Cixiidae). *Annales de la Société Entomologique de France (Nouvelle Série)* 34(1): 63–70.
- Tsaur SC, Hsu TC (2003) The Cixiidae of Taiwan, Part VII: Tribe Pintaliini (Hemiptera: Fulgoroidea). *Zoological Studies* 42(3): 431–443.
- Tsaur SC, Hsu TC, Van Stalle J (1988) Cixiidae of Taiwan, Part (I) Pentastirini. *Journal of Taiwan Museum* 41(1): 35–74.
- Zhang P, Chen XS (2013) Two new bamboo-feeding species of the genus *Neocarpia* Tsaur & Hsu (Hemiptera: Fulgoromorpha: Cixiidae: Eucarpiini) from Guizhou Province, China. *Zootaxa* 3641(1): 41–48. <https://doi.org/10.11646/zootaxa.3641.1.4>

***Cecidonium pampeanus*, gen. et sp. n.: an overlooked and rare, new gall-inducing micromoth associated with *Schinus* in southern Brazil (Lepidoptera, Cecidosidae)**

Gilson R.P. Moreira¹, Rodrigo P. Eltz¹, Ramoim B. Pase¹, Gabriela T. Silva²,
Sérgio A.L. Bordignon³, Wolfram Mey⁴, Gislene L. Gonçalves^{5,6}

1 Departamento de Zoologia, Instituto de Biociências, Universidade Federal do Rio Grande do Sul, Av. Bento Gonçalves 9500, 91501-970 Porto Alegre, RS, Brazil **2** PPG Biologia Animal, Departamento de Zoologia, Instituto de Biociências, Universidade Federal do Rio Grande do Sul, Av. Bento Gonçalves 9500, 91501-970 Porto Alegre, RS, Brazil **3** Programa de Mestrado em Avaliação de Impactos Ambientais, Universidade La Salle, Av. Victor Barreto, 2288, 92010-000 Canoas, RS, Brazil **4** Museum für Naturkunde, Leibniz Institute for Evolution and Biodiversity Science, Invalidenstraße 43, 10115 Berlin, Germany **5** PPG Genética e Biologia Molecular, Departamento de Genética, Instituto de Biociências, Universidade Federal do Rio Grande do Sul, Av. Bento Gonçalves 9500, 91501-970 Porto Alegre, RS, Brazil **6** Departamento de Recursos Ambientales, Facultad de Ciencias Agronómicas, Universidad de Tarapacá, Casilla 6-D, Arica, Chile

Corresponding author: *Gilson R.P. Moreira* (gilson.moreira@ufrgs.br)

Academic editor: *E. van Nieukerken* | Received 20 April 2017 | Accepted 7 August 2017 | Published 4 September 2017

<http://zoobank.org/F9D9BD39-1346-4F18-8EA1-7572C480F300>

Citation: Moreira GRP, Eltz RP, Pase RB, Silva GT, Bordignon SAL, Mey W, Gonçalves GL (2017) *Cecidonium pampeanus*, gen. et sp. n.: an overlooked and rare, new gall-inducing micromoth associated with *Schinus* in southern Brazil (Lepidoptera: Cecidosidae). ZooKeys 695: 37–74. <https://doi.org/10.3897/zookeys.695.13320>

Abstract

Galls induced by the larval stage of cecidosids (Lepidoptera: Cecidosidae) are complex, multi-trophic systems, still poorly studied. They may be associated with other insect feeding guilds, including inquilines, kleptoparasites, cecidophages, parasitoids, and predators. By causing death of the gall inducer early in life and altering the gall phenotype, inquilines may lead to misidentification of the true gall inducers. Here, we describe through light and scanning electron microscopy *Cecidonium pampeanus*, a new genus and species of cecidosid moth, from the Pampa biome, south Brazil. It induces unnoticed, small galls under swollen stems of *Schinus weinmannifolius* Mart. ex Engl. (Anacardiaceae). Such galls are severely attacked early in ontogeny either by unidentified parasitoids belonging to *Lyrcus* Walker (Pteromalidae) that feed upon the inducer, or by inquiline wasps of the genus *Allorhogas* Gahan (Braconidae). The inquilines modify the galls into large ones that last longer and promptly call attention. Free-living galls are rare and dehiscent, pupation of *C. pampeanus* occurring on the ground. Due to these reasons the true inducer has been

overlooked in this case for more than a century. Additionally we inferred a phylogeny for Cecidosidae using sequences from mitochondrial and nuclear loci, and characterized genetic variation and gene flow across ten populations. Despite its natural history similarities with the African genus *Scyrotis*, *Cecidonius* is a much younger lineage, more closely related to the Neotropical cecidosids. *C. pampeanus* populations, which are now confined to a few mountain areas within its distribution range due to habitat destruction, are also genetically isolated, requiring conservation measures.

Keywords

Anacardiaceae, cecidosid moths, conservation, insect galls, Neotropical region, taxonomy

Introduction

Insect-induced galls may consist of very complex, multitrophic-level systems including not only the gall inducers themselves, but also predators, cecidophages, parasitoids, kleptoparasites and inquilines, among other insects such as successors that use them for shelter. Kleptoparasites in particular invade galls, usurping the cecidogenous species and become stationary, feeding upon gall tissues until they complete their larval development, and may prey upon the inducer and other insects that eventually enter the usurped gall (e.g., Morris et al. 2000, Luz et al. 2015). They do not induce differentiation and growth of new tissues, only feeding on those that were induced to develop by their precursors. Inquilines, however, induce the development of new tissues, either similar to or different from original ones when they take over a given gall, generally killing the inducer by inanition (e.g., Brooks and Shorthouse 1988, van Noort et al. 2007). Thus, they may change substantially the size and shape of the gall they invade. Little attention has been paid to the important taxonomic consequences of this phenomenon, a potential difficulty factor in identification of hidden diversity in gall communities. Misidentification of the true gall inducers in such cases is obviously likely, since the inducer is eliminated from the system early in the gall ontogeny and no conspicuous trace of it may be left inside the gall. In addition, contrary to galls attacked either by kleptoparasites or inquilines that may stay attached to host plants, those free of them still containing the growing inducer may be dehiscent, with later development of immature stages occurring on the ground (e.g., van Noort et al. 2007, Luz et al. 2015). In this case, by altering the place of gall development in the field and thus enhancing the encounter of attacked galls by kleptoparasites and inquilines that stay attached to the host plant compared to free, detached ones, the possibility of missing the presence of the true inducers is substantially increased. Furthermore, depending on the rate of attack by other parasitoids and predators in association, natural densities of the true gall inducer would be reduced further, even becoming rare, and thus may be unnoticed. As a case study, here we describe one example of such a peculiar system, where the induction of a non-conspicuous, dehiscent gall by a cecidosid moth has been overlooked for more than a century, erroneously believed to be induced by their hymenopteran inquilines who do not originally induce galls but in fact modify them early in development into large and colorful, visually appealing galls.

Cecidosidae are poorly known monotrystian Heteroneura moths (*sensu* Davis 1998), comprising six genera and 18 species, all with ranges restricted to the southern hemisphere. They are among a few lepidopteran lineages with a Gondwanic distribution: one occurs in New Zealand, the monotypic genus *Xanadoses* Hoare & Dugdale; twelve in southern Africa, all belonging to *Scyrotis* Meyrick, and five in South America, two in *Dicranoses* Kieffer & Jörgensen, and three in the monotypic genera *Cecidoses* Curtis, *Eucecidoses* Brèthes, and *Oliera* Brèthes. *Xanadoses nielseni* Hoare & Dugdale is a bark-miner of several New Zealand bark trees, particularly within *Weinmannia* Linnaeus (Cunoniaceae). Larvae of African *Scyrotis* form galls on species of *Searsia* F.A. Barkley (Anacardiaceae) (van Noort et al. 2007). In this case, they may also be located in the leaves; these galls are known as “jumping-beans”. They exfoliate from the hostplant and drop to the ground, where they are propelled for short distances by the active pupa inside, a supposed adaptation to avoid excessive heat from the sun (Meyrick 1917, Davis 1998). Unfortunately, none of the immature stages of *Scyrotis* species have been described in detail yet. South American cecidosids induce galls either on the stem or on axillary buds of *Schinus* Linnaeus (Anacardiaceae), particularly *S. polygamus* (Cav.) Cabrera (*sensu* Cabrera 1938, Fleig 1987, 1989). Gall morphology and life history of *C. eremita* Curtis have been treated in detail by Wille (1926). The taxonomy was reviewed and immature stages and galls of *O. argentinana* Brèthès, and *D. capsulifex* Kieffer & Jörgensen were described respectively by Moreira et al. (2012) and San Blas and Davis (2013). Information gathered recently by the first author suggested that diversity of cecidosids is much greater in the Neotropics, and not only additional species of *Schinus* are used as host but also other Anacardiaceae, such as species of *Lithraea* Miers ex Hook. & Arn.

This study concerns the galls of *Schinus weinmannifolius* Mart. ex Engl., which are induced by an undescribed genus and species of Cecidosidae in southern Brazil. Although not fully explored yet, the existence of these galls has been known for a long time; their induction was wrongly associated with cynipid wasps (Tavares 1909, Wille 1926, Houard 1933, Sáiz and Núñez 1997). Here the gall, the immature stages, and adults of the true inducer are described under both light and scanning electron microscopy and provided information on its natural history, in conjunction with a parasitoid and an inquiline wasp frequently found in association with these galls. By conducting an analysis of concatenated mitochondrial (COI and 16S) and nuclear (Wingless) DNA sequences including putative members of all known Neotropical cecidosid lineages, we provide further support for the proposition of the new taxon. Considering the possibility that the new species could be closely related to the African lineages, two *Scyrotis* species are also included for the first time for comparison in the phylogenetic analysis of Cecidosidae. Given that extant populations of the new taxa are in low numbers and restricted to a reduced distribution range, a genetic structure analysis was carried out using *ca.* 1.5 kb of COI gene sequences. Statistical analysis was performed to describe the genetic diversity of this rare species. Data are discussed in the context of importance regarding use of integrative taxonomy, including molecular analyses, in the discovery of hidden insect diversity in gall communities and the corresponding conservation scenario.

Materials and methods

Morphology

Adult specimens used in this study were reared from galls in small plastic vials, which were maintained under controlled conditions (14 h light/10 h dark; 25 ± 2 °C) in the Laboratório de Morfologia e Comportamento de Insetos (LMCI), Departamento de Zoologia, Universidade Federal do Rio Grande do Sul (UFRGS), Porto Alegre city, RS. Dehiscent galls (approx. 20 in total) were collected from the ground, in the surroundings of *S. weinmannifolius* plants of an old grass field, located in a farm belonging to Antonio Malta, Coxilha das Lombas, 30°01'46"S, 50°36'40"W, 86m, 29.V.2012, Santo Antônio da Patrulha Municipality, Rio Grande do Sul State (RS), Brazil. Pupae were obtained later (September) by dissecting some galls under a stereomicroscope in the laboratory. Larvae were obtained by dissecting *S. weinmannifolius* branches, either from galls located under swollen bark (early instars) or erupted from the stem (later instars). Adults were pin-mounted and dried. Immature stages were fixed in Dietrich's fluid and preserved in 75% ethanol. Larvae used for DNA extraction came from several additional populations (listed below), and were preserved in 100% ethanol at -20 °C.

For descriptions of adult morphology the specimens were cleared in a 10% potassium hydroxide (KOH) solution, stained with Chlorazol black E and slide-mounted in either glycerine jelly or Canada balsam. Last instar larvae were prepared similarly for description of chaetotaxy. Observations were performed with the aid of a Leica® M125 stereomicroscope. Structures selected to be drawn were previously photographed with a Sony® Cyber-shot DSC-H10 digital camera attached to the stereomicroscope. Vectorised line drawings were then made with the software Corel Photo-Paint® X7, using the corresponding digitalized images as a guide. Additional specimens were used for scanning electron microscope analyses. They were dehydrated in a Bal-tec® CPD030 critical-point dryer, mounted with double-sided tape on metal stubs, coated with gold in a Bal-tec® SCD050 sputter coater and examined and photographed in a JEOL® JSM6060 scanning electron microscope at the Centro de Microscopia Eletrônica (CME) of UFRGS.

Molecular analysis

Mitochondrial and nuclear DNA sequences were used for two different levels of analysis of the undescribed genus and species: 1) to infer the phylogenetic status and relationships within Cecidosidae, and 2) to describe the genetic diversity and population structure of this rare taxon. For the first approach we used representative species of all members of Cecidosidae except *Xanadoses*, the corresponding samples coming from the tissue collection of LMCI: i.e., *C. eremita*, *Dicranoses congregatella* Kieffer & Jörgensen, *Eucecidoses minutanus* Brèthes, *O. argentinana*, an undescribed lineage from Chile (previously known to be closely related based on morphology) and *Scyrotis* (*Scy-*

rotis sp. and *S. granosa* Meyrick), a genus from Africa included for the first time in a molecular phylogeny. For the second approach we sampled 10 populations across the distribution range of *Cecidoniuss pampeanus* sp. n. (P1 to P10), including six individuals per site (Suppl. materials 3, 5). Previous analyses indicated there was no substantial addition of genetic variation by increasing corresponding sample size. Total genomic DNA was purified from fresh collected larval tissue of all Cecidosidae surveyed except *Scyrotis* (dried museum adult specimens were used), using the PureLink genomic DNA kit (Life, Invitrogen, USA) following the manufacturer's instructions.

For cecidosid phylogeny we used nucleotide sequences obtained from different molecular markers, selected because they evolve at different rates and provide phylogenetic resolution at different, overlapping taxonomic levels: two mitochondrial (1421 bp of the cytochrome oxidase subunit I [COI] and 474 bp of the 16S ribosomal RNA [16S] genes), and one nuclear (395 bp of the Wingless [Wg] gene) loci. For the genetic structure and variability approach, we amplified COI in 60 individuals, six from each population sampled. The selected molecular markers were amplified by polymerase chain reaction (PCR); primers and conditions used are described in the supplementary material (Suppl. material 1). PCR products were purified using the enzymatic method (exonuclease and alkaline phosphatase), sequenced with BigDye chemistry, and analysed in an ABI3730XL (Applied Biosystems Inc.). Chromatograms obtained from the automatic sequencer were read and sequences were assembled using the software CodonCode Aligner (CodonCode Corporation). Sequences generated in this study were deposited in the GenBank database (Suppl. material 3).

Sequence data were used for the reconstruction of a concatenated phylogenetic tree (COI+16S+Wg) with the Bayesian method in BEAST 2.02 (Bouckaert et al. 2014). The tree prior was set as a Yule calibrated process, using GTR + I for the COI partition and TN92+G for both 16S and Wg, selected with the Bayesian information criterion (BIC; Schwarz 1978) for each data set in jModelTest 2.1.2 (Darriba et al. 2012). The branch lengths were allowed to vary under a relaxed clock model with an uncorrelated log-normal distribution (Drummond et al. 2006). To adjust the molecular clock we used the fossil calibration point of Adeloidea (sensu van Nieukerken et al. 2011), about 120 ± 10 mya, with a log-normal distribution (Walhberg et al. 2013). The analysis was run for 10,000,000 Markov Chain Monte Carlo (MCMC) cycles and parameters were sampled every 1,000 cycles; this was repeated four times to test for MCMC convergence, and priors exceeded 200 to ensure effective sample sizes (ESS). Burn-in was determined in Tracer 1.5 (Drummond and Rambaut 2007) based on ESS and parameter trajectories, and the first 20% of trees were then removed with TreeAnnotator. Trees were observed and edited in FigTree v1.3.1 (Rambaut 2009). Clades with Bayesian Posterior Probability (BPP) $\geq 95\%$ were considered strongly supported. Pairwise genetic distances (p-distances) among lineages were calculated in MEGA 7 (Tamura et al. 2013).

Nucleotide and haplotype (gene) diversity indices were estimated for individuals grouped into ten populations (P1 to P10) with DnaSP 5.1 (Librado and Rozas 2009). To investigate the evolutionary relationships among COI-haplotypes a median-joining haplotype network (Bandelt et al. 1999) was constructed in NETWORK 5

(<http://www.fluxus-engineering.com/sharenet.htm>). Levels of genetic structure among populations were characterized using φ ST with Arlequin3.5 (Excoffier and Lischer 2010). Additionally, to investigate spatial patterns of genetic structure we assessed the correlation between genetic and geographic distances for all pairs of sampled individuals using a Mantel test (Mantel 1967). We also performed an Analysis of Molecular Variance (AMOVA; Excoffier et al. 1992) with Arlequin to assess more detailed quantitative differentiation among populations, performing two rounds of AMOVA employing different geographic clustering strategies: i) taking into account the vicariate effect of the Jacui River, and ii) using the genetic distance and haplotype relationship results. Finally, we investigated the demographic history of the new genus and species using neutrality tests (Tajima's D, Fu & Li' D* and F*, Fu's Fs) and mismatch distribution analysis (Rogers and Harpending 1992, Schneider and Excoffier 1999) with DnaSP.

Abbreviations of the institutions from which specimens were examined are:

- DZUP** Coll. Padre Jesus S. Moure, Departamento de Zoologia, Universidade Federal do Paraná, Curitiba, Paraná, Brazil.
- LMCI** Laboratório de Morfologia e Comportamento de Insetos, Universidade Federal do Rio Grande do Sul, Porto Alegre, Rio Grande do Sul, Brazil.

Results

Molecular phylogeny

The phylogenetic reconstruction corroborated our hypothesis of monophyly (well supported by posterior probability) for the new proposed genus (Fig. 1). Its sister taxon is the undescribed lineage from Chile (Cecidosidae sp.); it was close to *O. argentinana* among the described species of cecidosids. The dated phylogeny revealed the new genus as the youngest lineage among cecidosids, which emerged around 23.8 Mya (95% HDP 10.2–34.6 mya). Genetic distances of the new genus to other cecidosids ranged from 9 to 25%; less divergence was observed in relation to the sister species *Cecidonium* sp. and highest to *D. congregatella* (Table 1).

Taxonomy

***Cecidonium* Moreira & Gonçalves, gen. n.**

<http://zoobank.org/5029391A-325F-4BB4-A726-8D5F9FB78476>

Figs 2–9

Type species. *Cecidonium pampeanus* Moreira & Gonçalves, new species

Diagnosis. *Cecidonium* gen. n. bears several adult, pupal, larval, and gall features that in conjunction differentiate it from all cecidosid genera. Unlike other ce-

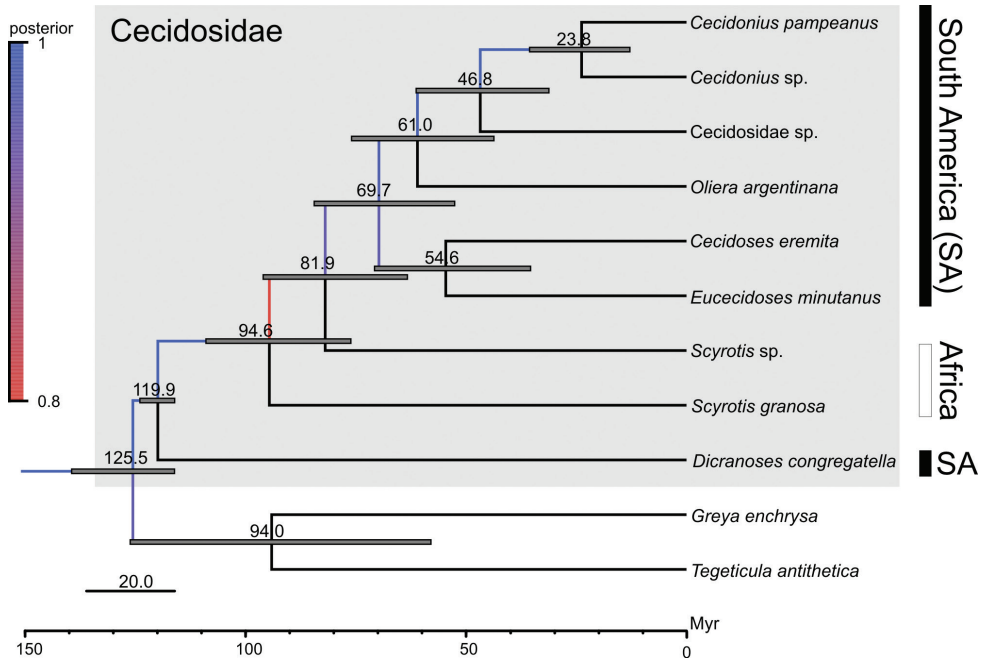


Figure 1. Molecular phylogeny of Cecidosidae. Bayesian time-calibrated consensus tree based on cytochrome oxidase subunit I (COI), r16S ribosomal (16S) and Wingless (Wg) genes. Prodoxidae (*Greya enchrysa* and *Tegeticula antithetica*) was used to root the tree. Colored branches indicate posterior probability support for the equivalent node following the legend. Dark gray bar indicates confidence interval for each node age estimate, presented in millions of years ago (Mya).

Table 1. Estimates of pairwise genetic distance (%) among nine Cecidosidae lineages based on DNA sequences (1420 base pairs of the cytochrome oxidase subunit I gene) using p-distance.

	<i>Cecidonium pampeanus</i>	<i>Cecidonium</i> sp.	<i>Cecidoses eremita</i>	<i>Dicranoses congregatella</i>	<i>Eucecidoses minutanus</i>	<i>Cecidosidae</i> sp.	<i>Oliera argentinana</i>	<i>Scyrotis</i> sp.	<i>Scyrotis granosa</i>
<i>Cecidonium pampeanus</i>	–								
<i>Cecidonium</i> sp.	9.0	–							
<i>Cecidoses eremita</i>	18.3	20.7	–						
<i>Dicranoses congregatella</i>	25.0	25.2	25.4	–					
<i>Eucecidoses minutanus</i>	13.8	18.6	18.3	23.2	–				
Cecidosidae sp.	16.1	18.3	18.5	23.7	17.8	–			
<i>Oliera argentinana</i>	13.7	16.4	17.5	21.8	16.3	15.1	–		
<i>Scyrotis</i> sp.	19.4	20.8	21.3	25.0	21.4	20.3	18.2	–	
<i>Scyrotis granosa</i>	23.7	27.4	26.9	28.8	27.8	25.8	24.5	27.3	–

cidosids, adults of *Cecidoniuss* have lateral cervical sclerites with anterior arms short and posterior ones with distal portion membranous. Females have a long ovipositor, bearing a large oviscapt cone with internal dorsal crest that extends cephalad within the seventh abdominal segment. In particular, they differ from those of the New Zealand *Xanadoses* that have a well-developed proboscis and five-segmented maxillary palpus (Hoare and Dugdale 2003) by having a vestigial proboscis and two-segmented maxillary palpus, among other characters. Unlike all species of the African *Scyrotis* that have forewings with four radial veins (Mey 2007), *Cecidoniuss* has five R-veins. With the exception of *Oliera*, which has small rudiments of galea (Moreira et al. 2012), other South American cecidosids show no vestiges of such structures. However, adults of *Cecidoniuss* have moderately well-developed galea. Contrary to those of *Oliera* where the maxillary and labial palpi are respectively three- and two-segmented, *Cecidoniuss* has the reverse; that is, two- and three-segmented maxillary and labial palpi, respectively. The pupa of *Cecidoniuss* is unique among all described cecidosids (those of *Scyrotis* are unknown), by having a stout and truncate cocoon cutter, flanked at the base by a pair of small, similarly shaped processes. In addition, in *Cecidoniuss* pupae the anterior margin of abdominal terga bear strong, posteriorly directed, transversally aligned spines that are much smaller in other genera. The larva of *Cecidoniuss* is also unique in having long thoracic setae, compared to short abdominal ones. They have two pair of stemmata; there is one in *Xanadoses*, and they are absent in other South American genera (larvae of *Scyrotis* are also unknown). Their woody, cylindrical galls are also unique, initially developing within swollen stems of *S. weinmannifolius* in southern Brazil. Later in ontogeny, they rupture the plant stem, thus growing externally. They are dehiscent, falling to the ground where pupation occurs. Contrary to those of *Scyrotis* (for detail, see von Noort et al. 2007), they do not exfoliate from the stem; they detach with their proximal base open, the corresponding orifice being clogged by larval feces.

Description of adults (Figs 2–4). Male and female similar in size and color; the body is covered with uniform, faded copper-coloured scales. Small moth, forewing length 4.16–4.58 mm (n = 4). **Head** (Fig. 3A): frons and vertex smooth, with sutures weakly developed; vestiture consisting of a pair of latero-dorsal scale tufts curved forward over the frons. Scales slender, lamellar, suberect and scattered over labrum, haustellum, maxillary, and labial palpi. Eyes relatively large, rounded; vertical diameter ~ 2.0x, minimum interocular distance across frons. Antennae median (~ 0.7x length of forewing); scape smooth except for medium dense pecten; flagellum filiform, with slender scales scattered only over dorsal half; ventral half with several elongate sensilla ca. 0.7x length of flagellomere. Labrum greatly reduced. Pilifers and mandibles absent. Haustellum moderately developed (~2/3 labial palpi length). Maxillary palpi short, 2-segmented; ratios of segments from base ~1.0:1.4. Labial palpi 3-segmented, bent anteriorly and upward (~2/3 eye width in length); ratio of segments from base ~1.0:1.8:1.6. **Thorax**: Anterior arms of laterocervical sclerites (Fig. 3B) short; posterior arms with distal portion weakly melanised. Metafurca (Fig. 3D, E) with slender, elongate postero-dorsal apophyses, free from secondary arms; antero-dorsal apodemes

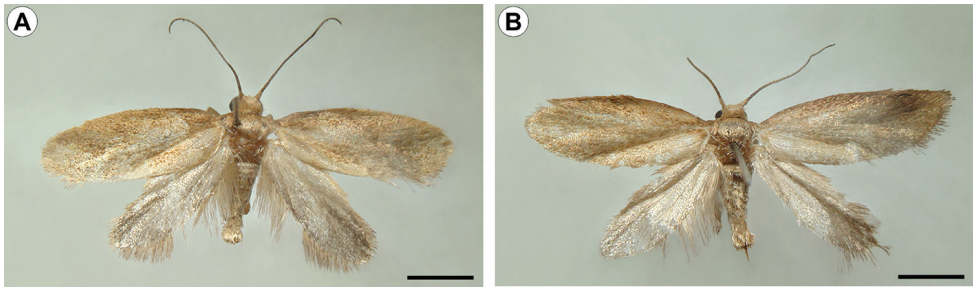


Figure 2. Pinned-dried *C. pampeanus* adults, dorsal view: **A** male (holotype, LMCI 188-4) **B** female paratype (LMCI 188-6). Scale bars: 2 mm.

present. Wings (Fig. 3C) lanceolate; microtrichia reduced in number; accessory cell present; retinaculum absent. Wing coupling consisting of ~20 frenular scales arising in two to three irregular rows near base of costa. Veins 13 in number, all reaching the margin; L/W index ~2.9; Sc ending near midpoint of wing margin, radius with 5 free branches, M 3-branched, CuA 2-branched, CuA1 and M3 well separated from each other basally, CuP faint distally and not stalked with 1A+2A. Hindwing: ~0.8 forewing in length, L/W index ~2.9; Sc and R stalked and ending distally at midpoint of wing margin, Rs unbranched, M 3-branched, M1 and M2 well separated, CuA 2-branched, CuA1 and M3 well separated, CuP faded, not stalked with 1A+2A. Legs (Fig. 3F) with spurs 0-2-4; epiphysis present. Tibial length proportion (anterior / medium / posterior legs) ~ 0.6:0.7:1.0. *Abdomen*: Sternum 2 with broad, U-shaped caudal rim; tergosternal connection absent. Male with remaining pre-genital segments unmodified. Female with abdominal segment A7 ~ 4x the length of A6; caudal margin bearing a dense ring of stout, elongate setae.

Male genitalia (Fig. 4A, B). Uncus moderately bilobed. Socii consisting of a pair of setigerous, dorsally directed lobes. Valva long and slender, with an elongate pectinifer along ventral margin extending ~ distal half-length of valva. Vinculum Y-shaped. Phallus (Fig. 4B) simple, slender, and tubular, rosette-like shaped anteriorly; vesica without cornuti. Juxta (Fig. 4B) elongate (~ 2/3 phallus length), slender, slightly spatulate distally and encircling phallus caudally. Saccus stout and tubular, ~ 1.3x length of valve.

Female genitalia (Fig. 4C, D). Oviscapt cone (*sensu* Kristensen 2003, San Blas and Davis 2013) present, with internal dorsal crest long, reaching the anterior portion of tergum seven. Anterior apophyses long, extending beyond fifth abdominal segment. Posterior apophyses ~1.5x length of anterior apophyses, and with anteriorly attached apodemes of similar width. Posterior apophyses are caudally fused to form an acute ovipositor, whose apex is compressed and sagittate, the lateral ridge bearing minute serrations. A typical primitive monotrysian reproductive system, with cloaca and vestibulum each bearing a pair of slender apodemes that extend anteriorly within abdominal segment 7; vestibulum without sclerotized structures; ductus and corpus bursae membranous, the latter saculiform, without signum; spermatheca connected to small, saculiform utriculus by a slightly coiled, afferent canal.

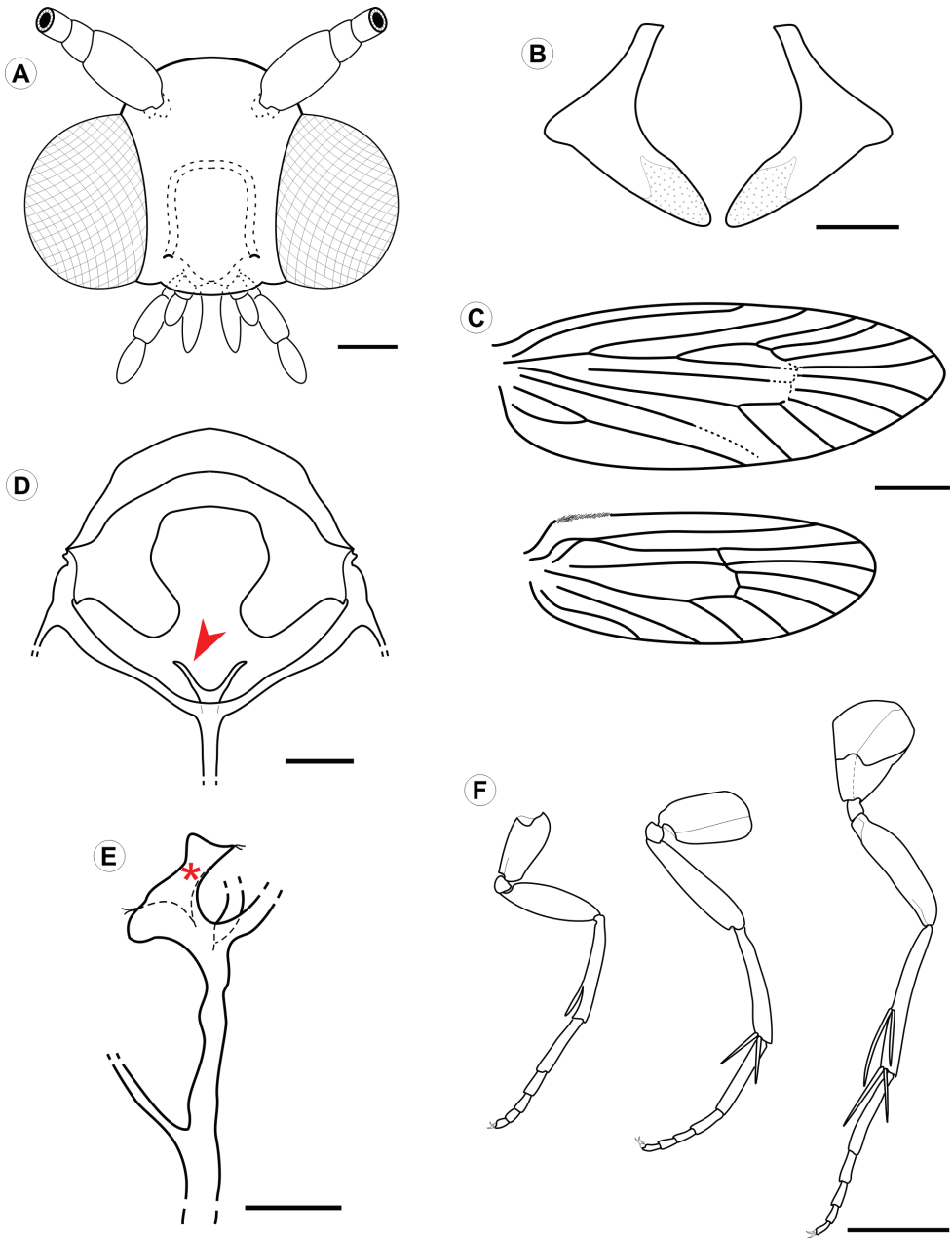


Figure 3. *Cecidonium pampeanus* adult morphology under light microscopy. **A** head, anterior view **B** lateral cervical sclerites, anterior; **C** fore- and hindwing venation, dorsal **D** metathoracic furcasternum, posterior (closed arrow points to left furcal apophysis) **E** metathoracic furcasternum in detail, lateral (asterisk indicates left furcal apophysis) **F** fore-, median- and hindlegs, from left to right, respectively. Scale bars: 0.25 (**A, D**); 0.1 mm (**B**); 1 mm (**C, F**); 0.2 mm (**E**).

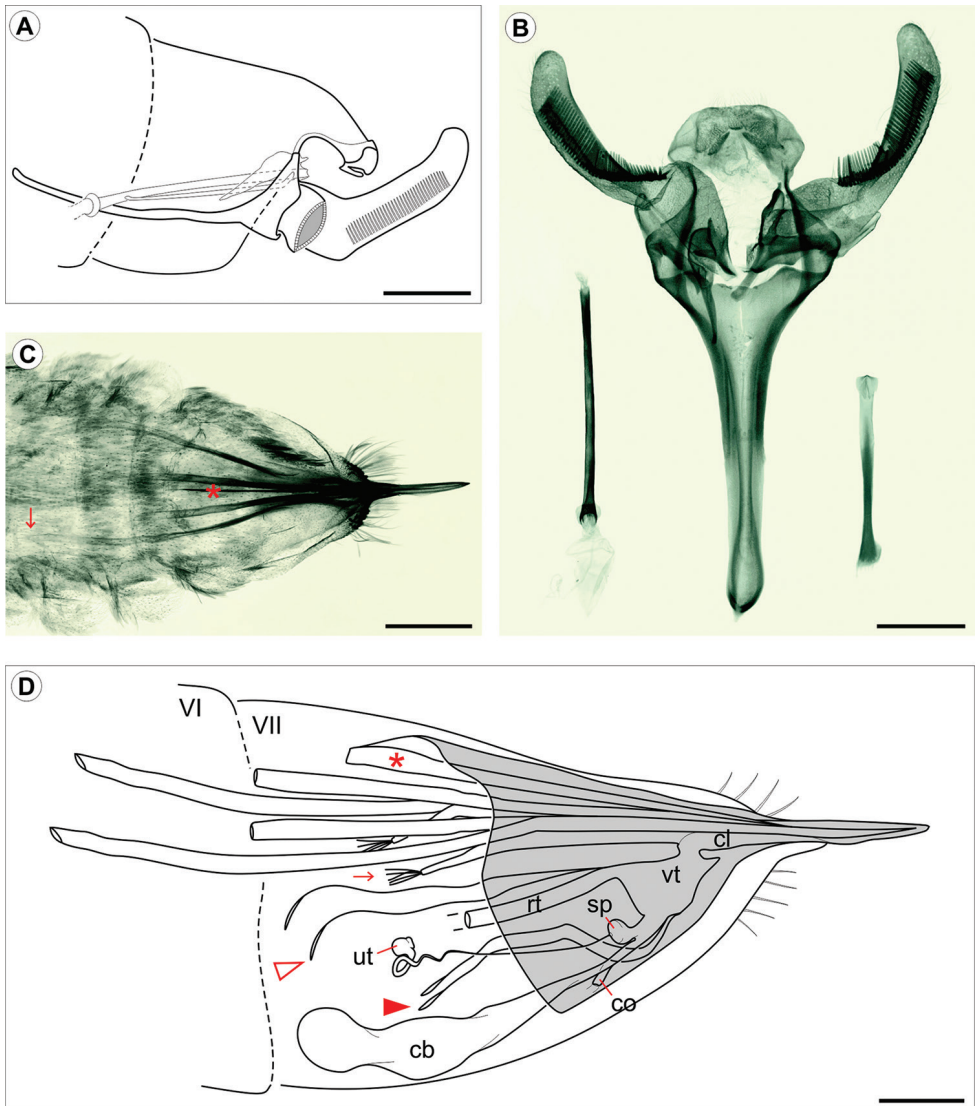


Figure 4. *Cecidonium pampeanus* genitalia morphology under light microscopy. **A** schematic representation of male genitalia, lateral view (left valve omitted) **B** dissected male genitalia, ventral, with detached phallus and juxta, on left and right side, respectively **C** female genitalia, dorsal **D** schematic representation of female genitalia, latero-dorsal. Roman numbers indicate abdominal segments. Oviscapt cone is represented in light gray in **D**. Arrows point to the end of left anterior apophysis in **C**, and to the apodeme of posterior apophysis in **D**. Asterisks indicate internal dorsal crest of oviscapt cone in **C** and **D**. Open and closed arrow heads point, respectively, to posterior apophyses and cloacal apodemes in **D**. Abbreviations: **cb** corpus bursae; **cl** cloaca; **co** common oviduct; **sp** spermatheca; **rt** rectum; **vt** vestibulum; **ut** utriculus of spermatheca. Scale bars: 0.25 mm.

Etymology. The genus name is derived from a composition between the Portuguese *Cecidia* (a gall; from the Greek, *kekidion*) with *Don* (an English nickname). Thus, the generic name means “Don’s gall”, named after Donald Davis from the Smithsonian Institution, USA, in recognition of his great contribution to the development of world lepidopterology, and in particular for having kindly introduced the first author to the study of Neotropical cecidosids a few years ago. The name is to be treated as masculine.

***Cecidoniuss pampeanus* Moreira & Gonçalves, sp. n.**

<http://zoobank.org/15DA6F09-4BF7-45CD-B25A-26DF60EDC383>

Figs 2–9

Diagnosis. As discussed for the monotypic genus.

Description of adults. As described for the monotypic genus.

Type material. Brazil: Old grass field, private farm belonging to Antonio Malta, Coxilha das Lombas, 30°01'46"S, 50°36'40"W, 86m, Santo Antônio da Patrulha Municipality, Rio Grande do Sul State (RS), Brazil; G.R.P. Moreira, H. A.Vargas, R. Brito & S.A.L. Bordignon; 29.V.2012, pinned-dry preserved adults, reared by the first author from dehiscent galls collected on the ground around patches of *Schinus weinmannifolius* Mart. ex Engl. plants. Holotype ♂: LMCI 188-4, emerged on 9.XI.2012; donated to DZUP (33.342). Paratypes: 1♂ (LMCI 188-7), emerged on 21.XI.2012, donated to DZUP (33.352); 1♀ (LMCI 188-6), with genitalia on slide (GRPM 50-127), emerged on 19.XI.2012, donated to DZUP (33.362).

Additional specimens used for morphological descriptions, with the same collection data as the type material: 1♂ (LMCI 188-5), emerged on 18.XI.2012, mounted on three slides in Canada balsam, genitalia (GRPM 50-124), head and thorax (GRPM 50-125) and wings (GRPM 50-126); three pupae (LMCI 188-8), three last instar larvae (LMCI 188-11), and several galls, dissected from galls induced on *S. weinmannifolius* plants, fixed in Dietrich’ fluid and preserved in 70% ethanol; two last instar larvae, mounted similarly on slides (GRPM 50-128 and 129).

Etymology. The epithet refers to Pampa, a biogeographic province within the Chacoan subregion (*sensu* Morrone 2006), predominantly composed of grasslands, and where *C. pampeanus* was first found.

Description of immature stages. *Larva* (Figs 5, 6, 9D, F): With five larval instars, which can be separated from each other by the head capsule width.

First instar (Fig. 6A, B). Head capsule width (average + standard error) = 0.066+0.009 mm; body length = 0.570+0.058 mm, n = 4. Head yellowish brown, with chewing mouthparts. Stemmata absent; antennae reduced, located close to mandibles; labrum subquadrate, with three pairs of minute setae; mandibles well developed, with four cusps along distal margin; maxilla with palpus and galea poorly developed; spinneret well developed, tubular; labial palpus one-segmented, bearing an apical sensillum. Thorax and abdomen creamy-white, cylindrical and U-shaped, with no developed primary setae; prothoracic shield, thoracic legs, prolegs, and abdominal calli absent.

Second instar (Fig. 9D). Similar in shape and color to fifth instar; head capsule width = $0.160+0.004$ mm; body length = $1.060 + 0.134$ mm, $n = 3$.

Third instar. Similar in shape and color to fifth instar; head capsule width = $0.217+0.005$ mm; body length = $2.078 + 0.052$ mm, $n = 3$.

Fourth instar. Similar in shape and color to fifth instar; head capsule width = $0.452+0.017$ mm; body length = $3.990 + 0.700$ mm, $n = 4$.

Fifth instar (Figs 5, 6C–L, 9F). Head capsule width = $0.898+0.031$ mm; body length = $7.190 + 1.722$ mm, $n = 5$. Head yellowish brown, with anterior margin orange-brown and lateral margin convex; frontoclypeus subtriangular, well-marked by pigmented adfrontal sutures, extending to apex of epicranial notch. Two well-developed, latero-located stemmata; antennae 2-segmented, with five sensilla, four short and one $\sim 5x$ longer the others; labrum slightly bilobed, with three pairs of setae on distal margin; mandible well developed with four cusps along distal margin and one seta basally on external surface; maxilla with palpus and galea reduced; spinneret tubular to conical; labial palpus one-segmented, with well-developed apical seta. Chaetotaxy consisting of 14 pairs of setae: F group unisetose; C group unisetose; A group trisetose; AF group unisetose; P group bisetose, reduced in length; S group trisetose, one reduced in length; SS group trisetose.

Thorax (T) and abdomen (A) creamy-white, cylindrical, slightly curved, covered with microtrichia. Prothoracic shield light yellowish; thoracic legs and abdominal prolegs absent; abdominal segments A2 to A7 with well-developed calli, located on posterior margin of terga. A10 composed of three lobes, one dorsal and two latero-ventral. Circular spiracles without elevated peritreme, laterally on T1, A1–8. Thoracic segments surrounded by short setae interspersed with long ones ($\sim 5x$ longer). T1 with 12 pairs of setae: D group bisetose; XD unisetose; SD unisetose, outside prothoracic shield; L group trisetose, anterior to spiracle; SV group trisetose; MV unisetose; V unisetose. T2–3 with 10 pairs of setae: D group bisetose; SD bisetose; MSD unisetose; L group bisetose; SV group bisetose; V unisetose.

Abdominal segments (AB) with only short setae that are more or less aligned on the middle region of each segment, which are tentatively named. AB1–7 with 6 pairs of setae: D group bisetose; L group trisetose, posterior to spiracles; V unisetose. AB8 with 8 pairs of setae: D group bisetose; SD group unisetose; L group tetrasetose, posterior to spiracles; V unisetose. AB9 with 5 pairs of setae: D group unisetose; SD group unisetose; L group unisetose; SV unisetose; V unisetose. A10 with six pairs of setae: D group bisetose; SD group unisetose; SV trisetose.

Pupa (Figs 7, 8). Length = $6.44+0.52$ mm; $n = 3$. Yellowish brown, with head, thorax, and abdominal spines becoming dark brown near adult emergence (Fig. 7C). Head with frontal process (gall-cutter) formed by three processes; one large, inverted U-shaped, located in the centre, which is flanked at the base by the other two that are $\sim 5x$ shorter than the central one, directed laterally and slightly bent to the anterior side (Figs 7, 8A, B). Antennae narrow, long, slightly surpassing forewing apex; prothorax a narrow transverse band between head and mesothorax; hindwings concealed by forewings, reaching posterior margin of sternum A6; pro- and mesothoracic legs

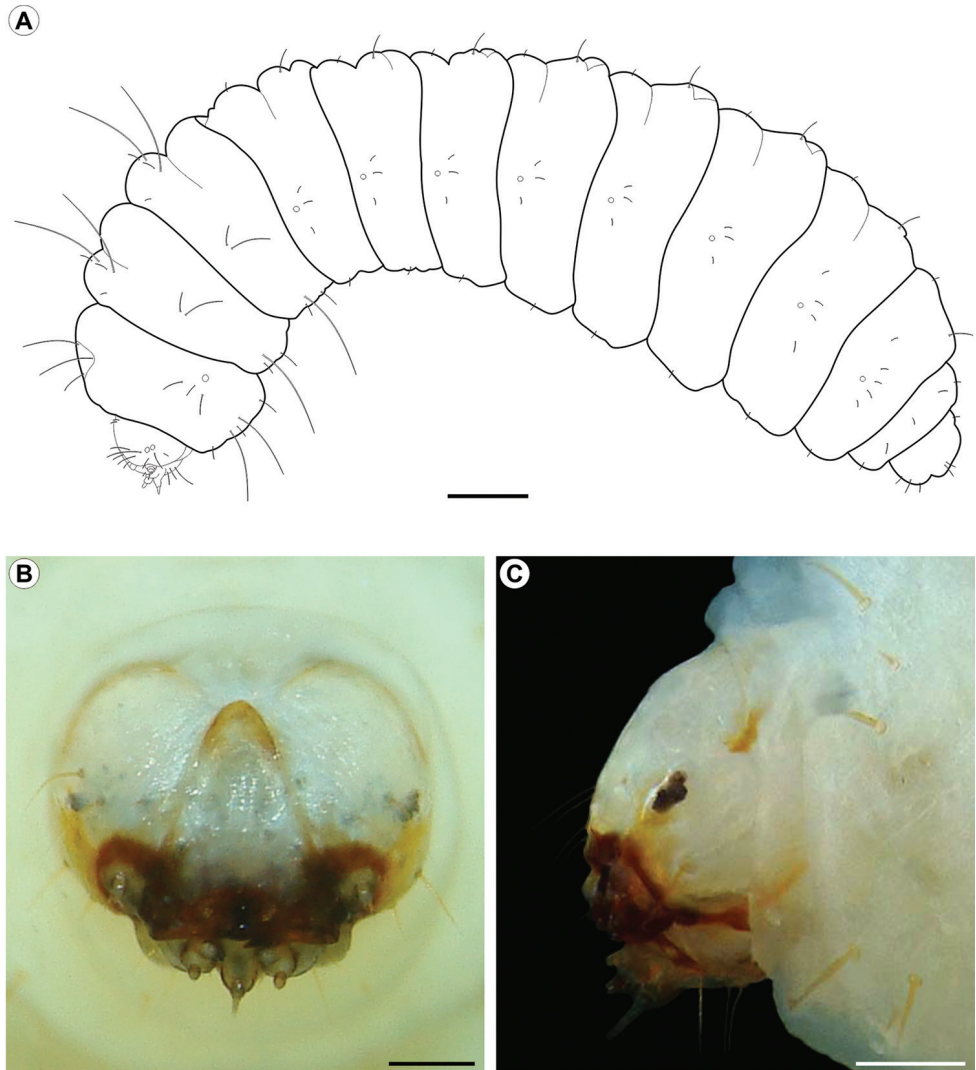


Figure 5. *Cecidoniopus pampeanus* last larval instar under light microscopy. **A** general schematic representation, lateral view **B, C** head, anterior, and lateral, respectively. Scale bars: 0.5 mm (**A**); 0.2 mm (**B, C**).

extended to A4 and A5, respectively; metathoracic legs reaching beyond forewing apex on segment A7 (Fig. 7). Frons and lateral portion of vertex with two pairs of setae each; tergum T2 with a pair of latero-dorsal setae; tergum T3 with a single seta on each side. Abdominal segments with central region covered by microtrichia; A2–9 with a transverse band of stout spines (Fig. 8E), near anterior margin of terga; tergum A10 with a pair of acute processes on posterior margin (Fig. 8F). Abdominal setae slightly shorter than thoracic, arranged in three rows (dorsal, supra- and subspiracular); one dorsal pair on segments A1–8; one supra-spiracular pair on segments A2–8; four subspiracular

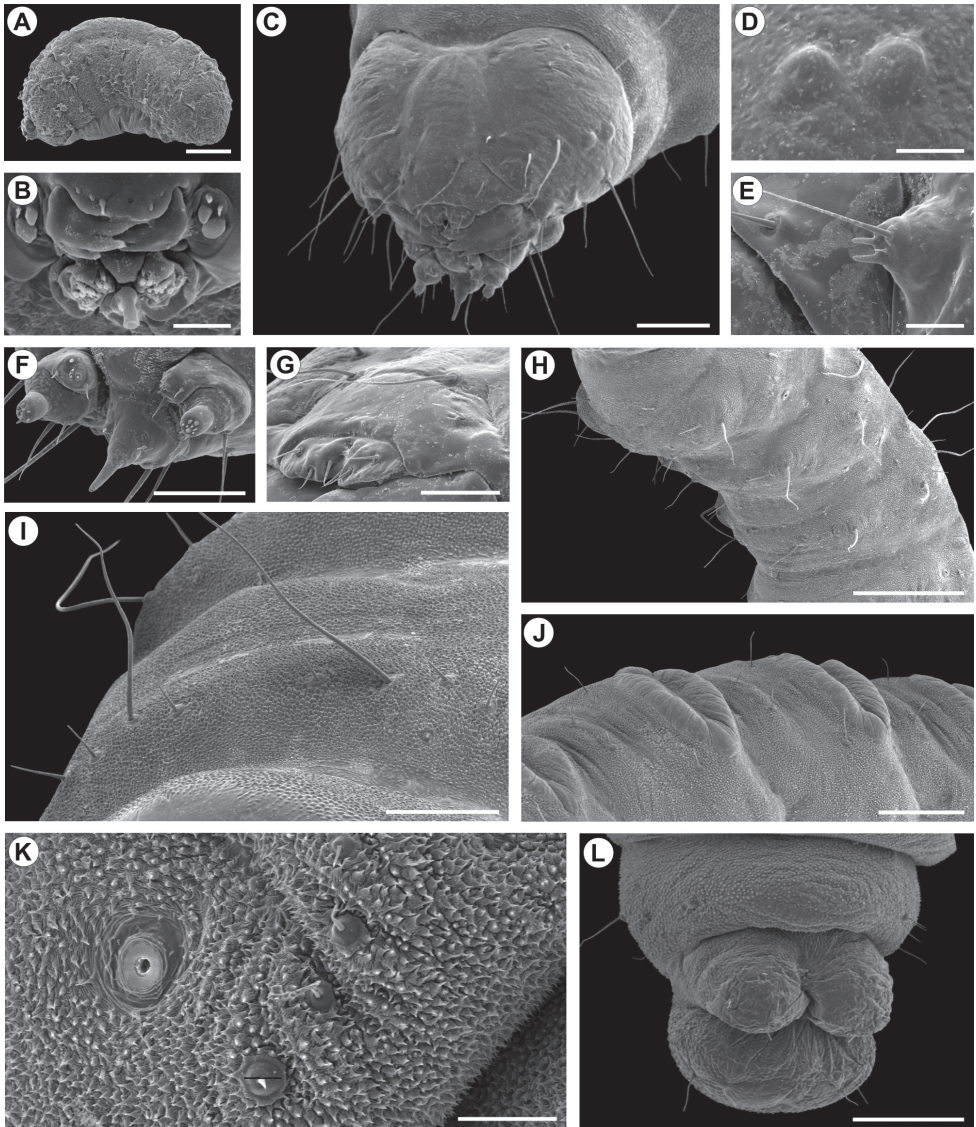


Figure 6. Morphology of *C. pampeanus* first (A, B) and last (C-L) larval instars under scanning electron microscopy. **A** general aspect, lateral view; **B**, buccal apparatus, anterior **C**, head, latero-dorsal **D** stemmata, lateral; **E**, left antenna, lateral **F** maxilla and labium, antero-lateral **G** labrum and clypeus, latero-dorsal **H** thorax, latero-ventral **I** meso- and metathorax in detail, with aligned setae of different lengths, antero-dorsal **J** second and third abdominal segments, showing tergal calli, latero-dorsal **K** eighth abdominal segment in detail, showing aligned secondary setae (arrows) and spiracle, lateral **L** last abdominal segments, ventral. Scale bars: 100 μm (**A, F, G**); 10 μm (**B**); 200 μm (**C**); 50 μm (**D, E, K**); 250 μm (**J**); 1 mm (**H, L**); 0.5 mm (**I**).

pairs on segments A3–6 (Fig. 8D); seven subspiracular pairs on A7–8; six pairs latero-ventrally on A10; spiracles with slightly elevated peritreme, laterally on A2–8, spiracle on A8 partially closed.

Natural history. The unilocular, club-shaped, green galls of *C. pampeanus* develop initially enclosed within swollen stems of *S. weinmannifolius* branches (Fig. 9B, C). Later on in ontogeny, they erupt from the stem surface, either as isolated units or in small groups, and may reach a few tens per branch (Fig. 9F). The larval chamber is almost cylindrical in shape (maximum length = 7.99 ± 0.58 mm; $n = 6$), and transverse to the stem axis. The external wall is shallow and thinner distally, formed as an expansion of the wood tissue under the bark (Fig. 9D–F). During the last larval instar, *C. pampeanus* galls have their wall somewhat annealed and ruptured at the base (Fig. 9G), when they fall freely to the ground containing the larva inside. The basal orifice left on these galls consequently is clogged by feces (Fig. 9I). These are continually deposited, then dry and solidify at the bottom of the gall chamber. After falling, the gall progressively dries up, turning a dark brown color (Fig. 9J). The external part may appear rotted in some old galls, when thin, longitudinally aligned grooves are found on the gall surface. Like *O. argentinana* galls (Moreira et al. 2012), those of *C. pampeanus* also lack an operculum. With the action of the frontal process and body contortions, the pupa opens an irregular orifice on the distal, weaker wall (Fig. 9H). By continuing these movements and anchoring the body laterally with its abdominal spines, the pupa pushes itself partially out of the gall. During this process, the anterior portion of the exuviae is split, allowing adult emergence. In all cases of adult emergence followed under laboratory conditions, the anterior part of the pupal exuviae (head and thorax) was found protruding to the outside, while the posterior third remained in the chamber.

Field collections carried out during five consecutive years at the type locality indicated that *C. pampeanus* is a univoltine species, larvae growing during the summer when young galls are seen on *S. weinmannifolius* stems. Fully developed galls containing last instar larvae have been collected mainly during autumn. Based on several dissections of galls on the ground that were field collected during the winter, it can be inferred that the species overwinters in the larval stage, pupation occurring in spring, and adults emerging later on. This time of the year coincides with full vegetative activity of *S. weinmannifolius* host plants, including production of new sprouts. In the populations of *S. weinmannifolius* located in the study area, several plants can be attacked by *C. pampeanus*, and many branches within a patch of plants can bear galls induced by them. Under severe attack by *C. pampeanus*, *S. weinmannifolius* stems may wilt, die, and then fall, but the underground portion may stay alive. Under low gall densities, however, the aerial portion of plants stay green throughout the year, the signs of detached galls appearing as small, cylindrical craters on their stem surface.

In the populations studied here, *C. pampeanus* larvae are only common to find in yearly stages, within those galls still under the bark. Free-living larvae are rarely found in the external galls. These are severely attacked by unidentified parasitoids belonging either to *Lyrcus* Walker (Pteromalidae) or to *Allorhogas* Gahan (Braconidae), whose taxonomy and biology will be treated in detail elsewhere. Larvae of *Lyrcus* are ectopara-

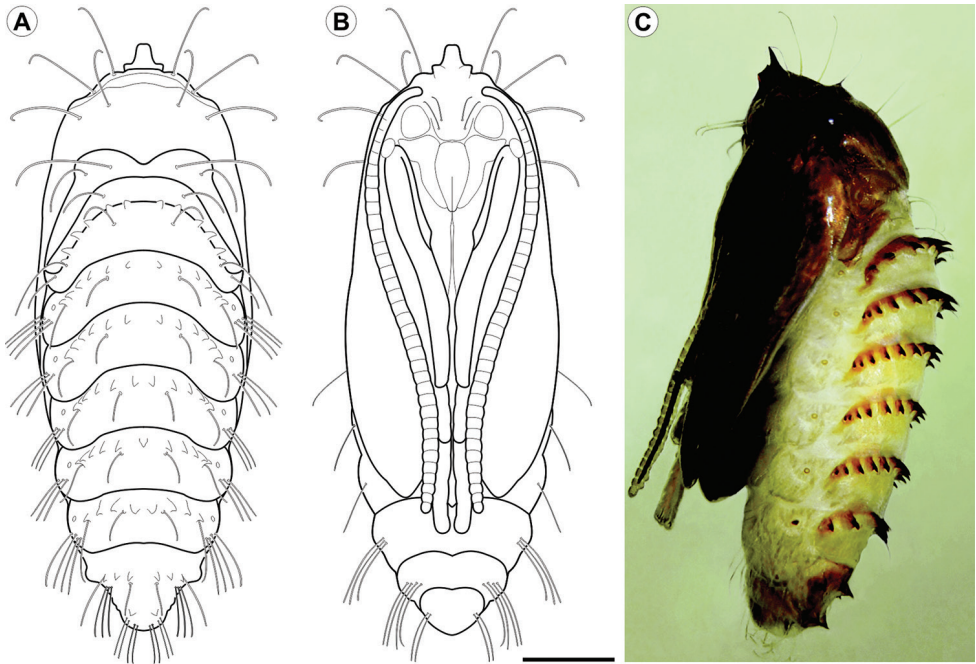


Figure 7. *Cecidoniuss pampeanus* pupa with light microscopy, under dorsal (A), ventral (B) and lateral (C) views. Scale bar: 1 mm.

sitoids found singly attached to *C. pampeanus* larvae inside the galls (Fig. 10A). They suck the internal contents of larvae, killing them and leaving only their exoskeletons intact. These parasitoids pupate inside *C. pampeanus* galls (Fig. 10B), which do not have their main shape changed, but turn a dark brown colour. In this case, galls stay attached to the stems for a longer time compared to ones free of parasitoids. After emergence, adults of *Lyrcus* open a characteristic, small orifice on the distal portion of the gall (Fig. 10C), through which they leave. By contrast, larvae of *Allorhogas* are gregarious and inquilines. They modify *C. pampeanus* galls, inducing production of additional tissue. When initially viewed externally in this case, *C. pampeanus* galls appear partially surrounded by this type of tissue (Fig. 10E). Later in ontogeny they are completely involved by such tissues, turning into globular, pinkish, large galls (up to 3.2 cm in diameter; $n = 8$) that last much longer in the field and promptly call attention (Fig. 10D, F). These galls are multilocular; larvae of inquilines are found individually in several chambers within (Fig. 10G). Pupation also occurs inside galls, that then dry up and turn dark brown; adults of inquilines leave through small circular orifices that are found on the gall surface (Fig. 10H).

Host-plant and distribution. Galls of *C. pampeanus* have been found only on branches of *Schinus weinmannifolius* Mart. ex Engl. (Anacardiaceae). This is a small shrub (up to 50-cm tall), originally found scattered in open savannas (Fig. 9A), hill tops and forest borders of southern South America, including central and south Bra-

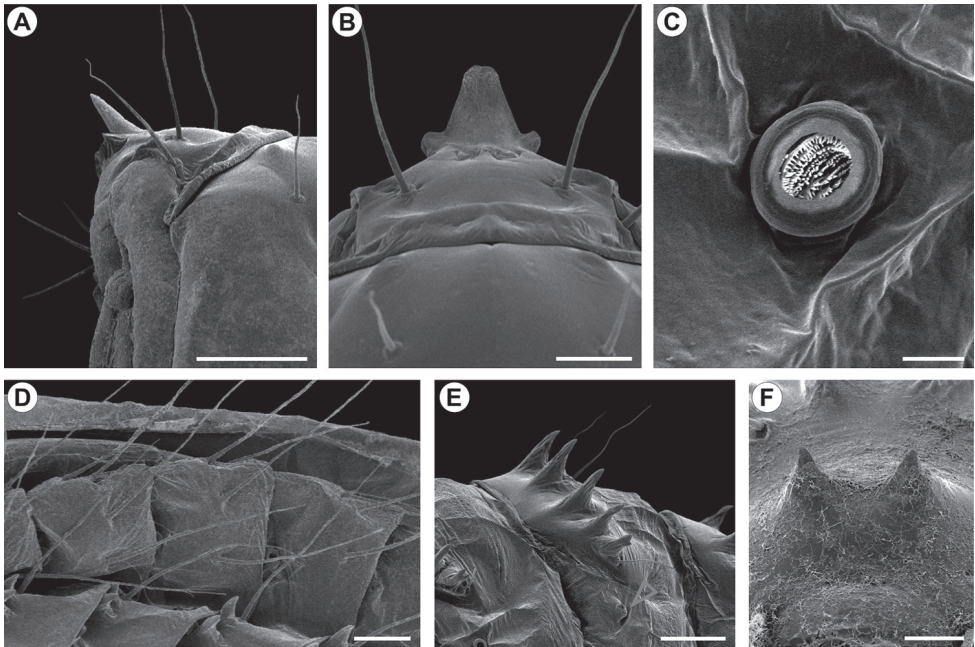


Figure 8. *Cecidonius pampeanus* pupal morphology with scanning electron microscopy. **A, B** head and prothorax, lateral and dorsal views, respectively **C** spiracle of sixth abdominal segment, dorsal **D** subspiracular setae from fourth to sixth abdominal segments, dorsal **E** tergal spines of eighth abdominal segment, lateral (arrow points to partially closed spiracle) **F** spines of tenth abdominal segment, posterior-dorsal. Scale bars: 0.5 mm(**A**); 0.25 mm (**B, C, E**); 0.1 mm (**D, F**).

zil, Paraguay, northeast Argentina and Uruguay (Barkley 1957, Luz 2011). However, populations of *S. weinmannifolius* bearing galls of *C. pampeanus* were found only in Rio Grande do Sul, the southernmost state of Brazil, particularly in the surroundings of Porto Alegre city (Fig. 11A) in the eastern limit of the Pampean province within the Chaco biogeographic region (*sensu* Morrone 2006). This region, also known as the Southeastern Highlands, since it reaches higher elevations than the remaining Pampean areas, includes several low-elevation hills (up to 300 m) that are more or less interwoven with fragments of semi-deciduous forests, herbaceous and shrub vegetation and single-layer grasslands, forming a mosaic. In this area a few, isolated, populations of *S. weinmannifolius* were found either as isolated plants or forming small patches (up to 3m in diameter), primarily located on hilltops and hill slopes, and a few scattered in the single-layer grasslands that prevail in the lower elevation areas.

Little is known about the biology or natural history of *S. weinmannifolius*. Although also found as isolated individuals, it usually forms small patches of plants, particularly in sandy soils. Preliminary field observations suggest that *S. weinmannifolius* is perennial, having a subterraneous habit of growth, forming stolons that grow just

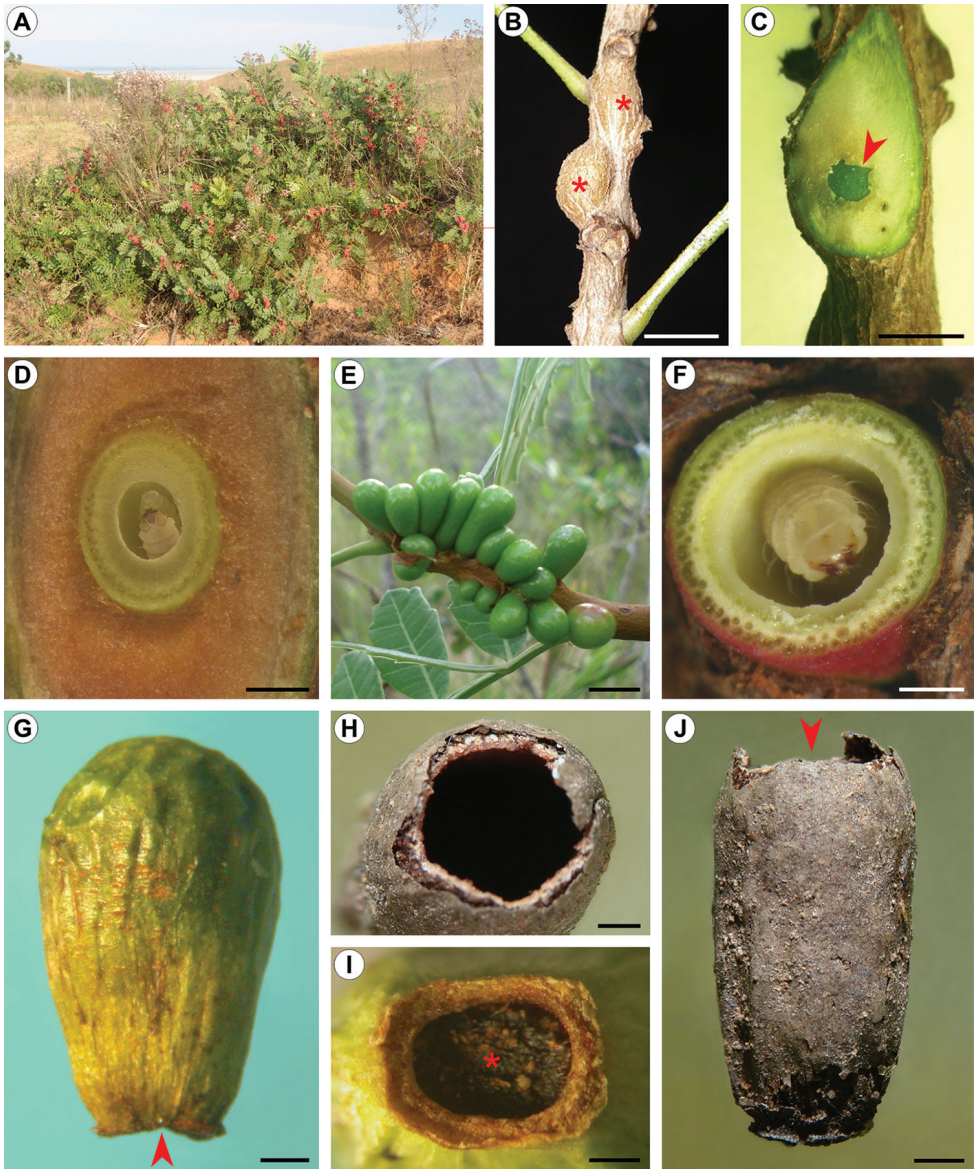


Figure 9. Natural history of *C. pampeanus* on *S. weinmannifolius*. **A** host plant patch at the type locality; **B** young developing galls within swollen stems (asterisks); **C** dissected swollen stem showing developing gall inside (indicated by arrow); **D** transversally sectioned young gall showing second instar larva inside; **E** group of external developing galls on branch; **F** transversally sectioned, full grown gall, showing last instar larva inside; **G** young dehiscent gall; **H** detail of emergence orifice left by adult on distal portion of old, empty gall (pointed by arrow in **J**); **I** detail of young dehiscent gall (arrow in **G**), showing orifice clogged by larval feces (asterisk); **J** old, empty, overwintered gall. Scale bars: 2 mm (**B**); 1 mm (**C**, **F**, **G**, **H**, **I**, **J**); 0.5 mm (**D**); 5 mm (**E**).

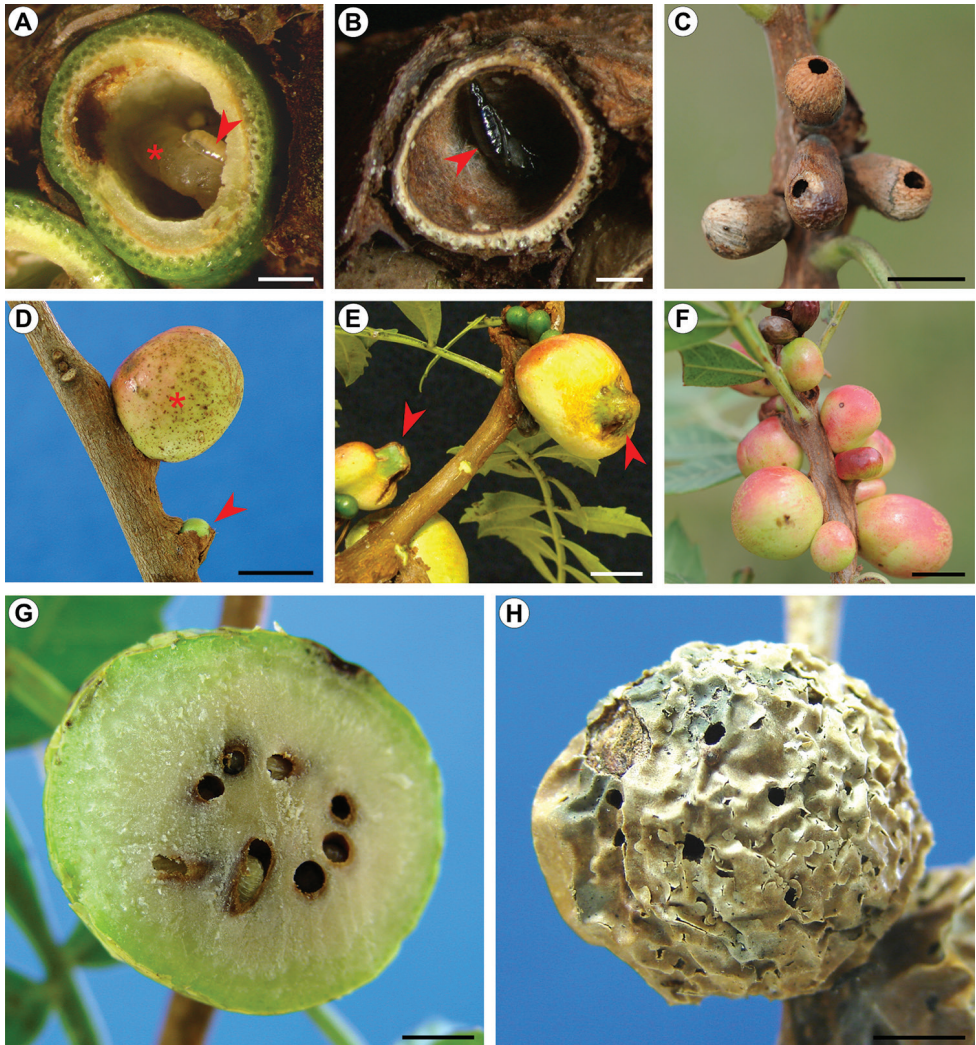


Figure 10. Hymenoptera fauna associated with *C. pampeanus* galls. **A** transversally sectioned, externally developing gall, showing inside a larva of *C. pampeanus* (asterisk) with attached larva (arrow) of *Lyracus* sp. (Pteromalidae) **B** transversally sectioned, dried gall, with pupa of *Lyracus* (arrow), after consumption of *C. pampeanus* larva **C** dried and empty attached galls showing orifices of emergence left by adults of *Lyracus* young, erupting, free of inquiline and adjacent inquiline attacked (*Allorhogas* sp., Braconidae) galls, indicated respectively by open arrow and asterisk **E** young galls of *C. pampeanus* (arrows) partially involved with gall tissue induced by inquilines **F** variation in size among *Allorhogas* galls early attacked **G** a full-developed inquiline-attacked gall showing larvae and pupae in cameras **H** senescent *Allorhogas* gall showing orifices of emergence (arrows) left by adults. Scale bars: 1 mm (**A, B, D, F**); 5 mm (**C**); 0.5 mm (**E, G, H**).

below ground and from which new sprouts emerge every year, starting in spring. At the type locality, the first flowers appear during November and the flowering season may last until March; fruits are found on plants from December to May. There is ap-

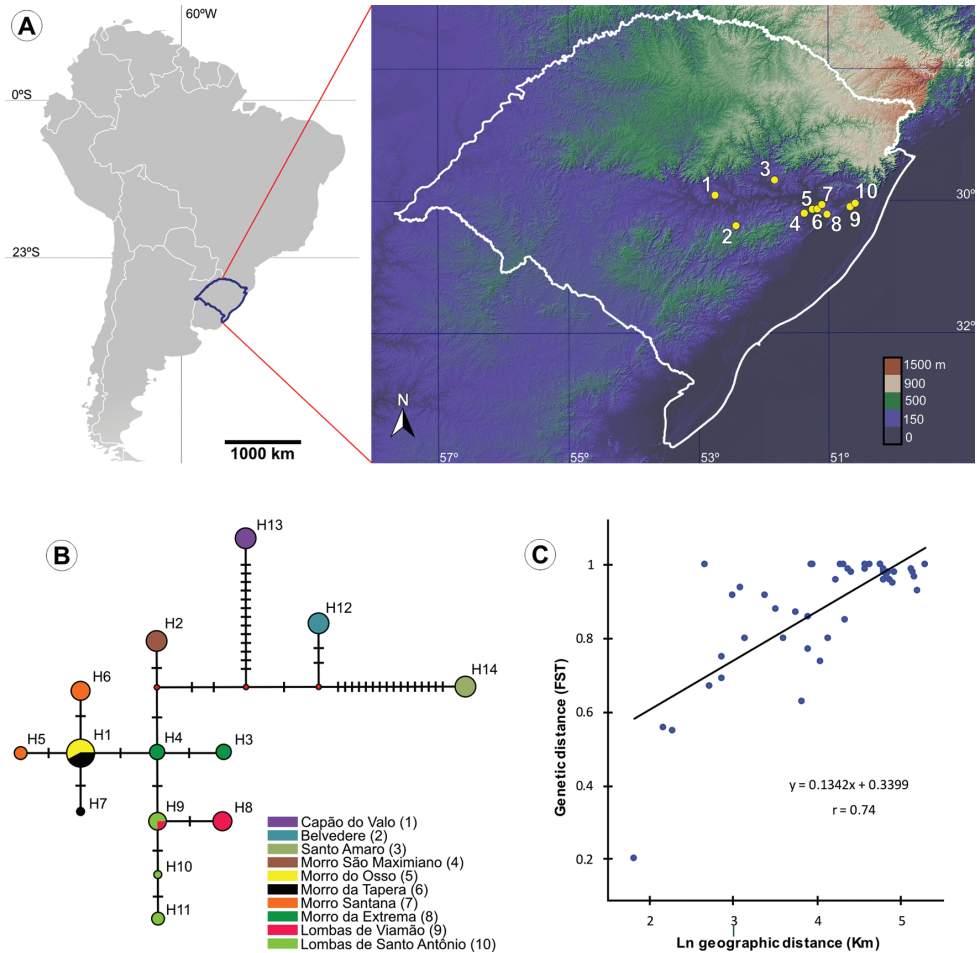


Figure 11. Geographic distribution and genetic variation among populations of *C. pampeanus* within Rio Grande do Sul State, Brazil; **A** localities of populations studied (see Suppl. material 3 for exact geographic coordinates and elevations) **B** evolutionary relationships of COI haplotypes across ten populations. The circles represent haplotypes; the diameter is proportional to the frequency in 60 analyzed individuals. Small red circles indicate intermediate vectors. Transversal bars represent mutational steps. Numbers in parentheses correspond to localities in the map (**A**) **C** correlation between pairwise geographic distance and estimates of gene flow (φ ST) ($P < 0.05$).

parently little if any vegetative growth during the winter, which is also the season when the aerial parts of *S. weinmannifolius* plants may wilt and die.

Population genetic structure. Inferences on the genetic variability of *C. pampeanus* resulted from 42 (3%) variable sites. Overall, haplotype (H_d) and nucleotide diversity (π) were 0.92 ± 0.01 and 0.0007 ± 0.0009 , respectively (Table 2). Individual populations presented H_d from 0.33 to 0.73 (P9 and P10, respectively) and π from 0.002 to 0.0013 (P9 and P10, respectively). A total of 14 haplotypes were found in

ten populations (Table 2; Fig. 11B). We found only one haplotype in each in P1 to P5; therefore, standard diversity indices and neutrality tests were not performed. From P6 to P9 two haplotypes per site were observed; P10 presented three haplotypes, the highest diversity. Except for H1 and H9, which were shared between P5/P6 and P9/P10 respectively, all were unique to each locality (Fig. 11B). Characterization of pairwise gene flow based on the F_{ST} index indicated significantly high levels of genetic structure in populations of *C. pampeanus*. Overall, F_{ST} ranged from 0.55 to 1 ($P < 0.05$) (Table 3). The lowest level observed was 0.20, between P5 and P6, not significant ($P > 0.05$). Spatial genetic structure assessed by the correlation between genetic and geographic distances indicated a significant pattern of isolation by distance for the ten populations ($r = 0.74$, $P < 0.01$) (Fig. 11C). Quantitative differentiation based on two groups of comparison reinforced the structure by distance pattern (Suppl. material 2). Both analyses (Jacuí River as a barrier and geographic distance) found similar values of F_{ST} (0.97; $P < 0.001$). However, when we grouped P2 with the cluster formed by P4 to P10 the divergence among groups was lower (46.45%; $P < 0.001$) than when we grouped it with P1 and P3 (58.73%; $P < 0.001$). Similarly, the divergence among populations within groups decreased from the first to the second scenario (51%, $P < 0.01$; 39.15%, $P < 0.001$, respectively).

Finally, analysis of demographic history by mismatch distribution indicated an overall multimodal pattern for *C. pampeanus* that is not compatible with a scenario of recent demographic expansion (Suppl. material 4). Single population analysis indicated a unimodal pattern, particularly for P9 that showed a possible scenario of expansion. In addition, overall neutrality tests yielded positive and non-significant values for all indices with respect to neutral expectations (Table 2). Single populations presented positive values, except P7 that showed negative values (but non-significant) for some parameters (i.e., Tajima's D and F_u and Li's D and F) and P9, that presented all negative (but non-significant) values.

Discussion

Taxonomy and phylogeny

Since it was proposed as a family by Brèthes (1916), the position of Cecidosidae remained for a long time uncertain until its affinity to the superfamily Adeloidea was clarified by Becker (1977), who regarded the group as endemic to South America. The affinity of *Scyrotis* with South American cecidosids was proposed later by Davis (1987). Molecular data provided here give further support to this taxonomic affinity, and show that the African *Scyrotis* are much older (ca. 90 Myr) than South American genera. Results also suggest there could exist more than one cecidosid lineage in Africa, since the two species we sequenced were 27% apart from each other in terms of genetic divergence in our analyses. The first studies on African cecidosids conducted by Meyrick (1909, 1913, 1928) clearly suggested the existence of at least three line-

Table 2. Summary of genetic variability of ten populations of *C. pampeanus* based on mitochondrial DNA sequences. Populations (Pop) are as follows: Capão do Valo (CV), Belvedere (Bel.), Santo Amaro (SA), Morro São Maximiliano (MSM), Morro do Osso (MO), Morro da Tapera (MT), Morro Santana (MS), Morro da Extrema (ME), Lombas de Viamão (LV) and Lombas de Sto. Antonio (LSA). Numbers from 1 to 14 indicate number of haplotypes found in each population. Hd, haplotype diversity; π , nucleotide diversity. Neutrality tests performed: Tajima's (D); Fu and Li's (D and F); Fu's (Fs). Asterisks indicate significant values, $P < 0.05$.

Pop.	Haplotypes														Hd	π	Neutrality tests			
	1	2	3	4	5	6	7	8	9	10	11	12	13	14			Tajima's	Fu and Li's		Fu's
																	D	D	F	Fs
CV													X		0.00	0.0000	–	–	–	–
Bel.														X	0.00	0.0000	–	–	–	–
SA														X	0.00	0.0000	–	–	–	–
MSM		X													0.00	0.0000	–	–	–	–
MO	X														0.00	0.0000	–	–	–	–
MT	X				X										0.53	0.0004	0.850	1.052	1.029	0.625
MS						X	X								0.33	0.0005	-1.131	-1.155*	-1.195	0.952
ME			X	X											0.60	0.0008	1.753	1.279	1.434	1.938
LV								X	X						0.33	0.0002	-0.933	-0.950*	-0.964	-0.003
LSA									X	X	X				0.73	0.0013	1.647	1.395	1.523	0.758
Overall															0.92	0.0068	-0.1362	1.775*	1.2683	2.886

ages of cecidosids, which can be separated by differences in the buccal apparatus of the adults. In fact, these lineages were initially grouped by him into different genera, which were later considered by Gozmány and Vári (1973) as synonyms of *Scyrotis* and treated as such ever since (for a detailed discussion, see Mey 2007). Two of these lineages are represented in our analysis by *Scyrotis* sp. and *S. granosa*; the former presents a rudimentary proboscis and maxillary palpi and the latter lacks such buccal structures. This question should be taken into account in revising the taxonomy and phylogeny of the family in the future, which is much needed. Although not linked to any *Scyrotis* species in particular, a field survey of galls conducted by van Noort et al. (2007) found them in association with several species of *Searsia* and suggested the existence not only of a wide variety of gall morphology but also considerable variation in life history styles among the African *Scyrotis*. It is unlikely that such variation will be conciliated within a single genus, which should be further explored. Unfortunately, this revision is pending upon description of the immature stages and gall morph types they induce, but as already said these aspects are still unknown for any African cecidosid species. The present study showed how valuable the inclusion of immature stages and galls is in taxonomic studies of cecidosids, whose adults in particular have relatively uniform morphology, especially regarding the genitalia (Mey 2007). In addition, our results support an accelerate evolutionary rate in all Cecidosidae lineages, as mentioned by Pellmyr and Leebens-Mack (1999) when a cecidosid (*C. eremita*) was used for the first time in a molecular phylogeny of Adeloidea. Similarly, Regier et al. (2015) in a family-level phylogenetic study based on 19 genes, found a high substitution rate in Cecidosidae when

including *C. eremita* and *D. capsulifex*, which they found in Incurvariidae as well. This faster evolution of cecidosids makes it difficult to resolve some internal evolutionary relationships within the group, generating phylogenetic uncertainties that are hard to overcome even by increasing markers, and should be further explored.

Cecidonius gen. n. resulted as a unique lineage in the present study from both morphological and molecular analyses. Also, interestingly, it appeared as one of the most recent lineages (ca. 24 Myr) to be evolved within the extant cecidosids. It diverged ca. 16% from the closest related lineage, an additional undescribed cecidosid taxon existing in Chile and Argentina, which was included in the present study for comparison. This undescribed taxon differs from *Cecidonius* by having adults that lack a rudimentary proboscis and having a three-segmented maxillary palpus, pupae bearing a gall-cutter with a different shape, larvae without long hair on thorax and galls with completely developed wall without basal orifice, and will be described elsewhere. Molecular findings also showed that although described as monotypic, there is at least one more species belonging to *Cecidonius*, associated with *Schinus terebinthifolius* Raddi, which is still awaiting description. This undescribed species diverged from *C. pampeanus* by more than 9% in DNA sequences. Its galls are conspicuous, morphologically different, and larger than those of *C. pampeanus*. They are relatively common in populations of *S. terebinthifolius* existing in southern Brazil. Unfortunately, we have no pupae or adults of this species yet, which apparently shares a similar life-history style and associated difficulties regarding rearing of *C. pampeanus*.

Life history

It took us a few years to obtain the small number of *C. pampeanus* pupae and adults used for description in this study. Although relatively abundant as young larvae when still under the bark of swollen stems, later instars of *C. pampeanus* occur at low density in the field. Collection of mature, dehiscent galls during later summer, either using cloth bags attached to the plants or picking by hand those that had naturally dropped to soil, always led to failure regarding development under laboratory conditions. Dissection of these galls demonstrated that larvae do not pupate, remaining alive in the last larval instar for months, eventually dying without any apparent cause. Interestingly, similar difficulties regarding rearing of *C. pampeanus* are also mentioned by Meyrick (1917) in relation to the African *Scyrotis*. *Cecidonius pampeanus* apparently diapauses for months in the last instar larva, which stays motionless within its dehiscent gall in the soil until pupation and adult emergence occur in the next growing season. Probably this species presents a seasonal adaptation (*sensu* Tauber, Tauber and Masaki 1986) to overcome the unfavourable low temperatures that prevent growth during winter, and also adjust its life cycle to the host plant phenology. As already mentioned, new growth shoots that are required for gall induction (Raman 1994, Yukawa 2000) start appearing on *S. weinmannifolius* plants during the spring. This time of the year coincides with adult emergence in the field, and supposedly also with oviposition in *C. pampeanus*. A group of approximately 20 galls were collected in the field by the first author during winter

Table 3. Pairwise estimates of gene flow based on φ -statistics (φ_{ST}) for cytochrome oxidase subunit I mitochondrial sequences in nine populations *C. pampeanus*. All comparisons were statistically significant ($P < 0.05$), except the value in bold.

	Capão do Valo	Belvedere	Santo Amaro	Morro São Maximiano	Morro do Osso	Morro da Tapera	Morro Santana	Morro da Extrema	Lombas de Viamão	Lombas de Santo Antônio
Capão do Valo	–									
Belvedere	1.0000	–								
Santo Amaro	1.0000	1.0000	–							
Morro São Maximiano	1.0000	1.0000	1.0000	–						
Morro do Osso	1.0000	1.0000	1.0000	1.0000	–					
Morro da Tapera	0.9846	0.9636	0.9875	0.9200	0.2000	–				
Morro Santana	0.9814	0.9583	0.9848	0.9166	0.6666	0.5500	–			
Morro da Extrema	0.9818	0.9538	0.9853	0.8800	0.8000	0.6909	0.7466	–		
Lombas de Viamão	0.9906	0.9787	0.9923	0.9565	0.9411	0.8631	0.8695	0.8000	–	
Lombas de Santo Antônio	0.9682	0.9276	0.9740	0.8521	0.8000	0.7368	0.7652	0.6285	0.5600	–

and kept under room temperature in the laboratory within plastic vials containing moist soil from the type locality. A few were dissected at fifteen-day intervals, rendering only last instar larvae. The first pupa in this case appeared in spring (October), and the adults, which were used in the present description, *ca.* one month later. The token stimuli that initially trigger and later break the diapause in *C. pampeanus* remain to be determined. We may speculate from above that the corresponding stimuli may be received during autumn by the dehiscent galls that are already in the soil.

Inquiline and parasitoid wasps

Allorhogas species are among a few braconid wasps having a phytophagous feeding habit. They are apparently relatively common and widespread in the Neotropics, all associated with galls, occurring in several plant families including Burseraceae, Fabaceae, Melastomataceae, Polygonaceae, Rubiaceae, and Solanaceae (e.g., Macedo and Monteiro 1989, Marsh et al. 2000, Marsh 2002, Pentead-Dias and Carvalho 2008, Chavarría et al. 2009, Centrella and Shaw 2010, 2013, Martínez et al. 2011, Martínez and Zaldívar-Riverón 2013). However, their biology is largely unknown, and it is still uncertain whether they are primary gall inducers or inquilines. A clear pattern always emerged during dissections of hundreds of galls from several *S. weinmannifolius* populations in the present study, demonstrating that they are inquilines. First, they were never found inside young galls that were located under swollen stem bark, where only young larvae

of *C. pampeanus* were always present. Second, erupted galls bearing either free-living *C. pampeanus* larvae or those attacked by *Lyracus* ectoparasitoids do not change their shape, but only those bearing *Allorhogas* that turn from cylindrical into globular galls. Third, *Allorhogas* immatures were always found within older, erupted and much larger, shaped-modified galls, where larvae of *C. pampeanus* were found dead. Fourth, as already described, a progressive transition in shape between galls free from such inquilines (cylindrical) to those attacked by them (globular) is found in the field, always in association with early development of *Allorhogas* larvae. Most of the *Allorhogas* studies listed above have a taxonomic bias and are based on descriptions of adults reared during extensive surveys, without including descriptions of immature stages. They lack information on gall ontogeny, and most importantly, about identification of trophic levels of insects present within these galls. Thus, the biological status of *Allorhogas* in those gall systems should be re-examined, since some of them may not induce galls but act as inquilines, the true gall inducers being either underexplored or missed in such cases.

Similar to what was described for the *Scyrotis* galls attacked by *Rhoophilus* Loewi (Hymenoptera: Cynipidae) inquilines (van Noort et al. 2007), space for a *C. pampeanus* larva within a given gall is progressively diminished with the development of tissues induced by *Allorhogas* larvae. In fact, in several cases in the present study during the dissections of medium-sized developing galls bearing *Allorhogas* inquilines, a dead *C. pampeanus* larva was found within a compressed space inside. From a gross morphology perspective, tissues induced to develop by *Allorhogas* are clearly different from those induced by the original inducer *C. pampeanus*, regarding thickness, consistency, and colour. In general, tissues present in insect galls are complex, and may structurally vary even within a given gall lineage (Stone and Schönrogge 2003). Specially the nutritious ones, which are absent on ungalled host plants, may also vary in complexity at a very fine scale not only among but also within galls. For example, when tissues produced by lepidopterans and hymenopterans are compared, differences between them emerge at the cell level in relation to the type, quantity, local and disposition of chemicals they store, among other characteristics (e.g., Ferreira and Isaias 2013, Vecchi et al. 2013). These tissues are used for feeding by the corresponding inducers independently, that is within their own distinctly located galls. This is not the case in the present system, where such tissues are induced by distantly related insect lineages and occur within the same gall. Thus, we suggest that tissues induced by *Allorhogas* species may inhibit feeding by *C. pampeanus*, whose larvae, by being confined in space, completely surrounded by tissues unsuitable for feeding, would be lead to death by inanition.

Additional field observations suggest that the existence of an inquiline association between *Allorhogas* species and galls of other cecidosids is common in southern Brazil. This is the case of the gall induced in *S. terebinthifolius* by the undescribed, additional species of *Cecidoniuss* already mentioned, as well as of those induced in *S. polygamus* by *C. eremita* and *E. minutanus*. Thus it seems that these braconid wasps parallel in the Neotropics the cynipid wasps that are inquilines of cecidosid galls in Africa (van Noort et al. 2007). Cynipids are found in South America, not acting as inquilines but as primary gall inducers, as for example in Fabaceae (e.g., Nieves-Aldrey and San Blas

2015). Unfortunately, little is known about the biology of the Neotropical species of *Lycrus*. They are diverse and difficult to identify in the Nearctic region, where many are important parasitoids of agricultural pests, primarily belonging to Coleoptera and Diptera (Gibson GAP, Agriculture and Agri-Food Canada, pers. comm.). According to preliminary observations there are additional insect species yet to be explored in association with *C. pampeanus* galls, including cecidophages, predators, hyperparasitoids and successors that use them as shelter. The latter may include other arthropods and are common in cecidosid galls, since some of these galls may last for years after adult emergence and thus be used by other insects for shelter and even for nesting (e.g., Wille 1926, Laroca 1972). We hope this study will stimulate additional studies on this topic, thus revealing fully the hidden diversity existing in association with these galls.

Genetic diversity and conservation biology

Our study provides strong evidence that *C. pampeanus* is under threat of extinction, and protection measures should be taken to conserve its remaining populations. The reasons are based primarily on the destruction of the host plant habitat. Open savannas of southern Brazil (= Brazilian 'Campos') where populations of *S. weinmannifolius* are found have been suffering from anthropic influence for decades, mostly caused by agriculture in general and/or cattle ranching, and recently from widespread expansion of *Eucalyptus* L'Heritier, *Acacia* Martius and *Pinus* Linnaeus plantations (Overbeck et al. 2007, Cordeiro and Hasenack 2009). A search by the first author for populations of *S. weinmannifolius* of which older dried material is preserved in the main herbaria in the region (e.g., UFPR/ Curitiba, Barbosa Rodrigues/Itajai; and UFRGS/Porto Alegre), suggested that most of these have disappeared since. In Parana state, for example, extant populations seem to be restricted to a few places, including the preserved area of Parque de Vila Velha, Ponta Grossa municipality. In Rio Grande do Sul scattered populations were located on high elevation steppes, as for example in Canela and São Francisco de Paula municipalities, and particularly at low elevations in the western portions of the Pampa biome. However, as already mentioned, extant populations of *S. weinmannifolius* bearing galls of *C. pampeanus* were restricted to small patches in the latter area. More importantly, these populations are distant and isolated from each other. Most of them are located at higher elevation, such as on hilltops and hill slopes interspersed with small bushes as already mentioned, where they are relatively more protected from anthropic influence. At least two of these areas (Morro do Osso and Morro Santana) are officially protected areas already, but the remaining populations are located on private property. *Schinus weinmannifolius* is considered a pasture weed, supposedly unpalatable to livestock, the reason for which we presume it has disappeared from most low elevation areas, where agriculture and cattle ranching prevail as the main economic activities. *Schinus weinmannifolius* is apparently heliophilous, and in consequence does not grow satisfactorily within plantations such as those composed of *Eucalyptus*, *Acacia* or *Pinus*, also common in the region.

There is no indication that adults of cecidosids feed actively, last long and disperse much; oviposition supposedly occurs on the plants surrounding those where they developed as immatures (e.g., San Blas and Davis 2013). The limited dispersal together with low connected patches of *S. weinmannifolius* resulted in ‘island’ populations of *C. pampeanus* with reduced variability. Moreover, high genetic structure and partition of variation based on geography corroborated a pattern of isolation by distance. The restricted distribution and small population sizes are important causes of reduced genetic diversity (Hamrick and Godt 1989), since the effects of natural selection and/or demographic changes may be more pronounced in such populations (Ellstrand and Elam 1993, Gibson et al. 2008). The low variability found in *C. pampeanus* possibly makes the species vulnerable for novel selection pressure. Whether populations would be affected by stochastic processes, particularly genetic drift, depends on gene flow within and among populations, among other ecological factors. We found significantly low levels of gene flow among populations of *C. pampeanus*. Haplotypes were mainly unique to each locality, except between Morro do Osso/Morro Tapera and Lombas de Viamão/Lombas de Santo Antônio; even so, the latter presented significant high F_{ST} values.

The low number of nucleotide differences between the haplotype pairs (except for H12, H13 and H14) and a multimodal curve in the mismatch distribution analysis of *C. pampeanus* indicate that population expansion is unlikely to have occurred. In contrast, the population of Lombas de Viamão presented an expansion pattern. According to Rogers and Harpending (1992) and Tajima (1989), bottlenecks may generate waves in the distribution of pairwise nucleotide differences. However, contrary to expansion, a population contraction leads to maintenance of genetic diversity over time. In a bottleneck model individuals differ in the average number of nucleotide changes when taken randomly from a given population. Such an effect leads to multipeak nucleotide distributions, as well as large pairwise differences between them (Harpending et al. 1998, Rogers and Harpending 1992). Additionally, when estimated by median-joining, the haplotype topology also did not support a population expansion scenario, as it did not fit into a typical star-like model (Harpending et al. 1998, Slatkin and Hudson 1991). The results suggest that demographic changes in populations of *C. pampeanus* are a consequence of ancient historical processes and recent decline, likely due to landscape disturbance.

The above-mentioned higher trophic level-associated fauna may be also under threat, considering that its existence depends on the success of *C. pampeanus*, the primary gall inducer. In other words, a whole community associated with *C. pampeanus* galls may go extinct in South Brazil, even before species that integrate it have been described, in the case of extinction of the primary gall inducer. A survey should be carried out to identify the unknown fauna associated with these galls. We also suggest that additional studies should examine the degree of specificity and inter-dependence of this fauna with *C. pampeanus* and its host plant. These actions should be prioritized when planning the corresponding conservation measures, since they are prerequisite to their implantation. Protection measures have been scarcely taken in relation to the

lepidopteran species that are under threat of extinction in the Neotropical region. In Brazil, actions in this regard have involved primarily the butterflies, in total 55 species that are officially considered under threat of extinction (Freitas and Marini-Filho 2011). However, microlepidoptera and associated plants are largely unknown in this country due to a corresponding taxonomic impediment (Aguilar et al. 2009), and thus they have been completely neglected from a conservation biology perspective. Within the gall-inducer and leaf-miner micromoths there are many species that are specialists on rare and/or endemic plants, particularly in the Brazilian Atlantic Forest, most yet to be discovered and/or described (Luz et al. 2014, Moreira et al. 2017). By being dependent on endemic hosts at a regional scale, these species in particular are under comparatively greater threat, because most of such plants are restricted in distribution (Lewinsohn et al. 2005). This study is apparently the first to suggest that a micromoth and its associated fauna should be taken into account in this regard in Brazil. It is also important to emphasize that the restricted number of extant *C. pampeanus* populations are located within the southern Brazilian “Campos” (= Pampean savanna) that is considered a diverse but neglected biome from a conservation biology perspective (Overbeck et al. 2007), and where no moth has ever been targeted from a conservation biology perspective.

Further remarks

This study also showed how important intensive, integrative taxonomic studies are to identify accurately the role of a cecidosid species in a given gall community. *Cecidonijs pampeanus* attracted our attention ca. 10 years ago as a cecidosid lineage by comparison of DNA sequences extracted from the larval stage, dissected from under the bark of swollen stems of *S. weinmannifolius*. For several years, its identification remained provisional, tied only to DNA similarity to other cecidosids, since for this new species morphology of the last larval instar, found later in the field, was also atypical compared to any known cecidosid. Full confirmation of the existence of this new lineage came when we finally obtained their pupae and reared them to adults. We inferred that the absence of such an approach led Tavares (1909: 8) to identify the true inducers of such *S. weinmannifolius* galls as “... *probabiliter Cynips incognita*” [... probably an undescribed *Cynips* Linnaeus species]. This action has prevented unraveling not only the true gall inducer, but also the diversity of fauna associated with such galls for more than a century, since his rationale was followed without being questioned by other authors (e.g., Wille 1926, Houard 1933, Sáiz and Núñez 1997). In other words, from Tavares’ original description until the present study, such galls have been treated as two trophic level systems, and their induction was erroneously associated with an unidentified species of Cynipidae (Hymenoptera). The Portuguese Jesuit priest Joaquim da Silva Tavares, also a naturalist who first described these galls, was a pioneer in the study and description of Brazilian cecidology during the first quarter of the last century. His descriptions were accurate and finely

illustrated, but most of them were based on the gall morph type only, not always being associated with precise identification of the corresponding inducers. We suppose the large and colourful *Allorhogas*-bearing galls, which appear as neat black and white photographs in his publication (Plate VIIi, figs 22, 23), called his attention to *S. weinmannifolius* plants at first sight in the field. As already mentioned, free-living external galls bearing *C. pampeanus* larvae are rarely found on *S. weinmannifolius* plants in the field, most being killed by *Lycrus* parasitoids, and thus they may never have been encountered by him. That is, the gall phenotype that is modified by the *Allorhogas* inquilines would have misguided him and led him to suggest the primary induction of such galls to be by cynipid wasps, based on the immature stages obtained when dissecting such galls, since those dissections were also illustrated by him (Plate VIII; figs 24, 25). He apparently did not rear to the adult stage of the assumed cynipid species at that time, since later on when working with the Brazilian melastomatacean galls he made comments on his disappointment about not ever having had a Brazilian cynipid specimen in his collection (Tavares 1917, p.19). In the same publication, he indirectly admitted having erroneously thought at first that these melastomatacean galls also looked like those induced by cynipids in Europe, but that he had changed his mind after having surprisingly obtained the first adult Lepidoptera reared from them.

Acknowledgements

Thanks are due to Prefeitura Municipal de Porto Alegre (Porto Alegre city), Nelson Matzemberger (Eldorado do Sul) and Antonio Malta (Santo Antonio da Patrulha), for allowing us to collect the specimens in areas under their care, and for providing assistance with field work. Gerson Buss, Rosângela Brito, Leonardo Re Jorge and Gislane von Poser (UFRGS), Gabriel Melo, the late Lucas Beltrami and Eduardo Carneiro (UFPR) assisted with field collections. Héctor Vargas (Universidad de Arica, Chile) and Germán San Blas (CONICET- Universidad Nacional de La Pampa, Argentina) provided cecidosid specimens for comparison. André Martins and Gabriel Melo (UFPR) identified the parasitoid and inquiline wasps, respectively. We acknowledge the staff members of CME/UFRGS and Thales O. Freitas (UFRGS) for the use of facilities and assistance with scanning electron microscopy and molecular analyses, respectively. Thanks are also due to Lafayette Eaton for editing the text. We are also grateful to Erik J. van Nieukerken (Naturalis Biodiversity Center, Netherlands), Carlos Lopez-Vaamonde (INRA, France) and Germán San Blas for suggestions that improved substantially the last version of the manuscript. G. L. Gonçalves, G.T. Silva and G.R.P. Moreira were supported by fellowships from CAPES/PNPd, CAPES/PPG-Ban/UFRGS and CNPq, respectively. R.P. Eltz and R.B. Pase were supported by the undergraduate research program of PROPESQ/UFRGS.

References

- Aguiar AP, Santos BF, Couri MS, Rafael JA, Costa C, Ide S, Duarte M, Grazia J, Schwertner CF, Freitas AVL, Azevedo CO (2009) Insecta. In: Rocha RM, Boeger WA (Orgs) Estado da Arte e Perspectivas para a Zoologia no Brasil. Editora UFPR, Curitiba, Brazil, 131–155.
- Bandelt HJ, Foster P, Röhl A (1999) Median-joining networks for inferring intraspecific phylogenies. *Molecular Biology and Evolution* 16: 37–48. <https://doi.org/10.1093/oxfordjournals.molbev.a026036>
- Barkley FA (1957) A study of *Schinus* L. *Lilloa* 28: 1–110.
- Becker VO (1977) The taxonomic position of the Cecidosidae Brèthes (Lepidoptera). *Polskie Pismo Entomologiczne* 47: 79–86.
- Bouckaert R, Heled J, Kuhnert D, Vaughan T, Wu C-H, Xie D, Suchard MA, Rambaut A, Drummond AJ (2014) BEAST 2: a software platform for Bayesian evolutionary analysis. *PLoS Computational Biology* 10: e1003537. <https://doi.org/10.1371/journal.pcbi.1003537>
- Brèthes J (1916) Estudio fito-zoológico sobre algunos lepidópteros Argentinos productores de agallas. *Anales de la Sociedad Científica Argentina* 82: 113–140.
- Brooks SE, Shorthouse JD (1988) Developmental morphology of stem galls of *Diplolepis nodulosa* (Hymenoptera: Cynipidae) and those modified by the inquiline *Periclistus pirata* (Hymenoptera: Cynipidae) on *Rosa blanda* (Rosaceae). *Canadian Journal of Botany* 76: 365–381.
- Cabrera AL (1938) Revisión de las Anacardiáceas Austroamericanas. *Revista del Museo de La Plata* 2: 3–64.
- Centrella ML, Shaw SR (2010) A new species of phytophagous braconid *Allorhogas minimus* (Hymenoptera: Braconidae: Doryctinae) reared from fruit galls on *Miconia longifolia* (Melastomataceae) in Costa Rica. *International Journal of Tropical Insect Science* 30: 101–107. <https://doi.org/10.1017/S1742758410000147>
- Centrella ML, Shaw SR (2013) Three new species of gall-associated *Allorhogas* wasps from Costa Rica (Hymenoptera: Braconidae: Doryctinae). *International Journal of Tropical Insect Science* 33: 145–152. <https://doi.org/10.1017/S1742758413000143>
- Chavarría L, Hanson PE, Marsh PM, Shaw SR (2009) A phytophagous braconid, *Allorhogas conostegia* n.sp. (Hymenoptera: Braconidae), in the fruits of *Conostegia xalapensis* (Bonpl.) D. Don (Melastomataceae). *Journal of Natural History* 43: 2677–2689. <https://doi.org/10.1080/00222930903243996>
- Cordeiro LP, Hasenack H (2009) Cobertura vegetal atual do Rio Grande do Sul. In: Pillar VP, Muller SC, Castilhos ZMS, Jacques AVA (Eds) Campos sulinos: Conservação e uso sustentável da biodiversidade. Ministério do Meio Ambiente, Brasília, 285–299.
- Darriba D, Taboada GL, Doallo R, Posada D (2012) jModelTest 2: more models, new heuristics and parallel computing. *Nature Methods* 9: 772. <https://doi.org/10.1038/nmeth.2109>
- Davis DR (1987) Heliozelidae (Incurvarioidea). In: Stehr FW (Ed.) *Immature insects*. Kendall/Hunt Publishing Company, Dubuque, 354–355.
- Davis DR (1998) The monotrysian Heteroneura. In: Kristensen NP (Ed.) *Lepidoptera, Moths and Butterflies*, vol. 1: Evolution, Systematics and Biogeography. *Handbook of Zoology* 4(35), Walter de Gruyter, Berlin, 65–90. <https://doi.org/10.1515/9783110804744.65>

- Drummond AJ, Ho SYW, Phillips MJ, Rambaut A (2006) Relaxed phylogenetics and dating with confidence. *PLoS Biology* 4: e88. <https://doi.org/10.1371/journal.pbio.0040088>
- Drummond AJ, Rambaut A (2007) Beast: Bayesian evolutionary analysis by sampling trees. *BMC Evolutionary Biology* 7: 214. <https://doi.org/10.1186/1471-2148-7-214>
- Ellstrand NC, Elam DR (1993) Population genetic consequences of small population size: implications for plant conservation. *Annual Review of Ecology and Systematics* 24: 217–242. <https://doi.org/10.1146/annurev.es.24.110193.001245>
- Excoffier L, Lischer HE (2010) Arlequin suite ver 3.5: a new series of programs to perform population genetics analyses under Linux and Windows. *Molecular Ecology Resources* 10: 564–567. <https://doi.org/10.1111/j.1755-0998.2010.02847.x>
- Excoffier L, Smouse PE, Quattro JM (1992) Analysis of molecular variance inferred from metric distances among DNA haplotypes: Application to human mitochondrial DNA restriction data. *Genetics* 131: 479–491.
- Ferreira BG, Isaias RMS (2013) Developmental stem anatomy and tissue redifferentiation induced by a galling Lepidoptera on *Marcetia taxifolia* (Melastomataceae). *Botany* 91: 752–760. <https://doi.org/10.1139/cjb-2013-0125>
- Flieg M (1987) Anacardiaceae. *Boletim Instituto de Biociências* 42: 1–72. [Flora Ilustrada do Rio Grande do Sul, 18]
- Flieg M (1989) Anacardiáceas. In: Reitz R (Ed.) *Flora Ilustrada Catarinense*. Herbário Barbosa Rodrigues, Itajaí, 1–64.
- Freitas AVL, Marini-Filho OJ (Orgs) (2011) Plano de ação nacional para conservação dos lepidópteros ameaçados de extinção. Instituto Chico Mendes de Conservação da Biodiversidade. Brasília, 124 pp. [Série Espécies Ameaçadas, 13]
- Gibson JP, Rice SA, Stucke CM (2008) Comparison of population genetic diversity between a rare, narrowly distributed species and a common, widespread species of *Alnus* (Betulaceae). *American Journal of Botany* 95: 588–596. <https://doi.org/10.3732/ajb.2007316>
- Gozmány LA, Vári L (1973) The Tineidae of the Ethiopian Region. *Transvaal Museum Memoir* 18: 1–238.
- Guindon S, Dufayard JF, Lefort V, Anisimova M, Hordijk W, Gascuel O (2010) New algorithms and methods to estimate Maximum-Likelihood phylogenies: assessing the performance of PhyML 3.0. *Systematic Biology* 59: 307–21. <https://doi.org/10.1093/sysbio/syq010>
- Hamrick JL, Godt MJW (1989) Allozyme diversity in plant species. In: Brown AHD, Clegg MT, Kahler AL, Weir BS (Eds) *Plant population genetics, breeding and genetic resources*. Sinauer, Sunderland, 43–63.
- Harpending HC, Batzer MA, Gurven M, Jorde LB, Rogers AR, Sherry ST (1998) Genetic traces of ancient demography. *Proceedings of the National Academy of Sciences* 95: 1961–1967. <https://doi.org/10.1073/pnas.95.4.1961>
- Hoare RJB, Dugdale JS (2003) Description of the New Zealand incurvariid *Xanadoses nielseni*, gen. n., sp. n. and placement in Cecidosidae (Lepidoptera). *Invertebrate Systematics* 17: 47–57. <https://doi.org/10.1071/IS02024>
- Houard C (1933) *Les zoocécidies des Plantes de l'Amérique du Sud et de l'Amérique Centrale*. Librairie Scientifique Hermann et Cie, Paris, 519 pp.

- Kristensen NP (2003) Skeleton and muscles: adults. In: Kristensen NP (Ed) Lepidoptera: Moths and Butterflies, vol. 2: Morphology, Physiology, and Development. Handbook of zoology 4(36), Walter de Gruyter, Berlin, 39–131. <https://doi.org/10.1515/9783110893724.39>
- Laroca S (1972) Notas sobre a biologia de *Hylaeus cecidonastes* Moure (Hymenoptera, Apoidea). Revista Brasileira de Biologia 32: 285–289.
- Librado P, Rozas J (2009) DnaSP v5: a software for comprehensive analysis of DNA polymorphism data. Bioinformatics 25: 1451–1452. <https://doi.org/10.1093/bioinformatics/btp187>
- Luz CLS (2011) Anacardiaceae R. Br. na flora fanerogâmica do Estado de São Paulo. Unpublished M.Sc. Thesis, São Paulo: Universidade de São Paulo.
- Luz FA, Gonçalves GL, Moreira GRP, Becker VO (2014) Three new cecidogenous species of *Palaeomystella* Fletcher (Lepidoptera, Momphidae) from the Brazilian Atlantic Rain Forest. ZooKeys 433: 97–127. <https://doi.org/10.3897/zookeys.433.7379>
- Luz FA, Gonçalves GL, Moreira GRP, Becker VO (2015) Description, molecular phylogeny, and natural history of a new kleptoparasitic species of gelechiid moth (Lepidoptera) associated with Melastomataceae galls in Brazil. Journal of Natural History 49: 1849–1875. <https://doi.org/10.1080/00222933.2015.1006284>
- Macedo MV, Monteiro RT (1989) Seed predation by a braconid wasp *Allorhogas* sp. (Hymenoptera). Journal of the New York Entomological Society 97: 358–362.
- Mantel N (1967) The detection of disease clustering and a generalized regression approach. Cancer Research 27: 209–220.
- Marsh PM (2002) The Doryctinae of Costa Rica (excluding the genus *Heterospilus*). Memoirs of the American Entomological Institute 70: 1–319.
- Marsh PM, Macedo MV, Pimentel MCP (2000) Descriptions and biological notes on two new phytophagous species of the genus *Allorhogas* from Brazil (Hymenoptera: Braconidae: Doryctinae). Journal of Hymenoptera Research 9: 292–297.
- Martínez JJ, Altamirano A, Salvo A (2011) New species of *Allorhogas* (Hymenoptera: Braconidae) reared from galls on *Lycium cestroides* Schtdl. (Solanaceae) in Argentina. Entomological Science 14: 304–308. <https://doi.org/10.1111/j.1479-8298.2011.00453.x>
- Martínez JJ, Zaldívar-Riverón A (2013) Seven new species of *Allorhogas* (Hymenoptera: Braconidae: Doryctinae) from Mexico. Revista Mexicana de Biodiversidad 84: 117–139. <https://doi.org/10.7550/rmb.31955>
- Mey W (2007) Cecidosidae (Lepidoptera: Incurvarioidea). In: Mey W (Ed.) The Lepidoptera of the Brandberg Massif in Namibia. Esperiana Memoir 4: 31–48.
- Meyrick E (1909) New South African Micro-Lepidoptera. Annals of the South African Museum 5: 349–379.
- Meyrick E (1913) Description of South African Micro-Lepidoptera. 4. Annals of the Transvaal Museum 3: 267–336.
- Meyrick E (1917) A jumping cocoon. Entomologist's Monthly Magazine 53: 62.
- Meyrick E (1928) Tineidae. Exotic Microlepidoptera 3: 429.
- Moreira GRP, Gonçalves GL, Eltz RP, San Blas G, Davis DR (2012) Revalidation of *Oliera* Brèthes (Lepidoptera: Cecidosidae) based on a redescription of *O. argentinana* and DNA analysis of Neotropical cecidosids. Zootaxa 3557: 1–19

- Moreira GRP, Pollo P, Brito R, Gonçalves GL, Vargas HÁ (2017) *Cactivalva nebularia*, gen. et sp. nov. (Lepidoptera: Gracillariidae): a new *Weinmannia* leaf miner from southern Brazil. *Austral Entomology*. <https://doi.org/10.1111/aen.12267>
- Morris DC, Mound LA, Schwarz MP (2000) *Advenathrips inquilinus*: a new genus and species of social parasites (Thysanoptera: Phlaeothripidae). *Australian Journal of Entomology* 39: 53–57. <https://doi.org/10.1046/j.1440-6055.2000.00146.x>
- Morrone JJ (2006) Biogeographic areas and transition zones of Latin America and the Caribbean Islands base on panbiogeographic and cladistics analyses of the entomofauna. *Annual Review of Entomology* 51: 467–94. <https://doi.org/10.1146/annurev.ento.50.071803.130447>
- Nieves-Aldrey JL, San Blas G (2015) Revision of the Neotropical genus *Eschatocerus* Mayr (Hymenoptera, Cynipidae, Eschatocerini) with biological notes and the first description of the terminal larva. *Zootaxa* 4012: 135–155. <https://doi.org/10.11646/zootaxa.4012.1.7>
- Nieukerken EJ van, Kaila L, Kitching IJ, Kristensen NP, Lees DC, Minet J, Mitter C, Mutanen M, Regier JC, Simonsen TJ, Wahlberg N, Yen S-H, Zahiri R, Adamski D, Baixeras J, Bartsch D, Bengtsson BÅ, Brown JW, Bucheli SR, Davis DR, De Prins J, De Prins W, Epstein ME, Gentili-Poole P, Gielis C, Hättenschwiler P, Hausmann A, Holloway JD, Kallies A, Karshol O, Kawahara A, Koster JC, Kozlov MV, Lafontaine JD, Lamas G, Landry J-F, Lee S, Nuss M, Park K-T, Penz C, Rota J, Schmidt BC, Schintlmeister A, Sohn JC, Solis MA, Tarmann GM, Warren AD, Weller S, Yakovlev VR, Zolotuhin VV, Zwick A (2011) Order Lepidoptera. In: Zhang Z-Q (Ed.) *Animal biodiversity: An outline of higher-level classification and survey of taxonomic richness*. *Zootaxa* 3148: 212–221.
- Noort S van, Stone GN, Whitehead VB, Nieves-Aldrey J-L (2007) Biology of *Rhoophilus loewi* (Hymenoptera: Cynipoidea: Cynipidae), with implications for the evolution of inquilinism in gall wasps. *Biological Journal of the Linnean Society* 90: 153–172. <https://doi.org/10.1111/j.1095-8312.2007.00719.x>
- Overbeck GE, Muller SC, Fidelisa A, Fadenhauer JP, Pillar VP, Blanco CC, Boldrini II, Both R, Forneck ED (2007) Brazil's neglected biome: The South Brazilian Campos. *Perspectives in Plant Ecology, Evolution and Systematic* 9: 101–116. <https://doi.org/10.1016/j.ppees.2007.07.005>
- Pellmyr O, Leebens-Mack JH (1999) Forty million years of mutualism: evidence for Eocene origin of yucca–yucca moth association. *Proceedings National Academy of Science* 96: 9178–9183. <https://doi.org/10.1073/pnas.96.16.9178>
- Penteado-Dias AM, Carvalho FM (2008) New species of Hymenoptera associated with galls on *Calliandra brevipes* Benth. (Fabaceae, Mimosoidea) in Brazil. *Revista Brasileira de Entomologia* 52: 305–310. <https://doi.org/10.1590/S0085-56262008000300001>
- Raman A (1994) Adaptation integration between gall-inducing insects and their host plants. In: Anathakrishnan TN (Ed.) *Functional dynamics of phytophagous insects*. Science Publishers, Lebanon, 249–275.
- Rambaut A (2009) Molecular evolution, phylogenetics and epidemiology: FigTree. <http://tree.bio.ed.ac.uk/software/figtree/>

- Regier JC, Mitter C, Kristensen NP, Davis DR, van Nieukerken EJ, Rota J, Simonsen TJ, Mitter KT, Kawahara AY, Yen S-H, Cummings MP, Zwick A (2015) A molecular phylogeny for the oldest (nonditrysian) lineages of extant Lepidoptera, with implications for classification, comparative morphology and life-history evolution. *Systematic Entomology* 40: 671–704. <https://doi.org/10.1111/syen.12129>
- Rogers AR, Harpending H (1992) Population growth makes waves in the distribution of pairwise genetic differences. *Molecular Biology and Evolution* 9: 552–569.
- San Blas G, Davis DR (2013) Redescription of *Dicranoses capsulifex* Kieffer and Jörgensen (Lepidoptera: Cecidosidae) with description of the immature stages and biology. *Zootaxa* 3682: 371–384. <https://doi.org/10.11646/zootaxa.3682.2.9>
- Sáiz F, Núñez C (1997) Estudio ecológico de las cecidias del género *Schinus*, especialmente las de hoja y de rama de *S. polygamus* y *Schinus latifolius* (Anacardiaceae), en Chile Central. *Acta Entomológica Chilena* 21: 39–59.
- Schneider S, Excoffier L (1999) Estimation of past demographic parameters from the distribution of pairwise differences when the mutation rates vary among sites: Application to human mitochondrial DNA. *Genetics* 152: 1079–1089.
- Schwarz GE (1978) Estimating the dimension of a model. *Annals of Statistics* 6: 461–464. <https://doi.org/10.1214/aos/1176344136>
- Slatkin M, Hudson RR (1991) Pairwise comparisons of mitochondrial DNA sequences in stable and exponentially growing populations. *Genetics* 129: 555–562.
- Stone GN, Schönrogge K (2003) The adaptive significance of insect gall morphology. *Trends in Ecology and Evolution* 18: 512–522. [https://doi.org/10.1016/S0169-5347\(03\)00247-7](https://doi.org/10.1016/S0169-5347(03)00247-7)
- Tajima F (1989) Statistical method for testing the neutral mutation hypothesis by DNA polymorphism. *Genetics* 123: 585–595.
- Tamura K, Stecher G, Peterson D, Filipski A, Kumar S (2013) MEGA6: molecular Evolutionary Genetics Analysis version 6.0. *Molecular Biology and Evolution* 30: 2725–2729. <https://doi.org/10.1093/molbev/mst197>
- Tavares JS (1909) Contributo prima ad cognitionem Cecidologiae Braziliae. *Broteria* 8: 5–29.
- Tavares JS (1917) As cecideas do Brazil que se criam nas plantas da familia das Melastomataceae. *Broteria* 15: 18–49.
- Tauber MJ, Tauber CA, Masaki S (1986) Seasonal adaptations of insects. Oxford University Press, New York, 426 pp.
- Vecchi C, Menezes NL, Oliveira DC, Ferreira BG, Isaias RMS (2013) The redifferentiation of nutritive cells in galls induced by Lepidoptera on *Tibouchina pulchra* (Cham.) Cogn. reveals predefined patterns of plant development. *Protoplasma* [Online] <https://doi.org/10.1007/s00709-013-0519-6>
- Walhberg N, Wheat CW, Peña C (2013) Timing and patterns in the taxonomic diversification of Lepidoptera (butterflies and moths). *PLoS ONE* 8: e80875. <https://doi.org/10.1371/journal.pone.0080875>
- Wille J (1926) *Cecidoses eremita* Curt. Und ihre Galle an *Schinus dependens* Ortega. *Zeitschrift für Morphologie und Ökologie der Tiere* 7: 1–101. <https://doi.org/10.1007/BF00540718>
- Yukawa J (2000) Synchronization of gallers with host plant phenology. *Population Ecology* 42: 105–113. <https://doi.org/10.1007/PL00011989>

Supplementary material 1

Table S1.

Authors: Gilson R.P. Moreira, Rodrigo P. Eltz, Ramoim B. Pase, Gabriela T. Silva, Sérgio A.L. Bordignon, Wolfram Mey, Gislene L. Gonçalves

Data type: molecular data

Explanation note: Primers and conditions used in polymerase chain reaction (PCR) to amplify COI, 16S and Wg genes.

Copyright notice: This dataset is made available under the Open Database License (<http://opendatacommons.org/licenses/odbl/1.0/>). The Open Database License (ODbL) is a license agreement intended to allow users to freely share, modify, and use this Dataset while maintaining this same freedom for others, provided that the original source and author(s) are credited.

Link: <https://doi.org/10.3897/zookeys.695.13320.suppl1>

Supplementary material 2

Table S2.

Authors: Gilson R.P. Moreira, Rodrigo P. Eltz, Ramoim B. Pase, Gabriela T. Silva, Sérgio A.L. Bordignon, Wolfram Mey, Gislene L. Gonçalves

Data type: statistical data

Explanation note: Analysis of Molecular Variance (AMOVA) using φ -statistics based on cytochrome oxidase subunit I mitochondrial sequences for groups of *C. pampeanus*, defined according to different dispersal barriers.

Copyright notice: This dataset is made available under the Open Database License (<http://opendatacommons.org/licenses/odbl/1.0/>). The Open Database License (ODbL) is a license agreement intended to allow users to freely share, modify, and use this Dataset while maintaining this same freedom for others, provided that the original source and author(s) are credited.

Link: <https://doi.org/10.3897/zookeys.695.13320.suppl2>

Supplementary material 3

Table S3.

Authors: Gilson R.P. Moreira, Rodrigo P. Eltz, Ramoim B. Pase, Gabriela T. Silva, Sérgio A.L. Bordignon, Wolfram Mey, Gislene L. Gonçalves

Data type: specimens data

Explanation note: Specimens used in this study for phylogenetic reconstruction and genetic structure analysis of *C. pampeanus*.

Copyright notice: This dataset is made available under the Open Database License (<http://opendatacommons.org/licenses/odbl/1.0/>). The Open Database License (ODbL) is a license agreement intended to allow users to freely share, modify, and use this Dataset while maintaining this same freedom for others, provided that the original source and author(s) are credited.

Link: <https://doi.org/10.3897/zookeys.695.13320.suppl3>

Supplementary material 4

Figure S1.

Authors: Gilson R.P. Moreira, Rodrigo P. Eltz, Ramoim B. Pase, Gabriela T. Silva, Sérgio A.L. Bordignon, Wolfram Mey, Gislene L. Gonçalves

Data type: statistical data

Explanation note: Graphs depicting the results of the mismatch distribution analysis for the total samples (*C. pampeanus*) and populations alone (P6 to P9). The analysis was performed with 1420 bp of COI sequences (excluding all sites with missing information or gaps).

Copyright notice: This dataset is made available under the Open Database License (<http://opendatacommons.org/licenses/odbl/1.0/>). The Open Database License (ODbL) is a license agreement intended to allow users to freely share, modify, and use this Dataset while maintaining this same freedom for others, provided that the original source and author(s) are credited.

Link: <https://doi.org/10.3897/zookeys.695.13320.suppl4>

Supplementary material 5

Figure S2.

Authors: Gilson R.P. Moreira, Rodrigo P. Eltz, Ramoim B. Pase, Gabriela T. Silva, Sérgio A.L. Bordignon, Wolfram Mey, Gislene L. Gonçalves

Data type: statistical data

Explanation note: Neighbor-Joining tree of *Cecidonius pampeanus* with the evolutionary distances computed using the Kimura 2-parameter method based on 1.6 Kb of cytochrome oxidase sequences. The analysis involved 60 individuals from 10 populations.

Copyright notice: This dataset is made available under the Open Database License (<http://opendatacommons.org/licenses/odbl/1.0/>). The Open Database License (ODbL) is a license agreement intended to allow users to freely share, modify, and use this Dataset while maintaining this same freedom for others, provided that the original source and author(s) are credited.

Link: <https://doi.org/10.3897/zookeys.695.13320.suppl5>

Taxonomic notes on two sibling species of *Metellina* from Asia (Araneae, Tetragnathidae)

Recep Sulhi Özkütük¹, Yuri M. Marusik^{2,3}, Kadir Boğaç Kunt¹, Mert Elverici^{4,5}

1 Department of Biology, Faculty of Science, Anadolu University, TR-26470, Eskişehir, Turkey **2** Institute for Biological Problems of the North, Portovaya Street 18, Magadan 685000, Russia **3** Department of Zoology & Entomology, University of the Free State, Bloemfontein 9300, South Africa **4** Department of Biological Sciences, Faculty of Arts and Sciences, Middle East Technical University, TR-06800 Ankara, Turkey **5** Department of Biology, Faculty of Science and Arts, University of Erzincan, TR-24100, Erzincan, Turkey

Corresponding author: *Recep Sulhi Özkütük* (sozkutuk@anadolu.edu.tr)

Academic editor: S. Li | Received 10 May 2017 | Accepted 17 August 2017 | Published 4 September 2017

<http://zoobank.org/32D8CCBF-6914-4E07-947F-6C5E349597BC>

Citation: Özkütük RS, Marusik YM, Kunt KB, Elverici M (2017) Taxonomic notes on two sibling species of *Metellina* from Asia (Araneae, Tetragnathidae). ZooKeys 695: 75–88. <https://doi.org/10.3897/zookeys.695.13611>

Abstract

Two sibling species, *Metellina orientalis* (Spassky, 1932) and *M. kirgisica* (Bakhvalov, 1974), occurring in the Middle East and Central Asia are redescribed and their distributions mapped. The previously unknown male of *M. kirgisica* is described for the first time. Stridulatory files on male chelicera of *Metellina* are also documented for the first time. The occurrence of *M. kirgisica* in Azerbaijan and Tajikistan and the presence of *M. orientalis* in Turkey are confirmed.

Keywords

Anatolia, Aranei, Metainae, Caucasus, Central Asia, Iran, new record, description

Introduction

Metellina Chamberlin & Ivie, 1941 is a small genus of Metainae spiders with seven named species occurring in the Holarctic (World Spider Catalog 2017). Two species, *M. curtisi* (McCook, 1894) and *M. mimetoides* Chamberlin & Ivie, 1941, are restricted to the Nearctic and all other species are known from West Palaearctic (from the Iberian Peninsula to Xinjiang). Three species occurring in Europe and both species known from the Nearctic are well studied due to several publications (Levi 1980; Roberts 1995, etc.).

Two easternmost Palearctic species, *M. kirgisica* (Bakhvalov, 1974) and *M. orientalis* (Spassky, 1932), are the least known species of the genus. The former is known by females only and sketchy drawings; although *M. orientalis* is relatively well known, some essential characters of this species are not documented, such as the cymbial spines or stridulatory files on male chelicera, as well as the stiff setae present on legs I and II. Distributions of the two species are not properly known due to past misidentifications. Difficulties were faced in discriminating between these two species during studies of Turkish, Caucasian, and Central Asian spiders; therefore, a comparative study of *M. kirgisica* and *M. orientalis* is provided.

Materials and methods

Specimens were photographed with a Canon EOS 7D camera attached to an Olympus SZX16 stereomicroscope and Leica DFC295 camera connected to a stereo microscope Leica S8AP0. SEM figures were made with a SEM JEOL JSM-5200 scanning microscope at the Zoological Museum, University of Turku, Finland and with a Zeiss Ultra Plus SEM device at the Anadolu University, Eskişehir. Digital images were montaged using CombineZP image stacking software. The epigyne was cleared in a KOH/water solution until soft tissues were dissolved. Photographs were taken in dishes with cotton or paraffin on the bottom to hold the specimens in position. All measurements are given in mm. Materials studied here are deposited in the Zoological Museum of the Moscow State University (ZMMU), Zoological Institute of St-Petersburg (ZISP), Zoological Museum, University of Turku (ZMUT), and Anadolu University, Zoological Museum (AUZM).

Taxonomy

Metellina Chamberlin & Ivie, 1941

Metellina Chamberlin & Ivie, 1941: 14; Levi 1980: 32; Álvarez-Padilla and Hormiga 2011: 779.

Type species. *Pachygnatha curtisi* McCook, 1894 from California.

Diagnosis. See Levi (1980) and Álvarez-Padilla and Hormiga (2011).

Metellina orientalis (Spassky, 1932)

Figs 1–6, 9–10, 17–19, 23–25, 29–36, 39, 47

Meta orientalis Spassky, 1932: 184, f. 5–8 (♂♀).

Metellina orientalis: Marusik 1985: 139; Marusik 1986: 19, f. 1.1–3 (♂♀); Malek Hosseini et al. 2015: 92, f. 3a–c (♂).

Examined specimens. TURKEY: *Konya* Province: 1♂, 2♀ (AUZM), Seydişehir District, Kuyucak Mountain, Kalafat Hill, Ferzene Cave (37°22'49.24"N 31°50'2.10"E), 27.03.2011 (R.S. Özkütük); 5♀ (AUZM), Derebucak District, Çamlık Town, Körükini Cave (37°20'53.94"N 31°37'38.53"E), 10.06.2011 (K.B. Kunt); 1♂, 2♀ (AUZM), Derebucak District, Çamlık Town, Döllüönüüni Cave (37°20'20.38"N 31°37'15.12"E), 10.07.2011 (R.S. Özkütük). *Erzincan* Province, 2♂, 4♀ (AUZM), Kemaliye District, Kozlupınar Village, Ala Cave (39°13'5.63"N 38°34'20.71"E), 20.03.2015 (M. Elverici) *Sivas* Province, 3♂, 1♀ (AUZM), Şarkışla District, Alaman Village, Camızlı Cave (39°35'8.91"N 36°15'12.13"E), 18.04.2016 (K.B. Kunt). ARMENIA: syntype 1♂ (ZISP), Goktscha Lake (=Sevan), Yelenovka, 13–16.08.1931 (M. Karpova). IRAN: *Kohgiluyeh and Buyer-Ahmad* Province, 1♂ 1♀ (ZMUT), Nevel Cave, 28.08.2011 (M.J. Malek Hosseini).

Diagnosis. Males of *M. orientalis* can be easily distinguished from all congeners, except for *M. kirgisica*, by having strong cymbial spines (Figs 17–19, 23, 25) lacking in other species. The two sibling species can be distinguished by the shape of paracymbial spur (*P*_s), which are rounded and claw-like in *M. orientalis* (Figs 19, 23) and spine-like in *M. kirgisica* (Figs 21–22). Females of *M. orientalis* are also very similar to those of *M. kirgisica* by having three pairs of abdominal humps (can be almost indistinct in some specimens) and a very similar epigyne. The epigyne in *M. orientalis* has a larger and wider median plate (cf. Fig 36, 39–40, 42) and a thinner “septum” (1/3 of median plate width vs. 1/2). Females can be easily distinguished by carapace pattern, poorly developed in *M. orientalis* (Fig. 4–5) and very complex in *M. kirgisica* (Figs 11–12).

Description. Measurements (♂/♀): total length 6.48/6.60; carapace 2.88/2.70 long, 2.24/2.04 wide; chelicerae 1.20/1.20 long; abdomen 3.60/3.90 long, 2.40/3.12 wide.

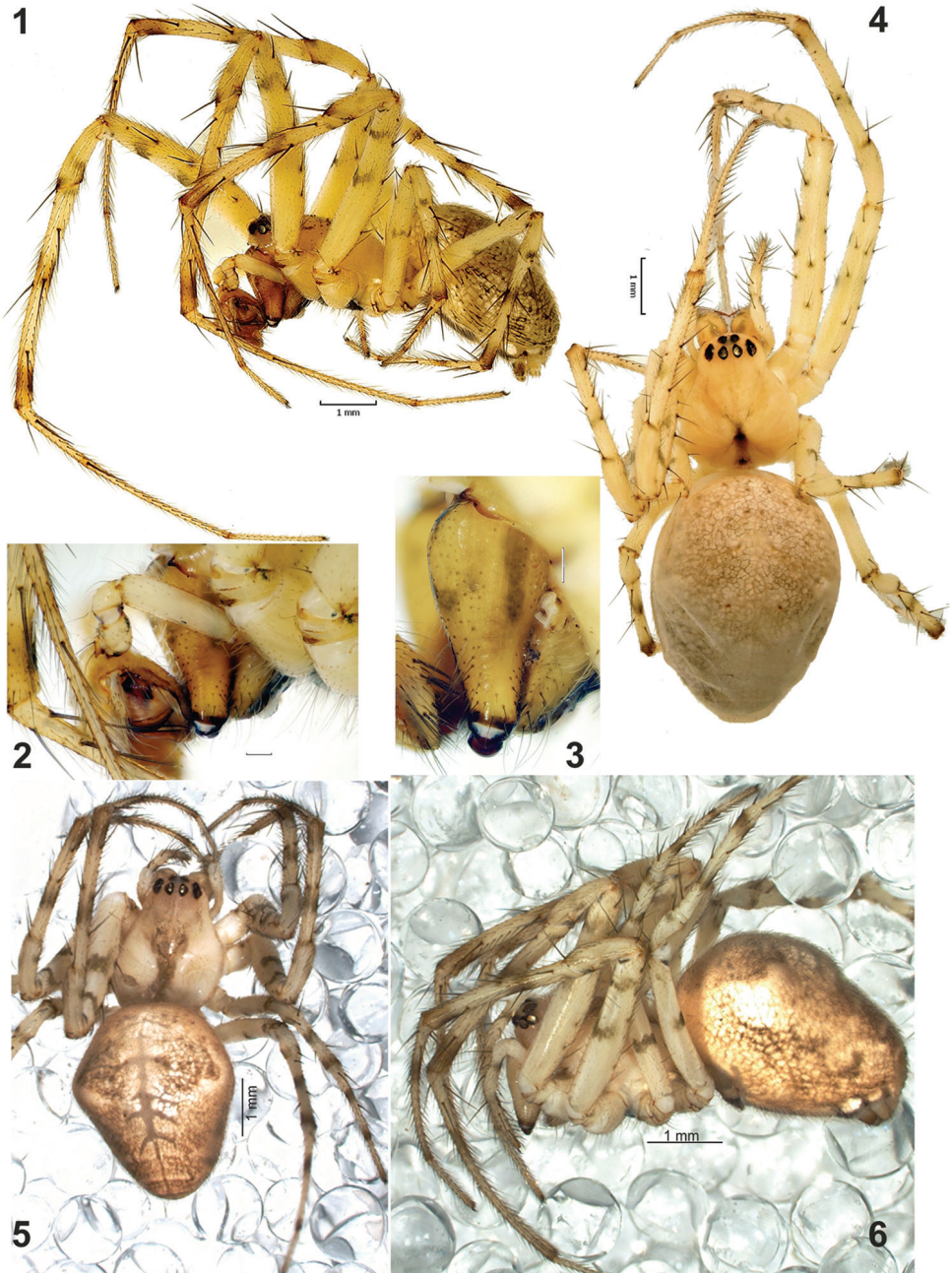
Female carapace with weak pattern (Fig. 5) or almost lacking any pattern (Fig. 4). Legs with numerous spines, stronger in males than in females. Legs light-coloured; femora, tibia and metatarsi of all legs with two dark rings (Figs 1, 4–6). Tibia-metatarsi of legs I and II with prolateral row of stiff, inflexible setae forming kind of catching basket. For leg measurements see Table 1.

Abdomen with three pairs of humps, almost indistinct in males. Anterior pair large and distinct in all females examined, two posterior pairs much smaller and can be indistinct. Pattern not distinct, in contrast to sibling species; venter with wide dark median band.

Male chelicera with five strong stridulating ridges and some smaller ones above and below. Male palp as in Figs 17–19, 23, 24, 30–33. Cymbium with more than a

Table 1. Leg measurements of *Metellina orientalis*.

♂/♀	Fe	Pa	Ti	Mt	Ta	Total
I	3.50/3.60	1.44/1.40	4.00/3.60	4.40/4.00	1.60/1.50	14.98/14.14
II	3.10/3.00	1.20/1.14	3.00/2.22	3.40/3.06	1.20/1.00	11.90/10.42
III	2.00/2.10	0.75/0.84	1.50/2.04	1.80/1.62	0.65/0.78	6.70/7.38
IV	2.88/2.94	0.78/0.84	2.10/2.28	2.40/2.40	0.90/0.90	9.06/9.36



Figures 1–6. Somatic characters of *Metellina orientalis*. **1** male habitus, lateral **2–3** anterior part of pro-soma showing chelicera with stridulating ridges **4–5** female habitus, dorsal; **6** female habitus, lateral. Scale bars 1 mm (**1, 4, 5, 6**); 0.2 mm (**2**).

dozen strong macrosetae in distal half. Paracymbium with finger-like ventral arm (*Pv*) covered with setae and a large extending dorso-retrolateral arm (*Pd*). Dorso-retrolateral arm gradually widens, its width subequal to width of cymbium. Dorso-distal part of the arm with deep depression dorsally (*Dd*), spur like process (*Ps*) and several rows of fine spines (*Fs*) clearly visible with SEM, but indistinct with light microscopy. Tegulum thin, as wide as conductor, transverse. Conductor (*Co*) long, with parallel margins, tip abrupt, with small membranous outgrowth (*Mo*), conductor entirely hides embolus in ventral view; embolus (*Em*) with large base (*Eb*) formed by two lobes; embolus gradually tapering, with widened tip.

Epigyne as in Figs 34–36, 39; simple, heavily sclerotized plate more than twice as wide than long, without any outgrowths; median plate (*Mp*) with septum-like sclerotised outgrowth (*Se*) three times thinner than width of median plate; median plate hexagonal, weakly sclerotized, wider than long. Anterior from epigynal plate with pair of transversal sclerotized plates (*Sp*, Fig. 34).

Distribution and notes. World Spider Catalog (2017) indicates distribution of the species as “Central Asia, Iran” although it was described from Armenia, located in the Caucasus and neighbouring with Turkey, which belong to the Middle East. Mikhailov’s catalogue (Mikhailov 2013) indicates the distribution of *M. orientalis* in the former USSR as Armenia, Kazakhstan, and Turkmenistan: *Metellina orientalis* was reported from Kazakhstan (Almaty) and Turkmenistan (Akhal-Teke) by Spassky (1952) but the two records of the species from Central Asia undoubtedly refer to the sibling species *M. kirgisica*, previously reported from Kyrgyzstan, Uzbekistan, Turkmenistan (Mikhailov 2013), and northwestern China, Xinjiang (Marusik et al. 2007).

This species was reported from Turkey for the first time by Karol (1967). She referred to Spassky (1932) and Charitonov (1936), although none of these publications deal with spiders of Turkey. Spassky (1932) described it from Armenia, and Charitonov (1936) just listed the species in his catalogue. Several surveys and checklists of Turkish spiders listed this species as occurring in Turkey with reference to Karol’s (1967) publications (Bayram 2002; Topçu et al. 2005; Bayram et al. 2017). Now we are able to confirm the presence of *M. orientalis* in Turkey.

Metellina kirgisica (Bakhvalov, 1974)

Figs 7–8, 11–15, 20–22, 26–28, 37–47

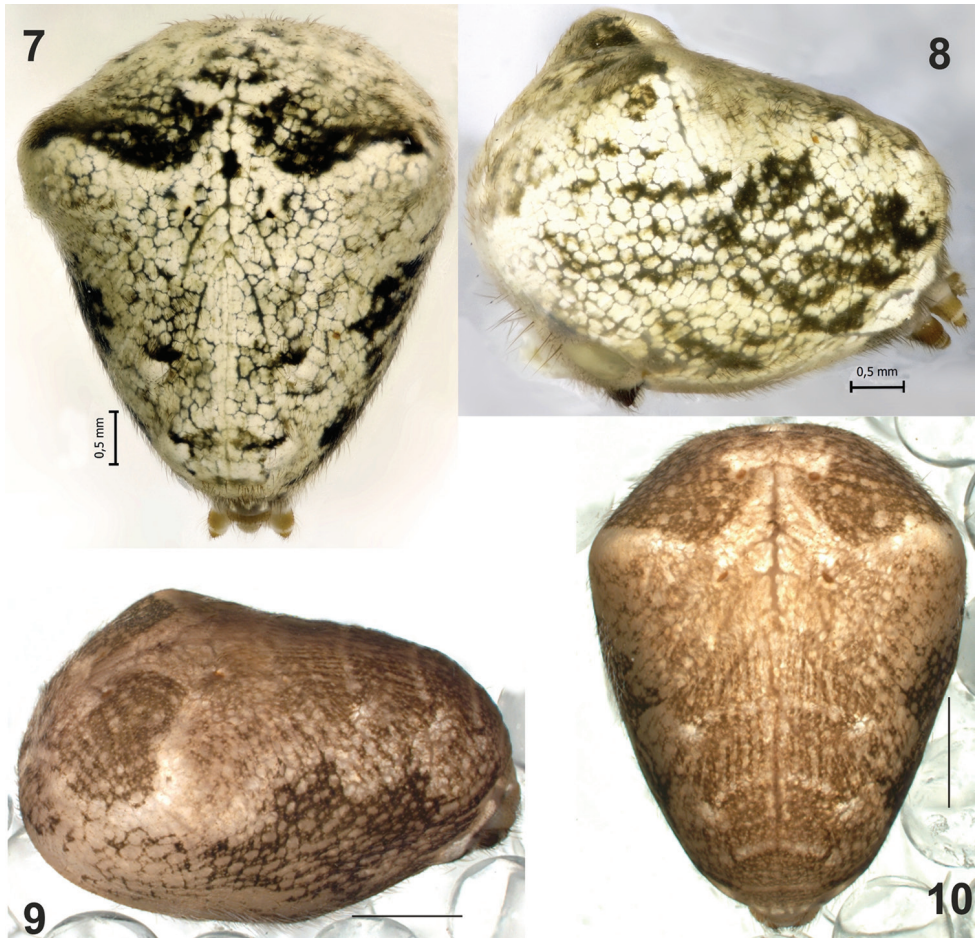
Meta orientalis: Spassky, 1952: 1977–198 (misidentification).

Meta kirgisicus Bakhvalov, 1974: 101, f. 6–7 (♀).

Meta kirgisica Bakhvalov, 1982: 136, f. 1 (♀); Bakhvalov 1983: 86, f. 1 (♀).

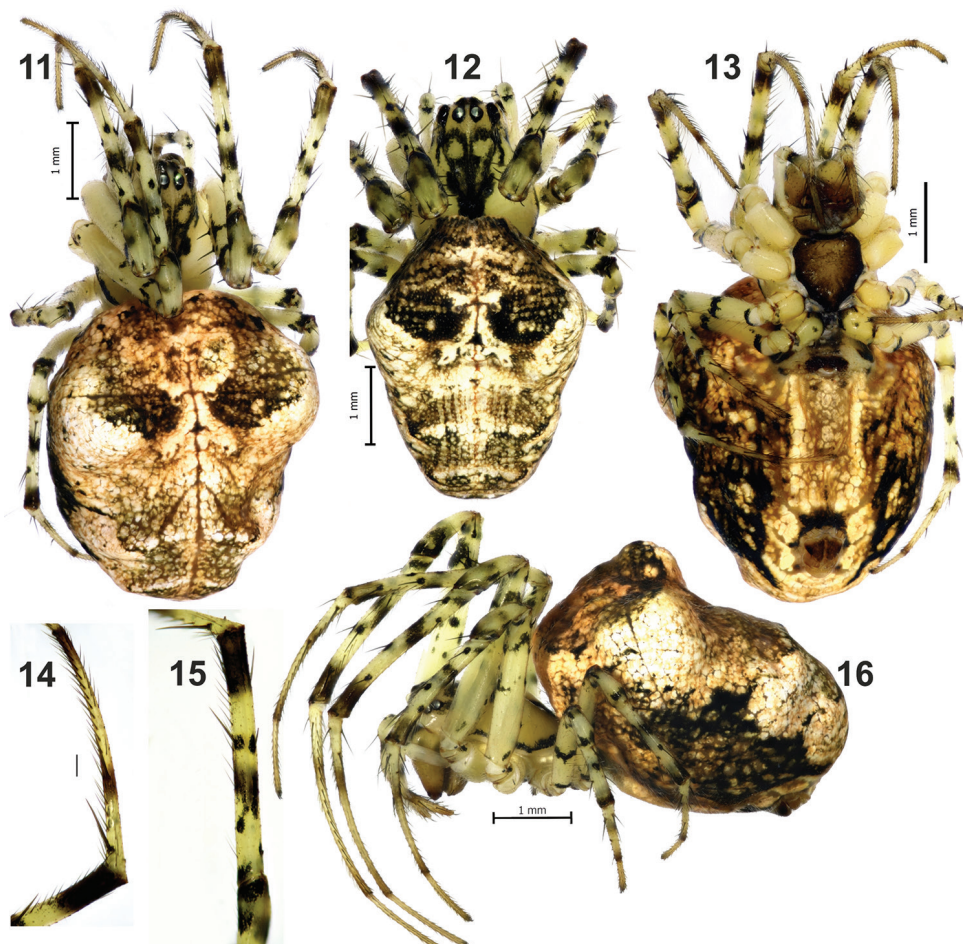
Metellina kirgisica: Marusik, 1989: 44; Marusik et al. 2007: 271, f. 31, 52 (♀).

Material examined. AZERBAIJAN: *Lenkoran* Dist.: 1♀ (ZMMU), env. of Aurora Vill., 38°40'N, 48°52'E, 23–28.04.2001 (Y.M. Marusik). KYRGYZSTAN: 1♂ (lost), Kirgizian Mt. Range, Ala-Archa River, ca. 42.645°N 74.480°E, 8.05.1983 (S.V.



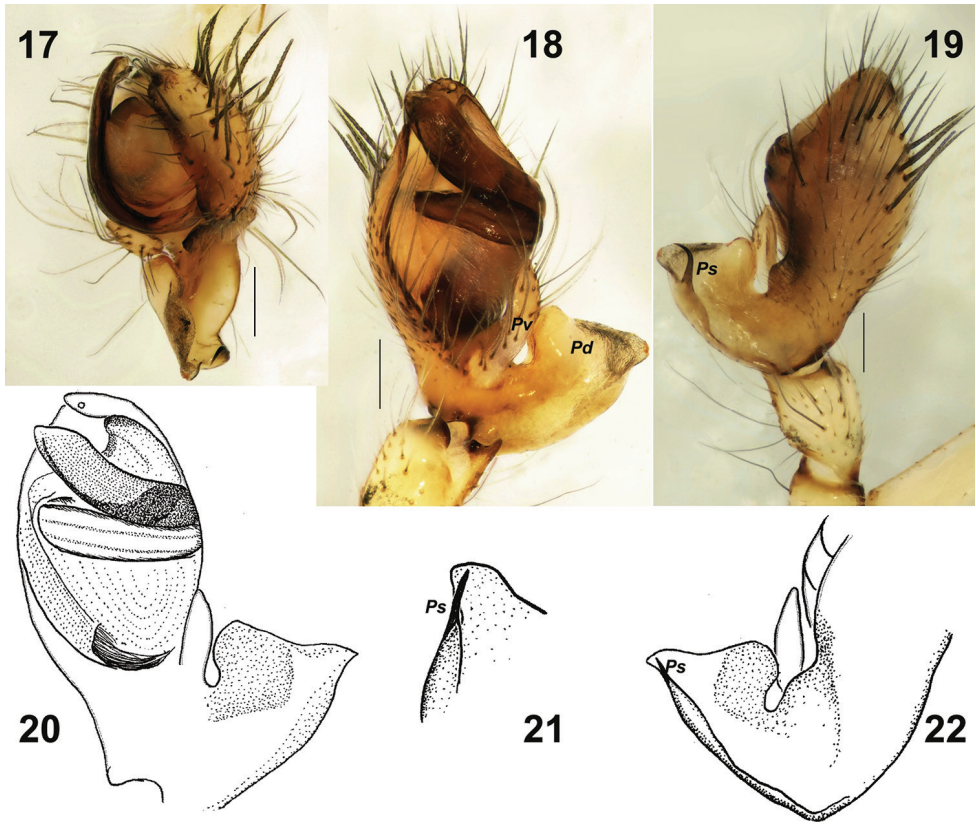
Figures 7–10. Abdomen of *Metellina kirgisica* (7–8) from Azerbaijan and *M. orientalis* (9–10) from Erzincan Province of Turkey. **7, 10** dorsal **8–9** lateral. Scalebars 0.5 mm (**7, 8**); 1 mm (**9, 10**).

Ovtchinnikov); 1♀ (lost), Chatkal Mt. Range, Sary-Chelek Reserve, Karangitun Gorge, ca. 41°40'N, 71°56'E, 3.05.1983 (S.L. Zonstein). TAJIKISTAN: *Khatlon* Area: 4♀ (ZMMU), Vose Distr., Khodzha-Mumin Mt., 37°45.941'N, 69°38.665'E, 474 m, 25.04.2015 (Y.M. Marusik); 1♀ (ZMMU), Khovaling Distr., Darai-Mukhtor, env. of "Vose Museum", 38°23.572'N, 69°57.910'E, 1579 m, 28.04.2015 (Y.M. Marusik); 2♀ (ZMMU) Hissar Mt. Range, Ramit Reserve, 38°44.605'N, 69°18.486'E, 1324 m, 1.05.2015 (Y.M. Marusik); 1♀ (ZMMU), environs of Dushanbe, Hissar Mt. Ridge, 38th km of Varzob Hwy, Takob Gorge, env. of Dehmalik Vill, 38°50.829'N, 68°54.637'E, 805 m, 8.05.2015 (Y.M. Marusik & M. Saidov). CHINA, *Xinjiang* Province 1♀ (ZMUT), 70 km southwest of Urumqi, Nantaizi, 43.399°N to 43.438°N, 87.214°E to 87.262°E, 1800–2100 m, 3.05.-28.06.2004 (N.R. Fritzén).



Figures 11–16. Somatic characters of *Metellina kirgisica* female from Tajikistan. 11–12 habitus, dorsal, showing differences in size and colour pattern 13, 16 habitus, ventral and lateral 14 metatarsus I pro-lateral, showing row of stiff setae 15 tibia I, prolateral. Scale bars 1 mm (11, 12, 13, 16); 0.2 mm (14).

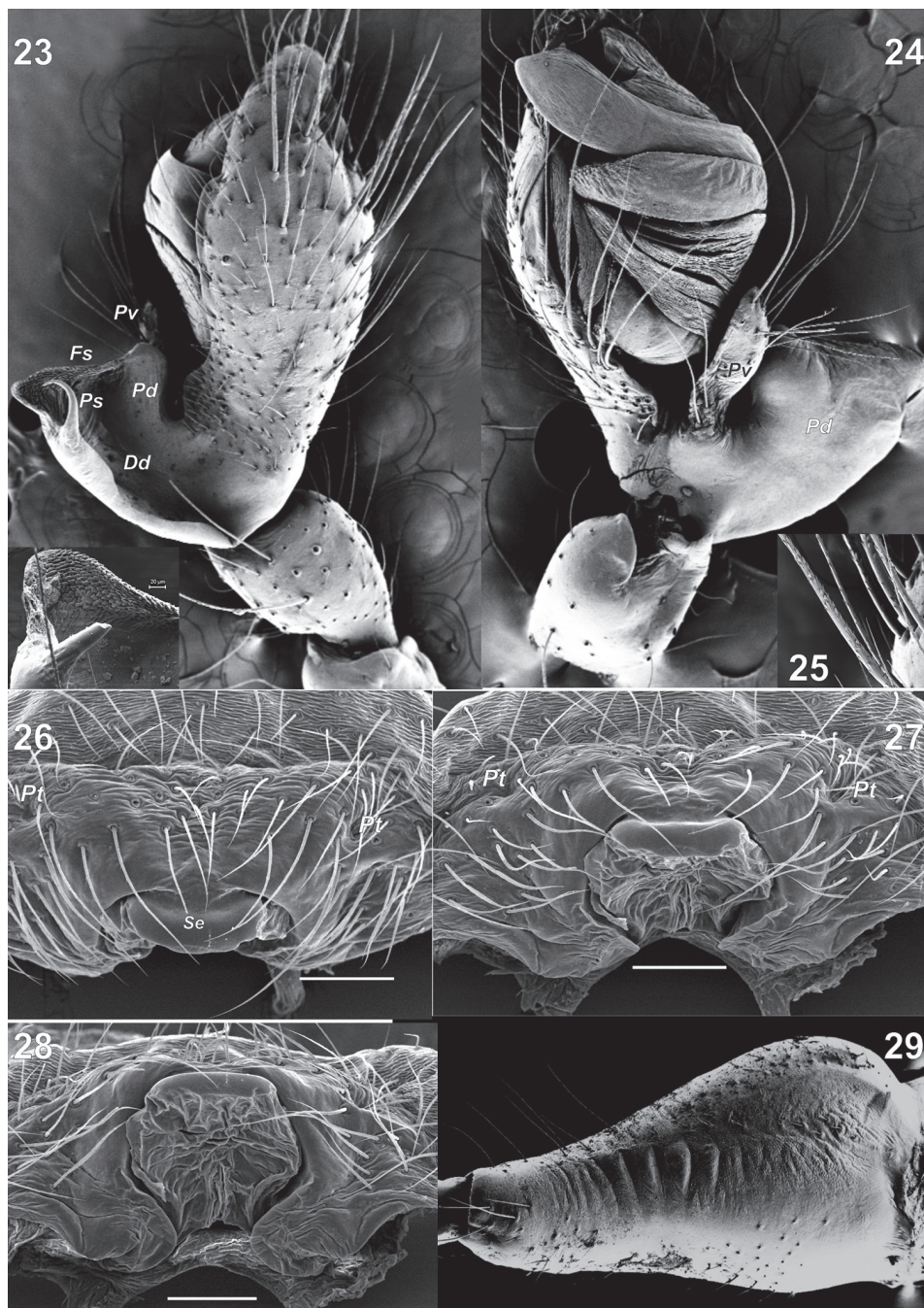
Note. Bakhvalov (1974) described *Meta kirgisicus* only in a key to the orb-weaving spiders of Kyrgyzstan. The type material was not mentioned. In the subsequent paper Bakhvalov (1982) described the same species as *Meta kirgisica* on the basis of the holotype female and several paratypes. This description was supplemented with new figures. A year later this species was described again based on the same material and figures (Bakhvalov, 1983). Bakhvalov (1982, 1983) indicated that types will be deposited in the Laboratory of Entomology of the Institute of Biology of Kirgizian Academy of Sciences. According to Sergei L. Zonstein (pers. comm.), who was working in that laboratory, Bakhvalov never deposited type specimens in the Laboratory of Entomology. After the death of Bakhvalov his private collection was taken by son, and its fate is unknown.



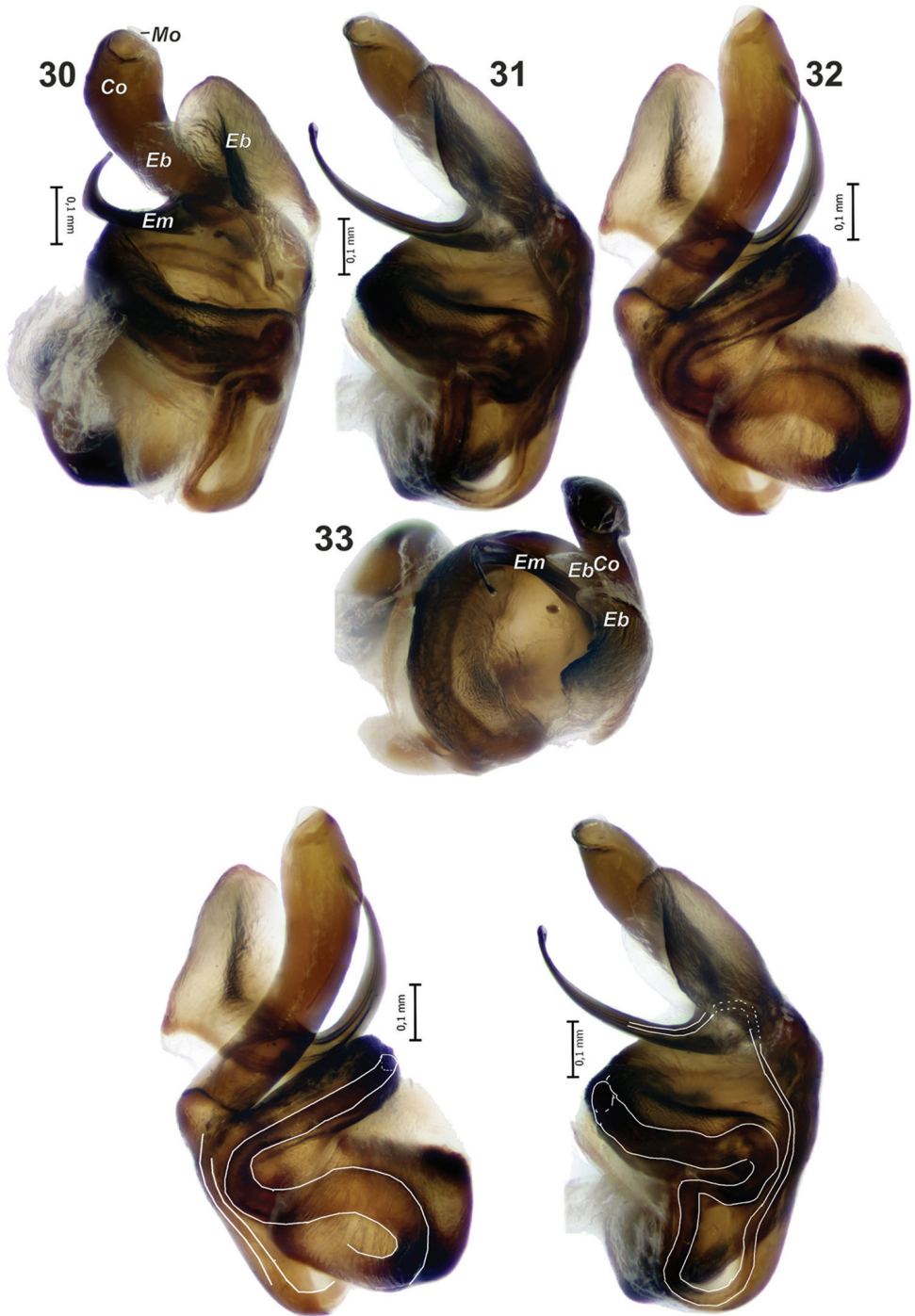
Figures 17–22. Male palp of *Metellina orientalis* (17–19) from Azerbaijan and *M. kirgisia* (20–22). 17 from above 18, 20 ventral 19, 22 dorsal 21 tip of paracymbium with spur. Pd dorso-retrolateral arm Ps spur like process Pv finger-like ventral arm. Scale bars 0.2 mm (17, 18, 19).

Diagnosis. Females of *M. kirgisia* can be distinguished from sibling *M. orientalis* by smaller size (carapace 2.0–2.1 long *vs.* 2.7), more developed pattern of carapace (cf. Figs 4–6 and 11–12, 16), and proportions of the median plate of epigyne (as long as wide *vs.* wider than long). Males of the two species can be distinguished by the shape of paracymbial spur (*Ps*), straight and spine-like in *M. kirgisia* and bent claw-like in *M. orientalis* (cf. Figs 19 and 21–22).

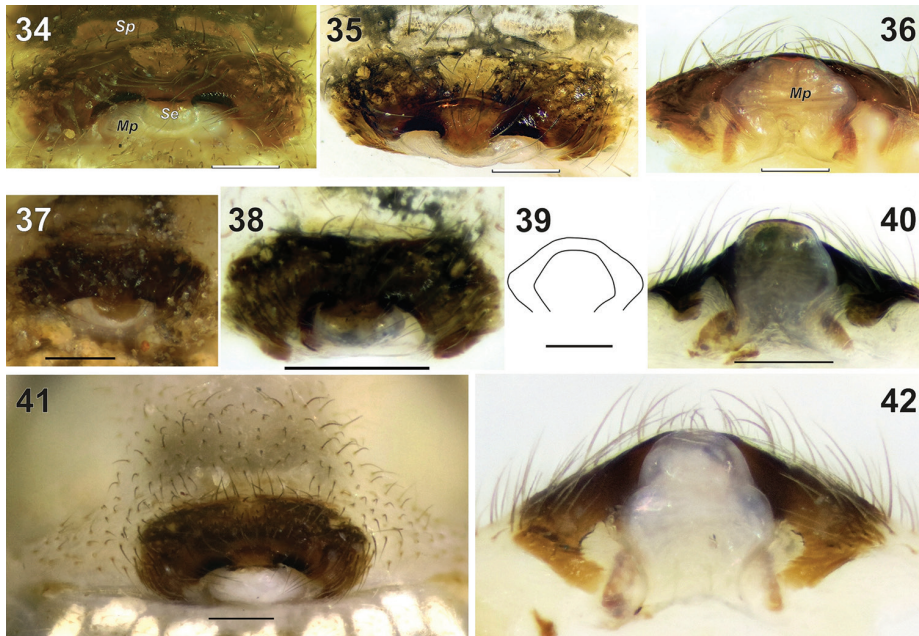
Description. Male. Measurements (male unavailable, specimen lost, palp was illustrated in 80th by YM). Female: total length 4.5–5.5; carapace 2.0–2.1 long, 1.5–1.7 wide. Carapace yellow with complex dark pattern and distinct marginal dark stripe (Figs 11–12, 16). Legs yellowish with dark annulation and dark spots around base of each spine; femora, tibia and metatarsus of legs with two dark rings, rings of femora thick and thin on tibia and metatarsi; coxae IV with blackish dot (Fig. 13); distal half of tibia and metatarsi I and II with row of stiff setae forming a kind of catching basket (Figs 14–15). For leg measurements see Table 2.



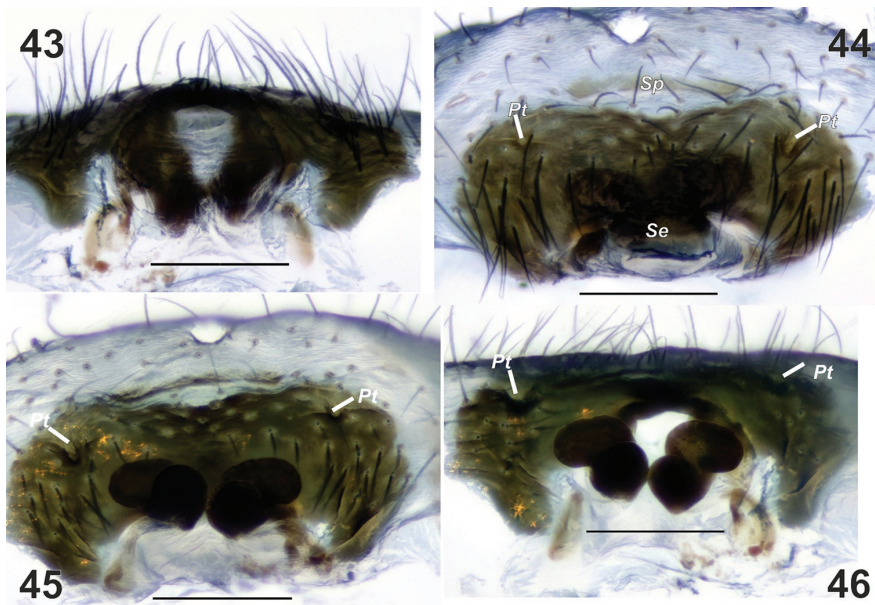
Figures 23–29. Copulatory organs and chelicera of *Metellina orientalis* (23–25, 29) from Konya Province of Turkey and *M. kirgisisca* (26–28). 23–24 male palp, dorsal and ventral 25 cymbial setae 26–28 epigyne, ventral, ventro-caudal and caudal 29 male chelicera, lateral. Abbreviations: *Dd* deep depression *Fs* fine spines *Pd* dorso-retrolateral arm *Ps* spur like process *Pt* lateral pits *Pv* finger-like ventral arm *Se* sclerotised outgrowth. Scale bars 0.2 mm (26, 27, 28).



Figures 30–33. Bulb of *Metellina orientalis*. **33** from above. Abbreviations: *Co* conductor *Eb* embolar base *Em* embolus *Mo* membranous outgrowth. Scale bars 0.1 mm.



Figures 34–42. Epigynes of *Metellina orientalis* (34–36, 39) and *M. kirgisica* (37–42). 34–35, 37–38, 41 ventral 36, 40, 42 caudal 39 outline of median plate of two species, showing differences in size and proportions 34–36 from Konya Province of Turkey 37–40 from Tajikistan 41–42 from Azerbaijan. Abbreviations: *Sp* sclerotized plate *Se* sclerotised outgrowth *Mp* median plate. Scale bars 0.2 mm



Figures 43–46. Macerated epigyne of *Metellina kirgisica*. 43 caudal 44 ventral 45 anterior 46 dorsal. *Pt* lateral pits *Se* sclerotised outgrowth *Sp* sclerotized plate. Scale bars 0.2 mm

Table 2. Leg measurements of *Metellina kirgısica*.

♀	Fe	Pt	Ti	Mt	Ta	Total
I	2.70	1.10	2.85	2.60	1.25	10.50
II	2.20	0.90	1.80	2.10	0.95	7.95
III	1.50	0.65	0.90	1.10	0.65	3.80
IV	2.15	0.70	1.40	1.55	0.75	6.50

**Figure 47.** Distribution records of *Metellina orientalis* (circle) and *M. kirgısica* (square).

Abdomen with three pairs of humps, anterior the largest, two posterior humps less distinct. Abdomen with distinct pattern as shown on Figs 11–13, 16; venter with wide light band.

Palp as in Figs 20–22; spination of cymbium not documented; paracymbium with weakly sclerotised ventral arm and large and broad dorsal arm; dorsal arm with spine-like spur (*Ps*).

Epigyne as in Figs 26–28, 37–46; almost instinct transversal sclerotised plate (*Sp*, Fig. 44) in front of epigynal plate, epigynal plate twice as wide as long, heavily sclerotised with pair of small lateral pits (*Pt*); median plate (*Mp*) weakly sclerotised except kind of septum (*Se*), septum twice as thin as median plate; median plate longer than wide; receptacles touching each other consisting of two lobes (Fig. 46).

Distribution. The species was previously known from Kyrgyzstan, Uzbekistan, Turkmenistan (Marusik 1989; Mikhailov 2013), and Xinjiang, China (Marusik et al. 2007). A search for literature records reveals that it was reported also from southeastern Kazakhstan (sub. *M. orientalis*: Spassky 1952). New material studied in this work reveals its occurrence in Tajikistan and eastern Azerbaijan (Fig. 47).

Acknowledgements

We thank Müjdat Çağlar (Eskişehir, Turkey) for provided assistance with SEM photography, Seppo Koponen (Turku, Finland) for arranging YM's stay in Turku and

work in the Zoological Museum, Alireza Zamani (Tehran, Iran) for providing comparative specimens from Iran, and Kirill Mikhailov (Moscow, Russia) for consultations on the distributions of *M. kirgisica* and *M. orientalis* in Central Asia. This study was supported by Anadolu University Scientific Research Projects Commission under the grant no: 1503F093.

References

- Álvarez-Padilla F, Hormiga G (2011) Morphological and phylogenetic atlas of the orb-weaving spider family Tetragnathidae (Araneae: Araneioidea). *Zoological Journal of the Linnean Society* 162: 713–879.
- Bakhvalov VF (1974) Identification key of the spider family Araneidae from Kirgizia. *Entomologiceskie issledovanija v Kirgizii* 9: 101–112. [In Russian]
- Bakhvalov VF (1982) New species of spiders (Aranei, Araneidae) from Tyan-Shan. *Entomologiceskie issledovaniya v Kirgizii* 15: 136–140. [In Russian]
- Bakhvalov VF (1983) New species of spiders (Aranei, Araneidae) of USSR fauna. *Entomologiceskie issledovaniya v Kirgizii* 16: 86–94. [In Russian]
- Bayram A (2002) Distributions of Turkish Spiders. In: Demirsoy A (Ed.) *Zoogeography of Turkey*. Meteksan Publications, Ankara, Turkey, 638–657. [In Turkish]
- Bayram A, Kunt KB, Danişman T (2017) The Checklist of the Spiders of Turkey. Version 2017. <http://www.spidersofturkey.info> [accessed on 09 May 2017]
- Charitonov DE (1936) Dopolneniye k katalogu russkich paukov Uchenye Zapiski Persmkgo Universiteta 2(1): 167–223. [In Russian]
- Karol S (1967) Turkish spiders. I. Preliminary list. Printing office of Ankara University, Ankara, 34 pp.
- Levi HW (1980) The orb-weaver genus *Mecynogea*, the subfamily Metinae and the genera *Pachygnatha*, *Glenognatha* and *Azilia* of the subfamily Tetragnathinae north of Mexico (Araneae: Araneidae). *Bulletin of the Museum of Comparative Zoology at Harvard College* 149: 1–74.
- Malek Hosseini MJ, Zamani A, Sadeghi S (2015) A survey of cave-dwelling spider fauna of Kohgiluyeh & Boyer-Ahmad and Fars Provinces, Iran (Arachnida: Araneae). *Revista Ibérica de Aracnología* 27: 90–94.
- Marusik YM (1985) A systematic list of the orb-weaving spiders (Aranei: Araneidae, Tetragnathidae, Theridiosomatidae, Uloboridae) of the European part of the USSR and the Caucasus. *Trudy Zoologicheskogo Instituta Akademii Nauk SSSR* 139: 135–140. [In Russian]
- Marusik YM (1986) A redescription of types of certain orb-weaving spiders (Araneidae, Tetragnathidae) from S. A. Spassky collection. *Vestnik Zoologii* 6: 19–22. [In Russian]
- Marusik YM (1989) New data on the fauna and synonymy of the USSR spiders (Arachnida, Aranei). In: Lange AB (Ed.) *Fauna i ekologiya paukov i skorpionov: Arakhnologicheskii Sbornik*. Akademia Nauk SSSR, Moscow, 39–52. [In Russian]
- Marusik YM, Fritzen NR, Song DX (2007) On spiders (Aranei) collected in central Xinjiang, China. *Arthropoda Selecta* 15: 259–276.

- Marusik YM, Larsen N (in press) A synopsis of African *Metellina* (Araneae, Tetragnathidae, Metinae) with a description of new species from South Africa. Vestnik Zoologii.
- Marusik YM, Özkütük RS, Kunt KB (2012) Spiders (Araneae) new to the fauna of Turkey. 10. Two new species records of Tetragnathidae. Anadolu University Journal of Science and Technology C2(2): 69–73.
- Mikhailov KG (2013) The spiders (Arachnida: Aranei) of Russia and adjacent countries: a non-annotated checklist. Arthropoda Selecta Supplement 3: 1–262.
- Roberts MJ (1995) Collins Field Guide: Spiders of Britain & Northern Europe. HarperCollins, London, 383 pp.
- Spassky SA (1932) Aranearum species novae. Bulletin du Muséum National d'Histoire Naturelle de Paris (2)4: 182–189.
- Spassky S (1952) Spiders of the Turanian zoogeographical province. Entomologicheskoe Obozrenie 32: 192–205. [In Russian]
- Topçu A, Demir H, Seyyar O (2005) A Checklist of the spiders of Turkey. Serket 9(4): 109–140.
- World Spider Catalog (2017) World Spider Catalog. Natural History Museum Bern. <http://wsc.nmbe.ch>, version 18.0 [accessed on 27 April 2017]

A genome-wide phylogeny of jumping spiders (Araneae, Salticidae), using anchored hybrid enrichment

Wayne P. Maddison^{1,2}, Samuel C. Evans¹, Chris A. Hamilton^{3,4,5}, Jason E. Bond^{3,4}, Alan R. Lemmon⁶, Emily Moriarty Lemmon⁷

1 Department of Zoology, University of British Columbia, 6270 University Boulevard, Vancouver, British Columbia, V6T 1Z4, Canada **2** Department of Botany and Beaty Biodiversity Museum, University of British Columbia, 6270 University Boulevard, Vancouver, British Columbia, V6T 1Z4, Canada **3** Department of Biological Sciences, Auburn University, Auburn, AL, USA **4** Auburn University Museum of Natural History, Auburn University, Auburn, AL, USA **5** Florida Museum of Natural History, University of Florida, 3215 Hull Rd, Gainesville, FL, 32611 **6** Department of Scientific Computing, Florida State University, Tallahassee, FL, USA **7** Department of Biological Science, Florida State University, Tallahassee, FL, USA

Corresponding author: Wayne Maddison (wayne.maddison@ubc.ca)

Academic editor: J. Miller | Received 31 May 2017 | Accepted 16 August 2017 | Published 4 September 2017

<http://zoobank.org/0C9E5956-2CDB-4BC5-9DCA-AFDC7538A692>

Citation: Maddison WP, Evans SC, Hamilton CA, Bond JE, Lemmon AR, Lemmon EM (2017) A genome-wide phylogeny of jumping spiders (Araneae, Salticidae), using anchored hybrid enrichment. ZooKeys 695: 89–101. <https://doi.org/10.3897/zookeys.695.13852>

Abstract

We present the first genome-wide molecular phylogeny of jumping spiders (Araneae: Salticidae), inferred from Anchored Hybrid Enrichment (AHE) sequence data. From 12 outgroups plus 34 salticid taxa representing all but one subfamily and most major groups recognized in previous work, we obtained 447 loci totalling 96,946 aligned nucleotide sites. Our analyses using concatenated likelihood, parsimony, and coalescent methods (ASTRAL and SVDQuartets) strongly confirm most previous results, resolving as monophyletic the Spartaeinae, Salticinae (with the hisponines sister), Salticoidea, Amycoidea, Saltafresia, and Simonida. The agoriines, previously difficult to place beyond subfamily, are finally placed confidently within the saltafresians as relatives of the chrysillines and hasariines. Relationships among the baviines, astioids, marpissoids, and saltafresians remain uncertain, though our analyses tentatively conclude the first three form a clade together. Deep relationships, among the seven subfamilies, appear to be largely resolved, with spartaeines, lyssomanines, and asemoneines forming a clade. In most analyses, *Onomastus* (representing the onomastines) is strongly supported as sister to the hisponines plus salticines. Overall, the much-improved resolution of many deep relationships despite a relatively sparse taxon sample suggests AHE is a promising technique for salticid phylogenetics.

Keywords

Dionycha, jumping spiders, salticids, systematics, phylogenomics

Introduction

Understanding the relationships of jumping spiders (Salticidae) long posed a challenge, given their diversity in forms and species (about 6,000 described, World Spider Catalog 2017). Recent data from a handful of sequenced genes has, however, begun to resolve many aspects of the group's broad phylogenetic structure (Maddison and Hedin 2003, Bodner and Maddison 2012, Maddison et al. 2014). Combined with morphological information, these results have led to a comprehensive phylogenetic classification (Maddison 2015) and are beginning to enable inferences about evolutionary patterns in salticids' structures, ecology, and behaviour. Two major gaps in knowledge remain to be filled, however, before the phylogeny can provide a high-resolution lens on salticid evolution. First, the great majority of known species are unstudied phylogenetically (and many others undiscovered taxonomically), and therefore few details are available about shallower phylogeny in most tribes and genera of the family. Second, the few genes studied do not give definitive answers in several key areas of the deeper parts of the phylogeny. Maddison et al. (2014) were unable to resolve the relationships among the seven subfamilies (as defined by Maddison 2015), except for the sister group relationship between Hisponinae and Salticinae. They were also unable to place the peculiar agoriines, and to determine the relationships among the baviines, Marpissoida, Astioida, and Saltafresia; support for the Saltafresia and Simonida was only tentative.

Our goal here is to answer remaining questions about broad salticid relationships, using data from across the genome. An efficient method to obtain data on hundreds of genes is Anchored Hybrid Enrichment (AHE; Lemmon et al. 2012; Lemmon and Lemmon 2013), a high-throughput genomics technique that uses probes designed for highly conserved DNA regions flanked by less-conserved regions. AHE has been applied for both deep and shallow relationships in spiders (Hamilton et al. 2016a,b), where it shows considerable promise for resolving phylogeny based on genome-wide data. We here apply AHE to salticids, using a combination of Spider Probe Kit versions 1 and 2 designed for spiders by Hamilton et al. (2016b, unpublished). The AHE Spider Probe Kit targets 585 phylogenetically-informative loci across the Order Araneae and delivers phylogenetic utility at both deep and shallow taxonomic depths. By providing a set of molecular markers that can be used to address evolutionary questions at multiple hierarchical levels, as well as across different research groups, the AHE Spider Probe Kit is being used to answer larger questions about spider phylogeny and evolution (Hamilton et al. 2016a,b).

Methods

Taxon sampling

Specimens sampled are listed in Table 1, representing 33 salticid genera belonging to 26 tribes and 6 subfamilies among the 30 tribes and 7 subfamilies currently recognized in the Salticidae (Maddison 2015). The one subfamily not sampled is the Eupoinae; the four tribes not represented are the amycoid tribe Huriini and the astioid tribes Neonini, Mopsini, and Vicirini. In addition, 12 dionychan outgroups are included, representing families inferred as more and less closely related to salticids by Wheeler et al. (2017). *Homalonychus* is used as the most distant outgroup.

When multiple specimens from a single genus (e.g. two *Hasarius*) were sampled, their DNA was pooled and they were treated as a single terminal taxon in analyses, resulting in 34 salticid and 12 outgroup terminal taxa (see “+” symbols in Table 1). This was done in an attempt to obtain our target DNA quantity of 500ng for sequencing. The one exception to this is *Sarinda*, whose DNA extraction and sequencing was done separately for two separate species. The specimens pooled for a terminal taxon appear to represent the same species in all cases but three. For *Agorius*, *Fluda*, and *Tisaniba*, two species were pooled for each (see Table 1), and thus those terminal taxa are chimeric. There is no doubt, based on morphology, that the two *Agorius* are sisters among the species included here, and likewise for the two *Fluda* and the two *Tisaniba*.

Voucher specimens are preserved in the Spencer Entomological Collection of the Beaty Biodiversity Museum (vouchers whose IDs in Table 1 start with “SCE”) and in the Auburn University Museum of Natural History (AUMNH) (vouchers with other IDs).

DNA extraction, sequencing, filtering, and alignment

Specimens were preserved in 95% ethanol, and stored between two months and 10 years before use. DNA extractions were done using the Qiagen DNEasy blood and tissue kit, using the protocol for <10 mg samples. The second through fourth pairs of legs were used if they provided sufficient sample volume; otherwise, the carapace and sometimes the distal part of the abdomen was added.

Library preparation, enrichment, and sequencing were conducted at the Center for Anchored Phylogenomics at Florida State University (<http://www.anchoredphylogeny.org>). After extraction, up to 500ng of each DNA sample was sonicated to a fragment size of ~300–800 bp using a Covaris E220 ultrasonicator. Indexed libraries were then prepared following Meyer and Kircher (2010), but with modifications for automation on a Beckman-Coulter Biomek FXP liquid-handling robot (see Hamilton et al. 2016b for details). Size-selection was performed after blunt-end repair using SPRI select beads

Table 1. Specimens from which Anchored Hybrid Enrichment data were obtained. A “+” at the start of a row indicates that that specimen’s DNA was combined with that of the previous specimen for sequencing, to yield a single analyzed terminal taxon.

Species	Voucher ID	Sex	Locality	Latitude - longitude
Salticidae				
<i>Agorius</i> aff. <i>borneensis</i> Edmunds & Proszynski, 2001	SCE0002	m	Malaysia: Sarawak: Mulu Nat. Pk.	4.05°N 114.86°E
+ <i>Agorius</i> sp.	SCE0035	f	Malaysia: Sarawak: Mulu Nat. Pk.	4.05°N 114.86°E
<i>Asemonea sichuanensis</i> Song & Chai, 1992	SCE0016	m	China: Guangxi: Ningming County	21.811°N 107.217°E
<i>Bavia aerticeps</i> Simon, 1901	SCE0008	m	Papua New Guinea: S. Highlands Prov.: Tualapa	5.283°S 142.498°E
<i>Breda apicalis</i> Simon, 1901	SCE0022	m	Ecuador: Orellana: Yasuni Res. Stn.	0.677°S 76.402°W
<i>Carrhotus sannio</i> (Thorell, 1877)	SCE0044	m	China: Guangxi: Ningming County	21.822°N 107.029°E
<i>Cocalodes macellus</i> (Thorell, 1878)	SCE0005	m	Papua New Guinea: S. Highlands Prov.: Putuwé	5.231°S 142.532°E
<i>Colonus sylvanus</i> (Hentz, 1846)	SCE0015	m	U.S.A.: Mississippi: Holmes County State Park	33.031°N 89.928°W
<i>Filuda</i> cf. <i>ista</i> Mello-Leitão, 1940	SCE0009	m	Ecuador: Orellana: Río Bigal Reserve	0.53°S 77.418°W
+ <i>Filuda elata</i> Galiano, 1986	SCE0057	m	Ecuador: Orellana: SE of Río Bigal Reserve	0.53-5°S 77.42°W
<i>Freyia decorata</i> (C. L. Koch, 1846)	SCE0012	m	Ecuador: Orellana: Yasuni Res. Stn.	0.674°S 76.397°W
<i>Habronattus ophrys</i> Griswold, 1987	SCE0065	m	Canada: British Columbia: Furry Creek	49.581°N 123.208°W
<i>Harmochirus brachiatus</i> (Thorell, 1877)	SCE0029	m	Malaysia: Sarawak: Kubah Nat. Pk.	1.605-6°N 110.185-7°E
<i>Hasarius adansonii</i> (Audouin, 1825)	SCE0011	m	Singapore: Labrador Park	1.27°N 103.80°E
+ <i>Hasarius adansonii</i> (Audouin, 1825)	SCE0049	m	China: Guangxi: Tianlin County	24.46°N 106.37°E
<i>Heliophanus lineiventris</i> Simon, 1868	SCE0039	m	Spain: Albacete: Villa de Chinchilla	38.9143°N 01.4618°W
<i>Idastrandia</i> sp.	SCE0031	f	Malaysia: Sarawak: Mulu Nat. Pk.	4.05°N 114.86°E
<i>Lapsias canadea</i> Maddison, 2012	SCE0020	m	Ecuador: Esmeraldas: Reserva Canandé	0.5167°N 79.1934°W
<i>Leitung porosa</i> (Wanless, 1978)	SCE0003	m	Malaysia: Sarawak: Lambir Hills Nat. Pk.	4.197-8°N 114.040°E
+ <i>Leitung</i> sp.	SCE0058	f	Malaysia: Sarawak: Lambir Hills Nat. Pk.	4.203°N 114.028-9°E
+ <i>Leitung</i> sp.	SCE0059	f	Malaysia: Sarawak: Lambir Hills Nat. Pk.	4.2025°N 114.0308°E
<i>Lysomanes viridis</i> (Walckenaer, 1837)	SCE0018	m	U.S.A.: Mississippi: Wall Doxey State Park	34.665°N 89.466°W
<i>Mintonia ramipalpis</i> (Thorell, 1890)	SCE0021	m	Malaysia: Sarawak: Mulu Nat. Pk.	4.038°N 114.813°E
<i>Myrmarachne</i> sp.	SCE0053,4	m	Malaysia: Pahang: Tanah Rata	4.46°N 101.40°E
<i>Naphrys pulex</i> (Hentz, 1846)	SCE0038	m	Canada: Muskoka Dist.: Port Cunnington	45.259°N 79.026°W
<i>Noegus</i> sp.	SCE0023	m	Ecuador: Orellana: Yasuni Res. Stn.	0.68°S 76.39°W

Species	Voucher ID	Sex	Locality	Latitude - longitude
<i>Onomastus</i> sp.	SCE0047	f	China: Guangxi: Fangchenggang City	21.683°N 107.649°E
+ <i>Onomastus</i> sp.	SCE0048	f	China: Guangxi: Ningming County	21.815°N 107.305°E
<i>Orthrus</i> aff. <i>muluensis</i> Wanless, 1980	SCE0040	f	Malaysia: Sarawak: Lambir Hills Nat. Pk.	4.199°N 114.037°E
+ <i>Orthrus</i> aff. <i>muluensis</i> Wanless, 1980	SCE0041	f	Malaysia: Sarawak: Lambir Hills Nat. Pk.	4.202°N 114.042°E
<i>Phidippus johnsoni</i> (Peckham & Peckham, 1883)	SCE0024	m	U.S.A.: Oregon: Mt. Hebo	45.214°N 123.755°W
<i>Salticus scenicus</i> (Clerck, 1757)	SCE0045	m	Canada: British Columbia: Kelowna	49.95°N 119.401°W
<i>Sarinda bentzi</i> (Banks, 1913)	AUMS16070	m	U.S.A.: Alabama: Elmore Co.	32.52265°N 86.0024°W
<i>Sarinda</i> sp.	SCE0046	m	Ecuador: Napo: Estación Biológica Jatun Sacha	1.067°S 77.617°W
<i>Sasacus</i> sp.	AUMS16722	f	U.S.A.: Washington: Northcreek	46.8908°N 123.1967°W
<i>Scopocira cyrilli</i> Costa & Ruiz, 2014	SCE0060,1,2	m	French Guiana: Commune Régina, les Nourages	4.0691°N 52.6689°W
<i>Sitircus fasciger</i> (Simon, 1880)	SCE0028	m	Canada: Ontario: Burlington	43.3507°N 79.7593°W
<i>Tisaniba bijibijan</i> Zhang & Maddison, 2014	SCE0050	f	Malaysia: Sarawak: Lambir Hills Nat. Pk.	4.200°N 114.036°E
+ <i>Tisaniba dik</i> Zhang & Maddison, 2014	SCE0051	f	Malaysia: Sarawak: Mulu Nat. Pk.	4.0380°N 114.8137°E
+ <i>Tisaniba dik</i> Zhang & Maddison, 2014	SCE0052	f	Malaysia: Sarawak: Mulu Nat. Pk.	4.0380°N 114.8137°E
<i>Titanattus</i> sp.	SCE0055,6	f	Brazil: Pará: Algodual	0.580°S 47.586°W
<i>Tomomingi</i> sp.	SCE0017	f	Gabon: Woleu-Ntem:Tchimbélé	0.629°N 10.404°E
<i>Yllenus arenarius</i> Simon, 1868	SCE0042,3	j	Poland: Kozki	52.361°N 22.870°E
Outgroups				
Clubionidae: <i>Clubiona</i> sp.	G1765	f	U.S.A.: California: Torrey Pines S.P.	32.92799°N 117.2575°W
Ctenidae: <i>Ctenus exlineae</i> Peck, 1981	G1699	f	U.S.A.: Arkansas: Stone Co., S. Calico Rock	35.9952°N 92.12200°W
Eutichuridae: <i>Cheiracanthium</i> sp.	G1048	m	U.S.A.: California: San Diego Co., Lake Murray	32.7862°N 117.0360°W
Gnaphosidae: <i>Zelotes</i> sp.	AUMS16708	f	U.S.A.: Washington: Stella	46.2614°N 123.1317°W
Homalonychidae: <i>Homalonychus theologus</i> Chamberlin, 1924	AUMS11918	f	U.S.A.: California: Imperial Co.	—
Lycosidae: <i>Alopecosa</i> sp.	AUMS16717	—	U.S.A.: Washington: Bear Canyon	46.71194°N 120.8906°W
Lycosidae: <i>Schizocosa salatrix</i> (Hentz, 1844)	AUMS19518	—	U.S.A.: Tennessee: Heck Hollow Road	36.3319°N 82.9552°W
Miturgidae: <i>Zora spinimana</i> (Sundevall, 1833)	ARA0192	f	Switzerland: Grison Alps, Alp Flix, Salatinas:	46.5131°N 9.6430°E
Oxyopidae: <i>Oxyopes</i> sp.	AUMS16731	m	U.S.A.: Alabama: Lee Co., Auburn	32.5820°N 85.4228°W
Philodromidae: <i>Philodromus barrowsi</i> Gertsch, 1934	SCE0063	m	U.S.A.: Arizona: Tumacacori	31.562°N 111.046°W
Thomisidae: <i>Coriarachne</i> sp.	AUMS16723	f	U.S.A.: Washington: Little Rock Road	46.8728°N 123.0239°W
Zoropsidae: <i>Zoropsis spinimana</i> (Dufour, 1820)	ARA1365	f	Slovenia: Ljubljana	46.0485°N 14.5079°E

(Beckman–Coulter Inc.; 0.9x ratio of bead to sample volume). Indexed samples were pooled at equal quantities (16 samples per pool), and then each pool was enriched using the AHE Spider Probe kit v1 developed by Hamilton et al. (2016b) and a modified v2 (Hamilton et al. unpublished), which has been refined to yield greater enrichment within araneomorph spiders than the original version. After enrichment, the two enrichment reactions were pooled in equal quantities and sequenced on one PE150 Illumina HiSeq 2500 lanes at Florida State University Translational Science Laboratory in the College of Medicine.

Prior to assembly, overlapping paired reads were merged following Rokyta et al. (2012). For each read pair, the probability of obtaining the observed number of matches by chance was evaluated for each possible degree of overlap. The overlap with the lowest probability was chosen if the p-value was less than 10^{-10} , a stringent threshold that helps avoid chance matches in repetitive regions (see Rokyta et al. 2012 for details). Read pairs failing to merge were utilized but left unmerged during the assembly.

Divergent reference assembly was used to map reads to the probe regions and extend the assembly into the flanking regions (see Prum et al. 2015 and Hamilton et al. 2016b for details). For this analysis, the *Aphonopelma*, *Aliatypus*, *Ixodes* and *Hypochilus* references (Hamilton et al. 2016b) were utilized as references. Preliminary matches were called if at least 17 of 20 spaced-kmer bases matched and the preliminary matches were confirmed if at least 55 of 100 consecutive bases matched. Assembly contigs derived from less than 23 reads were removed in order to reduce the effects of cross contamination and rare sequencing errors in index reads.

Orthology was determined among the homologous consensus sequences at each locus following Prum et al. (2015) and Hamilton et al. (2016b). Pairwise distances among homologs were computed for each locus based on the percent of shared continuous and spaced 20-mers. Sequences were clustered using a Neighbor-Joining algorithm by distance, but allowing at most one sequence per species to be in a given cluster. In order to reduce the effects of missing data, data were reduced by removing from downstream processing clusters that contained fewer than 50% of the species. The result of this assessment was 492 orthologous clusters (loci).

For all samples except *Tisaniba*, the nHomologs statistic presented in the Supplementary Table shows value near 1, indicating that at each locus approximately one homolog was recovered by the assembler. This is an indication that recent gene duplication and loss is very low in this group, and that our results are not compromised by the deep arachnid whole-genome duplication (Schwager et al. 2017). It also indicates that the individuals whose DNA was pooled for each species were quite similar (the assembler interpreted any differences at the level of allelic differences). This is not the case for *Tisaniba*, which had an elevated nHomolog value of 1.71, meaning that at 71% of the loci, two homologs were identified and separated into different consensus sequences. For these loci the orthology method would choose the consensus sequence most similar to that of the most similar relatives, and likely removed the other consensus from downstream analysis.

Sequences in each orthologous cluster were aligned using MAFFT v7.023b (Katoh and Standley 2013), using the `--genafpair` and `--maxiterate 1000` flags. The alignment for each locus was then trimmed/masked using the steps described in Hamilton et al. (2016b). Each alignment site was identified as “conserved” if the most commonly observed character was present in > 50% of the sequences. Each sequence was scanned for regions that did not contain at least 10 of 20 characters matching to the common base at the corresponding conserved site. Characters from regions not meeting this requirement were masked. Third, sites with fewer than 23 unmasked bases were removed from the alignment. Geneious version 7 (www.geneious.com; Kearse et al. 2012) was used to visually inspect each masked alignment and to remove regions of sequences identified as obviously misaligned or paralogous. Trimming resulted in some loci being deleted, yielding a final total of 447 loci. This represents a higher success rate than Hamilton et al. (2016), This represents a higher success rate than Hamilton et al. (2016), whose study had greater breadth, across all spiders, and used an older probe set.

In preparation for phylogenetic analyses, the 447 trimmed AHE loci were realigned individually with MAFFT version 7.058b (Katoh and Standley 2013) using the `L-INS-i` option (`--localpair --maxiterate 1000`). Although assigning codon positions could have allowed better model partitioning in the phylogenetic analysis, we were unable to do so because the loci are often relatively short (average about 560 bases; see Supplementary Table) and we lack a well-annotated reference transcriptome. Our attempts to assign codon positions via TransDecoder version 3.0.1 (Haas et al. 2013) yielded unrealistic results for many loci, and so we left codon positions unassigned.

Phylogenetic analyses

We inferred the phylogeny for the 46 taxa using Maximum Likelihood, parsimony, and SVDQuartets applied to a concatenated supermatrix of the 447 aligned loci, and using ASTRAL (a coalescent-based approach, like SVDQuartets) applied to ML-reconstructed gene trees of the 447 separate loci.

Two Maximum Likelihood (ML) analyses on the concatenated matrix were performed using RAxML version 8.2.8 (Stamatakis 2014). One left the matrix unpartitioned. The other used partitions chosen by PartitionFinder version 1.1.1 (Lanfear et al. 2012) based on an initial partition by locus. PartitionFinder grouped the loci via a relaxed clustering algorithm assuming linked branch lengths and evaluating 10% of schemes at each step according to BIC score. We used relaxed clustering as, for large datasets such as ours, it has been demonstrated to produce results consistently comparable to a greedy algorithm but with much more computational efficiency (Lanfear et al. 2014). The best scheme according to our PartitionFinder analyses grouped loci into 21 partitions. Both maximum likelihood analyses assumed the GTR+gamma+I model.

We present as our primary result the best-scoring ML tree from the partitioned supermatrix and 200 search replicates. Robustness of clade support was explored by a bootstrap analysis with 1000 replicates, in each of which 5 search replicates were done.

Parsimony bootstrap analysis was performed by PAUP* version 4.0a151 (Swofford 2002), with 1000 replicates, for each of which we used TBR branch rearrangement, multrees, maxtrees = 100, and 2 search replicates.

We also used two methods based on the multi-species coalescent model to infer the species phylogeny, SVDQuartets (Chifman and Kubatko 2015) and ASTRAL II (Mirarab et al. 2014). SVDQuartets was performed by PAUP* version 4.0a150 using exhaustive quartet sampling and 1000 bootstrap replicates. The ASTRAL analysis was performed by version 4.7.12 using default settings, based on the 447 gene trees, one from each locus, obtained by RAxML version 8.2.8 from a simple ML search (model GTRGAMMA, unpartitioned).

Results

Hybrid enrichment results are shown in the Supplementary Table. The 447 loci obtained in the final filtered data set represent for most taxa about 80 kb of nucleotide sequence. We were less successful at obtaining data for two taxa, with *Schizocosa sal-tatrix* having only 9377 nucleotides sequenced, and *Yllenus arenarius* having 36069 nucleotides. The “on target” percentage of *Yllenus* was low, suggesting either that its genome is unusually large, or that the sample included also some non-spider DNA. The other taxa had between 76,262 (*Clubiona*) and 91,238 (*Hasarius adansoni*) nucleotides sequenced. Alignments for each of the 477 loci are deposited, along with phylogenetic results, to Dryad (<http://dx.doi.org/10.5061/dryad.n2b3h>).

Fig. 1 shows the ML tree from the partitioned concatenated supermatrix. Bootstrap values are high for most clades. The unpartitioned ML, parsimony, ASTRAL and SVDQuartets gave largely concordant results, differing only where marked in Fig. 1 by -u, -p, -a, and -s respectively. In particular, unpartitioned ML places *Yllenus* as the sister to the rest of the Simonida (though with low bootstrap support); parsimony places *Yllenus* and *Naphrys* as sisters, and Freya as sister to *Harmochirus* and *Habronattus*; ASTRAL places *Bavia* as sister to the astioids and marpissoids, and *Yllenus* as the sister to the rest of the Simonida; SVDQuartets trades the positions of *Idastrandia* and *Hasarius* and rearranges the Simonida.

Discussion

This first genome-wide analysis of salticids resolves the group’s phylogeny with greater confidence than previous studies, confirming and extending those results based on far fewer genes (Maddison et al. 2014; Ruiz and Maddison 2015; Maddison 2015). The results corroborate the monophyly of the Salticinae, a major clade with more than

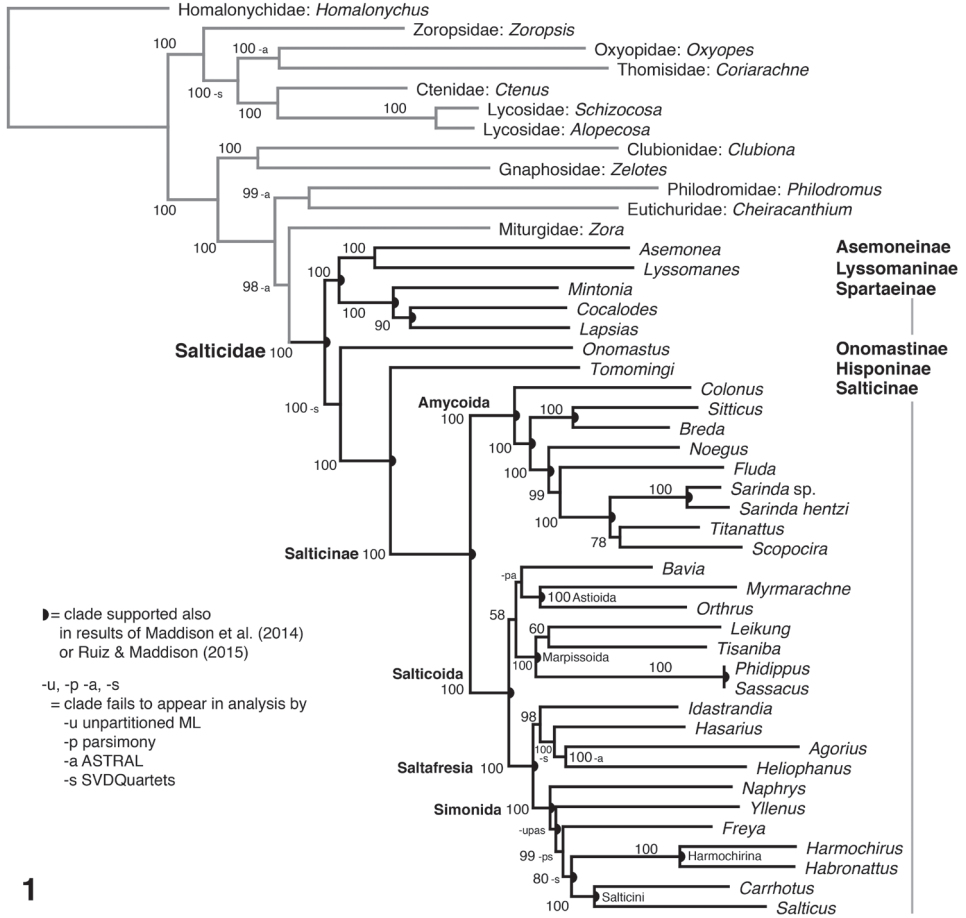


Figure 1. Maximum likelihood phylogeny from the partitioned concatenated matrix of 447 loci captured by Anchored Hybrid Enrichment. Numbers indicate percentage of likelihood bootstrap replicates showing the clade. Half circle indicates clades supported also in the results of Maddison et al. (2014) or, for the Amycoidea, of Ruiz and Maddison (2015). Letters u, p, a, and s indicate clades that fail to appear in the analyses by unpartitioned likelihood, parsimony, ASTRAL and SVDQuartets respectively.

90% of described salticid species, including most familiar species. The Spartaeinae, which includes the well-known *Portia*, is also supported (in our analysis: *Mintonia*, *Cocalodes*, *Lapsias*). Major clades corroborated within the Salticinae are the Salticoida (*sensu* Maddison 2015), Saltafresia, Simonida, Amycoidea, and Marpissoida (here: *Leikung*, *Tisaniba*, *Phidippus*, *Sassacus*). Other clades consistent with the previous results of Maddison et al. (2014, 8 genes, salticid-wide) and Ruiz and Maddison (2015, 5 genes, within the Amycoidea) are indicated with semicircles on Fig. 1.

The relationships among the subfamilies, previously poorly resolved (Maddison et al. 2014), are strongly supported in our analyses. Unsurprising is the relationship between

the Hisponinae and Salticinae, which has been supported by both molecular and morphological data (Maddison 2015). The relationship among asemoneines, lyssomanines and spartaeines was anticipated (Maddison et al. 2014) but not previously well supported.

A novel result is the placement of Onomastinae as sister to Hisponinae plus Salticinae. Onomastines, like the lyssomanines and asemoneines, are long-legged translucent spiders with complex palpi and an ocular area relatively small compared to other salticids (see Wanless 1980). The distinctive features of onomastines, lyssomanines and asemoneines might have been interpreted as ancestral for the family, or as synapomorphies uniting them (Maddison 2015). Their separate placement here suggests that either their form is convergent, or that the more familiar compact brown body with an expanded ocular area evolved independently in spartaeines and hisponines+salticines. We do note, however, that despite the 100% ML bootstrap support for onomastines+hisponines+salticines, not all analyses agree on this placement. The SVDQuartets analysis places *Onomastus* as sister to *Asemonea*+*Lyssomanes*+*Spartaeinae*, as also recovered from 8 genes by Maddison et al. (2014).

Within the Salticinae, our data have succeeded in resolving the placement of one puzzling group, the agoriines, whose position was problematic to Maddison et al. (2014). Our 447 locus data clearly supports placing the agoriines within the Saltafresia, in a group with chrysillines (here represented by *Heliophanus*) and hasariines. Most analyses place *Agorius* sister to *Heliophanus*, though ASTRAL places it with the nearby *Hasarius*. Maddison et al. (2014) found *Agorius* and its close relative *Synagelides* to have unstable placement, on long branches, and varying in position drastically among the different analyses. Interestingly, their All Genes salticine analysis (their figure 18) placed agoriines with the chrysillines, a placement strongly supported in our analyses. Maddison (2015) notes the similarities of the genitalia of agoriines with the two groups indicated as close relatives here, the chrysillines and hasariines.

The relationships among the four major subgroups of Salticoida (*sensu* Maddison 2015) — Marpissoida, Astioida, Baviini, and Saltafresia — were not resolved well by Maddison et al. (2014: 80). Bodner and Maddison (2012) suggested the first three form a clade, but this was not corroborated by the results of Maddison et al. (2014). Our data give support to Bodner and Maddison's conclusion, though weakly. All analyses place *Bavia* in a clade with the Marpissoida and Astioida (together forming the sister group to the Saltafresia), but bootstrap support is only 58% for likelihood, 67% for parsimony, and 100% for SVDQuartets. The weak support for this clade may indicate a rapid early radiation of the Salticoida, and may require considerably more data to corroborate or refute. Within the tentative clade of Baviini+Marpissoida+Astioida the detailed relationships are unresolved. Likelihood and SVDQuartets place *Bavia* with the astioids *Myrmarachne* and *Orthrus* but with bootstrap support less than 50% for ML, 56% for SVDQuartets; parsimony places *Bavia* as sister to the Marpissoida; ASTRAL places *Bavia* as sister to Marpissoida+Astioida.

Within the Simonida, the Harmochirina (*Harmochirus*, *Habronattus*) and Salticini (*Carrhotus*, *Salticus*) are confirmed each as monophyletic and as sister lineages, as per Maddison et al. (2014). Deeper relationships in the Simonida, among the tribes, are

unclear and vary by analysis. As shown in Fig. 1, likelihood recovers (*Naphrys*, (*Yllenus*, (*Freya*, (harmochirines, salticines))))), with *Naphrys* representing the Euphryini, *Yllenus* the Leptorchestini, and *Freya* the Aelurillini. However, ASTRAL obtains (*Y*,(*N*,(*F*,(*h*,*s*))))), SVDQuartets (*Y*,(*h*,(*N*,(*F*,*s*))))), and parsimony ((*Y*,*N*),((*F*,*h*),*s*)). A contributing factor to this poor resolution could be the poor sequence capture for *Yllenus*.

Given the strength of this broad data set and its concordance with previous results, we can now be reasonably confident in our current phylogenetic classification (Maddison 2015). Our results highlight what is needed for further progress. For the deeper parts of the phylogeny, most urgent is to include the Eupoinae, not only to determine their (currently ambiguous) placement (Maddison et al. 2014), but also because their inclusion would provide a test of the supported relationships among the subfamilies. Within the Salticinae, the most basic outstanding question concerns the relative relationships among baviines, astioids, marpissoids and saltafresians. To resolve this, a much larger fraction of the genome may be needed. Of course, even once our understanding of these broad relationships stabilizes, the bulk of salticid phylogeny remains still unresolved, as not only is there no explicit phylogenetic work on most of the described species, but many species remain to be discovered.

Acknowledgments

For assistance in collecting specimens we thank especially Edyta Piascik, Mauricio Vega, and Junxia Zhang. This work was supported by an NSERC Discovery grant to W. Maddison (RGPIN 261352-2013); National Science Foundation Doctoral Dissertation Improvement Grant – DEB-1311494 to CAH; an Auburn University Cellular and Molecular Biosciences Peaks of Excellence Research Fellowship (CAH).

References

- Bodner MR, Maddison WP (2012) The biogeography and age of salticid spider radiations (Araneae: Salticidae). *Molecular Phylogenetics and Evolution* 65: 213–240. <https://doi.org/10.1016/j.ympev.2012.06.005>
- Chifman J, Kubatko L (2015) Identifiability of the unrooted species tree topology under the coalescent model with time-reversible substitution processes, site-specific rate variation, and invariable sites. *Journal of Theoretical Biology* 374: 35–47. <https://doi.org/10.1016/j.jtbi.2015.03.006>
- Hamilton CA, Hendrixson BE, Bond JE (2016a) Taxonomic revision of the tarantula genus *Aphonopelma* Pocock, 1901 (Araneae, Mygalomorphae, Theraphosidae) within the United States. *ZooKeys* 560: 1–340. <https://doi.org/10.3897/zookeys.560.6264>
- Hamilton CA, Lemmon AR, Lemmon EM, Bond JE (2016b) Expanding anchored hybrid enrichment to resolve both deep and shallow relationships within the spider tree of life. *BMC Evolutionary Biology* 16: 212. <https://doi.org/10.1186/s12862-016-0769-y>

- Haas BJ, Papanicolaou A, Yassour M, Grabherr M, Blood PD, Bowden J, et al. (2013) De novo transcript sequence reconstruction from RNA-seq using the Trinity platform for reference generation and analysis. *Nature Protocols* 8: 1494–512. <https://doi.org/10.1038/nprot.2013.084>
- Katoh K, Standley D (2013) MAFFT multiple sequence alignment software version 7: improvements in performance and usability. *Molecular Biology and Evolution* 30: 3059–66. <https://doi.org/10.1093/molbev/mst010>
- Kearse M, Moir R, Wilson A, Stones-Havas S, Cheung M, Sturrock S, Buxton S, Cooper A, Markowitz S, Duran C, Thierer T, Ashton B, Meintjes P, Drummond A (2012) Geneious Basic: an integrated and extendable desktop software platform for the organization and analysis of sequence data. *Bioinformatics* 28: 1647–1649. <https://doi.org/10.1093/bioinformatics/bts199>
- Lanfear R, Calcott B, Ho S, Guindon S (2012) PartitionFinder: combined selection of partitioning schemes and substitution models for phylogenetic analyses. *Molecular Biology and Evolution* 29: 1695–701. <https://doi.org/10.1093/molbev/mss020>
- Lanfear R, Calcott B, Kainer D, Mayer C, Stamatakis A (2014) Selecting optimal partitioning schemes for phylogenomic datasets. *BMC Evolutionary Biology* 14: 82. <https://doi.org/10.1186/1471-2148-14-82>
- Lemmon AR, Emme SA, Lemmon EM (2012) Anchored Hybrid Enrichment for massively high-throughput phylogenomics. *Systematic Biology* 61: 717–726. <https://doi.org/10.1093/sysbio/sys049>
- Lemmon EM, Lemmon AR (2013) High-throughput genomic data in systematics and phylogenetics. *Annual Review of Ecology, Evolution, and Systematics* 44(1): 99–121. <https://doi.org/10.1146/annurev-ecolsys-110512-135822>
- Maddison WP (2015) A phylogenetic classification of jumping spiders (Araneae: Salticidae). *Journal of Arachnology* 43: 231–292. <https://doi.org/10.1636/ arac-43-03-231-292>
- Maddison WP, Hedin MC (2003) Jumping spider phylogeny (Araneae: Salticidae). *Invertebrate Systematics* 17: 529–549. <https://doi.org/10.1071/IS02044>
- Maddison WP, Li D, Bodner M, Zhang JX, Xu X, Liu Q, Liu F (2014) The deep phylogeny of jumping spiders (Araneae, Salticidae). *ZooKeys* 440: 57–87. <https://doi.org/10.3897/zookeys.440.7891>
- Mirarab S, Reaz R, Bayzid MS, Zimmermann T, Swenson MS, Warnow T (2014) ASTRAL: genome-scale coalescent-based species tree estimation. *Bioinformatics* 30: i541–8. <https://doi.org/10.1093/bioinformatics/btu462>
- Prum RO, Berv JS, Dornburg A, Field DJ, Townsend JP, Moriarty LE, Lemmon AR (2015) A comprehensive phylogeny of birds (Aves) using targeted next-generation DNA sequencing. *Nature* 526: 569–73. <https://doi.org/10.1038/nature15697>
- Rokyta DR, Lemmon AR, Margres MJ, Aronow K (2012) The venom-gland transcriptome of the eastern diamondback rattlesnake (*Crotalus adamanteus*). *BMC Genomics* 13: 1–23. <https://doi.org/10.1186/1471-2164-13-312>
- Ruiz GRS, Maddison WP (2015) The new Andean jumping spider genus *Uruguayu* and its placement within a revised classification of the Amycoidea (Araneae: Salticidae). *Zootaxa* 4040: 251–279. <https://doi.org/10.11646/zootaxa.4040.3.1>

- Schwager EE, Sharma PP, Clarke T, Leite DJ, Wierschin T, Pechmann M, Akiyama-Oda Y, Esposito L, Bechsgaard J, Bilde T, Buffry AD, Chao H, Dinh H, Doddapaneni HV, Dugan S, Eibner C, Extavour CG, Funch P, Garb K, Gonzalez LB, Gonzalez VL, Griffiths-Jones S, Han Y, Hayashi C, Hilbrant M, Hughes DST, Janssen R, Lee SL, Maeso I, Murali SC, Muzny DM, Nunes da Fonseca R, Paese CLB, Qu JX, Ronshaugen M, Schomburg C, Schönauer A, Stollewerk A, Torres-Oliva M, Turetzek N, Vanthournout B, Werren JH, Wolff C, Worley KC, Bucher G, Gibbs RA, Coddington J, Oda H, Stanke M, Ayoub NA, Prpic NM, Flot JF, Posnien N, Richards S, McGregor AP (2017) The house spider genome reveals an ancient whole-genome duplication during arachnid evolution. *BMC Biology* 15: 62. <https://doi.org/10.1186/s12915-017-0399-x>
- Stamatakis A (2014) RAxML version 8: a tool for phylogenetic analysis and post-analysis of large phylogenies. *Bioinformatics* 30(9): 1312–1313. <https://doi.org/10.1093/bioinformatics/btu033>
- Swofford DL (2002) PAUP*. Phylogenetic analysis using parsimony (* and other methods). Version 4. Sinauer Associates, Sunderland, MA.
- Wheeler WC, Coddington JA, Crowley LM, Dimitrov D, Goloboff PA, Griswold CE, Hormiga G, Prendini L, Ramírez MJ, Sierwald P, Almeida-Silva L, Alvarez-Padilla F, Arnedo MA, Benavides Silva LR, Benjamin SP, Bond JE, Grismado CJ, Hasan E, Hedin M, Izquierdo MA, Labarque FM, Ledford J, Lopardo L, Maddison WP, Miller JA, Piacentini LN, Platnick NI, Polotow D, Silva-Dávila D, Scharff N, Szűts T, Ubick D, Vink CJ, Wood HM, Zhang JX (2016) The spider tree of life: Phylogeny of Araneae based on target-gene analyses from an extensive taxon sampling. *Cladistics*, 1–43. <https://doi.org/10.1111/cla.12182>
- World Spider Catalog (2017) World Spider Catalog. Natural History Museum Bern, online at <http://wsc.nmbe.ch>, version 18.0. [Accessed on 21 April 2017]

Supplementary material I

Supplementary table of assembly statistics

Authors: Wayne P. Maddison, Samuel C. Evans, Chris A. Hamilton, Jason E. Bond, Alan R. Lemmon, Emily Moriarty Lemmon

Data type: Microsoft Excel Worksheet (.xlsx)

Explanation note: Statistics describing raw reads, loci, sequence lengths, and other aspects of sequencing assembly for each of the 34 salticid taxa and 12 outgroup taxa.

Copyright notice: This dataset is made available under the Open Database License (<http://opendatacommons.org/licenses/odbl/1.0/>). The Open Database License (ODbL) is a license agreement intended to allow users to freely share, modify, and use this Dataset while maintaining this same freedom for others, provided that the original source and author(s) are credited.

Link: <https://doi.org/10.3897/zookeys.695.13852.suppl1>

Occurrence and the ecological implication of a tropical anguillid eel *Anguilla marmorata* from peninsular Malaysia

Siti Raudah Abdul Kadir¹, Mohamad Hafiz Farhan Abdul Rasid²,
Kok Onn Kwong³, Li Lian Wong², Takaomi Arai⁴

1 Institute of Oceanography and Environment, Universiti Malaysia Terengganu, 21030 Kuala Terengganu, Terengganu, Malaysia **2** Institute of Tropical Aquaculture, Universiti Malaysia Terengganu, 21030 Kuala Terengganu, Terengganu, Malaysia **3** School of Biological Sciences, Universiti Sains Malaysia, Minden, Penang, Malaysia **4** Environmental and Life Sciences Programme, Faculty of Science, Universiti Brunei Darussalam, Jalan Tungku Link, Gadong, BE 1410, Brunei Darussalam

Corresponding author: Takaomi Arai (takaomi.arai@ubd.edu.bn)

Academic editor: N. Bogutskay | Received 19 April 2017 | Accepted 20 August 2017 | Published 5 September 2017

<http://zoobank.org/E9A259D7-7C35-4B76-8D41-D69A0748D4BE>

Citation: Abdul Kadir SR, Abdul Rasid MHF, Kwong KO, Wong LL, Arai T (2017) Occurrence and the ecological implication of a tropical anguillid eel *Anguilla marmorata* from peninsular Malaysia. ZooKeys 695: 103–110. <https://doi.org/10.3897/zookeys.695.13298>

Abstract

Recent studies suggested that accurate species identification in the tropical anguillid eels based on morphological examination requires confirmation by molecular genetic analysis. Previous studies found that two tropical anguillid eels, *Anguilla bicolor bicolor* and *A. bengalensis bengalensis*, were found in peninsular Malaysia (West Malaysia) based on morphological and molecular genetic analyses. This study is the first record of *A. marmorata* in peninsular Malaysia confirmed by both morphological and molecular genetic analyses. The present study also suggests that accurate tropical eel species identification is difficult by morphological identification alone; therefore, molecular genetic analysis is needed for precise species confirmation.

Keywords

Anguillid eel, giant mottled eel, molecular, species identification, tropical fish

Introduction

The anguillid eels of the genus *Anguilla* Schrank are widely distributed throughout the world. These eels have a catadromous life history, migrating between inland or coastal growth habitats and offshore spawning locations. Nineteen species or subspecies of *Anguilla* have been reported worldwide, thirteen of which occur in tropical regions. Of the thirteen species/subspecies found in tropical areas, seven species/subspecies inhabit western Pacific around Indonesia and Malaysia: *A. celebesensis* Kaup, *A. interioris* Whitely, *A. bengalensis bengalensis* Gray, *A. marmorata* Quoy & Gaimard, *A. borneensis* Popta, *A. bicolor bicolor* McClelland and *A. bicolor pacifica* Schmidt (Ege 1939, Castle and Williamson 1974, Arai et al. 1999).

Molecular phylogenetic research on freshwater eels have revealed that tropical eels are the most basal species originating in the Indonesian and Malaysian regions and that freshwater eels radiated from the tropics to colonize temperate regions (Minegishi et al. 2005). Recently, freshwater eel biology such as species composition, distribution, and life history has gradually accumulated in tropical eel species in Malaysian waters (e.g., Arai et al. 2012, 2015, 2017a, b, Arai and Chino 2013, Arai 2014, Abdul Kadir et al. 2015, Arai and Wong 2016, Wong et al. 2017). Identification of eels at the species level using morphological examination only is difficult because of similarities and overlapping of morphological characters, particularly in tropical anguillids (Arai et al. 2015, Arai and Wong 2016). Currently, two anguillid eels, *Anguilla bengalensis bengalensis* and *A. bicolor bicolor*, have been confirmed to occur in peninsular Malaysia (Arai et al. 2015, Arai and Wong 2016).

In the present study, two anguillid specimens were collected and examined from the Pondok Upeh River, Penang Island. As Arai et al. (2015) and Arai and Wong (2016) suggested that tropical eel species identification could be accurately validated by molecular genetic analysis after morphological observation, the specimens were subjected to identification using both morphological and mitochondrial cytochrome oxidase subunit I (COI) 16S ribosomal RNA (16S rRNA) sequence analyses. This paper describes the first confirmed record of a tropical anguillid eel, *Anguilla marmorata*, from peninsular Malaysia.

Materials and methods

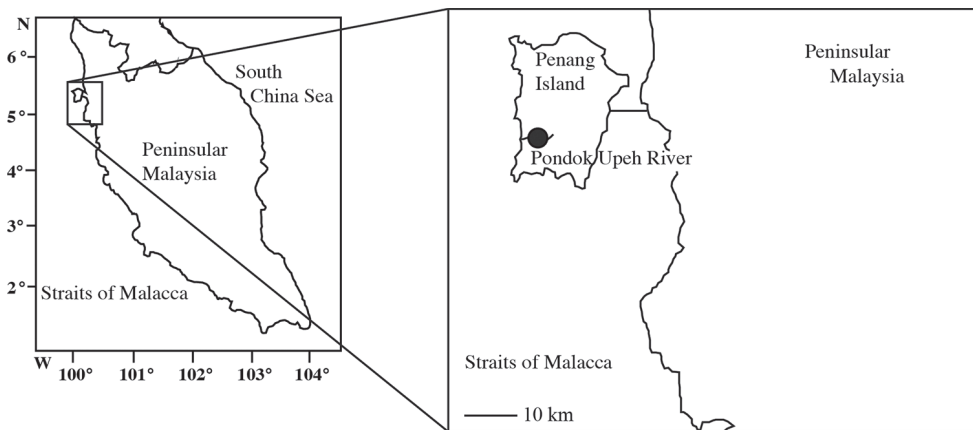
Eel samples and morphological analysis

Two anguillid specimens were collected by hook and line by local people in the Pondok Upeh River in Penang Island of peninsular Malaysia on 2 April 2015 (Fig. 1).

External measurements follow Ege (1939) and Watanabe et al. (2004), and the data are shown in Table 1. The fin difference index (**FDI**), which is the distance between the verticals from the origin of the dorsal fin (**Z**) to the anus (ano-dorsal length) relative to the total length (L_T) (Ege 1939) was calculated as follows: $FDI = 100 Z L_T^{-1}$. The number of teeth in the mid part of the maxillary band is abbreviated as NMM.

Table 1. Morphometric characteristics of *Anguilla marmorata* and *A. bengalensis bengalensis* as revealed by molecular genetic analyses.

Specimen number	SP26	TB316
Species by molecular genetic	<i>A. marmorata</i>	<i>A. bengalensis bengalensis</i>
Species by morphology	<i>A. celebesensis</i>	<i>A. marmorata</i>
Measurements (mm)		
Total length (Lt)	904	889
Standard length (SL)	886	975
Body weight (g)	2335	1579
Head length (HL)	136	127
Predorsal length (PD)	303	259
Preanal length (PA)	403	395
Length of intermaxillary-vomerine band (LV)	28.7	24.9
Length of left maxillary band (LM)	30.9	32.1
Number of teeth of mid part of maxillary band (NMM)	5	1
Width of mid part of maxillary band (WMM)	4.4	1.1
FDI (%)	11	15

**Figure 1.** Sampling site in the Pondok Upeh River in Penang Island of peninsular Malaysia.

Molecular genetic analysis

Two mitochondrial genes, cytochrome oxidase *c* subunit 1 (COI) and 16S ribosomal RNA (16S rRNA), were used. DNA was extracted from a dorsal fin clip of each specimen using Gentra Puregene Tissue Kit (QIAGEN, USA), according to the manufacturer's instructions. Total DNA concentration and quality was quantified using BioPhotometer Plus spectrophotometer (Eppendorf, Germany). Both mitochondrial cytochrome COI and 16S rRNA genes were amplified using primer pairs (Table 2) to validate the species identity of each specimen. PCR reaction and condition for COI gene was performed

Table 2. Primers used in this study.

Gene	Primer Sequences	Sources
Cytochrome oxidase subunit I (COI)	FF2d: 5'TTCTCCACCAACCACAARGAYATYGG3' FR1d: 3'CACCTCAGGGTGTCCGAARAAYCARAA5'	Ivanova et al. (2007)
16S rRNA	L2510: 5'CGC CTG TTT ATC AAA AAC AT 3' H3080: 5' CCG GTC TGA ACT CAG ATC ACG T 3'	Palumbi et al. (1991)

Table 3. Validation of species identity of collected specimens based on mitochondrial cytochrome oxidase subunit I (COI) and 16S ribosomal RNA (16S rRNA) genes using BLAST search in GenBank.

Morphological identification	Genetic identification	% Max identity (BLASTn)		GenBank Accession Number	
		COI	16S rRNA	COI	16S rRNA
SP26 <i>A. celebesensis</i>	<i>Anguilla marmorata</i>	94	99	KT728354	KT728352
TB316 <i>A. marmorata</i>	<i>Anguilla bengalensis bengalensis</i>	99	99	KT728353	KT728351

according to Abdul Kadir et al. (2015), whereas PCR amplification for 16S rRNA gene was conducted according to Arai and Wong (2016). PCR amplicons were purified using QIAquick® PCR Purification Kit (QIAGEN, USA), labeled with BigDye Terminator v.3.1 Cycle Sequencing Kit (Applied Biosystems Inc., USA), and sequenced bi-directionally on an ABI PRISM 3730xl Genetic Analyzer. Generated sequence trace files were manually edited and assembled using SeqMan Pro application in DNASTAR version 6.0 (DNASTAR Inc., USA). The contig sequences were compared for percentage similarity with the reference sequences in the GenBank using BLAST search. The sequences for both specimens were deposited to GenBank with accession numbers as listed in Table 3.

Results

The two specimens examined in this study had variegated markings on the body (Fig. 2a, b). However, one (SP26) had wide maxillary bands of teeth with a small number of NMM teeth (Fig. 2c) and 11 of FDI while the second specimen (TB316) had narrow maxillary bands of teeth with a higher NMM (Fig. 2d) and 15 of FDI.

SP26 was assigned into the first species group of the genus *Anguilla* (*A. celebesensis*, *A. interioris*, *A. megastoma* Kaup, *A. luzonensis* Watanabe, Aoyama and Tsukamoto) based on the variegated skin and wide maxillary bands of teeth (Ege 1939, Watanabe et al. 2004, Arai and Wong 2016). TB316 was assigned to the second group (*A. bengalensis bengalensis*, *A. bengalensis labiata* Peters, *A. marmorata*, *A. reinhardtii* Steindachner) based on variegated skin and narrow maxillary bands of teeth (Ege 1939, Watanabe et al. 2004, Arai and Wong 2016).



Figure 2. *Anguilla marmorata* and *A. bengalensis bengalensis* collected in the Pondok Upeh River in Penang Island of Peninsular Malaysia. **A** *Anguilla marmorata* (904 mm in TL) **B** *Anguilla bengalensis bengalensis* (889 mm in TL) **C** Wide maxillary bands of teeth of *A. marmorata* **D** Narrow maxillary bands of teeth of *A. bengalensis bengalensis*. DNA was extracted from dorsal fin clip of each specimen, and hence the posterior dorsal fin of each specimen is lacking.

The geographical distribution of anguillids is used in combination with key morphological characteristics to determine the classification of each species into four groups. Within the first group, *A. interioris*, *A. megastoma*, *A. luzonensis* exist in New Guinea, Solomon Islands, New Caledonia, Fiji Islands, Cook Islands, and northern Philippines (Ege 1939). Therefore, SP26 was considered to be *A. celebesensis* with a range of FDI from 6 to 12 and of NMM from 4 to 9 (Ege 1939, Watanabe et al. 2004).

Within the second group, *A. bengalensis labiata* and *A. reinhardtii* exist in the mid-southeastern region of Africa and eastern Australia and Tasmania, respectively (Ege 1939). Therefore, both species were not considered when identifying the samples in the present study. The FDI of the other two species, *A. bengalensis bengalensis* and *A. marmorata*, was studied further. According to the key morphological characteristics used for their identification (Ege 1939, Watanabe et al. 2004), the FDI of *A. marmorata* is in the range of 12 to 20, higher than that of *A. bengalensis bengalensis*, which ranges from 8 to 14 (Ege 1939, Watanabe et al. 2004). Based on the FDI of TB316, which equals 15, this specimen was identified as *A. marmorata*.

A total contrast was found in the species identification outcomes in the molecular genetic analysis when compared to the morphological observation. As shown in Table 3, molecular identification based on two genes confirms that SP26, which was morphologically identified as *A. celebesensis*, was in fact *A. marmorata*. On the other hand, specimen TB316 identified as *A. marmorata* was actually confirmed as *A. bengalensis bengalensis* based on the genetic results.

Discussion

The findings from this and previous studies (Arai et al. 2015, Arai and Wong 2016) have suggested that tropical eel species identification could be accurately validated by molecular genetic analysis after morphological observation. Misidentification using morphology has been reported for *A. borneensis* and *A. bicolor bicolor* (Arai and Wong 2016). Likewise, same mismatches between morphological identification and genetic identification were also found in TB316. Although TB316 was identified as *A. marmorata* by morphological key characters, it was identified as *A. bengalensis bengalensis* by molecular genetic analyses. The inconclusive morphological identification of these specimens is not merely a technical error, but, rather, is due to the inadequacy of the description of the key of morphological characteristics. Further, the species identity of both specimens from this study have been validated by a concrete molecular data of previous studies, in which putative voucher specimens of *A. bengalensis bengalensis* (Arai and Wong 2016) and *A. marmorata* (Wong et al. 2017) were morphologically examined for species confirmation. This verification process is necessary to ensure that our molecular data is solely based on correctly identified species, instead of referring to sequences in GenBank which may likely derived from misidentified specimens.

In previous studies, *Anguilla marmorata* was reported to exist in Langkawi Island, peninsular Malaysia (Ahmad and Lim 2006, Azmir and Samat 2010). However, after a thorough morphological re-examination by Ahmad and Lim (2006) of one sample of *A. marmorata* preserved in formalin, Arai (2014) discovered that the true identify of that particular sample was *A. bengalensis bengalensis*. In fact, the difficulty in distinguishing between *A. marmorata* and *A. bengalensis bengalensis* is augmented by their overlapping morphological characteristics. Furthermore, recent molecular studies also found that all eels that possess skin with variegated markings were identified as *A. bengalensis bengalensis* (Arai et al. 2015, Arai and Wong 2016); however, this is the first description of the occurrence of *A. marmorata* in peninsular Malaysia identified by molecular genetic analyses. The present and previous studies all lead to the conclusion that currently three eels, i.e., *A. bengalensis bengalensis*, *A. marmorata*, and *A. bicolor bicolor*, occur in peninsular Malaysia.

According to Jespersen (1942), the anguillid eels distributed in Java and Sumatra may have their spawning areas situated off the south-western coast of Sumatra. *Anguilla marmorata* in Malaysia might originate from spawning areas off Sumatra. However, the distance between the spawning area and recruitment area in peninsular Malaysia is con-

siderably larger than the distance between the islands of Java and Sumatra; therefore, the abundance of specimens that survive to reach peninsular Malaysia might be quite low. This would make *A. marmorata* difficult to identify in the area. Further field sampling should be undertaken, along with accurate species identification, in order to better understand the details of species composition and distribution of the tropical anguillid eels.

Acknowledgements

This study was financially supported by the Ministry of Higher Education Malaysia under the Fundamental Research Grant Scheme (Vot Nos. 59281 and 59406) and Universiti Brunei Darussalam under the Competitive Research Grant Scheme (Vot No. UBD/OVACRI/CRGWG(003)/161101).

References

- Abdul Kadir SR, Abdul Rasid MHF, Wong LL, Kwong KO, Arai T (2015) First record of albinism in a tropical anguillid eel *Anguilla bengalensis bengalensis* from Malaysia. *Marine Biodiversity Records* 8: e114. <https://doi.org/10.1017/S1755267215000950>
- Ahmad A, Lim KKP (2006) Inland fishes recorded from the Langkawi Islands, Peninsular Malaysia. *Malaysian Nature Journal* 59: 103–120.
- Arai T, Aoyama J, Limbong D, Tsukamoto K (1999) Species composition and inshore migration of the tropical eels *Anguilla* spp. recruiting to the estuary of the Poigar River, Sulawesi Island. *Marine Ecology Progress Series* 188: 299–303. <https://doi.org/10.3354/meps188299>
- Arai T, Chino N, Zulkifli SZ, Ismail A (2012) Notes on the occurrence of the tropical eel *Anguilla bicolor bicolor* in Peninsular Malaysia, Malaysia. *Journal of Fish Biology* 80: 692–697. <https://doi.org/10.1111/j.1095-8649.2011.03154.x>
- Arai T, Chino N (2013) Timing of maturation of a tropical eel, *Anguilla bicolor bicolor* in Malaysia. *Journal of Applied Ichthyology* 29: 271–273. <https://doi.org/10.1111/jai.12040>
- Arai T (2014) First record of a tropical mottled eel, *Anguilla bengalensis bengalensis* (Actinopterygii: Anguillidae) from the Langkawi Islands, Peninsular Malaysia, Malaysia. *Marine Biodiversity Records* 7: e38. <https://doi.org/10.1017/S1755267214000426>
- Arai T, Chin TC, Kwong KO, Siti Azizah MN (2015) Occurrence of the tropical eels, *Anguilla bengalensis bengalensis* and *A. bicolor bicolor* in Peninsular Malaysia, Malaysia and implications for the eel taxonomy. *Marine Biodiversity Records* 8: e28. <https://doi.org/10.1017/S1755267215000056>
- Arai T, Wong LL (2016) Validation of the occurrence of the tropical eels, *Anguilla bengalensis bengalensis* and *A. bicolor bicolor* at Langkawi Island in Peninsular Malaysia, Malaysia. *Tropical Ecology* 57: 23–31.
- Arai T, Abdul Kadir SR (2017a) Opportunistic spawning of tropical anguillid eels *Anguilla bicolor bicolor* and *A. bengalensis bengalensis*. *Scientific Reports* 7: 41649. <https://doi.org/10.1038/srep41649>

- Arai T, Abdul Kadir SR (2017b) Diversity, distribution and different habitat use among the tropical freshwater eels of genus *Anguilla*. Scientific Reports 7: 7593. <https://doi.org/10.1038/s41598-017-07837-x>
- Azmir IA, Samat A (2010) Diversity and distribution of stream fishes of Pulau Langkawi, Malaysia. Sains Malaysiana 39: 869–875.
- Castle PHJ, Williamson GR (1974) On the validity of the freshwater eel species *Anguilla ancestralis* Ege, from Celebes. Copeia 1974: 569–570. <https://doi.org/10.2307/1442564>
- Ege V (1939) A revision of the Genus *Anguilla* Shaw. Dana Report 16: 8–256.
- Jespersen P (1942) Indo-Pacific leptocephali of the Genus *Anguilla*. Dana Report 22: 1–128.
- Ivanova NV, Zemlak TS, Hanner RH, Hebert PD (2007) Universal primer cocktails for fish DNA barcoding. Molecular Ecology Notes 7: 544–548. <https://doi.org/10.1111/j.1471-8286.2007.01748.x>
- Minegishi Y, Aoyama J, Inoue JG, Miya M, Nishida M, Tsukamoto K (2005) Molecular phylogeny and evolution of the freshwater eels genus *Anguilla* based on the whole mitochondrial genome sequences. Molecular Phylogeny and Evolution 34: 134–146. <https://doi.org/10.1016/j.ympev.2004.09.003>
- Palumbi S, Martin A, Romano S, McMillan W, Stice L, Grabowski G (1991) The Simple Fool's Guide to PCR, Version 2. Honolulu: Department of Zoology and Kewalo Marine Laboratory.
- Watanabe S, Aoyama J, Tsukamoto K (2004) Reexamination of Ege's (1939) use of taxonomic characters of the genus *Anguilla*. Bulletin of Marine Science 74: 337–351.
- Wong LL, Abdul Kadir SR, Abdullah RAA, Lasuin CA, Kwong KO, Arai T (2017) Evidence supporting the occurrence and the ecological implication of giant mottled eel, *Anguilla marmorata* (Actinopterygii: Anguilliformes: Anguillidae), from Sabah, Borneo Island. Acta Ichthyologica et Piscatoria 47: 73–79. <https://doi.org/10.3750/AIEP/02072>

Normalup, a new genus of pselaphine beetle from southwestern Australia (Coleoptera, Staphylinidae, Pselaphinae, Faronitae)

Jong-Seok Park¹, Donald S. Chandler²

1 *S1-5 302, Major in Biology, Chungbuk National University, 1 Chungdae-ro, Seowon-gu, Cheongju-si, Chungbuk-do 28644, South Korea* **2** *Department of Biological Sciences, University of New Hampshire, Durham, NH 03824*

Corresponding author: *Jong-Seok Park* (jpark16@cbnu.ac.kr)

Academic editor: *Zi-Wei Yin* | Received 30 July 2017 | Accepted 16 August 2017 | Published 5 September 2017

<http://zoobank.org/091F6C64-9E8D-45DA-9F31-F5127DFA10CB>

Citation: Park J-S, Chandler DS (2017) *Normalup*, a new genus of pselaphine beetle from southwestern Australia (Coleoptera, Staphylinidae, Pselaphinae, Faronitae). ZooKeys 695: 111–121. <https://doi.org/10.3897/zookeys.695.19906>

Abstract

A new genus and three new species of the southwestern Australian pselaphine beetles belonging to the supertribe Faronitae are described: *Normalup* Park & Chandler, **gen. n.**, based on *Normalup afoveatus* Park & Chandler, **sp. n.**, *Normalup quadratus* Park & Chandler, **sp. n.**, and *Normalup minusculus* Park & Chandler, **sp. n.** Illustrations of their habitus and major diagnostic characters are provided, as well as distribution maps and a key to species.

Keywords

Biodiversity, biogeography, Faronini, taxonomy, Western Australia

Introduction

Two faronite genera, *Sagola* Sharp, 1874 with nine species and *Logasa* Chandler, 2001 with three species are known from Australia (Chandler 2001). The former genus includes 131 New Zealand species, and is considered to be a paraphyletic assemblage of species (Chandler 2001). A revision of the New Zealand fauna has been completed by Park and Carlton (2014a–b, 2015a–e).

In the initial steps of revising the Australian faronite fauna, which includes numerous undescribed species (Chandler 2001), it was found that three undescribed species form a morphologically distinctive group. These species are characterized by extremely large eyes, a deep and anteriorly open frontal sulcus, abdominal tergite IV is 1.5 times longer than V, and they also have a different thoracic foveal system from those of the other Australian groups. Foveal patterns have been used extensively for characterizing genera of Pselaphinae (Grigarick and Schuster 1980; Chandler 2001; Park and Carlton 2014a–b, 2015a–e).

Materials and methods

Thirty-six specimens were examined from the Field Museum of Natural History (FMNH), Chicago, Illinois, USA, and the Donald S. Chandler Collection (DSC), Durham, New Hampshire, USA. Six specimens were mounted on permanent slides to aid in observation of the internal characters and the fine external characters that are not apparent when using a dissecting microscope. Permanent microscopic slides were prepared using the techniques described by Hanley and Ashe (2003). Terminology for the foveal system follows Chandler (2001). Geographical coordinates are reported in Degrees and Decimal Minutes (**DDM**) format. Holotypes are deposited in the Western Australian Museum (**WAM**), Perth, Western Australia, Australia, and paratypes are deposited in the Field Museum of Natural History, the Western Australian Museum, the Australian National Insect Collection (**ANIC**), Canberra, ACT, Australia, and the Chungbuk National University Insect Collection (**CBNUIC**), Cheongju-si, Chungbuk-do, South Korea (indicated parenthetically). Specimen label data for the holotypes is transcribed verbatim. Data for paratypes are standardized for consistency. The map of Australia is created from SimpleMapper (Shorthouse 2010) and was subsequently modified.

Systematics

Nornalup Park & Chandler, gen. n.

<http://zoobank.org/691083BF-7137-48CF-BB87-7F735392CFCD>

Type species. *Nornalup afoveatus* Park and Chandler, sp. n., herein designated.

Diagnosis. Members of this genus are easily separated from other faronite genera by the following combination of characters: rostrum separated by distinct frontal sulcus (Fig. 3a); ventral surface of head swollen (Fig. 3b); eyes extremely large, longer than length of temples (Fig. 2g–l); frontal sulcus deep and wide, open anteriorly (Fig. 3a); mesoventrite with lateral mesosternal fovea and promesocoxal fovea (Fig. 3d); metaventrite with or without median metasternal fovea (Fig. 3d: arrow); abdominal length of tergite and sternite VI approximately 1.5 times longer than V (Fig. 1); female sternite IX bearing two pairs of long setae (Fig. 4a–c); species only known from Western Australia (Fig. 5).

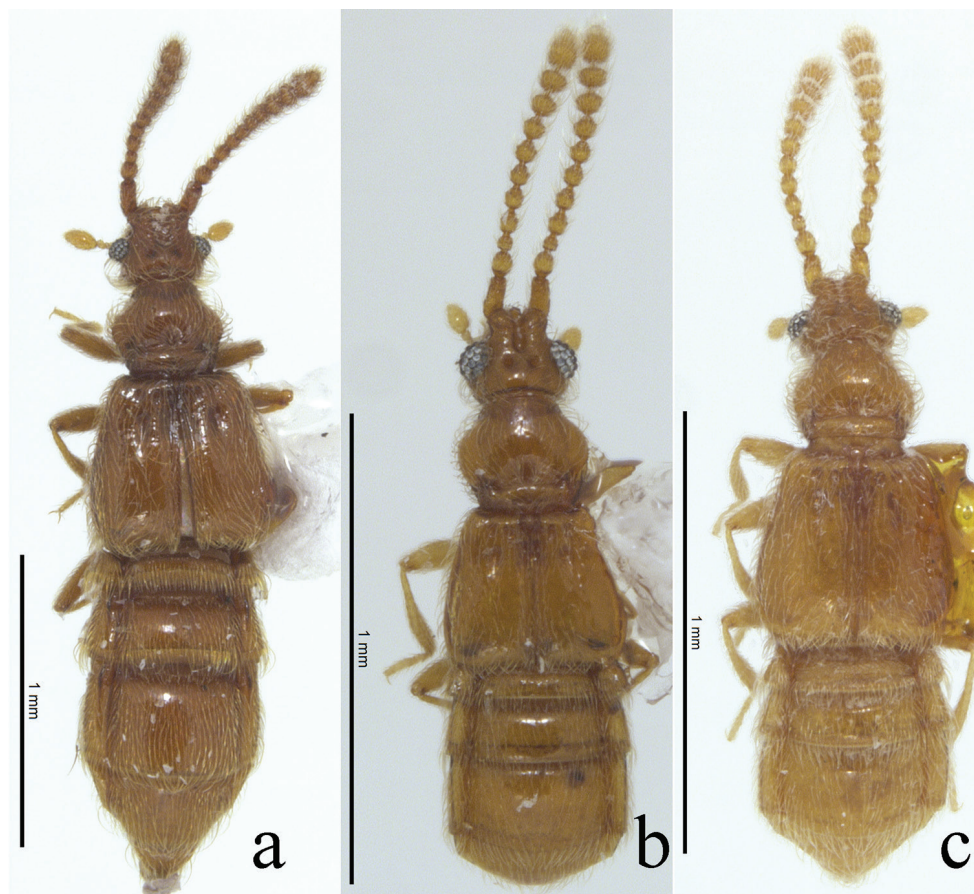


Figure 1. Habiti, dorsal view. **a** *Nornalup afoveatus* sp. n. **b** *N. quadratus* sp. n. **c** *N. minusculus* sp. n. Scale bars: 1 mm.

Description. Small body size, 1.1–2.5 mm (Fig. 1). Body yellowish to reddish-brown (Fig. 1). Head. Triangular with extremely large eyes, widest across eyes (Fig. 2g–l). Gular area convex (Fig. 3b). Male antennomeres longer than those of female. Male and female antennomeres with tubercles on 4–11 and 8–11, respectively (Fig. 2a–f). Frontal sulcus deep and wide, open anteriorly (Fig. 3a). *Thorax.* Prosternum as long as wide, widest at midpoint of prosternum (Fig. 3c). Prosternum with lateral procoxal and median procoxal fovea (Fig. 3c). Meso- and metathorax trapezoidal, longer than wide (Fig. 3d). Mes- and metaventrite with lateral mesosternal, promesocoxal and lateral mesocoxal foveae (Fig. 3d). Metaventrite with lateral metasternal foveae (Fig. 3d). *Abdomen.* Length of tergite and sternite VI approximately 1.5 times longer than V (Fig. 1). *Aedeagus.* Median lobe longer than parameres (Fig. 4d–i). Phallobase rounded (Fig. 4d–i). Parameres symmetrical, as wide as median lobe, bearing setae at apex (Fig. 4d–i).

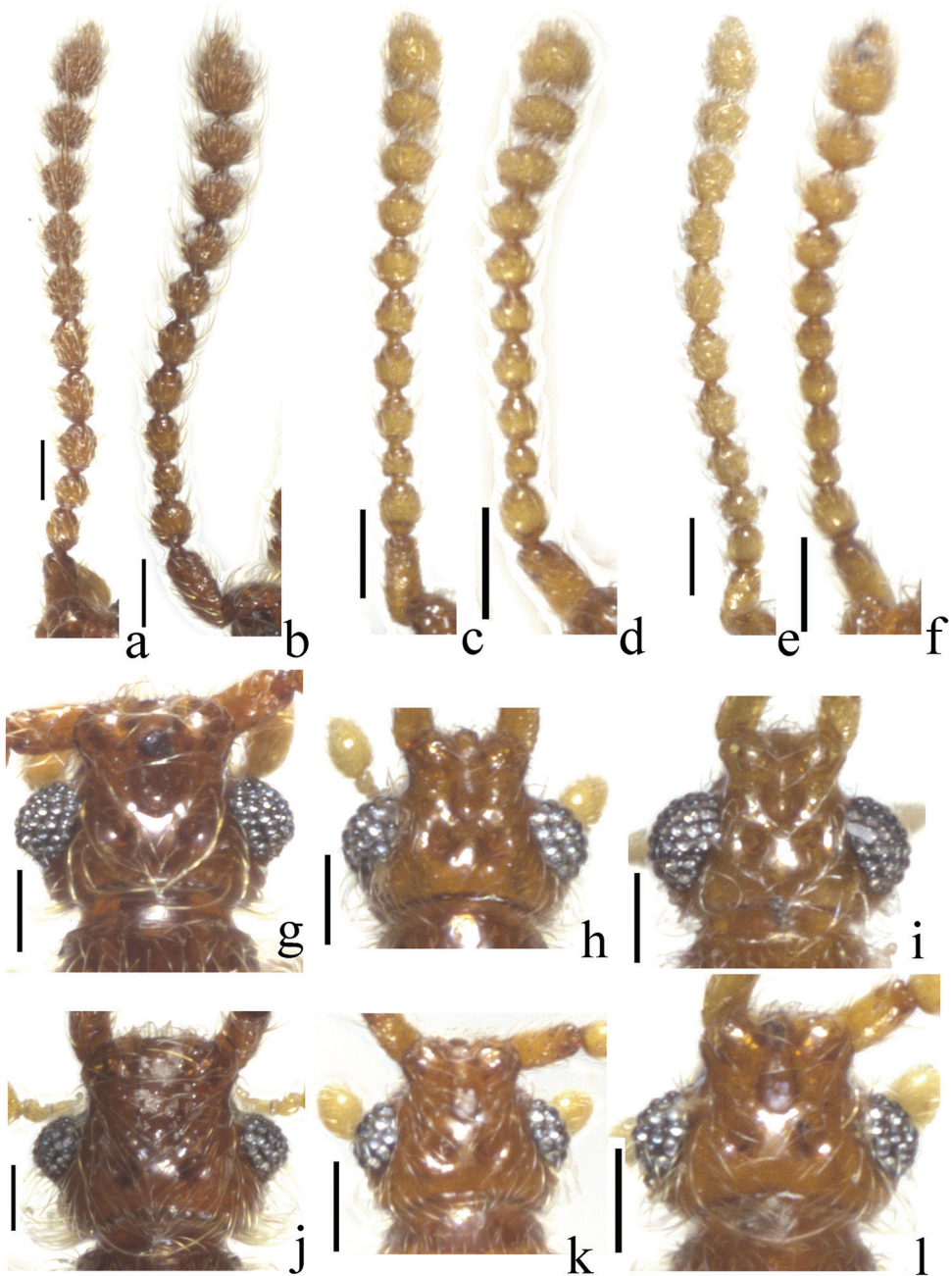


Figure 2. Antennae of *Nornalup afoveatus* sp. n. **a** male **b** female. Antennae of *N. quadratus* sp. n. **c** male **d** female. Antennae of *N. minusculus* sp. n. **e** male **f** female. Male heads, dorsal view **g** *N. afoveatus* sp. n. **h** *N. quadratus* sp. n. **i** *N. minusculus* sp. n. Female heads, dorsal view **j** *N. afoveatus* sp. n. **k** *N. quadratus* sp. n. **l** *N. minusculus* sp. n. Scale bars: 0.1 mm.

Etymology. *Nornalup* gen. n. is named for Nornalup, one of the national parks where one of the species was collected.

Distribution. Australia.

Comments about secondary sexual characters. Male specimens possess tubercles on antennomeres 4–11, but females have the tubercles on antennomeres 8–11 (Fig. 2a–f). Males have slightly larger eyes (Fig. 2g–l). Male abdominal sternite IX is usually fragile and is partially concealed by sternite VIII, rendering it simple and reduced in appearance. Females possess a more robust, rectangular abdominal sternite IX bearing two pairs of long setae (Fig. 4a–c) that are usually visible in ventral view.

Comments about biotic region. *Nornalup* gen. n. is found at the very southwestern corner of Australia, which is known as a global biodiversity hotspot (Hopper and Gioia 2004). This region has a higher average annual rainfall (300–1200 mm) than the surrounding more internal deserts of the mainland, and is mostly covered by *Eucalytus* forests (Hopper and Gioia 2004). Approximately 740 native vascular plants are known from this area, half of which are endemic (Hopper and Gioia 2004). All species are found in the karri (*E. diversicolor* F.Muell.), tingle (*E. jacksonii* Maiden), and jarrah (*E. marginata* Donn ex Sm.) forests unique to this area, where the distributions of three species do not overlap (Fig. 5).

Comments about related taxa. Based on thoracic foveal system, *Nornalup* gen. n. is closest to the genus *Sagola* Sharp. However, the frontal sulcus (Fig. 3a), abdominal length of tergite and sternite VI (Fig. 1), and form of the male aedeagus are not shared with any species of *Sagola* or other faronite genera. To understand the specific relationship with other faronites, phylogenetic analysis based on morphology and molecular data is needed.

Key to species of the genus *Nornalup* gen. n.

- 1 Elytra quadrate and flattened (Fig. 1b); metaventricle without median metasternal fovea (Fig. 3d: arrow); female abdominal sternite IX emarginate anteriorly (Fig. 4b: arrow).....*Nornalup quadratus* sp. n.
- Elytra longer than wide and convex (Fig. 1a, c); metaventricle with median metasternal fovea; female abdominal sternite IX straight anteriorly (Fig. 4a, c).....2
- 2 (1) Body length longer than 2.0 mm (Fig. 1a); apex of aedeagus with one small lobe (Fig. 4d: arrow); female abdominal sternite IX longer than wide, with oval sculpture (Fig. 4a).....*N. afoveatus* sp. n.
- Body length smaller than 2.0 mm (Fig. 1c); apex of aedeagus with two small lobes (Fig. 4h: arrow); female abdominal sternite IX as long as wide, without oval sculpture (Fig. 4c).....*N. minusculus* sp. n.

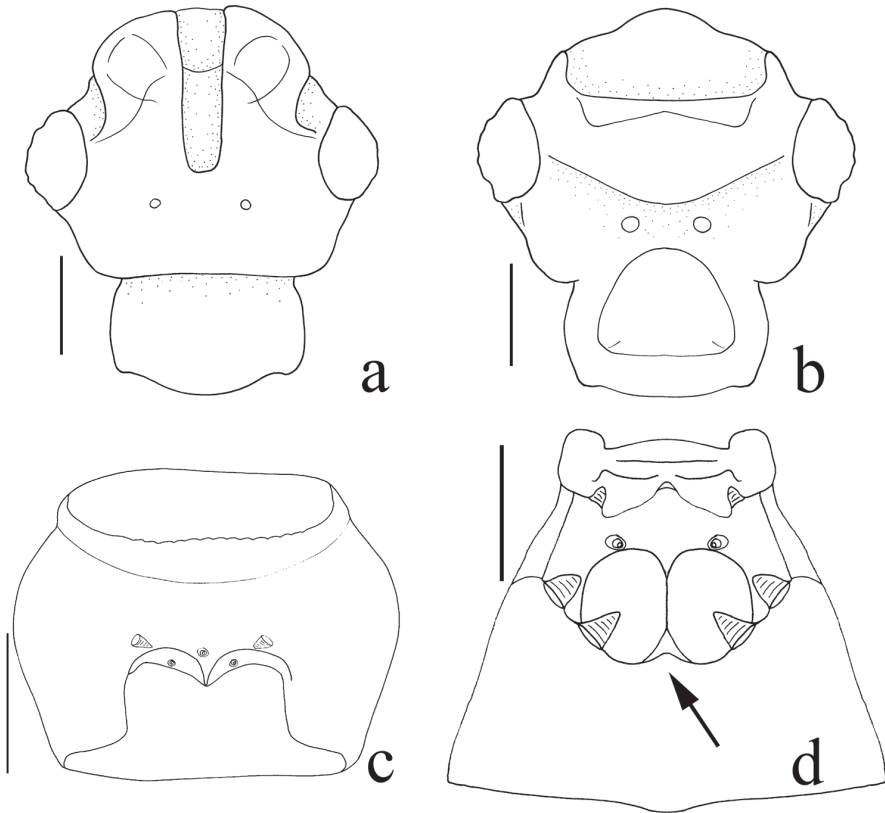


Figure 3. Heads of *Nornalup afoveatus* sp. n. **a** dorsal view **b** ventral view. *N. quadratus* sp. n. **c** prosternum, ventral view **d** meso- and metaventrite, ventral view. Scale bars: 0.1 mm.

***Nornalup afoveatus* Park & Chandler, sp. n.**

<http://zoobank.org/A773DD78-B39E-4792-B93E-3A94211F4C8E>

Figs 1a, 2a–b, 2g, 2j, 3a–b, 4a, 4d–e, 5

Type material. Holotype. Australia: Western Australia (WA): 1♂, aedeagus dissected and mounted in euparal on clear plastic card, “Australia: Western Australia: Walpole-Nornalup N.P., Anderson Rd., near Valley of the Giants Rd., 120m, 34°59.48'S, 116°52.35'E, 2 VIII 2004, tingle-*Allocasuarina*-karri (*Eucalyptus diversicolor*) forest; FMHD#2004-137, berl., leaf & log litter, A. Newton, M. Thayer, et al. 1111”. **Paratypes (n = 14; 7 males, 7 females). Australia: Western Australia:** 1♀ (CBNUIC, slide mounted), Warren N. P., Bicentennial Tree vic., 120 m, 34°29.73'S, 115°58.62'E, 30 VII–10 VIII 2004, kauri forest (*Eucalyptus diversicolor*), flight intercept trap, A. Newton & A. Solodovnikov, FMHD#2004-114, 1105; 1♂ (WAM), same as holotype; 1♂ (ANIC), 2–8 VIII 2004, flight intercept trap, A. Solodovnikov, A. Newton & M. Thayer, FMHD#2004-135, 1111; 1♂ (ANIC), Beedelup N. P., Beedelup Falls Rd.,

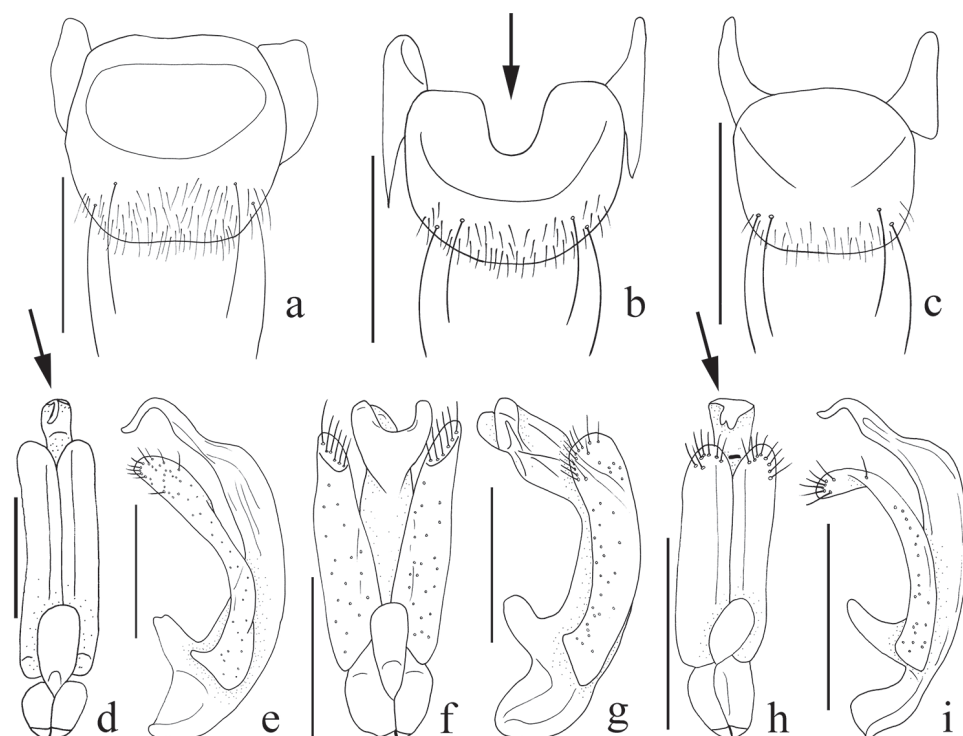


Figure 4. Female abdominal sternites IX, ventral view. **a** *Nornalup afoveatus* sp. n. **b** *N. quadratus* sp. n. **c** *N. minusculus* sp. n. Aedeagi of *N. afoveatus* sp. n. **d** dorsal view **e** lateral view. Aedeagi of *N. quadratus* sp. n. **f** dorsal view **g** lateral view. Aedeagi of *N. minusculus* sp. n. **h** dorsal view **i** lateral view. Scale bars: 0.1 mm.

150 m, 34°25.81'S, 115°53.098'E, 31 VII 2004, jarrah (*Eucalyptus marginata*) forest with *Banksia grandis*, *Xanthorrhoea*, A. Newton, M. Thayer, et al., FMHD#2004-128, 1109; 1♂ (FMNH), Warren N. P., Maidenbush Tr., 60 m, 34°30.515'S, 115°57.411'E, 29 VII 2004, old-growth karri forest (*Eucalyptus diversicolor*), A. Newton & D. Clarke, FMHD#2004-113, 1104; 1♂ (FMNH), Pemberton, The Cascades, 7 VII 1980, fungus & jarrah litter, S. Peck & J. Peck; 1♂ (CBNUIC), Brockman N. P., 23.5 km S Pemberton, 6 XII 1976, bark litter, J. B. Kethley, FMHD#76-5031; 1♂ (WAM), Walpole N. P., 5 km NE Coalbine, 5 XII 1976, fungal mat, J. B. Kethley, FMHD#76-470; 1♀ (FMNH), Beedelup N. P., Walk-through Tree vic., 100 m, 34°25.7'S, 115°58.63'E, 30 VII-10 VIII 2004, karri forest (*Eucalyptus diversicolor*), flight intercept trap, A. Newton & M. Thayer, FMHD#2004-116, 1106; 1♀ (CBNUIC), Brockman N. P., 8 XII 1976, leaf litter, debris u. canopy of karri, J. B. Kethley, FMHD#76-482; 1♀ (FMHD), Walpole N. P., 6 km NE Coalbine, 13 XII 1976, litter base of Red Tingle, J. B. Kethley, FMHD#76-493; 2♀♀ (WAM), Nornalup, Valley of Giants, 21 VI 1980, berl., tingle tree bark, S. Peck & J. Peck; 1♀ (ANIC), Walpole N. P., Collier Rd., 19 VI 1980, berl., tingle tree litter, S. Peck & J. Peck.

Diagnosis. This species can be distinguished from *N. quadratus* sp. n. by the longer elytra (Fig. 1a), larger body length (> 2.0 mm), presence of a median metasternal fovea, and the straight anterior margin of female abdominal sternite IX (Fig. 4a). This species is also separated from *N. minusculus* sp. n. by the greater body length (> 2.0 mm, Fig. 1a).

Description. Length 2.0–2.5 mm (Fig. 1a). *Head.* Male antennomeres 1–2 longer than wide, 3 subquadrate, 4–9 longer than wide, 10 subquadrate (Fig. 2a). Female antennomeres 1–2 longer than wide, 3 subquadrate, 4–6 longer than wide, 7–9 subquadrate, 10 weakly transverse (Fig. 2b). *Thorax.* Elytra rectangular and longer than wide (Fig. 1a). Hind wings fully developed. Metaventrite with median metasternal fovea. *Abdomen.* Female abdominal sternite IX with straight anterior margin (Fig. 4a). *Aedeagus.* Apex of male aedeagus with one small lobe, bended as L-shape in lateral view (Fig. 4e).

Distribution. Western Australia (Fig. 5: squares).

Habitat. Specimens of this species were collected using flight intercept traps, or by sifting leaf, bark, or fungus litter in *Eucalyptus* forests.

***Nornalup quadratus* Park & Chandler, sp. n.**

<http://zoobank.org/7A39C58D-F5CE-4A23-885C-870F86CE4BC3>

(Figs 1b, 2c–d, 2h, 2k, 3c–d, 4b, 4f–g, 5)

Type material. Holotype. Australia: Western Australia (WA): 1♂, aedeagus dissected and mounted in euparal on clear plastic card, “Australia: Western Australia: Avon Valley N.P., 1.3 km from entrance, 420m, 31°38.79'S, 116°17.94'E, 27 VII 2004, marris-jarrah (*Eucalyptus calophylla*-*E. marginata*) woodland; FMHD#2004-106, berl., leaf & log litter, A. Newton, D. Clarke, A. Solodovnikov 1102”. **Paratypes (n = 8; 4 males, 4 females).** **Australia: Western Australia:** 2♂♂ 2♀♀ (1♂ 1♀FMNH, 1♂ 1♀CBNUIC, 1♀ slide mounted), Avon Valley N. P., 1.3 km from entrance, 420 m, 31°38.79'S, 116°17.94'E, 27 VII-13 VIII 2004, marris-jarrah (*Eucalyptus calophylla*-*E. marginata*) woodland, flight intercept trap, A. Newton & M. Thayer, FMHD#2004-103, 1102; 1♀ (FMNH, slide mounted), 27 VII 2004, berl., *Banksia grandis* litter, M. Thayer, FMHD#2004-105, 1102; 2♂♂ 1♀ (1♂ 1♀WAM, 1♀ANIC, 1♂ slide mounted), same as holotype.

Diagnosis. This species can be distinguished from *N. afoveatus* sp. n. by the quadrate elytra (Fig. 1b), shorter body length (< 2.0 mm, Fig. 1b), lack of a median metasternal fovea (Fig. 3d: arrow), and emarginate anterior margin of female abdominal sternite IX (Fig. 4b: arrow). This species is also separated from *N. minusculus* sp. n. by the quadrate elytra (Fig. 1b), lack of a median metasternal fovea (Fig. 3d: arrow), and the emarginate anterior margin of female abdominal sternite IX (Fig. 4b).

Description. Length 1.1–1.5 mm (Fig. 1b). *Head.* Male antennomeres 1–2 longer than wide, 3 subquadrate, 4–6 longer than wide, 7–8 subquadrate, 9–10 weakly transverse (Fig. 2c). Female antennomeres 1–2 longer than wide, 3 subquadrate, 4–5 longer than wide, 6–8 subquadrate, 9–10 weakly transverse (Fig. 2d). *Thorax.* Elytra subquadrate (Fig. 1b). Hind wings reduced, half size of other species. Metaventrite without median metasternal fovea (Fig. 3d, arrow). *Abdomen.* Female abdominal sternite IX with

emarginate anterior margin (Fig. 4b). *Aedeagus*. Apical lobe of median lobe divided into two lobes as U-shape (Fig. 4f).

Distribution. Western Australia (Fig. 5: triangle).

Habitat. Specimens of this species were collected using flight intercept traps, or by sifting leaf, log, or *Banksia grandis* litter in *Eucalyptus* forests.

Comments. Both sexes of this species have the hind wings approximately half normal size when compared to the other species. However, four specimens were collected by flight intercept trap, so we speculate that this species still has the ability to fly.

***Nornalup minusculus* Park & Chandler, sp. n.**

<http://zoobank.org/E094EE5F-7D6B-4246-A02C-6170213E37D1>

(Figs 1c, 2e–f, 2i, 2l, 4c, 4h–i, 5)

Type material. Holotype. Australia: Western Australia (WA): 1♂, aedeagus dissected and mounted in euparal on clear plastic card, “Australia: Western Australia: Porongurup N.P., Nancy Peak Tr., Morgan’s View to The Pass, 450–600m, 34°40.8’S, 117°51.65’E, 6 VIII 2004, *Eucalyptus*; FMHD#2004-149, berl., leaf & log litter, Clarke & Grimbacher 1118”. **Paratypes (n = 9; 3 males, 6 females). Australia: Western Australia:** 1♂ 1♀ (CBNUIC), 40 km ESE Manjimup, 15 VII 1980, jarrah forest litter, S. Peck & J. Peck; 1♂ (WAM), 83 km NE Albany, Stirling Range N. P., Toolbrunup Peak, 700 m, 27 XII 1976, litter at stream edge. u. marri, below 1st talus, J. B. Kethley, FMHD#76-537; 1♂ (FMNH), Giant Tingle Area, 8 km NE Walpole, 19 XII 1976, Karri & Acacia l., J. B. Kethley, FMHD#76-514; 1♀ (FMNH), Porongurup N. P., Wansborough Walk at The Pass, 450 m, 34°40.69’S, 117°51.245’E, 6 VIII 2004, karri forest (*Eucalyptus diversicolor*), mostly young-growth, berl., leaf & log litter, A. Newton & M. Thayer, FMHD#2004-147, 1116; 2♀♀ (WAM, 1♀ slide mounted), Stirling Range N. P., Toolbrunup Peak Tr., 480–520 m, 34°23.4’S, 118°03.3’E, 5 VIII 2004, *Eucalyptus* forest & mallee, berl., leaf & log litter, D. Clarke & Grimbacher, FMHD#2004-146, 1115; 2♀♀ (ANIC, 1♀ slide mounted), 430–485 m, 34°23.5’S, 118°03.65’E, 5 VIII 2004, mallee *Eucalyptus*, berl., water-washed soil, 0–18 cm, D. Clarke, FMHD#2004-145, 1114; 1♀ (CBNUIC), 43 km E Albany, Two People’s Bay, Mt. Gardner, 150m, 1 I 1977, litter u. *Hibbertia* sp., J. B. Kethley, FMHD#77-88; 1♀ (ANIC), 220m, 1 I 1977, litter u. Marri, J. B. Kethley, FMHD#77-85.

Diagnosis. This species can be distinguished from *N. quadratus* sp. n. by the longer elytra (Fig. 1c), presence of a median metasternal fovea, and the straight anterior margin of female abdominal sternite IX (Fig. 4c). This species is also separated from *N. afoveatus* sp. n. by its smaller body length (< 2.0 mm, Fig. 1c).

Description. Length 1.2–1.6 mm (Fig. 1c). *Head*. Male antennomeres 1–2 longer than wide, 3 subquadrate, 4–9 longer than wide, 10 subquadrate (Fig. 2e). Female antennomeres 1–2 longer than wide, 3 subquadrate, 4–6 longer than wide, 7–8 subquadrate, 9–10 weakly transverse (Fig. 2f). *Thorax*. Elytra rectangular and longer than wide (Fig. 1c). Hind wings fully developed. Metaventricle with median metasternal

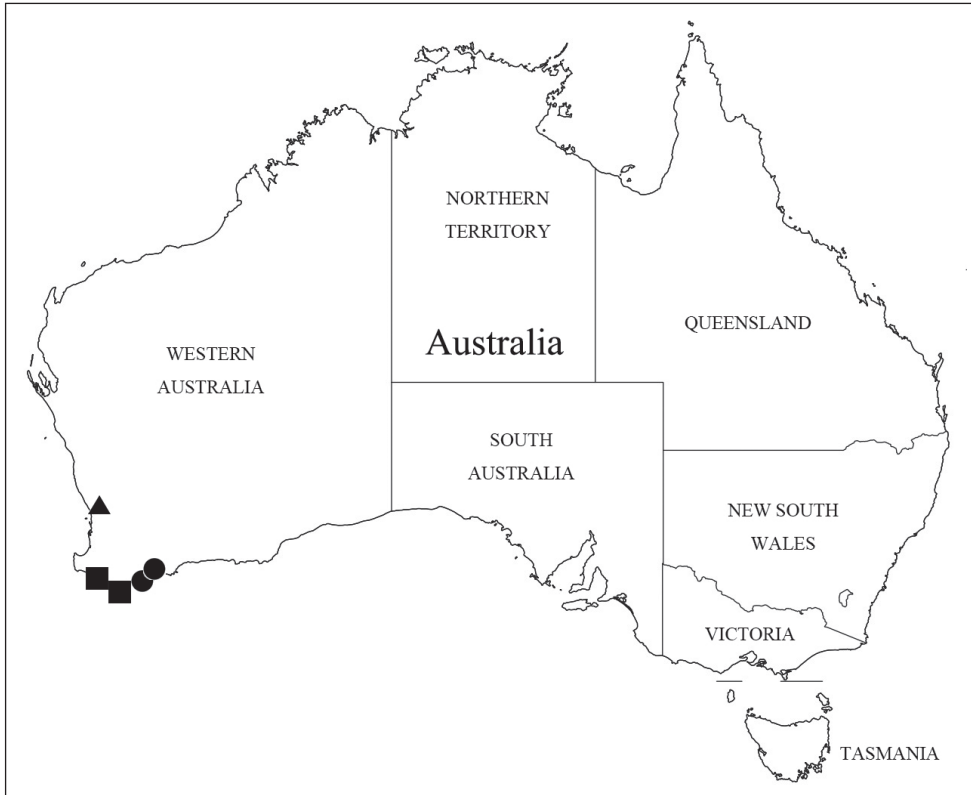


Figure 5. Known collection localities of *Nornalup* gen. n. *N. afoveatus* sp. n.: squares; *N. quadratus* sp. n.: triangle; *N. minusculus* sp. n.: circles.

fovea. *Abdomen.* Female abdominal sternite IX with straight anterior margin (Fig. 4c). *Aedeagus.* Apex of male aedeagus with two small lobes, bent into an L-shape in lateral view (Fig. 4i).

Distribution. Western Australia (Fig. 5: circles).

Habitat. Most specimens of this species were collected by sifting leaf and log litter, with one taken from water-washed soil in *Eucalyptus* forests.

Acknowledgements

We thank Margaret K. Thayer and Alfred Newton (Field Museum Natural History, Chicago, Illinois) for the loan of valuable specimens. Comments of anonymous reviewers and Chris Carlton (Louisiana State Arthropod Museum, Baton Rouge, Louisiana) guided substantial improvements to the manuscript. This work was supported by the research grant of the Chungbuk National University in 2017.

References

- Chandler DS (2001) Biology, Morphology, and Systematics of the Ant-like Litter Beetle Genera of Australia (Coleoptera: Staphylinidae: Pselaphinae). *Memoirs on Entomology, International*, Associated Publishers, Florida, 560 pp.
- Hanley RS, Ashe JS (2003) Techniques for dissecting adult aleocharine beetles (Coleoptera: Staphylinidae). *Bulletin of Entomological Research* 93: 11–18. <https://doi.org/10.1079/BER2002210>
- Grigarick AA, Schuster RO (1980) Discrimination of genera of Euplectini of North and Central America (Coleoptera: Pselaphinae). *University of California Publication in Entomology* 87: 56 pp. [79 pls]
- Park JS, Carlton CE (2014a) *Pseudostenosagola*, a new genus from New Zealand (Coleoptera: Staphylinidae: Pselaphinae: Faronitae). *Annals of the Entomological Society of America* 107(4): 734–739. <https://doi.org/10.1603/AN14025>
- Park JS, Carlton CE (2014b) A revision of New Zealand species of the genus *Sagola* (Coleoptera: Staphylinidae: Pselaphinae: Faronitae). *The Coleopterists Society Monograph Number 13*, 156 pp.
- Park JS, Carlton CE (2015a) *Brounea*, a new genus from New Zealand (Coleoptera: Staphylinidae: Pselaphinae), with descriptions of nine new species. *Zootaxa* 3990(4): 551–566. <https://doi.org/10.11646/zootaxa.3990.4.4>
- Park JS, Carlton CE (2015b) *Aucklandea* and *Leschenea*, two new monotypic genera from New Zealand (Coleoptera: Staphylinidae: Pselaphinae), and a key to New Zealand genera of the supertribe Faronitae. *Annals of the Entomological Society of America* 108(4): 634–640. <https://doi.org/10.1093/aesa/sav033>
- Park JS, Carlton CE (2015c) *Ahnea*, a new genus from New Zealand (Coleoptera: Staphylinidae: Pselaphinae), with description of a new species. *The Canadian Entomologist* 147: 381–389. <https://doi.org/10.4039/tce.2014.65>
- Park JS, Carlton CE (2015d) *Chandlerrea* and *Nunnea* (Coleoptera: Staphylinidae: Pselaphinae), two new genera from New Zealand with descriptions of three new species. *Florida Entomologist* 98(2): 588–592. <https://doi.org/10.1653/024.098.0231>
- Park JS, Carlton CE (2015e) *Pseudoexeirarthra*, a new genus from New Zealand (Coleoptera, Staphylinidae, Pselaphinae), with descriptions of seven new species. *Zookeys* 491: 95–118. <https://doi.org/10.3897/zookeys.491.9164>
- Shorthouse DP (2010) SimpleMappr, an online tool to produce publication-quality point maps. <http://www.simplemappr.net> [Accessed August 15, 2017]

The larvae of *Sericostoma bergeri* Malicky, 1973 and *Sericostoma herakles* Malicky, 1999 (Trichoptera, Sericostomatidae)

Johann Waringer¹, Hans Malicky²

1 Department of Limnology and Bio-Oceanography, University of Vienna, Althanstrasse 14, A-1090 Vienna, Austria **2** Sonnengasse 13, A- 3293 Lunz am See, Austria

Corresponding author: *Johann Waringer* (johann.waringer@univie.ac.at)

Academic editor: *R. Holzenthal* | Received 14 June 2017 | Accepted 14 August 2017 | Published 5 September 2017

<http://zoobank.org/009BB77E-8336-45AC-A892-D84D028F2C07>

Citation: Waringer J, Malicky H (2017) The larvae of *Sericostoma bergeri* Malicky, 1973 and *Sericostoma herakles* Malicky, 1999 (Trichoptera, Sericostomatidae). ZooKeys 695: 123–133. <https://doi.org/10.3897/zookeys.695.14531>

Abstract

This paper describes the previously unknown larvae of *Sericostoma bergeri* and *S. herakles* (Trichoptera: Sericostomatidae) restricted to European Ecoregion 6 (= Hellenic western Balkan). Information on the morphology of the larvae is given, and the most important diagnostic features are illustrated. *Sericostoma bergeri* and *S. herakles* can be easily separated from known sericostomatid larvae of Ecoregion 6 (*Schizopelex huettingeri*, *Oecismus monedula*, *Sericostoma flavicorne* and *S. personatum*) by the shape of the pronotum, presence or lack of a comma-like marking on the lateral protuberance, by the number of setae on abdominal dorsum IX, and by distribution patterns. With respect to the latter, *S. bergeri* is a micro-endemic of the Greek Islands of Euboea and Andros whereas *S. herakles* is an endemic of the Peloponnese. The species are integrated in a dichotomous key including the currently known Sericostomatidae larvae of the Hellenic western Balkan. In addition, ecological information on the two species is provided.

Keywords

Description, distribution, larva, identification, West Palearctic fauna

Introduction

From Europe, 18 species of genus *Sericostoma* Latreille, 1825 are known (Graf et al. 2008; Malicky 2004, 2005a, b, 2014), with four species also present in European Ecoregion 6 (= Hellenic western Balkan). From the latter, only *Sericostoma flavicorne* Schneider, 1845 and *Sericostoma personatum* (Kirby & Spence, 1826) were described

in the larval stage to date (Pitsch 1993). Several years ago, however, Hans Malicky managed to collect larvae and adults of the two remaining *Sericostoma* species of Ecoregion 6: *S. bergeri* Malicky, 1973 from the Greek islands of Euboea and Andros and *S. herakles* Malicky, 1999 from the Peloponnese. This material enabled us to infer reliable diagnostic characters for the larval description and to use this information for integrating the two species in the key of the previously known Sericostomatidae larvae of the Hellenic western Balkan provided by Karaouzas and Waringer (2017).

Material and methods

Three final instar larvae and numerous adults of *Sericostoma bergeri* were sampled by H. Malicky on the Greek island of Andros at Refmata (37°52'N, 24°50'E, 220 m a.s.l.) on 21 October 1980. In addition, one final instar larva and numerous adults of *S. herakles* were obtained by the same collector at Kefalarion, Peloponnese, Greece (37°54'N, 22°31'E, 670 m a.s.l.) on 19 May 1974. Immature stages were picked from the mineral substrate with forceps, adults were collected using light traps, and the material was preserved in 70% ethanol. The larvae were studied and photographed using a Nikon SMZ 1500 binocular microscope with DS-Fi1 camera and NIS-elements D 3.1 image stacking software for combining 6–46 frames in one focused image. Species association was enabled by the fact that both larvae and adults were collected at the same locations where other Sericostomatidae were lacking.

Deposition of voucher specimens: Final instar larvae of *Sericostoma bergeri* and *S. herakles* are deposited in the collections of the authors in Lunz am See and Vienna. Comparative material of *Schizopelex huettingeri* Malicky, 1974 (3 final instar larvae), *Oecismus monedula* (Hagen, 1859) (1 final instar larva) and *Sericostoma personatum* (Kirby & Spence, 1826) / *Sericostoma flavicorne* Schneider 1845 (15 final instar larvae) are deposited in the collection of J. Waringer (Vienna, Austria). We used the morphological terminology of Wiggins (1998), Pitsch (1993), and Waringer and Graf (2011).

Results

Sericostoma bergeri Malicky 1973

Description of the 5th instar larva.

Diagnosis. Pronotum with convex ventral border; anterolateral pronotal corner short and knob-like; with black comma-like marking on lateral protuberance; setal counts on abdominal dorsum IX 18–41.

Biometry. Body length of 5th instar larvae ranging from 16.0 to 17.5 mm, head width from 1.69 to 1.76 mm (n = 3).

Head. Head capsule roundish, dorsally medium to orange brown, posterolaterally and ventrally whitish; with slightly granulated surface and large, elongated, orange muscle

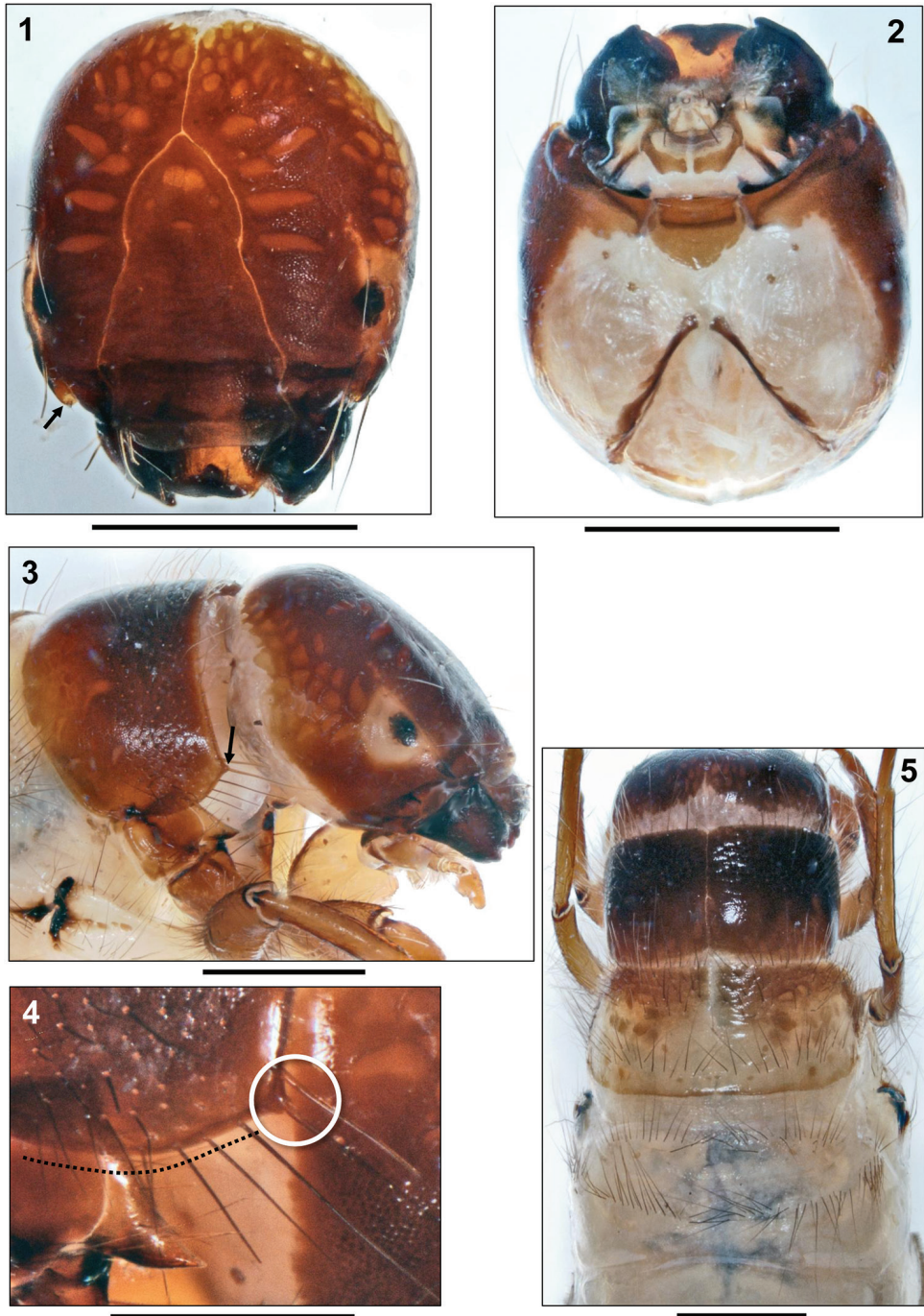
attachment spots (Figs 1–3). Distinct whitish spade-like patch present around each eye (Fig. 3). With ridge extending from posterodorsal corner of white spade-like ring around each eye (Fig. 3) to anterior parietal margin where ridge creates an inwardly-bending groove bearing the antenna (Fig. 1, arrow). Frontoclypeus with shallow central constriction; a shallow secondary constriction situated subapically near anterior border (Fig. 1). Head capsule with complete set of 18 pairs of primary setae: 10 dorsal and 2 ventral primary setae on each parietal, 6 pairs of primary setae on frontoclypeus. Labrum medium brown, narrowly rectangular, with 6 pairs of primary setae. Submentum separating the genae incompletely, broadly shield-shaped, light brown, with darker brown rectangular anterior sclerotization (Fig. 2). Mandibles blackish brown, of shredder type, with 4 terminal teeth (Fig. 2).

Thorax. Pronotum dark brown (Fig. 5), in some specimens slightly paler on posterior half (Fig. 3). Without transverse ridge present in other caddisfly taxa (e.g., Limnephilinae), heavily sclerotized, with anterolateral corner creating a tiny, knob-like projection (Fig. 4, white circle). The two pronotal plates mesially meeting in a narrow, straight suture; surface smooth (Fig. 5). Ventral pronotal margin curved (Fig. 4, dotted line). Each pronotal half covered by 223–235 setae concentrated on anterior pronotal section. Anterior pronotal margin with row of pale, curved setae (Fig. 3). Anterior process of propleuron long and corniform (Fig. 7, arrow). Mesodorsum covered by 4 sclerotized plates (2 large central, 2 small lateral), anterior border medium brown, with oval, pale muscle attachment spots, posterior section whitish, with brown muscle attachment spots (Fig. 5); suture between central and lateral plates inconspicuous (Fig. 6, arrows). Setal counts per central sclerite are 64–72 in anterior group and 25–30 in posterior group; lateral sclerite with 49–57 dark setae (Fig. 6).

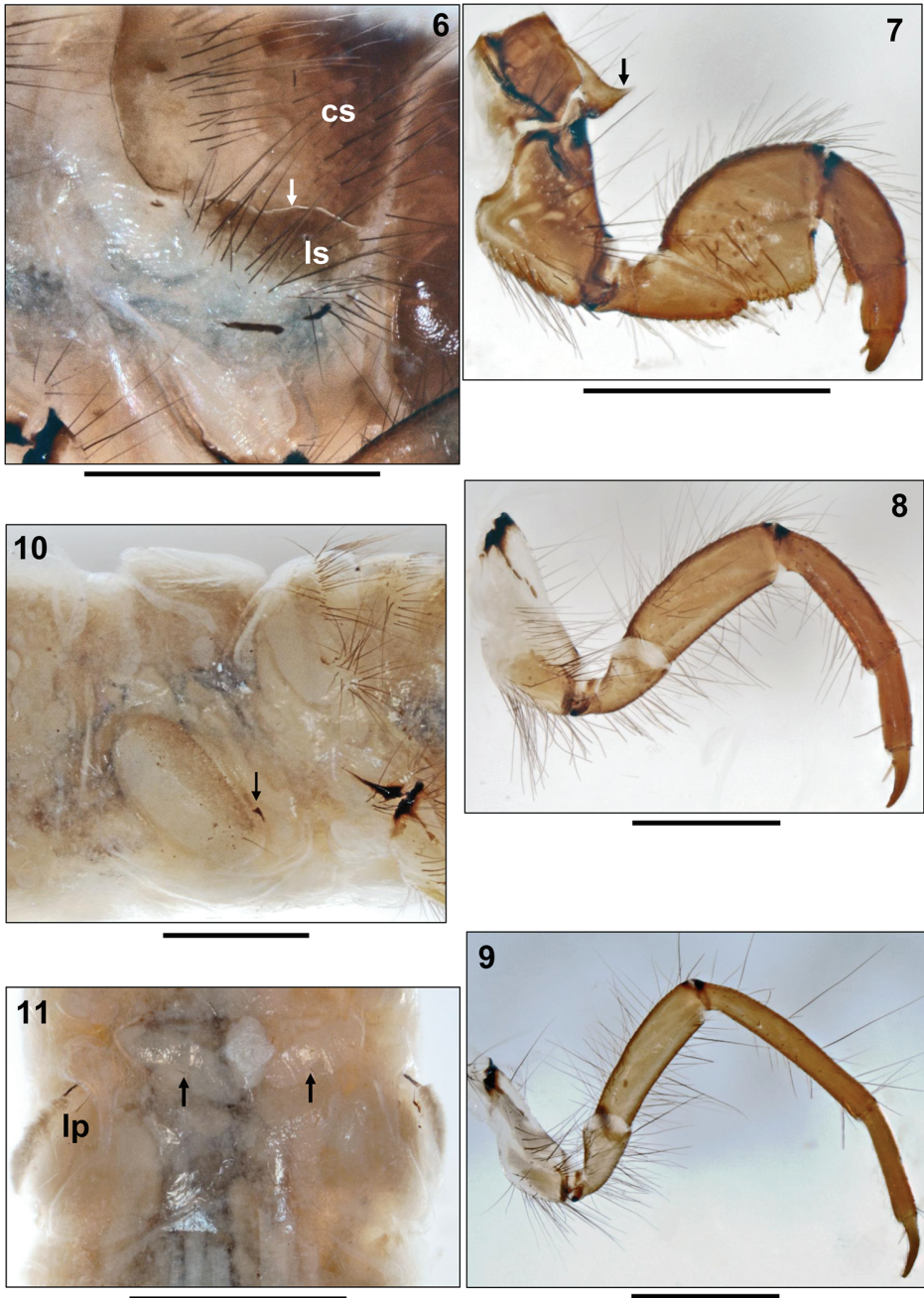
Prosternal sclerites and prosternal horn lacking. Metadorsum covered by colourless and barely visible weak sclerites arranged in 2 parallel transverse bands. Setal counts per sclerite are 27–35 setae in anterior group, 40–46 setae in posterior group (Fig. 5).

Legs medium to light brown (Figs 7–9). Foreleg short and stout, femur distally enlarged and flattened, thereby creating an edge interacting with tibia when bent inwards (Fig. 7). Coxa with ventral group of long black setae, trochanter with dense ventral brush of pale, flexible setae. Dorsal edge of femur with large groups of dark setae. Tibia with groups of long dark dorsal and ventral setae and with pale apical spine. Strong tarsal claw sickle-shaped, with stout pale basal spine. Midleg much more slender, coxa weakly sclerotized, femur not enlarged. Hind leg even more slender, tarsal claw elongated, setation less than in other legs (Figs 7–9).

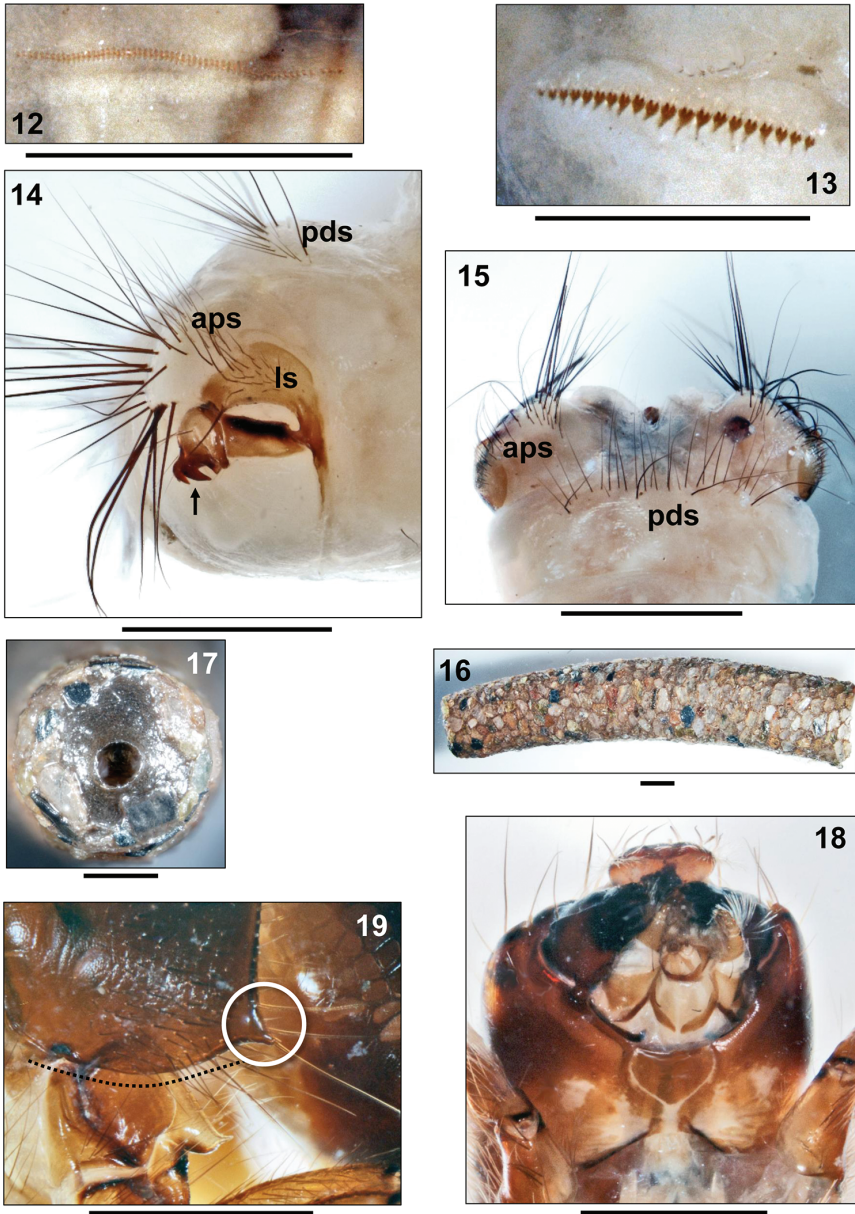
Abdomen. Abdominal segment I with 2 flat, oblique lateral and 1 low, inconspicuous dorsal protuberances (Fig. 10); setation consisting of 1 pair of ventral *sa*1 setae (Fig. 11, arrows) and 1 lateral protuberance seta per side (Fig. 11 lp). With black comma-like marking on lateral protuberance (Fig. 10, arrow). Gills consisting of tiny single (rarely double or triple) filaments and in presegmental position only. Dorsal gills present at most from abdominal segment I to VI, ventral gills from segment II to VII and lateral gills from II to III. Lateral fringe lacking; however, with lateral rows of tiny serrate lamellae on each side of abdominal segments III to VII (Fig. 12), and with row of forked lamellae on each side of segment VIII (Fig. 13).



Figures 1–5. *Sericostoma bergeri* Malicky, 1973, final instar larva. **1** Head, dorsal view (arrow: antenna) **2** Head, ventral view **3** Head and pronotum, right lateral view (arrow: anterolateral corner of pronotum) **4** Detail of pronotum (right lateral) showing small and knoblike anterolateral corner (white circle) and curved ventral outline (black dots) **5** Head, thorax and abdominal segment I, dorsal. Scale bars: 1 mm.



Figures 6–11. *Sericostoma bergeri* Malicky, 1973, final instar larva. **6** Right anterolateral section of mesonotum (arrow: suture between central and lateral mesonotal sclerite; cs: central sclerite; ls: lateral sclerite) **7** Right foreleg, posterior face (arrow: propleuron, anterior process) **8** Right midleg, posterior face **9** Right hind leg, posterior face **10** Metanotum and abdominal segment I, right lateral (arrow: lateral protuberance with black, comma-like marking dorsally of lateral protuberance seta) **11** Abdominal sternum I (arrows: single sa1 setae; lp: lateral protuberance seta). Scale bars: 1 mm.



Figures 12–19. **12–17** *Sericostoma bergeri* Malicky, 1973, final instar larva **12** Abdominal segment V, posterior section, left lateral, showing row of serrate lamellae **13** Abdominal segment VIII, anterior section, left lateral, showing row of forked lamellae **14** Tip of abdomen, right lateral (aps: setae on dorsum of anal proleg; ls: setae on lateral sclerite; pds: setae on posterodorsal border of abdominal dorsum IX; arrow: anal claw) **15** Tip of abdomen, dorsal (aps: setae on dorsum of anal proleg; pds: setae on posterodorsal border of abdominal dorsum IX) **16** Larval case, right lateral **17** Larval case, foramen posterior, reduced in diameter by silk membrane **18–19** *Sericostoma herakles* Malicky, 1999, final instar larva. **18** Head, ventral view **19** Detail of pronotum (right lateral) showing conically prolonged and pointed anterolateral corner (white circle) and curved ventral outline (black dots). Scale bars: 1 mm (except **12**, **13**: 0.5 mm).

Dorsal sclerite of abdominal segment IX lacking, soft cuticle with 18–41 black setae of almost equal length on posterodorsal border (Figs 14, 15pds). Dorsum of each anal proleg with cluster of 35–45 black setae (Figs 14, 15aps). Lateral sclerite of anal proleg with 28–35 black setae of varying length (Fig. 14ls). Anal proleg claw with sharply angled crook and dorsal accessory hook (Fig. 14, arrow).

Larval case. Cylindrical, tapering, curved, made of flat sandgrains of approximately uniform size, neatly arranged in a puzzle-like pattern, thereby creating a rather smooth surface (Fig. 16). Case length 15.7 to 17.6 mm, anterior width 3.3 to 4.1 mm, posterior width 2.6 to 2.8 mm (n= 3). Foramen posterior partly closed by a slightly conical, translucent silken membrane with round central hole 0.61 mm in diameter (Fig. 17).

Sericostoma herakles Malicky, 1999

Description of the 5th instar larva.

Diagnosis. Pronotum with convex ventral border; anterolateral pronotal corner conically prolonged and pointed; with black comma-like marking on lateral protuberance; setal counts on abdominal dorsum IX 18–41.

Biometry. Body length of 5th instar larva 13.7 mm, head width 1.93 mm (n = 1). All morphological characters identical to those of *S. bergeri* except as noted below.

Head. Head capsule dorsally medium brown, whitish coloration on ventral section of parietalia restricted to small oval patches (Fig. 18).

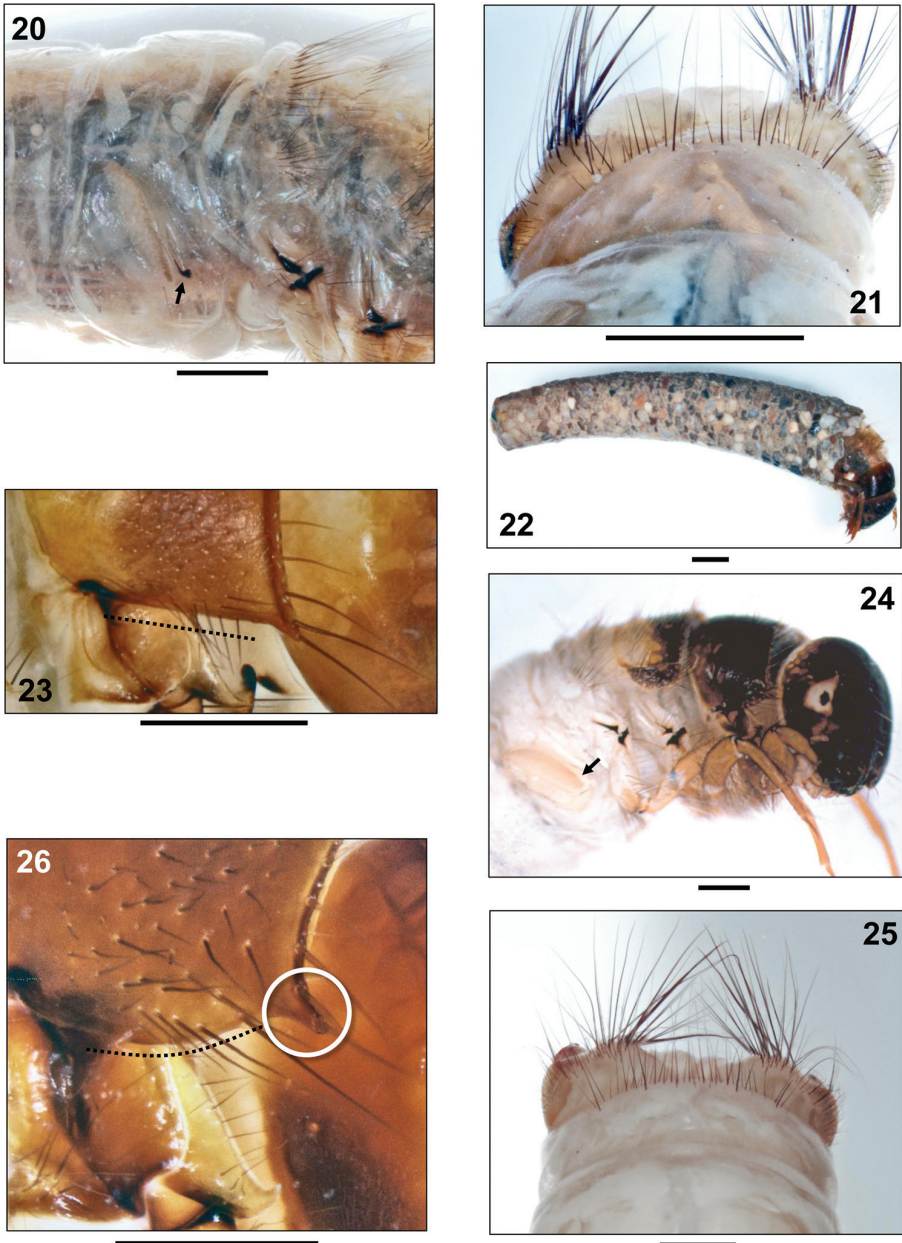
Thorax. Pronotum with convex ventral border (Fig. 19); anterolateral pronotal corner conically prolonged and pointed (Fig. 19, white circle). Each pronotal half covered by 190–220 setae concentrated on anterior pronotal section. Sclerotized plates on mesodorsum creamish white to light brown, with oval, pale muscle attachment spots. Setal counts per central sclerite are 69–85 in anterior group and 25–30 in posterior group; lateral sclerite with 57–80 dark setae. Setal counts per metanotal sclerite are 27–35 setae in anterior group, 50–65 setae in posterior group.

Abdomen. Lateral sclerite of anal proleg with 35–42 black setae of varying length.

Larval case. Case length 15.2 mm, anterior width 3.5 mm, posterior width 2.3 mm (n= 1).

Morphological separation of fifth instar larvae of *Sericostoma bergeri* Malicky, 1973 and *S. herakles* Malicky, 1999 from other European Trichoptera

A summary of morphological features for the identification of European caddisfly families was given by Waringer and Graf (2013). Within the framework of the Sericostomatidae key by Pitsch (1993), Wallace et al. (2003), and Waringer and Graf (2011), the larvae of the two Greek *Sericostoma* species can be separated from other species by the following features:



Figures 20–26. 20–22 *Sericostoma herakles* Malicky, 1999, final instar larva 20 Metanotum and abdominal segment I, right lateral (arrow: lateral protuberance with black, comma-like marking dorsally of lateral protuberance seta) 21 Tip of abdomen, dorsal 22 Larva in case, right lateral 23 *Schizopelex buettingeri* Malicky 1974, final instar larva. Pronotum, right lateral (dotted line: straight ventral margin of pronotum) 24–25 *Oecismus monedula* (Hagen 1859) 24 final instar larva, right lateral (arrow: lateral protuberance without black, comma-like marking dorsally of lateral protuberance seta) 25 Tip of abdomen, dorsal 26 *Sericostoma* sp., final instar larva. Detail of pronotum (right lateral) showing conically prolonged and pointed anterolateral corner (white circle) and curved ventral outline (black dots). Scale bars: 1 mm (except 23–26: 0.5 mm).

- pro- and mesonotum completely, metanotum incompletely sclerotized (metanotal sclerites may lack colour; Fig. 5);
- mesonotum divided into two large, central sclerites (Fig. 6cs) and two small, lateral sclerites (Fig. 6ls);
- with transportable cases (Fig. 16);
- prosternal horn lacking;
- abdominal dorsum IX unsclerotized (Fig. 15);
- abdominal segment I with one dorsal and two lateral protuberances (Fig. 10).

In the context of the Sericostomatidae larvae of European Ecoregion 6 (Hellenic western Balkan region), *Sericostoma bergeri*, and *S. herakles* can be identified by the following dichotomic key.

Key to the final instar *Sericostoma* larvae of European Ecoregion 6 (Hellenic western Balkan)

- 1 Pronotum with straight ventral border (Fig. 23, dotted line); abdominal dorsum IX with 18–41 setae (as in Fig. 15 pds); without black comma-like marking on lateral protuberance (as in Fig. 24, arrow) ***Schizopelex huettingeri* Malicky, 1974**
- Pronotum with convex ventral border (Figs 4, 19, dotted curvature); setal counts on abdominal dorsum IX either 18–41 or 48–74 (Figs 15, 25); with or without black comma-like marking on lateral protuberance (Figs 20, 24 arrows) **2**
- 2 Abdominal dorsum IX with 18–41 setae (Fig. 15); black comma-like marking present on lateral protuberance (Fig. 20, arrow) **3**
- Abdominal dorsum IX with 48–74 setae (Fig. 25); without black comma-like marking on lateral protuberance (Fig. 24, arrow) ***Oecismus monedula* (Hagen, 1859)**
- 3 Anterolateral corner of pronotum conically prolonged and pointed (Figs 19, 26)... ***Sericostoma herakles* Malicky, 1999** (endemic of the Peloponnese) or ***Sericostoma flavicorne* Schneider, 1845** / ***Sericostoma personatum* (Kirby & Spence, 1826)** (not separable) (unknown from the Peloponnese so far)
- Anterolateral corner of pronotum short and knob-like (Figs 3, 4); micro-endemic of the Greek Islands of Euboea and Andros..... ***Sericostoma bergeri* Malicky, 1973**

Ecology and distribution

In Europe, the Sericostomatidae fauna consists of *Cerasma cornuta* McLachlan, 1876, 6 species of *Notidobia* Stephens, 1829, 3 species of *Oecismus* McLachlan, 1876, 6 *Schizopelex* species and 18 *Sericostoma* species (García de Jalón and Vera 1978; Graf et al. 2008; Malicky

2004, 2005a, b, 2014; Ruíz-García and Ferreras-Romero 2014); of this inventory, three *Notidobia*, three *Oecismus*, one *Schizopelex* and four *Sericostoma* species have been recorded in European Ecoregion 6 (= Hellenic western Balkan). Here, the number of endemic caddisfly species is especially high: in Greece it is up to 72, yielding a proportion of 24% when compared with the overall Greek inventory of approximately 300 species. The Cyclades and Crete have the highest share of endemic species with species numbers reflecting permanent stream density; both are highest on Andros, Naxos, Ikaria and within the Ochi mountains in the south of Euboea. Indeed, on the verdant island of Andros, one third of the caddisfly fauna is endemic. Many endemics on this island have more widely distributed, close relatives within the region, e.g., *Tinodes* and *Hydropsyche* species. *Sericostoma bergeri* is such a typical micro-endemic of the Greek Islands of Euboea (Ochi mountains) and Andros. *S. bergeri* inhabits small springs and spring brooks on slate, shaded by riparian trees such as *Alnus glutinosa* (L.) Gaertn. and *Platanus orientalis* L. which release large amounts of leaf litter in the brooks. At typical habitats, water temperatures were 9.3–10.7 °C in April, 13.2–15.0 °C in May, 12.8–18.7 °C in June and 9.3–19.8 °C in October (Malicky 2014). The species is univoltine and stenochorous, peaking in emergence in May and June. In contrast to the high number of endemic species on the Greek islands, there are no significant concentrations of endemics on the Greek mainland, where most endemic species are widely spread over the mountains of central Greece or the Peloponnese (Malicky 2005b). A fine example of the latter is *Sericostoma herakles*; on the Peloponnese, this species has been mostly collected in large, calcareous mountain brooks with low annual and diurnal water temperature amplitudes (May morning water temperature: 8.1 °C, noon: 10.1 °C, evening: 9.5 °C; August evening: 14.2 °C, midnight: 13.8 °C; October morning: 12.0 °C, noon: 12.2 °C, evening: 12.0 °C [Malicky 2014]). The species is univoltine and on the wing from April to August, peaking in May; a single specimen has been collected as late as October (Malicky 2005b). The larvae of both species are detritivore-shredders, feeding on leaf litter from the woody riparian zone and aquatic vegetation, particularly mosses.

Acknowledgements

We are grateful to Dr. Ioannis Karaouzas, Athens, Greece, who provided comparative material, and Prof. Dr. Ralph Holzenthal and two anonymous reviewers for their helpful comments on this manuscript.

References

- García de Jalón D, Vera R (1978) La larva de *Schizopelex festiva* (Rambur, 1842) (Trich. Sericostomatidae). Boletín de la Asociación Española de Entomología 2: 117–122.
- Graf W, Murphy J, Dahl J, Zamora-Muñoz C, López-Rodríguez MJ (2008) Volume 1 – Trichoptera. In: Schmidt-Kloiber A, Hering D (Eds) Distribution and Ecological Preferences of European Freshwater Organisms. Pensoft Publishers, Sofia, Moscow, 388 pp.

- Karaouzas I, Waringer J (2017) The larva of *Schizopelex huettingeri* Malicky 1974 (Trichoptera: Sericostomatidae), including a preliminary key to the Sericostomatidae larvae of the Hellenic western Balkan regions. *Zootaxa* 4311: 271–279.
- Malicky H (2004) Atlas of European Trichoptera, Second edition. Springer, 359 pp.
- Malicky H (2005a) Ein kommentiertes Verzeichnis der Köcherfliegen (Trichoptera) Europas und des Mediterrangebietes. *Linzer biologische Beiträge* 37: 533–596.
- Malicky H (2005b) Die Köcherfliegen Griechenlands. *Denisia* 17: 1–240.
- Malicky H (2014) Lebensräume von Köcherfliegen (Trichoptera). *Denisia* 34: 1–280.
- Pitsch T (1993) Zur Larvaltaxonomie, Faunistik und Ökologie mitteleuropäischer Fließwasser-Köcherfliegen (Insecta: Trichoptera). *Landschaftsentwicklung und Umweltforschung. Schriftenreihe des Fachbereichs Landschaftsentwicklung, Sonderheft S8*, Technische Universität Berlin, 316 pp.
- Ruíz-García A, Ferreras-Romero M (2014) A new species of genus *Schizopelex* McLachlan (Trichoptera, Sericostomatidae), from the southern Iberian Peninsula. *Zootaxa* 3866: 297–300. <https://doi.org/10.11646/zootaxa.3866.2.8>
- Wallace ID, Wallace B, Philipson GN (2003) A key to the case-bearing caddis larvae of Britain and Ireland. *Freshwater Biological Association Scientific Publication* 61: 1–259.
- Waringer J, Graf W (2011) Atlas of Central European Trichoptera Larvae. Erik Mauch Verlag, Dinkelscherben, 468 pp.
- Waringer J, Graf W (2013) Key and bibliography of the genera of European Trichoptera larvae. *Zootaxa* 3640: 101–151. <https://doi.org/10.11646/zootaxa.3640.2.1>
- Wiggins GB (1998) Larvae of the North American Caddisfly Genera (Trichoptera), 2nd Edition. University of Toronto Press, Toronto, 457 pp.

Morphological analysis of *Trichomycterus areolatus* Valenciennes, 1846 from southern Chilean rivers using a truss-based system (Siluriformes, Trichomycteridae)

Nelson Colihueque¹, Olga Corrales¹, Miguel Yáñez²

1 Laboratorio de Biología Molecular y Citogenética, Departamento de Ciencias Biológicas y Biodiversidad, Universidad de Los Lagos, Avenida Alcalde Fuchslocher 1305, Casilla 933, Osorno, Chile **2** Departamento de Estadística, Universidad del Bío-Bío, Casilla 5-C, Concepción, Chile

Corresponding author: Nelson Colihueque (ncolih@ulagos.cl)

Academic editor: D. Bloom | Received 22 April 2017 | Accepted 24 July 2017 | Published 5 September 2017

<http://zoobank.org/CB0F1C25-1387-4C84-86B2-C06EBAEE40B5>

Citation: Colihueque N, Corrales O, Yáñez M (2017) Morphological analysis of *Trichomycterus areolatus* Valenciennes, 1846 from southern Chilean rivers using a truss-based system (Siluriformes, Trichomycteridae). ZooKeys 695: 135–152. <https://doi.org/10.3897/zookeys.695.13360>

Abstract

Trichomycterus areolatus Valenciennes, 1846 is a small endemic catfish inhabiting the Andean river basins of Chile. In this study, the morphological variability of three *T. areolatus* populations, collected in two river basins from southern Chile, was assessed with multivariate analyses, including principal component analysis (PCA) and discriminant function analysis (DFA). It is hypothesized that populations must segregate morphologically from each other based on the river basin that they were sampled from, since each basin presents relatively particular hydrological characteristics. Significant morphological differences among the three populations were found with PCA (ANOSIM test, $r = 0.552$, $p < 0.0001$) and DFA (Wilks's $\lambda = 0.036$, $p < 0.01$). PCA accounted for a total variation of 56.16% by the first two principal components. The first Principal Component (PC1) and PC2 explained 34.72 and 21.44% of the total variation, respectively. The scatter-plot of the first two discriminant functions (DF1 on DF2) also validated the existence of three different populations. In group classification using DFA, 93.3% of the specimens were correctly-classified into their original populations. Of the total of 22 transformed truss measurements, 17 exhibited highly significant ($p < 0.01$) differences among populations. The data support the existence of *T. areolatus* morphological variation across different rivers in southern Chile, likely reflecting the geographic isolation underlying population structure of the species.

Keywords

Morphological variability, morphometry, multivariate analysis, *Trichomycterus areolatus*, truss-based system

Introduction

Almost all species display morphological variation within and among populations in response to environmental and genetic factors, or as a consequence of behavioral and physiological differences (West–Eberhard 1989, Schwander and Leimar 2011). The effects of genetic factors on morphological variations have been well documented in natural populations of several fish species (e.g. Keeley et al. 2006, Taylor et al. 2011, Reid and Peichel 2010). Environmentally-induced morphological variation, or phenotypic plasticity (West–Eberhard 1989), has also been reported in fishes (Pakkasmaa and Piironen 2000, Reis et al. 2006, Bagherian and Rahmani 2009, Mir et al. 2013). In particular, hydrological condition of rivers may play an important role in the body shape changes of fishes. For example, water velocity could have a significant effect on different attributes of body shape, such as, head depth and length, caudal peduncle depth, caudal fin depth and length, and body depth, among others (Imre et al. 2002, Keeley et al. 2006, Grünbaum et al. 2007, Istead et al. 2015). These findings indicate that fishes are largely amenable to environmentally-induced morphological variations.

Trichomycterus genus is an interesting group of catfishes for the studying morphological variation because most species have a wide distribution in different habitats across a broad altitudinal and latitudinal range in South America. *Trichomycterus* belongs to the family Trichomycteridae, which is native to southern Central and South America (Berra 1981, Arratia 1990) and includes eight sub-families, 40 genera and >170 valid species (Eschmeyer et al. 2016). The particular biogeography of these catfishes often results in numerous isolated, slightly-differentiated populations, denoted by a marked intraspecific variation (Arratia 1990). However, the factors driving morphological variation in this group remain poorly understood.

In Chile, *Trichomycterus* is represented by five endemic species (Pardo et al. 2005), with *Trichomycterus areolatus* Valenciennes, 1846 (Siluriformes, Trichomycteridae) being a species characterized by inhabiting the rhithronic zone of freshwater systems of the Andean river basins (Arratia 1981, Vila et al. 1999). This small catfish, of less than 10 cm in length, inhabits a wide latitudinal and altitudinal range across the country, from 28 to 42°S (or a distance of about 1,500 km), and between zero and 4,000 meters above sea level, respectively (Vila et al. 1999, Dyer 2000, Unmack et al. 2009a). In addition, reproduction, feeding and shelter activities of this catfish regularly occur in habitats characterized by shallow water with a substratum of small stones with fine sand where there is rapid water velocity, located in the rhithronic zones of rivers (Arratia 1983, Campos 1985, García et al. 2012). In comparison with other sympatric freshwater fishes, either native or non-native, inhabiting Chilean river basins, ecological studies indicate that *T. areolatus* is relatively more abundant (Ruiz et al. 1993, Ruiz 1996, Valdovinos et al. 2012).

Morphological studies of *T. areolatus*, which have focused mainly on northern and central Chilean populations, indicated intraspecific variation for some morphological characters. Variation has been documented in the bones of caudal skeleton (Arratia et al. 1978, Arratia 1982, 1983) and in geometric characters at the head region (Pardo 2002). The origin of morphological variation in *T. areolatus* remains unknown, but

potential causes include local adaptation, due to the environmental variability of rivers, or geographic isolation of populations due to the physical separation between hydrographic basins (Pardo 2002). Another possible source of variation is the marked genetic structure of this species throughout its distribution range, associated with the low gene flow among drainage systems (Unmack et al. 2009a; Quezada–Romegialli et al. 2010). As studies undergone to date have mainly targeted northern and central regions of its range; it is unclear whether southern Chilean populations of *T. areolatus* exhibit similar levels of morphological variation. These catfish populations occupy a geographic zone of western of southern South America which, according to Hulton et al. (2002), was the site of a strong glaciation process (between latitudes 38° and 55°S) during the Last Glacial Maximum around 19,000–23,000 cal yr ago, with major ice sheets covering vast parts of the region. This geological may impacted the distribution of different species in southern Chile (Villagrán 1990). During this glaciation process, freshwater species survived in refuges and then recolonized rivers after glacial events. This process likely impacted the genetic structure of *T. areolatus* through tight bottlenecks across the distribution range, especially in basins subjected to significant ice cover during glaciation. In addition, the basins in southern Chile are made up of relatively short rivers that flow from east to west, each occupying large drainage areas. Rithonic biotopes represent about 70% of these basins (Campos 1985). In these hydrographic systems the movement of species is typically limited by connections among riverine systems, with the ocean providing an effective barrier at each river terminus. As a result of these topographic characteristics, *T. areolatus* populations between different basins are mostly isolated, which limits gene flow and promotes population subdivision. Studies to date on *T. areolatus* populations across southern Chile reveals high level of genetic divergence, which suggest limited movement between basins (Unmack et al. 2009a).

Morphometric variation between populations can provide a basis for population differentiation, which is an important tool for evaluating population structure and identifying discrete groups (Turan 1999). There are many studies on native Chilean freshwater fish that provide evidence for population or species discrimination based on traditional morphometric characters (Campos 1982, Gajardo 1987, Campos et al. 1996, Campos and Gavilán 1996). However, the alternative system of morphometric measurements called the truss network system (Strauss and Bookstein 1982, Winans 1987), constructed with the help of anatomical landmark points that enhance discrimination among groups, has been less explored for population structure analysis in freshwater fish. This type of morphometric analysis has been mostly applied to Chilean marine fish (e.g. Cortés et al. 1996, Gacitúa et al. 2008), to facilitate interpretation of the biological significance of population structures in species with wide distribution ranges.

In this study we determined the level of morphological variation in three *T. areolatus* populations collected from different river basins located in southern Chile. Given that these basins present particular hydrological conditions, we hypothesized that populations differ or segregate morphologically from each other, based on the river basin that they were sampled from. In order to address these objectives, we examined several specimens of each population based on 22 morphometric distance characters, using a truss network

that covers the body shape dimensions in a relatively homogeneous way. This ensured a significant amount of information about the shape of individuals was gathered. This dataset was then subject to multivariate analyses to evaluate the degree of population separation, and to identify the body regions that experienced shape variations.

Materials and methods

Study areas and sampling sites

Specimens were collected from the Tijeral (TIJ) ($n = 22$) ($40^{\circ}37'S$; $73^{\circ}02'W$) and Huilma (HUI) ($n = 32$) ($40^{\circ}43'S$; $73^{\circ}13'W$) Rivers in the Bueno River basin, Province of Osorno, 10th Region; and from the Biobío River (BIO) ($n = 50$) ($37^{\circ}11'S$; $72^{\circ}47'W$) in the Biobío River basin, Province of Biobío, 8th Region (Figure 1). These basins are located in southern Chile and originate in the western Andean Mountains at altitude above 1,000 meters and flow in a relatively straight line until reaching the Pacific Ocean. The basins are separated by about 500 km from north to south. The Biobío River basin ($36^{\circ}43'–38^{\circ}55'S$, $70^{\circ}49'–73^{\circ}10'W$) has a drainage area of 24,029 km² and represents Chile's third largest river basin. It has a length of about 400 km and a mean flow of 900 m³/s (Errazuriz et al. 2000). This basin shows marked changes in flow between seasons, from 391 to 3,697 m³/s (Dirección General de Aguas 2004a). From a hydrological perspective, the basin is nival and rapidly-filling, and its rivers are classified as torrential with a mixed regime. Local climatic conditions are warm-temperate with winter rains. Mean annual precipitation reaches from 730 mm to 1,072 mm, and the mean annual temperature is 14.7 °C (Errazuriz et al. 2000). The Bueno River basin ($39^{\circ}53'–41^{\circ}23'S$, $71^{\circ}43'–73^{\circ}15'W$) has a drainage area of 17,210 km² and a length of about 200 km. The mean flow is 570 m³/s (Errazuriz et al. 2000), ranging from 346 and 1106 m³/s (Dirección General de Aguas 2004b). Hydrological characteristics of the basin include a constant flow and weak slope, and its rivers are classified as quiet rivers with a lacustrine regulation. The climate is warm-temperate and rainy with Mediterranean influence. Mean annual precipitation and mean annual temperature is 2,490 mm and 12.0 °C, respectively (Errazuriz et al. 2000). In addition, the Biobío River basin has four-fold more suspended solids than the Bueno River basin (2,157 vs. 485 tons/month) (Brown and Saldivia 2000). Specimens were collected in September, October and December 2002, and March 2004 using two-pass electrofishing from 100 m of river bed, mainly in areas with small substrates and shallow water. The specimens were anesthetized with a lethal dose of benzocaine before identification as *T. areolatus* based on diagnostic characters as described by Arratia (1981). After identification, the specimens were fixed and deposited in the fish collection of the Laboratorio de Biología Molecular y Citogenética of the Universidad de Los Lagos, Osorno, Región de Los Lagos (LBMULA), under identification numbers LBMULA 363–366, LBMULA 369–375, LBMULA 382–386, LBMULA 388–412 and LBMULA 414–433. Moreover, dorsal fin rays were also counted, as an

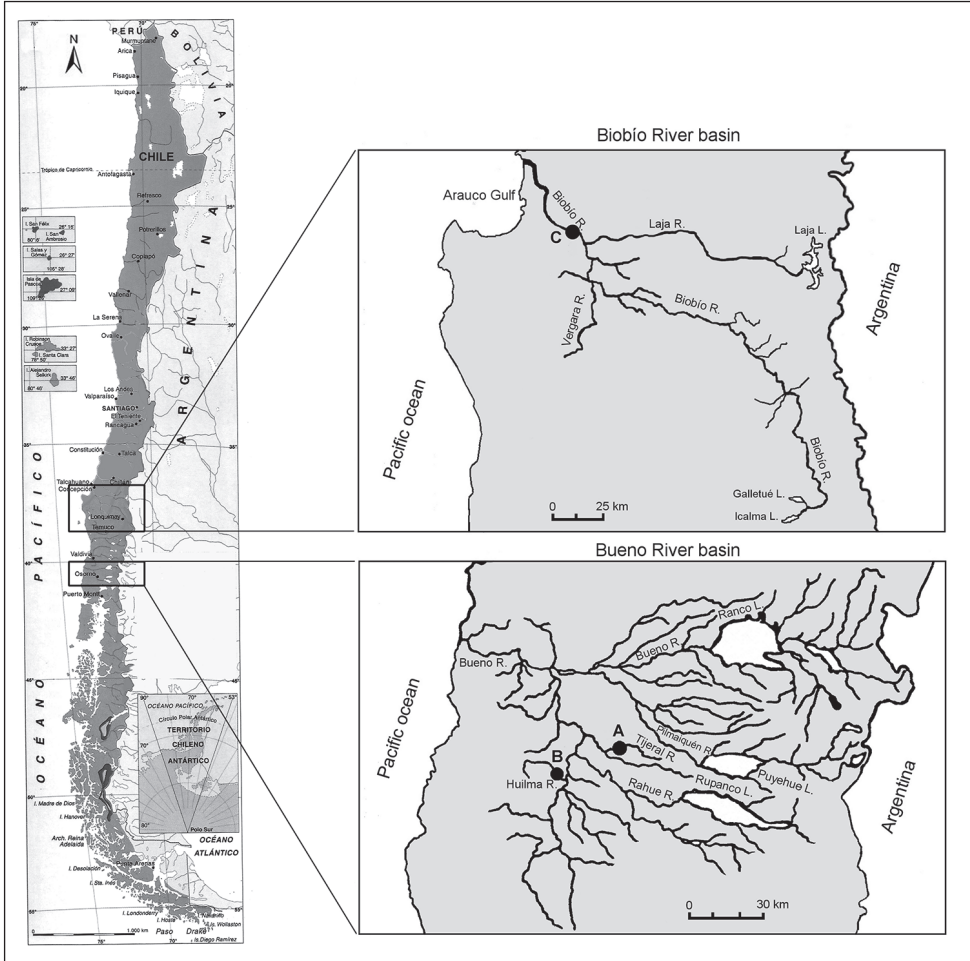


Figure 1. Location of sample sites of *Trichomycterus areolatus* populations located in two river basins from southern Chile. Bueno River basin: **A** Tijeral River, and **B** Huilma River; Biobío River basin: **C** Biobío River.

additional diagnostic character for enhanced differentiation this species from other trichomyterid catfish possibly distributed in southern Chile (e.g. *Hatcheria macraei* (Girard, 1855)), as has been suggested by Unmack et al. (2009b). Counts revealed that the specimens from all populations studied had the expected number of dorsal fin rays (TIJ= 6–8, HUI= 6–9, BIO= 4–8) for the species (Unmack et al. 2009b).

Morphometry procedure

Twenty-four morphometric characters were analyzed, including two conventional characters, total length and standard length, and 22 distance characters derived from

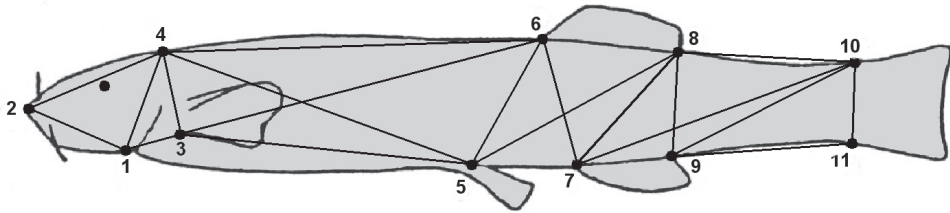


Figure 2. Position of the anatomical landmarks used to measure the size of 22 morphological characters on *Trichomycterus areolatus* based on a truss network. Definition of each character and its classification according to body shape dimension covered by them was as follows: **a** Head length, 1–2 = ventral tip of the operculum to tip of the head, 2–4 = tip of the head to posterior margin of the head **b** Head depth, 1–4 = ventral tip of the operculum to posterior margin of the head, 3–4 = base of the pectoral fin to posterior margin of the head **c** Anterior body length, 1–3 = ventral tip of the operculum to base of the pectoral fin, 3–5 = prepelvic length; 4–5 = posterior margin of the head to base of the pelvic fin; 3–6 = base of the pectoral fin to anterior base of the dorsal fin; 4–6 = predorsal length **d** Middle body depth, 5–6 = base of the pelvic fin to anterior base of the dorsal fin, 5–8 = base of the pelvic fin to posterior base of the dorsal fin, 6–7 = anterior base of the dorsal fin to anterior base of the anal fin, 7–8 = anterior base of the anal fin to posterior base of the dorsal fin **e** Middle body length, 5–7 = base of the pelvic fin to anterior base of the anal fin, 6–8 = dorsal fin base length, 7–9 = anal fin base length **f** Posterior body length, 7–10 = anterior base of the anal fin to dorsal posterior margin of the caudal peduncle, 9–10 = posterior base of the anal fin to dorsal posterior margin of the caudal peduncle **g** Peduncle depth, 8–9 = anterior caudal peduncle depth, 10–11 = posterior caudal peduncle depth **h** Peduncle length, 8–10 = dorsal caudal peduncle length, 9–11 = ventral caudal peduncle length.

a truss network constructed by interconnecting eleven landmarks representing the basic shape of the fish (Figure 2). The landmarks were selected for this particular fish species according to Winans (1987): 1) ventral tip of the operculum, 2) the most distal point of the head, 3) base of the pectoral fin, 4) posterior margin of the head, 5) base of the pelvic fin, 6) anterior base of the dorsal fin, 7) anterior base of the anal fin, 8) posterior base of the dorsal fin, 9) posterior base of the anal fin, 10) dorsal posterior margin of the caudal peduncle and 11) ventral posterior margin of the caudal peduncle. Several distance characters considered in this study covered the head and caudal regions of fish; these body areas are particularly interesting to analyze because, according to previous studies (Arratia 1982, 1983, Pardo 2002), *T. areolatus* populations may exhibit important morphological variation in these body regions. Truss measurements were performed manually on whole fixed specimens using a digital caliper with a precision of 0.01 mm. To reasonably eliminate any variation attributable to allometric growth, all measurements were standardized following Elliott et al. (1995), according to the following equation:

$$M_{adj} = M (L_s \cdot L_o^{-1})^b$$

where M_{adj} is the size adjusted measurement, M is the original measurement, L_s is the overall mean of the standard length (SL) for all fish from all samples in each

analysis and L_O = is the SL of the fish. Parameter b was estimated for each character from the observed data as the slope of the regression of $\log M$ on $\log L_O$.

Multivariate data analysis

Prior to statistical analysis the variables were analysed for conformance to assumptions regarding normal distribution and homogeneity of variance using the Kolmogorov–Smirnov (K-S) and Levene’s tests, respectively. Differences among populations were tested with an analysis of variance (ANOVA), either with parametric (one-way ANOVA) or non-parametric (Brown–Forsythe test) tests, using each character as a response variable. The Brown–Forsythe test was applied, given that some variables presented a heterogeneous variance among groups. The transformed data were subjected to principal component analysis (PCA) and discriminant function analysis (DFA) to evaluate any phenotypic differences among populations. Individual scores from PCA were used to construct a scatterplot to reveal the specimen groupings. The eigenvectors and eigenvalues were obtained from the PCA correlation matrix, which allowed the largest part of the variance of original variables to be reduced to a small number of components. The analysis evaluates the relationships among populations according to their proximity in the space defined by the components. Thus, plotting the component scores of specimens can reveal natural groupings, without *a priori* knowledge of such groupings. The significance of the separation among groups was determined using an analysis of similarity (ANOSIM) test. This test is a generalization of the univariate ANOVA and it has the property to consider all variables during the calculation of similarity among populations based on the Euclidean distance matrix. In this test, r -values range from 0 to 1, where 0 indicates no separation of groups and 1 corresponds to complete discrimination between groups (Clark 1993). Only 22 truss measurements were included in the PCA analyses. The number of principal components useful for this analysis was determined by using the Parallel Analysis (PA) based on the retaining of PCA eigenvalues from the data greater than PA eigenvalues from the corresponding random data (Franklin et al. 1995). Significant different ($p < 0.01$) truss measurements were further subjected to DFA for case classification using separate covariance matrix. This method is recommended to address the problem of inequality of covariance matrices among groups in DFA (Anderson and Bahadur 1962). The Wilks’s λ was used to compare the differences among all groups. The ability of the phenotypes to discriminate among populations was assessed with a cross-validation test. This required the removal of one individual from the original matrix, and then a discriminant analysis was performed with the remaining observations to classify the omitted individual. Performance was evaluated according to the percentage of correctly and incorrectly classified fish. The morphological distinctness of the population was defined as the percentage of correctly-classified individuals. Kolmogorov–Smirnov, ANOVA, Brown–Forsythe, and DFA analyses were carried out using SPSS v. 19 (IBM Corp., Armonk, NY, USA), while PCA and ANOSIM analyses were performed with MATLAB R2010a (The MathWorks, Inc.) and PAST v. 3.14 (Hammer et al. 2001), respectively.

Results

Table 1 shows the average values of TL, SL and the 22 truss measurements analyzed. Nineteen of 22 truss measurement were found to be significantly different among populations (Table 1), including 17 (1–2, 1–3, 1–4, 2–4, 3–4, 3–6, 4–6, 5–6, 5–7, 6–7, 6–8, 7–9, 7–10, 8–9, 8–10, 9–10, 9–11) with highly significant ($p < 0.01$) values that were further tested in multivariate analysis using DFA.

The PCA based on 22 truss measurements retained two components according to PA, explaining 56.16% of the total variance. The first (PC1) and second (PC2) principal components accounted for 34.73 and 21.44% of the total variance, respectively

Table 1. Morphometric data for 24 characters of three *Trichomycterus areolatus* populations from southern Chile.

Character	Tijeral River (Mean ± SD) (n = 22)	Huilma River (Mean ± SD) (n = 32)	Biobío River (Mean ± SD) (n = 50)	ANOVA (Exact p -value)
Total length, TL (cm)	7.02 ± 1.64	6.66 ± 0.92	6.16 ± 1.24	0.021*
Standard length, SL (cm)	6.27 ± 1.53	5.66 ± 0.75	5.51 ± 1.17	0.036*
Truss measurements (cm)				
1–2	1.04 ± 0.29	0.96 ± 0.12	0.58 ± 0.10	<0.001***(\$)
1–3	0.25 ± 0.12	0.17 ± 0.08	0.46 ± 0.08	<0.001***
1–4	0.63 ± 0.16	0.59 ± 0.11	0.49 ± 0.08	<0.001***(\$)
2–4	0.80 ± 0.19	0.74 ± 0.14	0.84 ± 0.14	<0.001***(\$)
3–4	0.73 ± 0.18	0.63 ± 0.13	0.53 ± 0.09	<0.001***(\$)
3–5	1.82 ± 0.71	1.80 ± 0.30	1.94 ± 0.39	0.024*(§)
4–5	2.51 ± 0.56	2.29 ± 0.35	2.20 ± 0.44	0.858 ^{NS}
3–6	2.57 ± 0.69	2.32 ± 0.37	2.48 ± 0.53	<0.001***
4–6	2.89 ± 0.70	2.60 ± 0.42	2.65 ± 0.54	<0.001***
5–6	0.96 ± 0.28	0.77 ± 0.15	0.96 ± 0.26	<0.001***
5–7	0.99 ± 0.39	0.74 ± 0.30	0.93 ± 0.23	0.004**(\$)
6–7	0.94 ± 0.24	0.81 ± 0.16	0.77 ± 0.17	0.007**
5–8	1.56 ± 0.48	1.48 ± 0.29	1.36 ± 0.29	0.053 ^{NS}
6–8	0.85 ± 0.27	0.89 ± 0.21	0.61 ± 0.13	<0.001***(\$)
7–8	0.75 ± 0.26	0.69 ± 0.16	0.66 ± 0.12	0.929 ^{NS} (§)
7–9	0.33 ± 0.15	0.36 ± 0.12	0.41 ± 0.10	<0.001***(\$)
8–9	0.53 ± 0.19	0.42 ± 0.08	0.49 ± 0.10	<0.001***(\$)
7–10	1.86 ± 0.53	1.63 ± 0.24	1.84 ± 0.42	<0.001***
8–10	1.30 ± 0.39	1.0 ± 0.19	1.44 ± 0.32	<0.001***
9–10	1.40 ± 0.38	1.15 ± 0.17	1.36 ± 0.29	<0.001***
9–11	1.22 ± 0.36	0.98 ± 0.20	1.25 ± 0.28	<0.001***
10–11	0.57 ± 0.16	0.48 ± 0.09	0.48 ± 0.10	0.040*

* $p < 0.05$, ** $p < 0.01$, *** $p < 0.001$

§Significance from Brown–Forsythe test

n = sample size

NS = not significant

Table 2. Component loadings of the first two principal components derived from PCA based on the correlation matrix of 22 truss measurements of *Trichomycterus areolatus* populations from southern Chile. Characters of greater contribution on each component are in bold.

		Component	
		PC1	PC2
Eigenvalue		7.640	4.716
Explained variance (%)		34.728	21.438
Cumulative variance (%)		34.728	56.166
Character	Body shape dimension		
1–2	Head length	-0.177	-0.341
1–3	Anterior body length	0.324	0.046
1–4	Head depth	-0.148	-0.282
2–4	Head length	0.209	0.134
3–4	Head depth	-0.126	-0.307
3–5	Anterior body length	0.250	-0.130
4–5	Anterior body length	-0.062	0.031
3–6	Anterior body length	0.253	0.039
4–6	Anterior body length	0.159	-0.002
5–6	Middle body depth	0.237	-0.083
5–7	Middle body length	0.222	-0.170
6–7	Middle body depth	0.066	-0.293
5–8	Middle body depth	0.060	-0.382
6–8	Middle body length	-0.109	-0.381
7–8	Middle body depth	0.096	-0.346
7–9	Middle body length	0.226	-0.139
8–9	Peduncle depth	0.239	-0.180
7–10	Posterior body length	0.259	-0.036
8–10	Peduncle length	0.324	0.080
9–10	Posterior body length	0.314	0.036
9–11	Peduncle length	0.310	0.045
10–11	Peduncle depth	0.127	-0.274

(Table 2). Thus, PC1 was the most important component contributing to separation among populations. These differences were primarily because of the strong loading of 1–3, 2–4, 3–5, 3–6, 5–6, 5–7, 7–9, 8–9, 7–10, 8–10, 9–10, and 9–11 characters. Most of these characters were involved in longitudinal body shape changes (i.e., shape changes corresponding to the anterior-posterior body that reflect length changes) either at the head (2–4), anterior body (1–3, 3–5 and 3–6) or caudal peduncle (8–10 and 9–11) regions. Strong loading of characters involved in body depth shape variation (i.e., corresponding shape changes of the dorsal-ventral body axis) at the dorsal fin in the middle body (5–6) and caudal peduncle (8–9) regions, were also observed (Table 2). In the case of PC2, within the eight characters that exhibited strong loadings, most were associated to body depth shape variation either at head (1–4 and 3–4), dorsal fin in the middle body (6–7, 5–8 and 7–8) or caudal peduncle (10–11) regions.

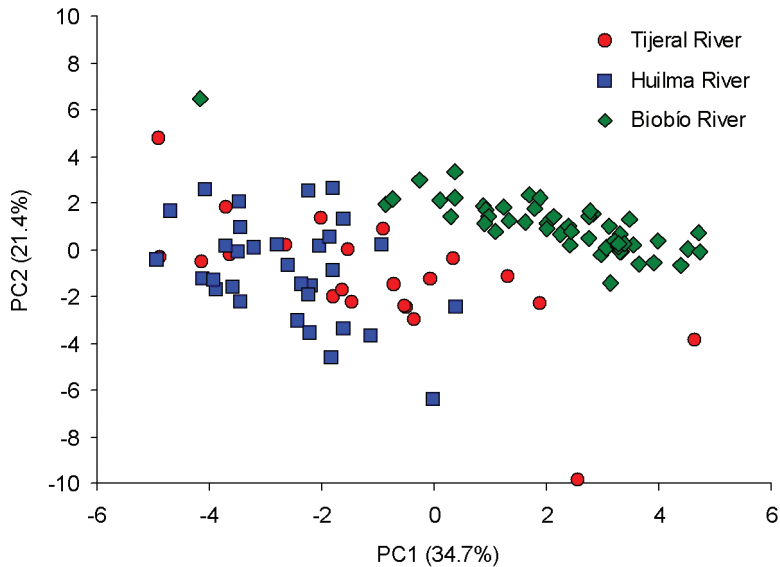


Figure 3. Scatterplot for individual scores from Principal Component Analysis (PC1 on PC2) of three *Trichomycterus areolatus* populations from southern Chile according to 22 truss measurements derived from a truss network.

The scatter-plot of PC1 and PC2 scores for each sample revealed no overlapping (TIJ and HUI vs. BIO) or some overlapping (TIJ vs. HUI) dot clusters among *T. areolatus* populations (Figure 3). There were highly significant difference between populations based on the ANOSIM test ($r = 0.552$, $p < 0.0001$).

The DFA based on 17 truss measurements with highly significant ($p < 0.01$) differences among populations produced two discriminant functions. The first (DF1) and second (DF2) discriminant functions explained 95.7% and 4.3% of the total variance, respectively, together accounting for 100% of the morphological variation. This result was supported by the high canonical correlations among the discriminant functions and groups, which had values of 0.969 y 0.641 for the first and second functions, respectively. Furthermore, both DF1 and DF2 generated statistically significant differences among the groups (Wilks's $\lambda = 0.036$, $\chi^2 = 309.803$, d.f. = 34, $p < 0.01$). This result indicated significant morphological differences among the three populations. The DF1 vs DF2 scatter-plot revealed a clear separation among the point clouds for the three populations (Figure 4), a result that was consistent with the clusters observed in the PCA scatter-plot. The structure matrix (Table 3), which shows the intra-group correlations between each of the characters and the discriminant functions, revealed 17 truss measurements with high correlations. The variables with meaningful loading on DF1 were 1–2, 1–3, 6–8, 2–4, 3–6, 1–4, 7–10 and 4–6, while on DF2 they were 9–10, 8–9, 8–10, 3–4, 5–7, 9–11, 7–9, 6–7 and 5–6, showing that these characters were mainly responsible for differences among the populations. In DF1 all variables

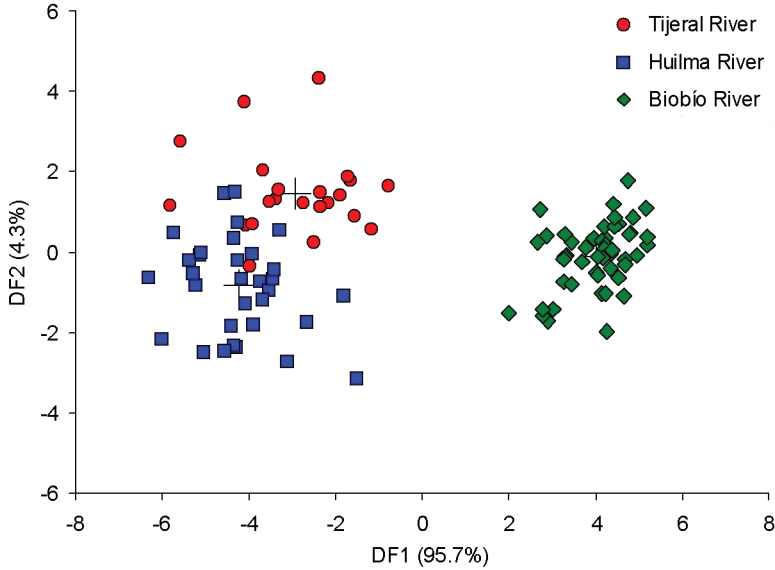


Figure 4. Scatterplot for individual scores from Discriminant Function Analysis (DF1 on DF2) of three *Trichomycterus areolatus* populations from southern Chile according to 17 truss measurements derived from a truss network. Crosses indicate group centroids.

Table 3. Structure matrix coefficients that show the intra-group correlations between each of the characters and the discriminant functions. Characters of greater contribution in each discriminant function are in bold.

Character	Body shape dimension	Function	
		DF1	DF2
1-2	Head length	-0.428	0.353
1-3	Anterior body length	0.390	0.142
6-8	Middle body length	-0.227	-0.173
2-4	Head length	0.220	-0.152
3-6	Anterior body length	0.190	-0.071
1-4	Head depth	-0.149	0.121
7-10	Posterior body length	0.139	0.102
4-6	Anterior body length	0.121	0.014
9-10	Posterior body length	0.234	0.378
8-9	Peduncle depth	0.116	0.376
8-10	Peduncle length	0.263	0.372
3-4	Head depth	-0.183	0.356
5-7	Middle body length	0.069	0.332
9-11	Peduncle length	0.217	0.311
7-9	Middle body length	0.109	-0.290
6-7	Middle body depth	-0.054	0.285
5-6	Middle body depth	0.121	0.223

Table 4. Percentage of *Trichomycterus areolatus* specimens from populations of southern Chile correctly classified into their original group and after cross-validation.

Group	Population	Tijeral River	Huilma River	Biobío River	Total
Original (%)†	Tijeral River	81.8	18.2	0.0	100
	Huilma River	9.4	90.6	0.0	100
	Biobío River	0.0	0.0	100	100
Cross-validated (%)‡	Tijeral River	77.3	18.2	4.5	100
	Huilma River	6.3	90.6	3.1	100
	Biobío River	0.0	0.0	100	100

†The 93.3% of originally grouped cases were correctly classified

‡The 92.3% of cross-validated grouped cases were correctly classified

represent measurements covering the entire body of the fish; in contrast, these were concentrated mostly in the tail region in DF2.

Discriminant function analysis showed 93.3% correct classification of individuals into their original populations, and the cross-validation test produced comparable results (92.3%) (Table 4). The percentage of correctly-classified fish was highest in all populations, with 100% in BIO, 81.8% in TIJ and 90.6% in HUI. The last two populations included a slight mixture of individuals from each other.

Discussion

The results of this study obtained from the truss-based morphometrics indicated that *T. areolatus* from southern Chile showed significant phenotypic heterogeneity among the populations. Both multivariate analyses using PCA and DFA suggested three distinct phenotypic populations of *T. areolatus*. The segregation among populations was confirmed by PCA and DFA scatter-plot based on scores for each sample that showed non-, or slight, overlapping clusters of points for each population. This result was also supported by the percentage of correctly-classified individuals, where 93.3% of individuals showed correct classification into their respective groups by DFA, indicating low intermingling among the populations. Populations of the Tijeral plus Huilma Rivers versus the Biobío River showed non-overlapping, possibly due to the large distances among drainages. This was not the case in the morphological parameters of populations of the Tijeral River versus the Huilma River that showed some overlapping between populations, which may be attributed to the small geographic distances between them given that both belong to the same drainage in southern Chile (Buena River basin) and probably share more similar environmental conditions. Our results are similar to those of Pardo (2002) who reported morphometric variation based on the geometric morphometric technique in two *T. areolatus* populations from different river basins of south-northern Chile. Our results also agree with Arratia (1982, 1983) who reported phenotypic heterogeneity in this species, particularly, among popula-

tions collected across central Chile, although the differences were found in the bones of the caudal skeleton.

The PCA confirmed that the variation in morphological measurements of the study populations of *T. areolatus* involved several characters related to the head region, body depth, and caudal peduncle. For example PC1, which was the most important component contributing to separation between populations (34.72% of the total explained variance), presented twelve characters with strong loading on this component, associated with body length and depth. For their part, PC2 that was also an important component (21.44% of the total explained variance), showed characters mainly associated to body depth variation in the head region, including the caudal peduncle region. Thus, the morphological variation registered in *T. areolatus* populations by PCA revealed changes on several body regions and/or dimensions.

Understanding the origin of morphological differences between populations of *T. areolatus* is challenging. This is because fish morphology is a complex phenotype that is determined by genetics and environment factors, and the interaction between them (Poulet et al. 2004, Keeley et al. 2006, Schwander and Leimar 2011, Colihueque and Araneda 2014). In addition, other forces such as ontogeny, performance, fitness and behavior may also change the body shape (Walker 2010). Thus, for example, phenotypic variability among populations may arise without major genetic differentiation as a consequence of the isolation of portions of a population within local habitats or when they occupy heterogeneous habitats across their distribution range. In other cases, genetic differentiation among populations precedes phenotype divergence (Schwander and Leimar 2011). It is also possible that preexisting genetic differences among current populations can be enhanced by their isolation, resulting in a notable inter-population structuring (Esguícero and Arcifa 2010). Previous molecular studies of *T. areolatus* across its distribution range reveal a high level of genetic differentiation among populations within and between watersheds (Unmack et al. 2009a, Quezada-Romegialli et al. 2010). This high degree of genetic divergence seem to be related to geographic isolation and the subsequent low genetic flow among populations of this species, given that Chilean watersheds flow relatively straight from the east (Andean mountains) to the west (Pacific Ocean), limiting opportunities for contact despite relatively short geographical distances among populations. Thus, the morphological variations observed in the present study for *T. areolatus* might be due to genetic differences among the populations. In natural populations of other fish species, the association between genetic differentiation and morphology variation among populations has been well-supported. In particular, Keeley et al. (2006) demonstrated that differences in external morphological traits among rainbow trout, *Oncorhynchus mykiss* (Walbaum, 1792) populations had a significant genetic component. In addition, these authors proposed that this morphological distinction could be, at least in part, a response to natural selection in contrasting environments. Taylor et al. (2011) after analyzing several populations of the same species from British Columbia, came to a similar conclusion, since they observed a significant positive correlation between genetic and morphological divergence among populations.

The morphometric variations observed among different populations of *T. areolatus* in the present study might also be associated with phenotypic plasticity in response to the different environmental factors of various habitats. Included within these factors are the hydrological characteristics of rivers, given that available data reveal an important influence of some hydrological parameters on body shape variation in fishes. For example, several studies have shown that water velocity can modify body shape in various fish species, such as salmonids (Pakkasmaa and Piironen 2000), Caspian cyprinid, *Alburnus chalcoides* (Güldenstädt, 1772) (Bagherian and Rahmani 2009) and the Indian major carp, *Labeo rohita* (Hamilton, 1822) (Mir et al. 2013). Differences in the water current have also been cited as an important factor that can affect body shape variation in Brazilian epigeal and hypogean *Ancistrus* catfishes (Reis et al. 2006). In addition, experimental data on the brook charr, *Salvelinus fontinalis* (Mitchill, 1814) (Imre et al. 2002), the Arctic charr, *Salvelinus alpinus* (Linnaeus, 1758) (Grünbaum et al. 2007), the rainbow trout (Keeley et al. 2006), and gibbose centrarchid species (Istead et al. 2015) also revealed that changes in water velocity may affect the morphology of different areas of fish body, such as head depth and length, caudal peduncle depth, caudal fin depth and length, body depth, pelvic fin and dorsal fin lengths. These findings provide strong support that the hydrological conditions of the rivers may play an important role in morphology variations in fishes. Of note is that the study populations of *T. areolatus* belong to different basins in southern Chile (Biobío River basin and Bueno River basin) whose hydrological conditions are dissimilar with respect to various parameters, such as, quantity of water flow, turbidity and temperature (Dirección General de Aguas 2004a,b). In addition, Biobío River basin experiences significantly more variable water flow throughout the year than Bueno River basin, resulting in rapid filling during various periods of the year, and therefore, exhibiting more turbulent water conditions than Bueno River basin (Erzuriz et al. 2000). Future controlled or field experiments should be undertaken to reveal the degree of body shape variation of *T. areolatus* populations from southern Chile that could be attributed to environmental variability among rivers. This variability is may be related to water current velocity given that habitats with high water current are preferentially used by this species, compared with other sympatric species (García et al. 2012).

The truss-based morphometrics represent a system of morphometric measurements that enhance discrimination between group, based on a systematic detection of body shape differences in both diagonal and horizontal and vertical directions (Strauss and Bookstein 1982, Winans 1987). One of the properties of this system is to ensure uniform coverage of the landmark configuration, being able to capture information about the shape of an organism. This class of morphometric analysis has been less explored in catfish, in spite of its potential to facilitate interpretation of morphology variation through multivariate analysis, such as PCA. In our case, the truss-based system showed a high performance to distinguish *T. areolatus* populations based on morphological data, and also to determine the specific body shape characters that contributed to such variations.

In conclusion, the findings of this study based on truss-based morphometrics indicated significant morphological variations among three *T. areolatus* populations from southern Chile. Thus, these results suggest an underlying population structure of the species.

Acknowledgments

The suggestions and constructive comments of all those who helped to improve the final version of this manuscript are gratefully acknowledged. The authors are very grateful to the people who helped during the field works. We also wish to thank to Dr. Juan Francisco Gavilán for providing collaboration in this study.

References

- Anderson TW, Bahadur RR (1962) Classification into two multivariate normal distributions with different covariances matrices. *Annals of Mathematical Statistics* 33: 420–431. <https://doi.org/10.1214/aoms/1177704568>
- Arratia G (1981) Géneros de peces de aguas continentales de Chile. Museo Nacional de Historia Natural, Santiago de Chile (Chile), 108 pp.
- Arratia G (1982) Esqueleto caudal de peces siluriformes y sus tendencias evolutivas (Diplomystidae y Trichomycteridae). *Boletín del Museo Nacional de Historia Natural (Chile)* 39: 49–61.
- Arratia G (1983) The caudal skeleton of Ostariophysan fishes (Teleostei): intraspecific variation in Trichomycteridae (Siluriformes). *Journal of Morphology* 177: 213–229. <https://doi.org/10.1002/jmor.1051770208>
- Arratia G (1990) The South American Trichomycterinae (Teleostei: Siluriformes), a problematic group. In: Peters G, Hutterer R (Eds) *Vertebrates in the tropics*. Alexander Koenig Zoological Research Institute and Zoological Museum, Bonn, 395–403.
- Arratia G, Chang A, Menu-Marque S, Rojas G (1978) About *Bullockia* gen. nov., *Trichomycterus mendozensis* n. sp. and revision of the family Trichomycteridae (Pisces, Siluriformes). *Studies of Neotropical Fauna and Environment* 13: 157–194. <https://doi.org/10.1080/01650527809360539>
- Bagherian A, Rahmani H (2009) Morphological discrimination between two populations of shemaya, *Chalcalburnus chalcoides* (Actinopterygii, Cyprinidae) using a truss network. *Animal Biodiversity and Conservation* 32: 1–8.
- Berra T (1981) *An atlas of distribution of the freshwater fish families of the world*. University of Nebraska Press, Lincoln, USA, 197 pp.
- Brown E, Saldivia JE (2000) Informe nacional sobre la gestión del agua en Chile. Comisión Económica para América Latina y el Caribe, Santiago de Chile, 101 pp.
- Campos H (1982) Sistemática del género *Cheirodon* (Pisces: Characidae) en Chile con descripción de una nueva especie. *Análisis de multivarianza*. *Studies of Neotropical Fauna and Environment* 17: 129–162. <https://doi.org/10.1080/01650528209360606>

- Campos H (1985) Distribution of the fishes in the Andean rivers in the south of Chile. *Archive of Hydrology* 104: 169–191.
- Campos H, Gavilán JF (1996) Diferenciación morfológica entre *Percichthys trucha* y *Percichthys melanops* (Perciformes: Percichthyidae) entre 36° y 41° L.S (Chile y Argentina), a través de análisis multivariados. *Gayana Zoológica* 60: 99–120.
- Campos H, Gavilán JF, Murillo V, Alarcón P (1996) Presencia de *Cheirodon australe* (Pisces: Characidae) en el Lago Tarahuín (Isla Grande de Chiloé, 42°40'S, Chile) y su significado zoogeográfico. *Medio Ambiente* 13: 69–79.
- Clarke KR (1993) Non-parametric multivariate analyses of changes in community structure. *Australian Journal of Ecology* 18: 117–143. <https://doi.org/10.1111/j.1442-9993.1993.tb00438.x>
- Colihueque N, Araneda C (2014) Appearance traits in fish farming: progress from classical genetics to genomics, providing insight into current and potential genetic improvement. *Frontiers in Genetics* 5: 1–8. <https://doi.org/10.3389/fgene.2014.00251>
- Cortés NA, Oyarzún C, Galleguillos R (1996) Diferenciación poblacional en sardina común, *Strangomera bentincki* (Norman, 1936). II. Análisis multivariado de la morfometría y la merística. *Revista de Biología Marina, Valparaíso* 31: 91–105.
- Dirección General de Aguas (DGA) (2004a) Diagnóstico y clasificación de los cursos y cuerpos de agua según objetivos de calidad: cuenca del Río Bio Bio. Santiago de Chile, Chile, 179 pp.
- Dirección General de Aguas (DGA) (2004b) Diagnóstico y clasificación de los cursos y cuerpos de agua según objetivos de calidad: cuenca del Río Bueno. Santiago de Chile, Chile, 141 pp.
- Dyer B (2000) Systematic review and biogeography of the freshwater fishes of Chile. *Estudios Oceanológicos, Chile*, 19: 77–98.
- Elliott NG, Haskard K, Koslow JA (1995) Morphometric analysis of orange roughy (*Hoplostethus atlanticus*) off the continental slope of southern Australia. *Journal of Fish Biology* 46: 202–220. <https://doi.org/10.1111/j.1095-8649.1995.tb05962.x>
- Erazuriz A, Cereceda P, González J, González M, Henríquez M, Rioseco R (2000) Manual de geografía de Chile. 3ª ed. Andrés Bello, Santiago de Chile, Chile, 443 pp.
- Eschmeyer W, Fricke R, van der Laan R (2016) Catalog of fishes: genera, species, references [Electronic version]. California Academy of Sciences. <http://researcharchive.calacademy.org/research/ichthyology/catalog/fishcatmain.asp> [accessed: November 2, 2016]
- Esguicero ALH, Arcifa MS (2010) Fragmentation of a Neotropical migratory fish population by a century-old dam. *Hydrobiologia* 638: 41–53. <https://doi.org/10.1007/s10750-009-0008-2>
- Franklin SB, Gibson DJ, Robertson PA, Pohlmann JT, Fralish JS, Scott B, David J, Philip A, John T, James S (1995) Parallel Analysis: a method for determining significant principal components. *Journal of Vegetation Science* 6: 99–106. <https://doi.org/10.2307/3236261>
- Gacitúa S, Oyarzún C, Veas R (2008) Análisis multivariado de la morfometría y merística del robalo *Eleginops maclovinus* (Cuvier, 1830). *Revista de Biología Marina y Oceanografía* 43: 491–500. <https://doi.org/10.4067/S0718-19572008000300008>
- Gajardo G (1987) *Basilichthys microlepidotus* (Jenyns, 1842) and *Basilichthys australis* Eigenmann, 1927 (Pisces: Teleostei, Atherinidae): comments on their morphological differentiation. *Studies of Neotropical Fauna and Environment* 22: 223–236. <https://doi.org/10.1080/01650528709360735>

- García A, González J, Habit E (2012) Caracterización del hábitat de peces nativos en el río San Pedro (cuenca del río Valdivia, Chile). *Gayana Especial* 75: 36–44. <https://doi.org/10.4067/S0717-65382012000100004>
- Grünbaum T, Cloutier R, Mabee PM, Le François NR (2007) Early developmental plasticity and integrative responses in Arctic Charr (*Salvelinus alpinus*): effects of water velocity on body size and shape. *Journal of Experimental Zoology (Mol Dev Evol)* 308B: 396–408. <https://doi.org/10.1002/jez.b.21163>
- Hammer Ø, Harper D, Ryan P (2001) Past: Paleontological statistics software package for education and data analysis. *Paleontologia Electronica* 4: 1–9.
- Hulton NRJ, Purves RS, McCulloch RD, Sugden DE, Bentley MJ (2002) The Last Glacial Maximum and deglaciation in southern South America. *Quaternary Science Reviews* 21: 233–241. [http://dx.doi.org/10.1016/S0277-3791\(01\)00103-2](http://dx.doi.org/10.1016/S0277-3791(01)00103-2)
- Imre I, McLoughlin RL, Noakes DLG (2002) Phenotypic plasticity in brook charr: changes in caudal fin induced by water flow. *Journal of Fish Biology* 61: 1171–1181. <https://doi.org/10.1006/jfbi.2002.2131>
- Istead A, Yavno S, Fox M (2015) Morphological change and phenotypic plasticity in response to water velocity in three species of Centrarchidae. *Canadian Journal of Zoology* 93: 879–888. <https://doi.org/10.1139/cjz-2015-0096>
- Keeley ER, Parkinson EA, Taylor EB (2006) The origins of ecotypic variation of rainbow trout: a test of environmental vs. genetically based differences in morphology. *Journal of Evolutionary Biology* 20: 725–736. <https://doi.org/10.1111/j.1420-9101.2006.01240.x>
- Mir JI, Sarkar UK, Dwivedi AK, Gusain OP, Jena JK (2013) Stock structure analysis of *Labeo rohita* (Hamilton, 1822) across the Ganga basin (India) using a truss network system. *Journal of Applied Ichthyology* 29: 1097–1103. <https://doi.org/10.1111/jai.12141>
- Pakkasmaa S, Piironen J (2000) Water velocity shapes juvenile salmonids. *Evolutionary Ecology* 14: 721–730. <https://doi.org/10.1023/A:1011691810801>
- Pardo R (2002) Diferenciación morfológica de poblaciones de *Trichomycterus areolatus* Valenciennes, 1846 (Pisces: Siluriformes: Trichomycteridae) de Chile. *Gayana* 66: 203–205. <https://doi.org/10.4067/S0717-65382002000200015>
- Pardo R, Scott S, Vila I (2005) Análisis de formas en especies Chilenas del género *Trichomycterus* (Osteichthyes: Siluriformes) utilizando morfometría geométrica. *Gayana* 69: 180–183. <https://doi.org/10.4067/S0717-65382005000100023>
- Poulet N, Berrebi P, Crivelli AJ, Lek S, Argillier C (2004) Genetic and morphometric variations in the pikeperch (*Sander lucioperca* L.) of a fragmented delta. *Archiv für Hydrobiologie* 159: 531–554. <https://doi.org/10.1127/0003-9136/2004/0159-0531>
- Quezada–Romegialli C, Fuentes M, Véliz D (2010) Comparative population genetics of *Basilichthys microlepidotus* (Atheriniformes: Atherinopsidae) and *Trichomycterus areolatus* (Siluriformes: Trichomycteridae) in north central Chile. *Environmental Biology of Fishes* 89: 173–186. <https://doi.org/10.1007/s10641-010-9710-1>
- Reis RE, Trajano E, Hingst–Zaher E (2006) Shape variation in surface and cave populations of the armoured catfishes *Ancistrus* (Siluriformes: Loricariidae) from the São Domingos karst area, upper Tocantins River, Brazil. *Journal of Fish Biology* 68: 414–429. <https://doi.org/10.1111/j.1095-8649.2005.00891.x>

- Ruiz VH (1996) Ictiofauna del Río Laja (VIII Región, Chile): Una evaluación preliminar. Boletín de la Sociedad de Biología de Concepción, Chile 67: 15–21.
- Ruiz VH, López MT, Moyano HI, Marchant M (1993) Ictiología del Alto Bio Bio. Gayana Zoología 57: 77–88.
- Schwander T, Leimar O (2011) Genes as leaders and followers in evolution. Trends in Ecology and Evolution 26: 143–151. <https://doi.org/10.1016/j.tree.2010.12.010>
- Strauss RE, Bookstein FL (1982) The truss: body form reconstructions in morphometrics. Systematic Zoology 31: 113–135. <https://doi.org/10.2307/2413032>
- Taylor EB, Tamkee P, Keeley ER, Parkinson EA (2011) Conservation prioritization in widespread species: the use of genetic and morphological data to assess population distinctiveness in rainbow trout (*Oncorhynchus mykiss*) from British Columbia, Canada. Evolutionary Applications 4: 100–115. <https://doi.org/10.1111/j.1752-4571.2010.00136.x>
- Turan C (1999) A note on the examination of morphometric differentiation among fish populations: the truss system. Turkish Journal of Zoology 23: 259–263.
- Unmack PJ, Bennin AP, Habit EM, Victoriano PF, Johnson JB (2009a) Impact of ocean barriers, topography, and glaciation on the phylogeography of the catfish *Trichomycterus areolatus* (Teleostei: Trichomycteridae) in Chile. Biological Journal of the Linnean Society 97: 876–892. <https://doi.org/10.1111/j.1095-8312.2009.01224.x>
- Unmack PJ, Habit EM, Johnson JB (2009b) New records of *Hatcheria macraei* from Chilean Province. Gayana 73: 102–110. <https://doi.org/10.4067/S0717-65382009000100013>
- Valdovinos C, Habit E, Jara A, Piedra P, González J, Salvo J (2012) Dinámica espacio-temporal de 13 especies de peces nativos en un ecotono lacustre-fluvial de la Cuenca del Río Valdivia (Chile). Gayana Especial 75: 45–58. <https://doi.org/10.4067/S0717-65382012000100005>
- Vila I, Fuentes L, Contreras M (1999) Peces límnicos de Chile. Boletín del Museo Nacional de Historia Natural, Chile 48: 61–75.
- Villagrán C (1990) Glacial climates and their effects on the history of the vegetation of Chile: A synthesis based on palynological evidence from Isla de Chiloé. Review of Palaeobotany and Palynology 65: 17–24. doi: [http://dx.doi.org/10.1016/0034-6667\(90\)90052-K](http://dx.doi.org/10.1016/0034-6667(90)90052-K)
- Walker JA (2010) An integrative model of evolutionary covariance: a symposium on body shape in fishes. Integrative and Comparative Biology 50: 1051–1056. <https://doi.org/10.1093/icb/icq014>
- West-Eberhard MJ (1989) Phenotypic plasticity and the origins of diversity. Annual Review of Ecology and Systematics 20: 249–278. <https://doi.org/10.1146/annurev.es.20.110189.001341>
- Winans G (1987) Using morphometric and meristic characters for identifying of fish. In: Kumpf H, Vaught R, Grimes C, Johnson A, Nakamura E (Eds) Stock identification workshop. US Department of Commerce, National Oceanic and Atmospheric Administration, National Marine Fisheries Service, Panama City Beach, Florida, 135–146.